Radiation from the inset dielectric guide: Applications to antenna arrays and transitions

Sewell, P. D.

Award date:
1991

Awarding institution:
University of Bath

RADIATION FROM THE INSET DIELECTRIC GUIDE:

APPLICATIONS TO ANTENNA ARRAYS AND TRANSITIONS.

Submitted by P.D.Sewell

for the degree of PhD

of the University of Bath,

1991.

ProQuest LLC
789 East Eisenhower Parkway
P.O. Box 1346
Ann Arbor, MI 48106-1346

SUMMARY.

The objective of this thesis is to quantify the effects of radiation from the Inset Dielectric Guide,(I.D.G.).

The I.D.G. has demonstrated excellent potential both as a transmission medium and a basis for leaky-wave antennas and belongs to a class of open nonseparable waveguides that have been proposed for use in the millimeter band.

The theoretical analysis of I.D.G. circuit and antenna elements requires the complete mode spectrum of the I.D.G.,which previously,had not been rigorously derived.

A hybrid transverse characteristic Green's function is presented that allows the complete mode spectra of open nonseparable structures to be recovered.In particular,the continuous radiation modes of the I.D.G.,the microstrip loaded I.D.G. and slotline with finite thickness metallisation have been identified.

Transitions between closed rectangular waveguide and the I.D.G. have been analysed and have shown excellent agreement between experimental and theoretical values,confirming both the validity and utility of the mode spectra developed.

Radiating strips and patches on the I.D.G.,from which leaky-wave antennas may be constructed,have been analysed,demonstrating several interesting phenomena and providing building blocks from which linear arrays may be synthesised.

It is concluded,that the commercial exploitation of the millimeter band will require the complete mode spectra of open nonseparable waveguides.This thesis presents a method that permits their derivation and further demonstrates their role in the development of practical circuit components.

ACKNOWLEDGEMENTS.

I would like to express my thanks to my supervisors,Professor T.Rozzi and Dr S.Pennock,whose guidance and inspiration provided a very stimulating and enjoyable environment within which to work.

I would also like to thank my colleagues in the Wolfson laboratory for both their friendship and the many helpful discussions.

This work was funded by a grant from the Science and Engineering Council,(Award No 88302717).

PUBLICATIONS ARISING FROM THIS WORK.

1) "The Continuous Spectrum of Open Waveguides of Nonseparable Cross-Section",T.Rozzi and P.Sewell,submitted to IEEE trans. antennas and prop.

2) "The Continuous Spectrum of the Inset Dielectric Guide and its Application to Waveguide Transitions",P.Sewell and T.Rozzi,submitted to IEEE trans. microwave theory and techniques.

3) "The Hybrid Continuous Spectrum of the Inset Dielectric Guide and its Application to Rectangular Waveguide to I.D.G. Transitions",P.Sewell and T.Rozzi,to appear in the 21st European microwave Conf.,Stuttgart,1991.

CONTENTS.

CHAPTER 1.

INTRODUCTION.

1.1) Introduction.

With the ever increasing demands being placed upon communication and radar systems,there has been a steady increase in the operating frequencies of these systems.

Higher operating frequencies promise greater channel capacity and allow wider channel separation,thus reducing cross-channel interference.The decrease in wavelength,not only offers the possibility of higher resolution radar systems,but also the construction of physically small antennas with large electrical apertures to improve the efficiency,security and resistance to interference of point to point communication systems.For many applications,such as airborne radar,personal communications and satellite systems,the compact nature of high frequency technologies is also of prime importance.

In the past few decades considerable attention has been directed toward the millimeter waveband,(30-300GHz),in an attempt to realise these advantages,[1].Early experiments were disappointing due to atmospheric absorption,a process not fully characterised until later.In fact today,not only are the propagation windows in the spectrum utilised,but also the high absorption bands, which find applications in the fields of secure battlefield and ship to ship communications and weather forecasting.

Exploitation of any region of the electromagnetic spectrum requires the development of four areas;

i) Coherent source generation.

ii) Propagation and passive circuit media.

iii) Antenna structures.

iv) Active devices.

Sources have been produced that cover many of the frequencies in the millimeter band,including refined travelling wave tubes,klystrons and magnetrons developed from the centimeter band and gas lasers developed from from the far infared region.Currently the use of solid state sources,such as gunn and impatt diodes,is restricted to applications requiring less than 100W of continuous power,[2].

To date,active devices are not widely commercially available for much of the higher frequencies of the millimeter band and fall outside the scope of this thesis.

The remaining two aspects listed above,propagation media and antenna structures,have generated increasing interest in the past 20 years,although the transition from the centimeter to the millimeter band has required the development of new technologies to overcome performance and manufacturing difficulties.

The next section shall briefly discuss the progress that has been made in developing this aspect of the millimeter band,concluding with an introduction to the Inset Dielectric Guide,(I.D.G.),the main concern of this thesis.The following section considers the emergence of a promising new class of leaky wave antennas formed in dielectric waveguide.Section (1.4) discusses the methods currently available for the analysis of discontinuity problems that allow both circuit components and antennas to be designed without resorting to an empirical approach.The final section outlines the work to be presented in the remainder of

this thesis.

1.2) Millimeter Wave circuit Technologies.

Although in principle the circuit technologies currently used in the centimeter band,such as hollow metallic waveguides,microstrip and finline may be dimensionally scaled for use in the millimeter band,in practice frequency limits are set by manufacturing tolerances and material performance.Not only does manufacture become difficult and expensive,but in general the circuitry becomes increasingly lossy as the operating frequency is increased.Therefore considerable attention has been directed toward developing alternative circuit technologies for use in the millimeter band.Although several technologies have been proposed and developed,no one has yet gained universal acceptance.

The main criteria that need to be satisfied by these new technologies are;

i) Cost,both in terms of materials and fabrication methods.

ii) Ease of manufacture and mechanical robustness.

iii) Low material and radiation losses.

iv) Simple active device integration.

v) The ability to realise passive circuits such as couplers and filters.

Printed circuit techniques,such as microstrip and slotline,figure 1a and b,are well proven in the centimeter band and are simple to manufacture.The use of special substrate materials,such as sapphire and fused quartz,can extend the useful operating range of microstrip up to 100Ghz,however,above this frequency these structures become increasingly lossy with Q factors of the order 100.Notwithstanding this,the ease of manufacture and device integration of

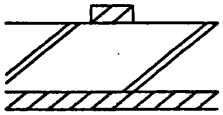

a) Microstrip.

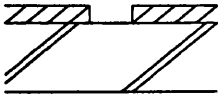

b) Slotline.

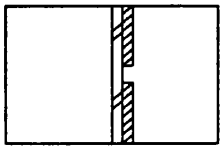

c) Finline.

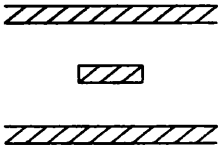

d) Stripline.

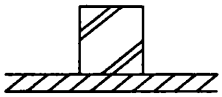

e) Image Line.

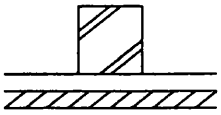

f) Insular Guide.

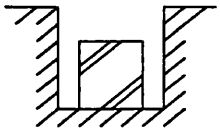

g) Trapped Image Line.

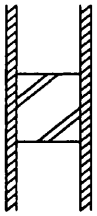

h) Nonradiative Guide.

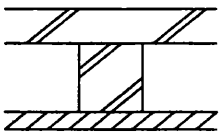

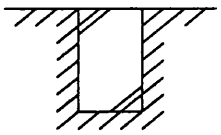

i) Inverted Strip Dielectric Waveguide. j) Inset Dielectric Guide.

Figure 1.1) Millimeter Wave Structures.

microstrip,has motivated its continued development and some microstrip components operating at up to 220Ghz are now available,[3,4].

A problem that is encountered with printed circuit technologies is the excitation of surface waves in the grounded substrate at any discontinuity,[5].Not only does this contribute to the overall loss,but it also causes undesirable crosstalk between components.

The relatively low loss finline structure has proved popular for many applications for frequencies between 25-150GHz,[6].Although housed in a split block,resembling rectangular waveguide,unlike the latter,the tight manufacturing tolerances are placed upon the printed substrates,rather than on the block.The printed substrates may be produced using conventional photolithographic techniques and allow simple integration of beam lead devices.However,as the frequency of operation is increased,finline suffers progressively from unacceptable losses.

Most common centimeter band technologies and those just discussed support a quasi-T.E.M. or fast wave fundamental mode.An alternative approach is to consider structures that support surface wave propagation.These structures utilise dielectric interfaces to guide power and typically have Q factors of several thousands due to the concentration of the fields in a low loss dielectric,[7,8].

Image line,figure 1e, has received considerable attention as a propagation media,[9],although its initial promise has not been fulfilled due to excessive bending losses and radiation from any discontinuities.In addition,its manufacture is not particularly simple either,as it is difficult to maintain tight tolerances when machining the dielectric.This is especially true when,in order to reduce conduction losses,an an insulating layer is introduced to give insular line,shown in figure 1f.The large bending losses of image line arise as a consequence of the lack of

lateral field confinement and,in attempt to overcome this difficulty,trapped image line has been proposed,[10].Although bending losses are reduced,it is only at the expense of fabrication simplicity.

Other structures,illustrated in figure 1,such as inverted strip dielectric guide,[11],and nonradiative guide,[12],whilst similar to image line also possess improved loss performance,although interest in these structures as propagation media seems to be waning,again probably due to manufacturing difficulties.

Inset dielectric guide may be considered as a special case of trapped image line and in fact has previously been analysed as an intermediate structure in this context,[13].As the fields are excellently confined to the dielectric region,the bending losses are low compared to image line,[14].The the structure is relatively simple to construct as,unlike image line,the I.D.G. does not necessarily require precision machining of dielectric materials and may be fabricated by moulding dielectric material into a preformed slot.Alternatively,for lightweight applications,the I.D.G may be formed by depositing a thin metallic coating on three sides of a precut dielectric bar.In contrast to image line or insular line,the construction of the I.D.G. does not require the bonding of dielectrics,which is advantageous due to the lossy nature of most bonding materials.

Although dielectric guides,and in particular the I.D.G.,satisfy many of the criteria previously set out,their success will be determined by the simplicity of active device integration and ease with which passive networks,such as couplers and filters,may be realised.A complication that arises in this context is the open nature of this class of guides.Consequently,any discontinuity causes power to be lost through radiation.Whilst the I.D.G.,for example,may be relatively insensitive to surface imperfections and bends,the design of circuit components must be

undertaken with due regard to minimising radiation losses.However,in contrast,the deliberate excitation of radiation has allowed a new class of leaky wave antennas to be proposed.

1.3) Dielectric Leaky-Wave Antennas.

Leaky-wave antennas are structures that 'leak' part of the guided power as radiation.More precisely,in many cases they are structures that possess a complex pole that lies in the nonspectral Riemann sheet of the propagation constant plane close to the real axis.Although these leaky-wave poles do not belong to the spectrum of the structure,the deformation of the branch cut integral describing the radiation field,may cross these poles,which then often dominate the far field distributions,[15].

Originally continuously slotted rectangular waveguide and later arrays of discrete slots,were the first examples of such antennas and in fact it was consideration of their behaviour that led to the realisation that leaky-waves exist,[16].

In the millimeter band leaky-wave antennas formed from dielectric waveguides have many advantages over their counterparts.Compared to conventional reflector based antennas,dielectric waveguide antennas are more compact and lightweight.This is particularly important for airborne radar applications,which often currently involve complicated hydraulic scanning systems that are bulky and expensive.Not only may leaky-wave planar arrays be electrically scanned,but they may also be conformally mounted onto the skin of an aircraft.Although microstrip patch antennas have also been developed for these applications,they suffer from three main drawbacks,narrow bandwidth,(at best a few per cent),poor polarisation properties and interelement coupling by the excitation of surface waves in the substrate,[17].

Arrays in dielectric guides have been formed using both dielectric discontinuities and metallic radiators.The former class have their origins in optical waveguide gratings,commonly employed as beam couplers and frequency sensitive reflectors for distributed feedback lasers,[16].Scannable grating arrays have been investigated in image line and inverted strip line,[18-21],and whilst promising are hampered by their relatively complicated manufacture.

Arrays formed from metallic radiators can be produced using conventional photolithographic techniques and are consequently attractive for commercial exploitation.Such arrays formed in image line,[22,23],dielectric rod,[24,25],trapped image line,[26] and the I.D.G.[27,28,29] have been both theoretically and experimentally investigated.

An important consideration for planar arrays is the coupling between guides in close proximity.For example,coupling between parallel image lines limits their use in such arrays,whereas in contrast,the relative isolation of parallel I.D.G.'s makes them ideally suited to such an application.

One of the main objectives of this thesis is to develop a rigorous method to allow I.D.G. leaky wave antennas to be analysed and synthesised,without excessive experimentation.

The I.D.G. has two fundamental modes of operation,either an $H.E._{10}$ mode in a deep slot I.D.G. or an $E.H._{11}$ mode in a shallow slot I.D.G.,[30].In both configurations the guided fields are almost maximal at the air-dielectric interface,which is therefore an ideal location for the introduction of radiating elements.Transverse metallic strips placed upon a deep slot I.D.G. produce vertically polarised radiation,which,due to the minor contribution from the transverse magnetic field of the fundamental mode,does not suffer from the cross-polarisation difficulties experienced with microstrip patch antennas.Similarly

longitudinal strips,when excited by the fundamental mode of the shallow slot I.D.G.,produce horizontally polarised radiation which is useful for many applications.

Experimental studies have shown that I.D.G. leaky-wave antenna arrays may be successfully formed in this manner and exhibit many desirable features although to date,their accurate design has been hampered by a lack of a rigorous,complete spectrum for the I.D.G.

1.4) The Analysis and synthesis of circuit components and Antenna structures.

The accurate analysis and synthesis of circuit elements and antenna arrays relies on an ability to model discontinuities.Although uniform quasi-infinite gratings and antenna arrays may be analysed as periodic structures supporting leaky-waves,practical components are often nonuniform and far from infinite.

In general there are two approaches to modelling discontinuities:purely numerical methods and analytic techniques,[31].The former category includes techniques such as the finite difference method and the finite element method which,with ever increasing computer power,are finding favour in many fields.

These methods solve Maxwell's equations on a microscopic level,using a finite difference and a variational formulation of Maxwell's equations respectively.In the former method the fields and their derivatives are expressed in terms of the fields at the nodes of a mesh superimposed on the structure.Substitution of these quantities into Maxwell's equations yields a matrix equation which may then be solved for the nodal field values.Although not essential,a variational formulation of Maxwell's equations can be used to improved the convergence of the solution,[32].The finite difference method does not suffer from the appearance of spurious solutions that can complicate a finite element analysis,although it is only strictly accurate for regular meshes and

therefore does not allow targeting of problematic regions such as sharp corners.Recently,the finite element method has overshadowed the finite difference method as is does allow the use of nonuniform meshes.In this method the structure is decomposed into a mesh of elements,such as triangles for a plane,and the fields in each element approximated by a low order polynomial,determined by interpolating between preselected nodes within the element.Substitution of these polynomials into a variational formulation of Maxwell's equations and applying continuity between the elements again results in a matrix equation that may be solved for the nodal field values,[33,34].As commented above,spurious solutions have been a problem in some finite element analyses,although various methods have been developed to overcome this difficulty,[31].A further limitation is the ability to consider open structures.In certain circumstances a combination of finite elements and analytical techniques has been applied,in which the fields within some predetermined nonphysical boundary are treated with finite elements and those external to the boundary using a spectral approach,[35].

The alternative to purely numerical techniques is to use an analytical approach based upon a spectral representation of the fields.An arbitrary solution to Maxwell's equations may be expressed as a superposition of the modes of the structure,where the modes are the eigenfunctions of Maxwell's equations,subject to the boundary conditions imposed by the structure,[36].Theoretically,once the modes are known,it is possible to use their orthogonality properties to identify the expansion coefficients and thus the solution to the problem.Unfortunately,not only are there an infinite number of modes,but often the solution may still only be expressed as that of an integral equation.However,the solution of this integral equation may be obtained using a technique,such as Galerkin's method,in which a physical understanding of the nature of the solution can have a profound influence upon the ease with which the solution may be recovered.This is the main

advantage of the analytical approach,namely that it allows the analyst to use their experience to optimise the formulation of the problem that is finally solved by numerical evaluation.

In comparing numerical and analytical techniques there are two considerations to make.Firstly the ease and efficiency with which,if at all,the solution may be determined.Numerical methods are continually being refined,in terms of efficiency,the elimination of spurious solutions and the range of problems that they can tackle and advances in computer power,have alleviated the common criticism that they are time consuming and require extensive computer facilities.The principle advantage of numerical methods is the ease with which they may be applied to structures with complex geometries.However,for many common structures it is possible to apply analytical methods and derive results more efficiently than by purely numerical means.Solutions to more complex structures can then be built from those of the elementary problems.Employing both an understanding of the physical situation and mathematical ingenuity,can,in some circumstances,yield a good approximation to the solution in a closed form and,even if this is not the case,the problem may be reduced to a form far more amenable to accurate and efficient numerical solution than otherwise possible.

The second consideration is more esoteric.It has been stated above that a physical understanding of the problem can often lead to simpler methods of solution being found.Further,as argued by Collin,[37],it is often the case that practical developments have been proposed to capitalise on properties predicted from an analytical concept and it is interesting to wonder if some advances would have been made if powerful computers had been available 40 years ago.Purely numerical methods can only ever solve a sequence of particular problems rather than a class,and,although results may be interpolated,they yield little further to aid

an understanding of the principles involved.It seems reasonable to argue that numerical and analytical approaches are complementary,neither can be applied to every situation and each has its own advantages.

This thesis is concerned with the spectral approach to electromagnetic problems.Clearly in order to pursue the spectral approach outlined above,the complete mode spectrum of the structure of interest must be available.This is available for 1 dimensional and 2 dimensional separable sections.The main objective of this thesis is to develop a method that allows the complete modal spectrum of open nonseparable structures to be identified.By nonseparable it is meant that the transverse geometry,and hence the modes,of the structure cannot be represented in the form X(x).Y(y).This is a class that includes many of the structures discussed above that are being developed for use in the millimeter band.

The spectrum of open waveguides comprises of two types of mode.There are discrete modes,often referred to as bound modes,which may,or may not,exist in a given situation.These modes,as the name implies,are characterised by discrete values of the propagation constant and are bound to the structure.These are the modes which are exploited for transmission purposes and many methods are available to recover their shape and dispersion relationships,[31,36,38].In addition to the discrete modes,open waveguides also possess a continuum of radiation modes.These modes radiate power away from the structure and are characterised by a continuous propagation constant.Any discontinuity causes these modes to be excited and power to be radiated,whether intentionally,as in an antenna,or not.The continuous modes of separable open waveguides are amenable to identification by the separation of variables,[36],or instead by a scalar transverse characteristic Green's function approach,[38].Until recently,the continuous modes of

nonseparable open structures have received little attention.It is the identification of these modes,and in particular those of the I.D.G.,that are the principle concern of this thesis.

1.5) The Structure of the Thesis.

Chapter 2 shall expand upon the spectral approach,briefly introduced above,for solving electromagnetic problems,highlighting the role of the complete mode spectrum and its use in constructing an inversion operator to Maxwell's equations,the Green's function.

A novel vector transverse characteristic Green's function shall be presented that allows the complete mode spectra of open nonseparable structures to be identified.

Chapter 3 shall demonstrate the use of this method to recover the complete spectra of open separable structures,for which closed form solutions are already available.

The strength of the method shall be demonstrated in chapter 4,in which the continuous spectrum of the I.D.G. shall be derived.

Subsequently these modes shall be used in chapters 5 and 6 to rigorously analyse rectangular waveguide to I.D.G. transitions and radiating patches on the I.D.G. respectively.

Chapter 7 derives the continuous spectrum of the microstrip loaded I.D.G.,a structure that is useful in the analysis of certain I.D.G. leaky wave arrays.

Chapter 8 extends the method developed in chapter 2,to include structures,specifically slotline with finite metallisation thickness,that have more than one nonseparable interface.

Finally,chapter 9 shall discuss future studies suggested,and draw conclusions from,the work presented in this thesis.

1.6) References.

1) J.Wiltse,"History of Millimeter and Submillimeter Waves",IEEE trans. microwave theory and techniques,vol MTT-32,no9 Sept 84,pp1118-1127.

2) J.Dunlop and D.Smith,"Telecommunications Eng.",Van Nostrand Reinhold (UK),1984.

3) H.Meinel,"Millimeter-Wave Technological Advances since 1985 and future Trends",IEEE trans. microwave theory and techniques,vol MTT-39,no 5,May 91,pp759-767.

4) D.Williams,"Millimeter-Wave Components and Subsystems built using Microstrip Technology",IEEE trans. microwave theory and techniques,vol MTT-39,no 5 May 91,pp768-774.

5) T.Oxley and C.Burnett,"MM-Wave Hybrid Microstrip Technology",Microwave J. pt 1,Mar 86,pt 2,May 86.

6) W.Harokopus,L.Katehi,W.Ali-Ahmed and G.Rebeiz,"Surface Wave Excitation from Open Microstrip Discontinuities",IEEE trans. microwave theory and techniques,vol MTT-39,no 7,July 91,pp1098-1107.

7) R.Gelsthorpe,N.William,s and N.Davey,"Dielectric Waveguide;a low cost technology for millimeter wave integrated circuits,The Radio and Electronic Engineer,vol 52,no 11/12 pp522-528.

8) R.Knox,"Dielectric Waveguide Microwave Integrated Circuits-An Overview",IEEE trans. microwave theory and techniques,vol MTT-24,no 11,Nov 76,pp806-814.

9) D.King,"Properties of Dielectric Image Lines",IRE trans. microwave theory and techniques,vol MTT-3,no 3,Mar 55,pp75-81.

10) T.Itoh and B.Adelseck,"Trapped Image Guide for millimeter-Wave Circuits",IEEE trans. microwave theory and techniques,vol MTT-28,no 12,Dec 80,pp1433-1436.

11) T.Itoh,"Inverted Strip Dielectric Waveguide for Millimeter-Wave Integrated Circuits",IEEE trans. microwave theory and techniques,vol MTT-24,no 11,Nov 76,pp821-827.

12) T.Yoneyama and S.Nishida,"Nonradiative Dielectric Waveguide for Millimeter-Wave Integrated Circuits",IEEE trans. microwave theory and techniques,vol MTT-29,pp1188-1192.

13) W.Zhou and T.Itoh,"Analysis of Trapped Image Line using Effective Dielectric Constant and Surface Impedances",IEEE trans. microwave theory and techniques,vol MTT-30,no 12,Dec 82,pp2163-2166.

14) S.Hedges and T.Rozzi,"The Loss Analysis of Inset Dielectric Guide including Bending Loss and a Comparison with Image Line",proc 17th european microwave conf,Rome,Sept 87,pp933-938.

15a) T.Tamir and A.Oliner,"Guided Complex Waves : part 1,Fields at an Interface",proc I.E.E.,vol 110,no 2,Feb 63,pp310-324.

15b) A.Oliner,S-T Peng,T-I Hsu and A.Sanchez,"Guided Complex Waves : part 2,Relation to Radiation Patterns" ,proc I.E.E.,vol 110,no 2,Feb 63,pp325-334.

16) A.Oliner,"Historical Perspectives on Microwave Field Theory",IEEE trans. microwave theory and techniques,vol-32,no 9,Sept 84,pp1021-1045.

17) A.Rudge,K.Milne,A.Olver and P.Knight,"The Handbook of Antenna Design,Vols 1 and 2",Peregrinus,London,1986.

18) F.Schwering and S-T Peng,"Design of Dielectric Grating Antennas for Millimeter-Wave Applications",IEEE trans. microwave theory and techniques,vol MTT-31,no 2,Feb 83,pp199-209.

19) T.Ohira,M.Tsutsumi and N.Kumagai,"Radiation of Millimeter Waves from a grooved Ferrite Image Line",proc IEEE,vol 70,June 82,pp682-683.

20) H.Maheri,M.Tsutsumi and N.Kumagai,"Experimental Studies of Magnetically Scannable Leaky-Wave Antennas having a Corrugated Ferrite Slab/Dielectric layer Structure",IEEE trans. antennas and prop.,vol AP-36,no 7,July 88,pp911-917

21) T.Itoh,"Application of Gratings in a Dielectric Waveguide for Leaky-Wave Antennas and Band-Reject Filters",IEEE trans. microwave theory and techniques,vol MTT-25,no 12,Dec 77,pp1134-1137

22) K.Solbach and B.Adelseck,"Dielectric Image Line Leaky Wave Antenna for Broadside Radiation",Electronics letts.,vol 19,no 16,4th Aug,pp640-641.

23) K.Solbach,"E-band Leaky Wave Antenna using Dielectric Image line with etched Radiating Elements",1979 IEEE MTT-S International Microwave Conf. digest,pp214-216.

24) S.Kabayashi et al,"Dielectric Rod Leaky-Wave Antennas for Millimeter-Waves",IEEE trans. Antennas and prop.,vol AP-29,pp822-824.

25) R.Mittra and R.Kastner,"A Spectral Domain Approach for Computing the Radiation Characteristics of a Leaky-Wave Antenna for Millimeter-Waves",IEEE trans. Antennas and prop.,vol AP-29,pp652-654.

26) T.Itoh and B.Adelseck,"Trapped Image Guide Leaky-Wave Antennas for millimeter Wave applications",IEEE trans. Antennas and prop.,vol AP-30,no 3,May 82,pp505-509.

27) T.Rozzi,L.Ma,R de Leo and A.Morini,"Equivalent Network of Transverse Dipoles on Inset Dielectric Guide:Application to Linear Arrays",IEEE trans. Antennas and prop.,vol Ap-38,no 3,Mar 90,pp380-385.

28) T.Rozzi and L.Ma,"Scattering by Dipoles in I.D.G. and Application to Millimeter Antennas",proc 17th European microwave conf.,Rome,Sept 87,pp543-548.

29) T.Rozzi,R de Leo and A.Morini,"Analysis of the 'microstrip-Loaded Inset Dielectric Guide",1989 MTT-S digest,pp923,926.

30) T.Rozzi and S.Hedges,"Rigorous Analysis and Network Modelling of the Inset Dielectric Guide",IEEE trans. microwave theory and techniques,vol MTT-35,no 9,Sept 87,pp823-834.

31) S.Saad,"Review of Numerical Methods for the Analysis of Arbitrarily-Shaped Microwave and Optical Dielectric Waveguides",IEEE trans. microwave theory and techniques,vol MTT-33,no 10,Oct 85,pp894-899.

32) E.Schweig and W.Bridges,"Computer Analysis of Dielectric Waveguides:A Finite Difference Method",IEEE trans. microwave theory and techniques,vol MTT-32,no 5,May 84,pp531-541.

33) J.Reddy,"Applied Functional Analysis and Variational Methods in Engineering",McGraw Hill,1986.

34) D.Jones,"Methods in Electromagnetic Wave Propagation,vol 1",Oxford, 1987.

35) M.Koshiba and K.Hiragama,"Application of Finite Elements to Arbitrarily Shaped Discontinuities in Dielectric Waveguide",IEE proc,vol 135,pt H,Feb 88,pp8-12.

36) R.Collin,"Field Theory of Guided Waves",McGraw Hill,1960.

37) R.Collin,"The Role of Analysis in the Age of Computers:View from the Analytical Side",IEEE Antennas and Propagation Magazine,vol 32,no 4,Aug 90,pp27-31.

38) L.Felsen and N.Marcuvitz,"Radiation and Scattering of Waves",Prentice Hall,1973.

CHAPTER 2.

THE SPECTRAL APPROACH TO ELECTROMAGNETIC PROBLEMS.

The general problem that is posed in the analysis of electromagnetic systems,is to determine the response of the system to a given source.The source and response may be defined in many forms,depending upon the context of the analysis,although they are fundamentally related through Maxwell's equations.Consequently it is essential to consider the properties and methods of solving Maxwell's equations.

For linear media,Maxwell's equations,in their most general form,may be stated as;

$$\nabla \times \underline{E}(\underline{r},t) = -\frac{\partial}{\partial t}\underline{\underline{\mu}}(\underline{r},t) \cdot \underline{H}(\underline{r},t)$$

$$\nabla \times \underline{H}(\underline{r},t) = \underline{J}(\underline{r},t) + \frac{\partial}{\partial t}\underline{\underline{\varepsilon}}(\underline{r},t) \cdot \underline{E}(\underline{r},t)$$

$$\nabla \cdot \underline{\underline{\mu}}(\underline{r},t) \cdot \underline{H}(\underline{r},t) = 0 \qquad (2.1)$$

or more compactly,in the form of the operator equation;

$$\begin{pmatrix} -\frac{\partial}{\partial t}\underline{\underline{\varepsilon}}(\underline{r},t) & \nabla \times \\ -\nabla \times & -\frac{\partial}{\partial t}\underline{\underline{\mu}}(\underline{r},t) \end{pmatrix} \begin{pmatrix} \underline{E}(\underline{r},t) \\ \underline{H}(\underline{r},t) \end{pmatrix} = \begin{pmatrix} \underline{J}(\underline{r},t) \\ \underline{0} \end{pmatrix} \qquad (2.2)$$

As discussed in the introduction,there are two approaches to solving this equation.The first is to apply purely numerical techniques,such as the finite element method,and the second,is to use the spectral representation of the fields and currents to construct an inverse operator,such that;

$$\begin{pmatrix} -\frac{\partial}{\partial t}\underline{\underline{\varepsilon}}(\underline{r},t) & \nabla\times \\ -\nabla\times & -\frac{\partial}{\partial t}\underline{\underline{\mu}}(\underline{r},t) \end{pmatrix}^{-1} \begin{pmatrix} \underline{J}(\underline{r},t) \\ \underline{0} \end{pmatrix} = \begin{pmatrix} \underline{E}(\underline{r},t) \\ \underline{H}(\underline{r},t) \end{pmatrix} \tag{2.3}$$

The objective of this work is to determine the complete mode spectrum of nonseparable open waveguides and subsequently construct and utilise this inverse operator.The approach is based upon certain results available from functional analysis and it is now appropriate to review the essential theorems that shall be applied later.

2.1) Application of the Spectral Theorem to Linear partial differential operators.

This section shall introduce the spectral theorem and its application to linear partial differential operators.It shall be shown that the inversion operator,used to solve an operator equation,may be developed from a knowledge of the spectrum of the operator.The following section shall then discuss the characteristic Green's function method of determining the spectrum of the operator.

It is not possible or appropriate to present more than a review of the essential theorems that shall be applied later,further details may be found in references [1-5].

The problem under consideration is to determine the response,$\underline{\psi}(\underline{r})$,of a system to a given source,$\underline{f}(\underline{r})$.The system may be characterised by the operator equation;

$$L\underline{\psi}(\underline{r}) = \underline{f}(\underline{r}) \tag{2.1.1}$$

and the boundary conditions associated with the range and domain of the operator L.Attention shall be restricted to linear partial differential operators.

The inverse operator,L^{-1},defined by the equation;

$$\underline{\psi}(\underline{r}) = L^{-1}\underline{f}(\underline{r}) \tag{2.1.2}$$

shall be expressed in terms of its spectral representation.Before this spectral representation may be introduced and derived from the spectral theorem,it is necessary to define the spectrum of an operator.

The spectrum of the operator L is defined as the set of complex values,λ,for which the operator L-λ does not have a bounded inverse.Therefore if λ lies in the spectrum of L there does not exist a value of m,such that;

$$< (L-\lambda)^{-1}\underline{x}(\underline{r}),\underline{x}(\underline{r}) > \leq m < \underline{x}(\underline{r}),\underline{x}(\underline{r}) > \tag{2.1.3}$$

holds for all $\underline{x}(\underline{r})$ within the domain of L.The inner product < , > is chosen in accordance with the range and domain of L.

Application of this definition to a linear partial differential operator,L,reveals two possibilities;

i) If λ_n is an eigenvalue of L,ie λ_n is a solution to the equation;

$$(L-\lambda_n)\underline{\phi}_n(\underline{r}) = \underline{0} \tag{2.1.4}$$

then clearly the operator $(L-\lambda_n)^{-1}$ is unbounded.For λ_n to be a strict eigenvalue the corresponding eigenfunction $\underline{\phi}_n(\underline{r})$ must lie in the domain of L.The set of eigenvalues $\{\lambda_n\}$,which always consists of discrete values,constitutes the point spectrum of the operator L.

ii) The second possibility is that there may exist values of λ for which;

$$(L-\lambda)\underline{\phi}_\lambda(\underline{r}) = \underline{0} \tag{2.1.5}$$

although the functions $\underline{\phi}_\lambda(\underline{r})$ do not have bounded norms and therefore cannot lie in the domain of L.These values of λ constitute the continuous spectrum of L.As the

name implies,these values are not discrete but are grouped into continuous sets.As $\underline{\phi}_\lambda(\underline{r})$ does not lie in the domain of L,λ and $\underline{\phi}_\lambda(\underline{r})$ cannot be a strict eigensolution of L,although they are often referred to as an improper eigensolution of L.

Now that the spectrum of L has been defined,the central theorem underlying the spectral approach,the spectral theorem,may be introduced.

The spectral theorem states that the proper and improper eigenfunctions of the operator L are linearly independent.This is a somewhat simplified statement,but it is sufficient for the present context.

Consequently,if the eigenfunctions may be shown to be complete and span the domain of L,then an arbitrary function within the domain may be expressed as a linear combination of these functions,ie;

$$\underline{\psi}(\underline{r}) = \sum_n \gamma_n \underline{\phi}_n(\underline{r}) + \int d\lambda\, \gamma_\lambda \underline{\phi}_\lambda(\underline{r}) \tag{2.1.6}$$

This expansion is referred to as the spectral representation of $\underline{\psi}(\underline{r})$

The advantage of the spectral representation is apparent upon application of the operator L.

$$L\underline{\psi}(\underline{r}) = \sum_n \gamma_n \underline{\phi}_n(\underline{r})\lambda_n + \int d\lambda\, \gamma_\lambda \underline{\phi}_\lambda(\underline{r})\lambda \tag{2.1.7}$$

If $L\underline{\psi}(\underline{r})$ in this form is equated to the spectral representation of the function $\underline{f}(\underline{r})$;

$$\underline{f}(\underline{r}) = \sum_n \alpha_n \underline{\phi}_n(\underline{r}) + \int d\lambda\, \alpha_\lambda \underline{\phi}_\lambda(\underline{r}) \tag{2.1.8}$$

then the solution to the operator equation,equation (2.1.1),is immediately identified as;

$$\underline{\psi}(\underline{r}) = \sum_n \frac{\alpha_n \underline{\phi}_n(\underline{r})}{\lambda_n} + \int d\lambda\, \frac{\alpha_\lambda \underline{\phi}_\lambda(\underline{r})}{\lambda} \tag{2.1.9}$$

Before this expression may be used to derive the inverse operator,L^{-1},it is necessary to explicitly relate the coefficients α_n and α_λ to the function $\underline{f}(\underline{r})$.

As stated above,the proper and improper eigenfunctions of L form a linearly independent set,however,they are not necessarily orthogonal.In general they satisfy a biorthogonality relationship of the form;

$$< \underline{\phi}_n(\underline{r}),\underline{\phi}^{\Lambda}_m(\underline{r}) > = \delta_{mn}$$

$$< \underline{\phi}_n(\underline{r}),\underline{\phi}^{\Lambda}_\lambda(\underline{r}) > = 0$$

$$< \underline{\phi}_\lambda(\underline{r}),\underline{\phi}^{\Lambda}_{\lambda'}(\underline{r}) > = \delta(\lambda - \lambda') \qquad (2.1.10)$$

The functions $\underline{\phi}^{\Lambda}_m(\underline{r})$ and $\underline{\phi}^{\Lambda}_\lambda(\underline{r})$ are the proper and improper eigenfunctions of the adjoint operator to L,L^{Λ}.

The adjoint operator is defined as the operator for which the expression;

$$< L\underline{x}(\underline{r}),\underline{y}(\underline{r})) = < \underline{x}(\underline{r}),L^{\Lambda}\underline{y}(\underline{r}) > \qquad (2.1.11)$$

holds for all $\underline{x}(\underline{r})$ and $\underline{y}(\underline{r})$ in the domain and range of L.Further,it may be proved that the spectrum of L^{Λ} is the conjugate to that of L when the inner product is defined on a complex linear space and equal to that of L when the inner product is defined on a real linear space.

The Dirac delta function,appearing in the biorthogonality relationship between the improper eigenfunctions,highlights the non-bounded nature of these functions and also their continuous dependence upon the parameter λ.

The biorthogonality relationship between the eigenfunctions of the operator L and its adjoint L^{Λ},allows the coefficients α_n and α_λ in equation (2.1.8) to be evaluated as;

$$\alpha_n = < \underline{\phi}^{\Lambda}_n(\underline{r}),\underline{f}(\underline{r}) > \quad : \quad \alpha_\lambda = < \underline{\phi}^{\Lambda}_\lambda(\underline{r}),\underline{f}(\underline{r}) > \qquad (2.1.12)$$

If these expressions are substituted into equation (2.1.9),then the response of the system may be written as;

$$\underline{\psi}(\underline{r}) = \sum_{n} \frac{\phi_n(\underline{r}) < \phi_n^{\Lambda}(\underline{r}), \underline{f}(\underline{r}) >}{\lambda_n} + \int d\lambda \, \frac{\phi_\lambda(\underline{r}) < \phi_\lambda^{\Lambda}(\underline{r}), \underline{f}(\underline{r}) >}{\lambda} \tag{2.1.13}$$

Now that the response $\underline{\psi}(\underline{r})$ has been expressed in terms of the source,$\underline{f}(\underline{r})$,it is possible to seek the general inverse operator,L^{-1}.

If the inverse operator is defined to be of the form;

$$L^{-1}\underline{f}(\underline{r}) = < \underline{\underline{G}}(\underline{r},\underline{r}'), \underline{f}(\underline{r}') > \tag{2.1.14}$$

then it is apparent that the kernel,$\underline{\underline{G}}(\underline{r},\underline{r}')$,known as the Green's function,is given by;

$$\underline{\underline{G}}(\underline{r},\underline{r}') = \sum_{n} \frac{\phi_n(\underline{r})\phi_n^{\Lambda}(\underline{r}')}{\lambda_n} + \int d\lambda \, \frac{\phi_\lambda(\underline{r})\phi_\lambda^{\Lambda}(\underline{r}')}{\lambda} \tag{2.1.15}$$

Thus to summarise:if the spectral representation associated with the operator L and its adjoint,L^{Λ},is determined,then the inverse operator,L^{-1},may be expressed by means of a Green's function whose spectral representation is given in equation (2.1.15).

Now that it has been demonstrated that the inverse operator may be developed from a knowledge of the spectrum of an operator,it is necessary to consider in detail how this spectrum may be determined.

2.2) The Characteristic Green's function Method.

As discussed above,the spectrum of the operator L is defined as the set of values of λ for which;

$$(L - \lambda)\underline{\phi}_\lambda(\underline{r}) = \underline{0} \tag{2.2.1}$$

where $\underline{\phi}_\lambda(\underline{r})$ may be either a proper or an improper eigenfunction.

The method used to determine the spectrum and the eigenfunctions of L will obviously depend upon the particular system under consideration and for a given system there may,in fact,exist a variety of techniques,both numerical and analytical.It is often found that if the domain of the operator is dimensionally separable,then the separation of variables permits analytic solutions to be identified.Naturally it must be ensured that all the possible solutions have been recovered and that they are normalised in accordance with equation (2.1.10).

The characteristic Green's function method is a technique that obtains the complete,correctly normalised,spectrum in one fell swoop.This section shall introduce the characteristic Green's function and demonstrate its utility in the derivation of the spectrum and the eigenfunctions of an operator L.

Consider the inhomogeneous equation;

$$(L-\lambda)\underline{g}(\underline{r})=\underline{f}(\underline{r}) \tag{2.2.2}$$

where λ is not contained within the spectrum of L.Again an inverse operator,$(L-\lambda)^{-1}$,may be defined and expressed in terms of a Green's function,in this case known as the characteristic Green's function.

$$(L-\lambda)^{-1}\underline{f}(\underline{r})=\underline{g}(\underline{r})=-<\underline{\underline{G}}(\underline{r},\underline{r}';\lambda),\underline{f}(\underline{r}')> \tag{2.2.3}$$

It is noted that the characteristic Green's function is symbolically distinguished from the Green's function of the previous section by its arguments.

The motivation for considering this inhomogeneous operator equation and its inverse,is that the characteristic Green's function may be expressed in two forms.Naturally,it may be written in terms of the spectral representation associated with the operator L and,in addition,it may be shown that it is also the solution to the inhomogeneous equation,(2.2.2),for a particular source function.The equivalence of the two forms subsequently permits the identification

of the spectrum of the operator L.

The spectral representation of the characteristic Green's function may be determined in a similar manner to that of the Green's function of the previous section.The spectral representations of the functions $\underline{f}$ and $\underline{g}$;

$$\underline{f}(\underline{r}) = \sum_n \underline{\phi}_n(\underline{r}) < \underline{\phi}_n^{\dagger}(\underline{r}), \underline{f}(\underline{r}) > + \int d\lambda \, \underline{\phi}_\lambda(\underline{r}) < \underline{\phi}_\lambda^{\dagger}(\underline{r}), \underline{f}(\underline{r}) >$$

$$\underline{g}(\underline{r}) = \sum_n \underline{\phi}_n(\underline{r}) \alpha_n + \int d\lambda \, \underline{\phi}_\lambda(\underline{r}) \alpha_\lambda \tag{2.2.4}$$

are substituted into equation (2.2.3),which identifies the spectral representation of the characteristic Green's function to be;

$$\underline{\underline{G}}(\underline{r},\underline{r}'\lambda) = \sum_n \frac{\underline{\phi}_n(\underline{r})\underline{\phi}_n^{\dagger}(\underline{r}')}{\lambda - \lambda_n} + \int d\lambda' \, \frac{\underline{\phi}_\lambda(\underline{r})\underline{\phi}_\lambda^{\dagger}(\underline{r}')}{\lambda - \lambda'} \tag{2.2.5}$$

The second means of determining the characteristic Green's function is recovered by applying the operator $(L - \lambda)$ to equation (2.2.3).

$$\underline{f}(\underline{r}) = -< (L - \lambda)\underline{\underline{G}}(\underline{r},\underline{r}';\lambda), \underline{f}(\underline{r}') > \tag{2.2.6}$$

demonstrating that the characteristic Green's function is also the solution to the inhomogeneous equation;

$$(L - \lambda)\underline{\underline{G}}(\underline{r},\underline{r}';\lambda) = -\underline{\underline{I}}\,\delta(\underline{r}-\underline{r}') \tag{2.2.7}$$

where $\underline{\underline{I}}$ is the identity operator.

The connection between the spectrum of the operator L and the characteristic Green's function may be made,if the spectral representation of the latter is integrated around a contour,C, in the complex λ plane that encloses all of its singularities.Evaluation of the integral using the residue theorem gives;

$$\frac{1}{2\pi j}\int_C d\lambda\, \underline{\underline{G}}(\underline{r},\underline{r}';\lambda) = \sum_n \underline{\phi}_n(\underline{r})\underline{\phi}_n^{\wedge}(\underline{r}') + \int d\lambda\, \underline{\phi}_\lambda(\underline{r})\underline{\phi}_\lambda^{\wedge}(\underline{r}') \qquad (2.2.8)$$

Therefore,if the characteristic Green's function may be somehow determined by solving equation (2.2.7),then it is apparent from equation (2.2.8),that the point spectrum of L consists of the values of λ for which it is singular.Similarly the values of λ corresponding to any branch cuts in the complex plane constitute the continuous spectrum of L.The corresponding proper and improper eigenfunctions may then be identified,usually by inspection,from the explicit form of equation (2.2.8).

The specific method used to solve equation (2.2.8) for the characteristic Green's function will depend upon the operator L and its domain,although it is usual in a multidimensional system for one or more of the dimensions to be separable.

Consider the example of two dimensional separable system with eigensolutions defined by;

$$(L - \lambda_{mn})\underline{\Psi}_{mn}(x,y) = \underline{0} \qquad (2.2.9)$$

The separable nature allows this equation to be written in the form;

$$(L_x + L_y - \lambda_{mn})\underline{\Phi}_m(x)\chi_n(y) = \underline{0} \qquad (2.2.10)$$

from which it may be seen that the functions,$\Phi_m(x)$ and $\chi_n(y)$ are the eigensolutions of the equations;

$$(L_x - \lambda_m)\underline{\Phi}_m(x) = \underline{0} \;:\; (L_y - \lambda_n)\chi_n(y) = 0 \qquad (2.2.11)$$

where $\lambda_{mn} = \lambda_m + \lambda_n$.

The two dimensional eigenfunctions,$\underline{\Psi}_{mn}(x,y)$,may then be derived from the two,one dimensional,characteristic Green's functions as;

$$\sum_{p} \underline{\Psi}_p(x,y)\underline{\Psi}_p^A(x',y') = \left(\frac{1}{2\pi j}\int_{C_m} d\lambda_m \underline{\underline{G}}(x,x';\lambda_m)\right)\left(\frac{1}{2\pi j}\int_{C_n} d\lambda_n\, G(y,y';\lambda_n)\right) \qquad (2.2.12)$$

[It is noted that the summation w.r.t. p is symbolic not necessarily literal.]

The spectral representation of an arbitrary function will now involve summations and integrations w.r.t. two independent variables;

Attention shall now be refocused upon the application of the preceding theory to the electromagnetic system characterised by Maxwell's equations.

2.3) Application of the Spectral Theorem to Maxwell's Equations.

The theory of the preceding sections has demonstrated a technique that may be used to solve Maxwell's equations,by means of constructing an inverse operator.Before the procedure may be pursued,it is necessary to formulate Maxwell's equations into an operator equation and to determine the domain of functions upon which it operates.Similarly an adjoint operator and its domain must be identified.

Equation (2.2) expresses Maxwell's equations in the form of the following operator equation;

$$\begin{pmatrix} -\partial t\underline{\underline{\varepsilon}}(\underline{r},t). & \nabla\times \\ -\nabla\times & -\partial t\underline{\underline{\mu}}(\underline{r},t). \end{pmatrix}\begin{pmatrix} \underline{E}(\underline{r},t) \\ \underline{H}(\underline{r},t) \end{pmatrix} = \begin{pmatrix} \underline{J}(\underline{r},t) \\ \underline{0} \end{pmatrix} \qquad (2.3.1)$$

For arbitrary linear media,this is the most basic operator equation that characterises the system.However,for most practical applications it is possible to use the specific properties of the structure to derive an alternative,simpler,operator equation.For example,if the media is isotropic,then the permeability and permittivity dyadics may be,a priori,replaced by scalar functions.This process often results in an operator that is its own adjoint.If,in addition,the domains of the operator and its adjoint are identical,then the operator is known as self adjoint.

This section shall show,that for the structures that are the subject of this work,the operator equation may be reformulated such that the operator is its own adjoint,but with differing domains.Thus the operator is not self adjoint.The difference between the two domains may be most simply observed with the operator in the form of equation (2.3.1).

The domain of this operator is the set of functions satisfying the following criteria,[5]:

i) $\hat{n}(\underline{r},t)\times\underline{E}(\underline{r},t)=\underline{\underline{Z}}(\underline{r},t).\underline{H}(\underline{r},t)$ where $\underline{\underline{Z}}(\underline{r},t)$ is a known dyadic and $\hat{n}(\underline{r},t)$ is the normal to the enclosing surface.For an open structure,this surface may be regarded as being at infinity,in which case,this condition is replaced by the requirement that the fields are bounded at infinity,ie the radiation condition,[6].

ii) $\int dV\int dt\ \underline{E}(\underline{r},t).\underline{E}(\underline{r},t)+\underline{H}(\underline{r},t).\underline{H}(\underline{r},t)$ is finite,ie the domain consists of functions having a bounded norm.

iii) $\begin{pmatrix}\underline{J}(\underline{r},t)\\ \underline{0}\end{pmatrix}=\begin{pmatrix}\underline{E}(\underline{r},t)\\ \underline{H}(\underline{r},t)\end{pmatrix}=\begin{pmatrix}\underline{0}\\ \underline{0}\end{pmatrix}$ for $t<t_1$,ie the system is causal. (2.3.2)

It is simple to show that the adjoint operator to that of equation (2.3.1),is;

$$\begin{pmatrix}\partial t\underline{\underline{\varepsilon}}^{A}(\underline{r},t). & -\nabla\times\\ \nabla\times & \partial t\underline{\underline{\mu}}^{A}(\underline{r},t).\end{pmatrix}\begin{pmatrix}\underline{E}^{A}(\underline{r},t)\\ \underline{H}^{A}(\underline{r},t)\end{pmatrix}=\begin{pmatrix}\underline{J}(\underline{r},t)^{A}\\ \underline{0}\end{pmatrix} \qquad (2.3.3)$$

where $\underline{\underline{\varepsilon}}^{A}(\underline{r},t)$ and $\underline{\underline{\mu}}^{A}(\underline{r},t)$ are the adjoint permittivity and permeability dyadics.

The domain of the adjoint operator is the set of functions satisfying;

i) $\hat{n}(\underline{r},t)\times\underline{E}^{A}(\underline{r},t)=\underline{\underline{Z}}^{A}(\underline{r},t).\underline{H}^{A}(\underline{r},t)$

ii) $\int dV\int dt\underline{E}(\underline{r},t)^{A}.\underline{E}^{A}(\underline{r},t)+\underline{H}^{A}(\underline{r},t).\underline{H}^{A}(\underline{r},t)$ is finite.

iii) $\begin{pmatrix} J^A(\underline{r},t) \\ \underline{0} \end{pmatrix} = \begin{pmatrix} \underline{E}^A(\underline{r},t) \\ \underline{H}^A(\underline{r},t) \end{pmatrix} = \begin{pmatrix} \underline{0} \\ \underline{0} \end{pmatrix}$, for $t > t_2$.

It is observed that the imposition of causality constrains the domains of the operator and its adjoint to consist of outgoing and incoming waves respectively,[5].Consequently the two domains are mutually exclusive.Even though the operator and its adjoint shall be reformulated such that they are functionally identical,the operator is not self adjoint.

The structures under consideration shall be assumed to be time invariant and consist of a number of isotropic regions,each of which has a scalar permeability and permittivity,albeit different for each region.

For such structures the original operator equation may be reformulated to the wave equation;

$$[\nabla \times \nabla \times + \varepsilon\mu\partial^2 t\,] \begin{pmatrix} \underline{E}(\underline{r},t) \\ \underline{H}(\underline{r},t) \end{pmatrix} = \begin{pmatrix} -\mu\partial t \underline{J}(\underline{r},t) \\ \nabla \times \underline{J}(\underline{r},t) \end{pmatrix} \tag{2.3.4}$$

Unfortunately the source function for the magnetic field vector has become a little more complicated.However,it is clear that the system response is completely characterised by the electric field vector which,once determined,may be substituted into Maxwell's equations to give the magnetic field vector.Therefore the response of the system may be completely described by the solution to;

$$[\nabla \times \nabla \times + \varepsilon\mu\partial^2 t\,] \underline{E}(\underline{r},t) = -\mu\partial t \underline{J}(\underline{r},t) \tag{2.3.5}$$

It is this equation that shall be considered analogous to the operator equation

$$L\underline{\psi}(\underline{r}) = \underline{f}(\underline{r}) \tag{2.3.6}$$

and to which the theorems of the preceding sections shall be applied.

Section 2.4 shall demonstrate how the electric field characteristic Green's

function may be developed for structures that,in general,possess both a point spectrum and a continuous spectrum.In particular,the technique presented allows the complete spectrum of nonseparable open structures to be derived.

Section 2.5 shall use this spectrum to formulate the Green's function and hence the inverse operator to Maxwell's equations.

Finally section 2.6 shall consider a slight reformulation to allow inhomogeneous and lossy structures to be treated more succinctly.

2.4) The Electric field Characteristic Green's function.

The electric field characteristic Green's function is defined as the solution to;

$$(\nabla\times\nabla\times-\varepsilon\mu\partial^2 t-\lambda)\underline{\underline{G_E}}(\underline{r},\underline{r}',t,t';\lambda)=-\underline{\underline{I}}\,\delta(\underline{r}-\underline{r}')\delta(t-t') \tag{2.4.1}$$

It is immediately apparent,that the operator may be expressed as the sum of a time operator and a spatial operator.This is a consequence of the time invariance of the structure.Therefore the electric field characteristic Green's function and eigenfunctions may be written in the following,separable,form;

$$\underline{\underline{G_E}}(\underline{r},\underline{r}',t,t';\lambda)=\underline{\underline{G_E}}(\underline{r},\underline{r}';\lambda_\tau)G_E(t,t';\lambda_t)\quad:\quad\lambda=\lambda_\tau+\lambda_t \tag{2.4.2}$$

$$\underline{\Psi}(\underline{r},t;\lambda)\underline{\Psi}^A(\underline{r}',t';\lambda)=\underline{\psi}(\underline{r};\lambda_\tau)\underline{\psi}^A(\underline{r}';\lambda_\tau)T(t;\lambda_t)T^A(t';\lambda_t)$$

$$=\left(\frac{1}{2\pi j}\int_{C_\tau}d\lambda_\tau\,\underline{\underline{G_E}}(\underline{r},\underline{r}';\lambda_\tau)\right)\left(\frac{1}{2\pi j}\int_{C_t}d\lambda_t\,G_E(t,t';\lambda_t)\right) \tag{2.4.3}$$

Substitution of equation (2.4.2) into equation (2.4.1),identifies the time and spatial characteristic Green's functions as the solutions to;

$$(\nabla\times\nabla\times-\lambda_\tau)\underline{\underline{G_E}}(\underline{r},\underline{r}';\lambda_\tau)=-\underline{\underline{I}}\,\delta(\underline{r}-\underline{r}')$$

$$(\varepsilon\mu\partial^2 t + \lambda_t)G_E(t,t',\lambda_t) = \delta(t-t') \tag{2.4.4}$$

These two equations may now be analysed independently for the dyadic spatial and the scalar time,characteristic Green's functions,which then may be substituted into equation (2.4.3) to give the complete electric field eigenfunctions.

2.4.1) The Time Characteristic Green's function.

Consider the possibility that the scalar time characteristic Green's function,$G_E(t,t';\lambda_t)$,may be written in the form;

$$G_E(t,t';\lambda_t) = \frac{e^{j\omega|t-t'|}}{\gamma(\lambda_t)} \quad : \quad \omega^2\varepsilon\mu = k^2 = +\lambda_t \tag{2.4.5}$$

where it is noted that causality requires that Im [ω] > 0.

This form is suggested as the functions $e^{\pm j\omega t}$ are known to be solutions to the homogeneous equation;

$$(\varepsilon\mu\partial^2 t + \lambda_t)T(t;\lambda_t) = 0 \tag{2.4.6}$$

and,in addition,the second derivative w.r.t. time of $e^{j\omega|t-t'|}$ results in a dirac delta function at t=t'.

In order to ensure that this singularity is of the correct strength,the expression for $G_E(t,t';\lambda_t)$,given in equation (2.4.5),is substituted into equation (2.4.4) which is then integrated w.r.t. time,ie;

$$\left[\varepsilon\mu\partial t\frac{e^{j\omega|t-t'|}}{\gamma(\lambda_t)}\right]_{t=t'-0}^{t=t'+0} = 1 \quad : \quad \rightarrow \gamma(\lambda_t) = 2j\omega\varepsilon\mu \tag{2.4.7}$$

and hence;

$$G_E(t,t;\lambda_t) = \frac{e^{j\omega|t-t'|}}{2j\omega\varepsilon\mu} \tag{2.4.8}$$

As discussed in section 2.2,the integration of $G_E(t,t';\lambda_t)$ around a closed

contour in the complex λ_t plane,permits the time eigenfunctions,$T(t;\lambda_t)$,to be identified,in this case by inspection.$G_E(t,t';\lambda_t)$ is a multivalued function of λ_t and therefore it is necessary to introduce a branch cut along the negative real axis of the λ_t plane.This branch cut defines the boundary between the proper and improper Riemann sheets.Upon the former the fields are bounded with time,whereas upon the latter they increase exponentially with time.

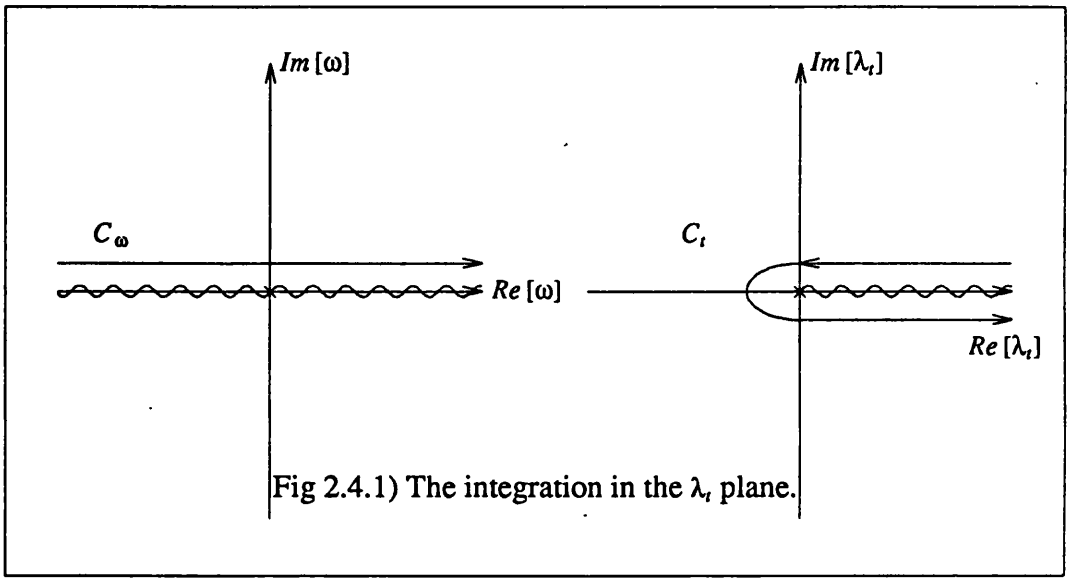

Fig 2.4.1) The integration in the λ_t plane.

As the only singularities of $G_E(t,t';\lambda_t)$ are the branch points,the integration in the complex λ_t plane may be evaluated as;

$$\frac{1}{2\pi j}\int_{C_t} d\lambda_t\, G_E(t,t';\lambda_t) = \frac{1}{2\pi j}\int_{-\infty}^{\infty} d\omega(-2)\omega\varepsilon\mu\frac{e^{j\omega|t-t'|}}{2j\varepsilon\mu\omega} = \int_{-\infty}^{\infty} d\omega\frac{e^{j\omega|t-t'|}}{2\pi}$$

$$= \int_{-\infty}^{\infty} d\omega T(t;\lambda_t)T^{A}(t';\lambda_t) \qquad (2.4.9)$$

recovering the familiar fourier integral functions;

$$T(t;\lambda_t)=\frac{e^{j\omega t}}{\sqrt{2\pi}} \quad : \quad T^A(t;\lambda_t)=\frac{e^{-j\omega t}}{\sqrt{2\pi}} \quad : t > t'$$

$$T(t;\lambda_t)=\frac{e^{-j\omega t}}{\sqrt{2\pi}} \quad : \quad T^A(t;\lambda_t)=\frac{e^{j\omega t}}{\sqrt{2\pi}} \quad : t < t' \qquad (2.4.10)$$

The method used to construct the time characteristic Green's function relied upon the identification of its functional form by inspection.For the spatial characteristic Green's function,this is clearly not possible and a more formal approach must be adopted.

2.4.2) The Spatial Characteristic Green's function.

The previous section relied upon the separation of variables to isolate a one dimensional characteristic Green's function,which could then be solved in a relatively simple manner.This process has reduced the problem to that of determining the spatial characteristic Green's function defined by;

$$(\nabla\times\nabla\times-\lambda_\tau)\underline{\underline{G}}_E(\underline{r},\underline{r}';\lambda_\tau)=-\underline{\underline{I}}\,\delta(\underline{r}-\underline{r}') \qquad (2.4.11)$$

Unfortunately,at this stage the previous process falters.If the structure is nonseparable in the transverse plane,then neither the transverse characteristic Green's function,nor the transverse eigenfunctions,may be written in a separable form.Clearly an alternative,more general,approach is required.

As discussed in section 2.2,the spectrum of the operator $\nabla\times\nabla\times$ comprises,in general,of a discrete spectrum and a continuous spectrum.The spectrum of a closed structure is purely discrete,whereas that of an open structure may be purely continuous,as in the case of a solid conducting bar,or contain both a discrete and a continuous spectrum,for example the case of microstrip.

Transverse resonance has been applied to both open and closed,separable and nonseparable structures,yielding their discrete spectra,[5,7,8,9].However,a rigorous derivation of the continuous spectrum of nonseparable open structures has not,to date,been achieved.

After a brief review of the transverse resonance method,a rigorous,generalised method shall be presented that permits the complete mode spectrum of a nonseparable open structure to be determined.

2.4.3) The Transverse Resonance Method.

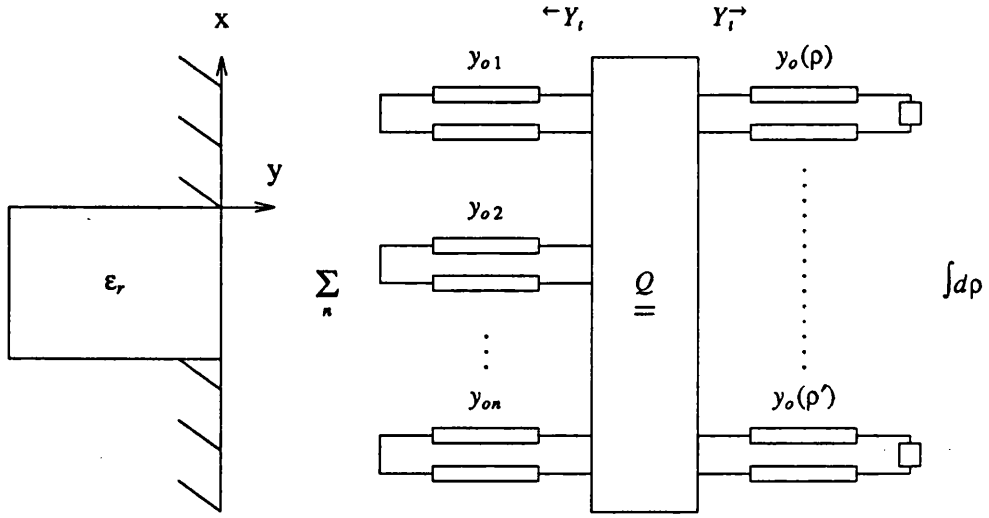

Fig 2.4.2) The Transverse Equivalent Network of the I.D.G.

The transverse resonance method approaches the solution of the eigenvalue equation;

$$(\nabla \times \nabla \times - \lambda_r)\underline{\psi}(\underline{r};\lambda_r) = \underline{0} \quad : \quad \nabla \cdot \underline{\psi}(r;\lambda_r) = 0 \quad \rightarrow \quad (\nabla^2 + \lambda_r)\underline{\psi}(r;\lambda_r) = 0 \qquad (2.4.12)$$

directly,by considering the transverse equivalent network of the structure.

For example,consider the Inset Dielectric Guide and its transverse equivalent network shown in figure (2.4.2).Each separable region may be modelled as a superposition of transmission lines,discrete in the bounded region,continuous in the open region.Q is the admittance transformer associated with the,possibly nonseparable,interface.

For cylindrical structures such as waveguides,it is possible to separate the dependence of the eigenfunctions upon z and $\underline{r}_t$ and write them in the form;

$$(\nabla_t^2 + \lambda_{r_t})\underline{\phi}(\underline{r}_t;\lambda_{r_t}) = \underline{0} \quad : \nabla_t^2 = \partial^2 x + \partial^2 y$$

$$(\partial^2 z + \lambda_z)Z(z;\lambda_z) = \underline{0}$$

$$\underline{\psi}(\underline{r};\lambda_r) = \underline{\phi}(\underline{r}_t;\lambda_{r_t})Z(z;\lambda_z) \quad : \quad \lambda_r = \lambda_{r_t} + \lambda_z \tag{2.4.13}$$

A scalar characteristic Green's function,$G_E(z,z';\lambda_z)$,developed in an analogous manner to that of $G_E(t,t';\lambda_t)$ above,may be shown to be;

$$G_E(z,z';\lambda_z) = \frac{e^{j\beta|z-z'|}}{2j\beta} \quad : \quad \lambda_z = \beta^2 \, , \, Im[\beta] < 0$$

from which it follows that;

$$Z(z;\lambda_z) = \frac{e^{-j\beta z}}{\sqrt{2\pi}} \quad : \quad Z^A(z;\lambda_z) = \frac{e^{j\beta z}}{\sqrt{2\pi}} \quad : z > z'$$

$$Z(z;\lambda_z) = \frac{e^{j\beta z}}{\sqrt{2\pi}} \quad : \quad Z^A(z;\lambda_z) = \frac{e^{-j\beta z}}{\sqrt{2\pi}} \quad : z < z' \tag{2.4.14}$$

recalling that causality requires that the fields consist of outgoing,and the adjoint fields of incoming waves.

To determine the transverse eigenfunctions,$\underline{\phi}(\underline{r}_t;\lambda_{r_t})$,the following argument

is employed.

For finite voltages and currents to exist on the transmission lines in the absence of any sources,the transverse admittance seen at any point, $^{\leftarrow}Y_t + Y_t^{\rightarrow}$,must be identically zero.The expression for the transverse admittance for a given structure is a function of the parameter λ_{r_t} and for certain values,the eigenvalues,vanishes.

These discrete values of λ_{r_t} constitute the point spectrum of the operator ∇_t^2 and physically correspond to the bound,or surface,modes of the structure.Whilst for nonseparable structures the discrete eigenvalues and the functional form of the bound modes are recovered,ensuring the correct normalisation still requires the direct integration of the eigenfunctions over the guide cross-section,which may not be that straightforward.

However,transverse resonance cannot recover the continuous spectrum of a guide.This may may be illustrated by considering the transverse network of the lossless Inset Dielectric Guide.The admittance presented by the open region to a mode of the continuous spectrum has both real and imaginary parts,whereas that presented by the slot is purely imaginary.Consequently the total transverse admittance seen by a continuous eigenfunction is always nonzero and hence not identified by transverse resonance.

It shall now be demonstrated how the correctly normalised complete spectrum of both closed and open nonseparable structures may be rigorously derived.

2.4.4) The Spatial Characteristic Green's function for open nonseparable Structures.

The spatial characteristic Green's function may be decomposed into solenoidal and lamellar components,$\underline{\underline{G}}_E^S(\underline{r},\underline{r}';\lambda_r)$ and $\underline{\underline{G}}_E^L(\underline{r},\underline{r}';\lambda_r)$.It is apparent,from

equation (2.4.4),that these components are defined by;

$$(\nabla^2 + \lambda_\tau)\underline{\underline{G}}_E^s(\underline{r},\underline{r}';\lambda_\tau) = \left[\underline{\underline{I}}\delta(\underline{r}-\underline{r}')\right]^s \quad : \quad \nabla . \underline{\underline{G}}_E^s(\underline{r},\underline{r}';\lambda_\tau) = 0 \quad : \quad \nabla' . \underline{\underline{G}}_E^s(\underline{r},\underline{r}';\lambda_\tau) = 0 \qquad (2.4.15)$$

$$\underline{\underline{G}}_E^l(\underline{r},\underline{r}';\lambda_\tau) = \left[\frac{\underline{\underline{I}}\delta(\underline{r}-\underline{r}')}{\lambda_\tau}\right]^l \quad : \quad \nabla \times \underline{\underline{G}}_E^l(\underline{r},\underline{r}';\lambda_\tau) = \underline{0}: \quad \nabla' \times \underline{\underline{G}}_E^l(\underline{r},\underline{r}';\lambda_\tau) = \underline{0} \qquad (2.4.16)$$

The source functions are,respectively,the solenoidal and lamellar components of the dyadic delta function.

$$\nabla . \left[\underline{\underline{I}}\delta(\underline{r}-\underline{r}')\right]^s = 0 \quad : \quad \nabla \times \left[\underline{\underline{I}}\delta(\underline{r}-\underline{r}')\right]^l = \underline{0}$$

$$\nabla' . \left[\underline{\underline{I}}\delta(\underline{r}-\underline{r}')\right]^s = 0 \quad : \quad \nabla' \times \left[\underline{\underline{I}}\delta(\underline{r}-\underline{r}')\right]^l = \underline{0} \qquad (2.4.17)$$

Clearly $\underline{\underline{G}}_E^l(\underline{r},\underline{r}';\lambda_\tau)$ is analytic at all points of the λ_τ plane except the origin and shall be left in this form for the moment.

Direct solution for the solenoidal part,$\underline{\underline{G}}_E^s(\underline{r},\underline{r};\lambda_\tau)$,is complicated by the source function,$\left[\underline{\underline{I}}\delta(\underline{r}-\underline{r}')\right]^s$,that appears in equation (2.4.11) and therefore it is more convenient to adopt an indirect approach.

The solenoidal electric field eigenfunctions,both proper and improper,are defined by;

$$(\nabla^2 + \lambda_\tau)\underline{E}^s(\underline{r};\lambda_\tau) = \underline{0} \quad : \quad \nabla . \underline{E}^s(\underline{r};\lambda_\tau) = 0 \qquad (2.4.18)$$

In general there exists a two component magnetic vector potential satisfying;

$$(\nabla^2 + \lambda_\tau)\underline{A}(\underline{r};\lambda_\tau) = \underline{0} \qquad (2.4.19)$$

such that the three component electric field vector,derived from it,satisfies equation (2.4.18).In fact,which two components A consists of is arbitrary and may be chosen as appropriate to the particular structure under consideration.The price of involving only two components is that the magnetic vector potential will contain both a lamellar and solenoidal part.Under the Lorentz guage,the electric

and magnetic fields may be derived as,[7];

$$\partial t\underline{E}(\underline{r},t) = \left(-\partial^2 t + \frac{\nabla\nabla.}{\varepsilon\mu}\right)\underline{A}(\underline{r},t) \tag{2.4.20}$$

$$\mu\underline{H}(\underline{r},t) = \nabla \times \underline{A}(\underline{r},t) \tag{2.4.21}$$

the former of which,given the $e^{j\omega t}$ time dependence of the eigenfunctions determined above,may be written as;

$$\underline{E}(\underline{r};\omega) = -j\omega\left(\underline{\underline{I}}. + \frac{\nabla\nabla.}{k^2(\underline{r}_t)}\right)\underline{A}(\underline{r};\omega) \tag{2.4.22}$$

The equivalent inhomogeneous equations to those of (2.4.18) and (2.4.19) are;

$$(\nabla^2 + \lambda_\tau)\underline{E}^s(\underline{r};\lambda_\tau) = \underline{f}_E^{\tau}(\underline{r}) \quad : \quad \nabla . \underline{E}^s(\underline{r};\lambda_\tau) = 0 \quad : \quad \nabla . \underline{f}_E^{\tau}(\underline{r};\lambda_\tau) = 0 \tag{2.4.23}$$

$$(\nabla^2 + \lambda_\tau)\underline{A}(\underline{r};\lambda_\tau) = \underline{f}_A(\underline{r}) \tag{2.4.24}$$

with $\underline{E}^s(\underline{r};\lambda_\tau)$ and $\underline{A}(\underline{r};\lambda_\tau)$ related through (2.4.22).

Clearly the three component source,$\underline{f}_E^{\tau}(\underline{r})$,and the two component source,$\underline{f}_A(\underline{r})$,are also related,although in order to derive this relationship,it is necessary to make an observation concerning the adjoint fields.The solenoidal electric field and magnetic vector potential eigenfunctions are separable w.r.t. z and $\underline{r}_t$,their z-dependence being given by the functions in (2.4.14).It is important to realise that,if the z-dependence of a field is $e^{-j\beta z}$,then that of its adjoint is $e^{+j\beta z}$ and not $e^{(-j\beta z)^*}$.Although for real β this distinction is superfluous,at a later stage β will become complex and then it will be necessary.In addition,as the complex type inner product is appropriate for the transverse eigenfunctions,it is known that the eigenvalues of the adjoint problem are the conjugates of those of the original problem.Therefore the transverse eigenfunctions and their adjoints are defined as

solutions to;

$$(\nabla_t^2 + \lambda_{\tau_t})\underline{E}^s(\underline{r}_t;\lambda_{\tau_t}) = \underline{0} \;:\; (\nabla_t^2 + \lambda_{\tau_t}^*)[\underline{E}^s(\underline{r}_t;\lambda_{\tau_t}^*)]^A = \underline{0} \tag{2.4.25}$$

Conjugating the first of these equations and comparing with the second,reveals that $[\underline{E}^s(\underline{r}_t;\lambda_{\tau_t}^*)]^A = [R\underline{E}^s(\underline{r}_t;\lambda_{\tau_t})]^*$,where $R = (\underline{\underline{I}}_t - \hat{z}\hat{z})$.The reflection operator,R,is included to ensure that the adjoint eigenfunctions are solenoidal.Physically,this is consistent with the outgoing and incoming wave nature of the eigenfunctions and their adjoints.Having now related the fields and their adjoints,it is possible to relate $f_{\underline{E}}^s(\underline{r})$ and $f_{\underline{A}}(\underline{r})$.

If the inner products of equations (2.4.23) and (2.4.24) are formed respectively with $\underline{A}^A(\underline{r};\lambda_\tau)$ and $[\underline{E}^S(\underline{r};\lambda_\tau)]^A$,we get;

$$<\underline{A}^A(\underline{r};\lambda_\tau),(\nabla^2 + \lambda_\tau)\underline{E}^s(\underline{r};\lambda_\tau)> - <[\underline{E}^s(\underline{r};\lambda_\tau)]^A,(\nabla^2 + \lambda_\tau)\underline{A}(\underline{r};\lambda_\tau)>$$

$$= <\underline{A}^A(\underline{r};\lambda_\tau),f_{\underline{E}}^s(\underline{r})> - <[\underline{E}^s(\underline{r};\lambda_\tau)]^A,f_{\underline{A}}(\underline{r})> \tag{2.4.26}$$

Using Green's theorem,the complex definition of the inner product,$<\underline{a}(\underline{r}),\underline{b}(\underline{r})> = \iiint dV\, \underline{a}^*(\underline{r}).\underline{b}(\underline{r})$ and the result of the preceding discussion,it may be shown that the left side of (2.4.26) is zero and hence

$$<\underline{A}^A(\underline{r};\lambda_\tau),f_{\underline{E}}^s(\underline{r})> = <[\underline{E}^s(\underline{r};\lambda_\tau)]^A,f_{\underline{A}}(\underline{r})> \tag{2.4.27}$$

Armed with this result the following approach may now be pursued.A characteristic Green's function for the magnetic vector potential is defined by;

$$(\nabla^2 + \lambda_\tau)\underline{\underline{G}}_{\underline{A}}(\underline{r},\underline{r}';\lambda_\tau) = \hat{p}\hat{p}\,\delta(\underline{r}-\underline{r}') \tag{2.4.28}$$

where $\hat{p}$ specifies an arbitrary plane.This permits the magnetic vector potential,excited by an arbitrary source tangential to the plane $\hat{p}$,to be identified.A restricted set of such sources will result in the excitation of a solenoidal electric field.The magnetic vector potential from which this electric field may be

derived,may then be directly related to the solenoidal electric field source,$\underline{f}_E^s(\underline{r})$,by using equation (2.4.27).Finally,applying equation (2.4.22),term by term,relates the excited solenoidal electric field to $\underline{f}_E^s(\underline{r})$, and permits the solenoidal electric transverse characteristic Green's function to be determined.

Consider,initially,a structure consisting of two homogeneous separable regions having a common nonseparable interface in the x-z plane,as illustrated by the Inset Dielectric Guide in figure (2.4.2).In this case it is appropriate to consider the dyadic $\hat{p}\hat{p}$ as $\hat{x}\hat{x} + \hat{z}\hat{z}$.

The problem may be viewed as a discontinuity analysis between the two separable regions,with a current lying in the x-z plane.

As before,the time and the z-dependence of the magnetic vector potential eigenfunctions may be determined by the separation of variables,leaving the following equation defining the magnetic vector potential transverse characteristic Green's function;

$$(\nabla_t^2 + \lambda_{r_t})\underline{\underline{G}}_A(\underline{r}_t,\underline{r}_t';\lambda_{r_t}) = -(\hat{x}\hat{x} + \hat{z}\hat{z})\delta(\underline{r}_t-\underline{r}_t') \tag{2.4.29}$$

Consider expressing $\underline{\underline{G}}_A(\underline{r}_t,\underline{r}_t';\lambda_{r_t})$ in the form;

$$\underline{\underline{G}}_A(\underline{r}_t,\underline{r}_t';\lambda_{r_t}) = \sum_v \frac{\underline{\underline{A}}_v^+(\underline{r}_t;\lambda_{r_t})[\underline{\underline{E}}_v^-(\underline{r}_t';\lambda_{r_t})]^A}{\gamma_v(\lambda_{r_t})} \quad : \quad y \geq 0$$

$$\underline{\underline{G}}_A(\underline{r}_t,\underline{r}_t';\lambda_{r_t}) = \sum_v \frac{\underline{\underline{A}}_v^-(\underline{r}_t;\lambda_{r_t})[\underline{\underline{E}}_v^+(\underline{r}_t';\lambda_{r_t})]^A}{\gamma_v(\lambda_{r_t})} \quad : \quad y \leq 0 \tag{2.4.30}$$

where the two component vectors,$\underline{A}_v^+(\underline{r}_t;\lambda_{r_t})$,$\underline{A}_v^-(\underline{r}_t;\lambda_{r_t})$,$\underline{E}_v^+(\underline{r}_t;\lambda_{r_t})$ and $\underline{E}_v^-(\underline{r}_t;\lambda_{r_t})$,satisfy the homogeneous Helmholtz equation in the regions above and below the nonseparable interface,ie;

$$(\nabla_t^2 + \lambda_{r_t})\underline{E}_v^+(\underline{r}_t;\lambda_{r_t}) = 0 \quad :y > 0 \quad :(\nabla_t^2 + \lambda_{r_t})\underline{E}_v^-(\underline{r}_t;\lambda_{r_t}) = 0 \quad :y < 0$$

$$\underline{E}_v^{\pm}(\underline{r}_t;\lambda_{r_t}) = \hat{x}E_{vx}^{\pm}(\underline{r}_t;\lambda_{r_t}) + \hat{z}E_{vz}^{\pm}(\underline{r}_t;\lambda_{r_t})$$

$$(\nabla_t^2 + \lambda_{r_t})\underline{A}_v^+(\underline{r}_t;\lambda_{r_t}) = 0 \quad :y > 0 \quad : \quad (\nabla_t^2 + \lambda_{r_t})\underline{A}_v^-(\underline{r}_t;\lambda_{r_t}) = 0 \quad :y < 0 \qquad (2.4.31)$$

Similar relationships are satisfied by the adjoint quantities.

The electric field vector has been used with a view to substituting equation (2.4.27) at a later stage and also removes the magnetic vector potential from the final expression for the electric transverse characteristic Green's function.

To ensure the continuity of $\underline{\underline{G}}_A(\underline{r}_t,\underline{r}_t';\lambda_{r_t})$,it is necessary to set;

$$\underline{A}_v^+(x,0;\lambda_{r_t}) = \underline{A}_v^-(x,0;\lambda_{r_t}) \quad ; \quad \underline{E}_v^+(x,0;\lambda_{r_t}) = \underline{E}_v^-(x,0;\lambda_{r_t}) \qquad (2.4.32)$$

It is clear,that if the expression for $\underline{\underline{G}}_A(\underline{r}_t,\underline{r}_t';\lambda_{r_t})$ is substituted into equation (2.4.30),then the discontinuity in the derivative w.r.t. y at y=y',results in a singularity of the form $\underline{\underline{F}}(x,x')\delta(y-y')$.

The function $\underline{\underline{F}}(x,x')$ may be found by integrating equation (2.4.29) w.r.t. y,ie;

$$\int_{-\infty}^{\infty} dy\ (\nabla_t^2 + \lambda_{r_t})\underline{\underline{G}}_A(\underline{r}_t,\underline{r}_t';\lambda_{r_t}) =$$

$$\sum_v \left[\frac{\partial y \underline{A}_v^+(\underline{r}_t;\lambda_{r_t})\left[\underline{E}_v^-(\underline{r}_t';\lambda_{r_t})\right]^A}{\gamma_v(\lambda_{r_t})} - \frac{\partial y \underline{A}_v^-(\underline{r}_t;\lambda_{r_t})\left[\underline{E}_v^+(\underline{r}_t';\lambda_{r_t})\right]^A}{\gamma_v(\lambda_{r_t})} - \right]_{y=y'} = -(\hat{x}\hat{x} + \hat{z}\hat{z})\delta(x-x') \quad (2.4.33)$$

As the magnetic vector potential does not contain a y-directed component,its derivative w.r.t. y is simply;

$$\partial y \underline{A}_v^{\pm}(\underline{r}_t;\lambda_{r_t}) = \mu \underline{H}_v^{\pm}(\underline{r}_t;\lambda_{r_t}) \times \hat{y} \qquad (2.4.34)$$

and hence equation (2.4.33) may be written as;

$$\mu\sum_{\nu}\left[\frac{\underline{E}^{A}_{\nu}(\underline{r}_t';\lambda_{\tau_t})\,\underline{H}_{\nu}(\underline{r}_t;\lambda_{\tau_t})\times\hat{y}}{\gamma_{\nu}(\lambda_{\tau_t})}\right]_{y=y'-0}^{y=y'+0}=-(\hat{x}\hat{x}+\hat{z}\hat{z})\delta(x-x') \tag{2.4.35}$$

It is important to observe,that this is not an identity,rather the condition that must be satisfied if it is possible to express $\underline{\underline{G}}_A(\underline{r}_t,\underline{r}_t';\lambda_{\tau_t})$ in the form of equation (2.4.30).This condition will indeed be satisfied if $\mu\left[\underline{H}_{\nu}(\underline{r}_t,\lambda_{\tau_t})\times\hat{y}\right]_{y=y'-0}^{y=y'+0}$ forms a complete,linearly independent,basis that spans the interface,with $\underline{E}^{A}_{\nu}(x,y',\lambda_{\tau_t})$ as the adjoint basis.Recalling that $\underline{E}^{A}_{\nu}(\underline{r}_t;\lambda_{\tau_t})=(R\underline{E}_{\nu}(\underline{r}_t;\lambda_{\tau_t}))^{*}$,allows this requirement to be written as the orthogonality condition;

$$\mu\int_{-\infty}^{\infty}dx\left[\frac{R\underline{E}_{\mu}(\underline{r}_t;\lambda_{\tau_t})\,.\,\underline{H}_{\nu}(\underline{r}_t;\lambda_{\tau_t})\times\hat{y}}{\gamma_{\nu}(\lambda_{\tau_t})}\right]_{y=y'-0}^{y=y'+0}=-\delta_{\nu\mu} \tag{2.4.36}$$

or as;

$$\mu\int_{-\infty}^{\infty}dx\left[\frac{R\underline{E}_{\mu}(\underline{r}_t;\lambda_{\tau_t})\times\underline{H}_{\nu}(\underline{r}_t;\lambda_{\tau_t})\,.\,\hat{y}}{\gamma_{\nu}(\lambda_{\tau_t})}\right]_{y=y'-0}^{y=y'+0}=-\delta_{\nu\mu} \tag{2.4.37}$$

Using the solutions to this equation,the magnetic vector potential characteristic Green's function is given by;

$$\underline{\underline{G}}_A(\underline{r}_t,\underline{r}_t';\lambda_{\tau_t})=\sum_{\nu}\frac{\underline{A}^{+}_{\nu}(\underline{r}_t;\lambda_{\tau_t})[\underline{E}^{-}_{\nu}(\underline{r}_t';\lambda_{\tau_t})]^{A}}{-\mu\int_{-\infty}^{\infty}dx\left[R\underline{E}_{\nu}(\underline{r}_t;\lambda_{\tau_t})\times\underline{H}_{\nu}(\underline{r}_t;\lambda_{\tau_t}).\hat{y}\right]_{y=0^{-}}^{y=0^{+}}}\quad :y\geq 0$$

$$\underline{\underline{G}}_A(\underline{r}_t,\underline{r}_t';\lambda_{\tau_t})=\sum_{\nu}\frac{\underline{A}^{-}_{\nu}(\underline{r}_t;\lambda_{\tau_t})[\underline{E}^{+}_{\nu}(\underline{r}_t';\lambda_{\tau_t})]^{A}}{-\mu\int_{-\infty}^{\infty}dx\left[R\underline{E}_{\nu}(\underline{r}_t;\lambda_{\tau_t})\times\underline{H}_{\nu}(\underline{r}_t;\lambda_{\tau_t}).\hat{y}\right]_{y=0^{-}}^{y=0^{+}}}\quad :y\leq 0 \tag{2.4.38}$$

The magnetic vector potential characteristic Green's function that acts on $\underline{f}^{s}_{E}(\underline{r})$ to give $\underline{A}(\underline{r})$,such that the electric field derived from it is solenoidal,may be found by

substituting equation (2.4.27);

$$\underline{\underline{G}}_A(\underline{r}_t,\underline{r}_t';\lambda_{r_t}) = \sum_{\nu} \frac{\underline{A}_\nu^+(\underline{r}_t;\lambda_{r_t})[\underline{A}_\nu^-(\underline{r}_t';\lambda_{r_t})]^A}{-\mu \int_{-\infty}^{\infty} dx \left[\underline{RE}_\nu(\underline{r}_t;\lambda_{r_t}) \times \underline{H}(\underline{r}_t;\lambda_{r_t}).\hat{y}\right]_{y=0^-}^{y=0^+}} \quad :y \geq 0$$

$$\underline{\underline{G}}_A(\underline{r}_t,\underline{r}_t';\lambda_{r_t}) = \sum_{\nu} \frac{\underline{A}_\nu^-(\underline{r}_t;\lambda_{r_t})[\underline{A}_\nu^+(\underline{r}_t';\lambda_{r_t})]^A}{-\mu \int_{-\infty}^{\infty} dx \left[\underline{RE}_\nu(\underline{r}_t;\lambda_{r_t})) \times \underline{H}_\nu(\underline{r}_t;\lambda_{r_t}).\hat{y}\right]_{y=0^-}^{y=0^+}} \quad :y \leq 0 \qquad (2.4.39)$$

The solenoidal electric field characteristic Green's function may now be found by simply replacing the terms $\underline{A}_\nu^\pm(\underline{r}_t;\lambda_{r_t})$ by $\underline{E}_\nu^\pm(\underline{r}_t;\lambda_{r_t})$;

$$\underline{\underline{G}}_E^s(\underline{r}_t,\underline{r}_t';\lambda_{r_t}) = \sum_{\nu} \frac{\underline{E}_\nu^+(\underline{r}_t;\lambda_{r_t})[\underline{A}_\nu^-(\underline{r}_t';\lambda_{r_t})]^A}{-\mu \int_{-\infty}^{\infty} dx \left[\underline{RE}_\nu(\underline{r}_t;\lambda_{r_t}) \times \underline{H}_\nu(\underline{r}_t;\lambda_{r_t}).\hat{y}\right]_{y=0^-}^{y=0^+}} \quad :y \geq 0$$

$$\underline{\underline{G}}_E^s(\underline{r}_t,\underline{r}_t';\lambda_{r_t}) = \sum_{\nu} \frac{\underline{E}_\nu^-(\underline{r}_t;\lambda_{r_t})[\underline{A}_\nu^+(\underline{r}_t';\lambda_{r_t})]^A}{-\mu \int_{-\infty}^{\infty} dx \left[\underline{RE}_\nu(\underline{r}_t;\lambda_{r_t}) \times \underline{H}_\nu(\underline{r}_t;\lambda_{r_t}).\hat{y}\right]_{y=0^-}^{y=0^+}} \quad :y \leq 0 \qquad (2.4.40)$$

Finally it is recalled that the characteristic Green's function,as defined in section 2.2,must act on the total source rather than its predetermined solenoidal or lamellar constituents,ie the source to $\underline{\underline{G}}_E^s(\underline{r}_t;\underline{r}_t';\lambda_{r_t})$,defined in (2.4.15),is $\underline{f}_E(\underline{r})$ not $\underline{f}_E^s(\underline{r})$.This modification may be made by substituting $-j\omega\underline{A}(\underline{r}_t;\lambda_{r_t}) = \underline{E}^S(\underline{r}_t;\lambda_{r_t}) + \frac{j\omega}{k^2}\nabla\nabla\underline{A}(\underline{r}_t;\lambda_{r_t})$ and recognising that,$< (\underline{E}^S(\underline{r}_t;\lambda_{r_t}) + \frac{j\omega}{k^2}\nabla\nabla\underline{A}(\underline{r}_t;\lambda_{r_t})) , \underline{f}_E^s(\underline{r}_t) >$ $= < \underline{E}^s(\underline{r}_t;\lambda_{r_t}),\underline{f}_E^s(\underline{r}_t) > = < \underline{E}^s(\underline{r},\lambda_{r_t}),\underline{f}_E(\underline{r}_t)$.Thus the required transverse characteristic Green's function is given by;

$$\underline{\underline{G}}_E^s(\underline{r}_t,\underline{r}_t';\lambda_{r_t}) = \sum_{\nu} \frac{\underline{E}_\nu^+(\underline{r}_t;\lambda_{r_t})[\underline{E}_\nu^-(\underline{r}_t';\lambda_{r_t})]^A}{-j\omega\mu \int_{-\infty}^{\infty} dx \left[\underline{RE}_\nu(\underline{r}_t;\lambda_{r_t}) \times \underline{H}_\nu(\underline{r}_t;\lambda_{r_t}).\hat{y}\right]_{y=0^-}^{y=0^+}} \quad :y \geq 0$$

$$\underline{\underline{G}}^{s}_{E}(\underline{r}_t,\underline{r}_t';\lambda_{r_t}) = \sum_{\nu} \frac{\underline{E}^{-}_{\nu}(\underline{r}_t;\lambda_{r_t})[\underline{E}^{+}_{\nu}(\underline{r}_t';\lambda_{r_t})]^{A}}{-j\omega\mu\int_{-\infty}^{\infty} dx \left[\underline{RE}_{\nu}(\underline{r}_t;\lambda_{r_t}) \times \underline{H}_{\nu}(\underline{r}_t;\lambda_{r_t}).\hat{y}\right]_{y=0^-}^{y=0^+}} \quad :y \le 0 \qquad (2.4.41)$$

Noting that an additional '-' sign is introduced due to the change of sign of the source for the solenoidal part the electric characteristic Green's function compared to that of the magnetic vector potential.

Now that the solenoidal part of the electric field characteristic Green's function has been determined,there are two further aspects that must be considered before the eigenfunctions may be identified.The next section shall detail the process by which the vectors $\underline{E}^{\pm}_{\nu}(\underline{r}_t;\lambda_{r_t})$,satisfying the orthogonality condition of equation (2.4.37),may be found.The following section shall discuss the contour integration of the characteristic Green's function in the complex λ_{r_t} plane that allows the eigenfunctions to be explicitly identified.

2.4.5) Formulation of the Transverse Eigenvalue Equation.

The transverse characteristic Green's function has been constructed from a complete set of linearly independent electric field vectors,$\underline{E}_{\nu}(\underline{r}_t;\lambda_{r_t})$,defined by the biorthogonality relationship;

$$\int_{-\infty}^{\infty} dx \left[\frac{\underline{RE}_{\mu}(\underline{r}_t;\lambda_{r_t}) \times \underline{H}_{\nu}(\underline{r}_t;\lambda_{r_t}) \,.\, \hat{y}}{\gamma_{\nu}(\lambda_{r_t})}\right]_{y=y'-0}^{y=y'+0} = -\delta_{\nu\mu} \qquad (2.4.42)$$

This section shall discuss the general approach used to determine these vectors.

It is helpful to attribute a physical interpretation to the quantity $\left[\underline{RE}_{\mu}(\underline{r}_t;\lambda_{r_t}) \times \underline{H}_{\nu}(\underline{r}_t;\lambda_{r_t})\right]_{y=y'-0}^{y=y'+0}$.

Obviously,this term has the dimesions of power,although it is incorrect to interpret it as the net power leaving the interface,due to the presence of the reflection operator,R.Rather,this quantity may be regarded as term from a reciprocity relationship between the fields and their adjoints.

This expression appears in the denominator of the characteristic Green's function,implying that,if $\underline{H}_v(\underline{r}_t;\lambda_{r_t})\times\hat{y}$ is continuous across the interface,then the transverse characteristic Green's function is singular.As,in this case,the source has been interpreted as a current tangential to the interface,this will only occur if the source is identically zero.Of course the existence of continuous,non trivial,fields in the absence of a source is indicative of a discrete eigenfunction,confirming the premise that the singularities of the transverse characteristic Green's function occur at the discrete eigenvalues.

The continuous eigenfunctions require a source to sustain their existence,although this source is considered to be at an infinite distance from the interface.It shall be shown in the following section,that the continuous eigenfunctions are constructed from two terms,each of which either sources or sinks power at the interface.These two terms are $\underline{\underline{G}}_E(\underline{r}_t,\underline{r}_t';\lambda_{r_t})$ evaluated on opposite sides of a branch cut.Each term has the same transverse electric field at the interface,although in the open region,one is constructed from incoming waves and the other from outgoing waves.When combined in the appropriate manner,the net source required at the interface is zero,resulting in a standing wave representation in the open region.

Physically,the continuous eigenfunctions may be regarded as the result of a scattering process.A source at an infinite distance from the interface,excites a packet of waves propagating toward the interface.These are scattered and result in both standing waves and exponentially decaying terms in the open region.It is

probable,that in the future an alternative method of deriving the continuous eigenfunctions of nonseparable structures may be based upon this interpretation,as this has already achieved for separable ones,[3].

At this point,it is apparent that the transverse resonance method is a particular case of this more general formulation.Recalling that transverse resonance seeks the values of λ_{r_t} for which the transverse admittance vanishes,it is observed that this is equivalent to requiring continuity of $\underline{H}_v(\underline{r}_t;\lambda_{r_t})\times\hat{y}$ across the interface.Therefore transverse resonance is a method of locating the singularities of the transverse characteristic Green's function without requiring its explicit form.However,it is equally apparent,that as the transverse characteristic Green's function is not singular at either of the points used to construct a continuous eigenfunction,transverse resonance cannot identify these points.

Returning now to the orthogonality condition,this may be written,without loss of generality,in the form;

$$-j\omega\mu\int_{-\infty}^{\infty}dx\left[R\underline{E}_\mu(\underline{r}_t;\lambda_{r_t})\times\underline{H}_v(\underline{r}_t;\lambda_{r_t})\cdot\hat{y}\right]_{y=y'-0}^{y=y'+0}$$

$$=-j\delta_{v\mu}(P_v+jQ_v)=-j\delta_{v\mu}P_v(1-jcot\alpha_v(\lambda_{r_t})) \qquad (2.4.43)$$

where $-j\delta_{v\mu}(P_v(\lambda_{r_t})+jQ_v(\lambda_{r_t}))$ is the denominator of $\underline{\underline{G}}_E(\underline{r}_t,\underline{r}_t';\lambda_{r_t})$ and P_v,Q_v and $\alpha_v(\lambda_{r_t})$ are,by definition,real quantities.$cot\alpha_v(\lambda_{r_t})$ has been introduced as it shall be shown later that α_v appears as the phase shift in the standing wave representation of the continuous eigenfunctions.

Expressing $-j\omega\mu\int_{-\infty}^{\infty}dx\left[R\underline{E}_\mu(\underline{r}_t;\lambda_{r_t})\times\underline{H}_v(\underline{r}_t;\lambda_{r_t})\cdot\hat{y}\right]_{y=y'-0}^{y=y'+0}$ in the form $-j\delta_{v\mu}P_v(1-jcot\alpha_v(\lambda_{r_t}))$,requires the solution of the following eigenvalue equation;

$$cot\alpha_v \,\mathrm{Re}\left[\omega\mu \int_{-\infty}^{\infty} dx \left[R\underline{E}_\mu(\underline{r}_t;\lambda_{r_t}) \times \underline{H}_v(\underline{r}_t;\lambda_{r_t}) \cdot \hat{y}\right]_{y=y'-0}^{y=y'+0}\right]$$

$$= \mathrm{Im}\left[\omega\mu \int_{-\infty}^{\infty} dx \left[R\underline{E}_\mu(\underline{r}_t;\lambda_{r_t}) \times \underline{H}_v(\underline{r}_t;\lambda_{r_t}) \cdot \hat{y}\right]_{y=y'-0}^{y=y'+0}\right] \qquad (2.4.44)$$

In each of the two separable regions of the structure,the vector $\underline{E}_v(\underline{r}_t;\lambda_{r_t})$ may be expressed as a linear combination of solutions to the homogeneous Helmholtz equation,with expansion coefficients determined from the transverse electric fields at the interface.The vector $\underline{H}_v(\underline{r}_t;\lambda_{r_t})$ on each side of the interface can then be expressed by means of admittance operators acting upon $\underline{E}_v(\underline{r}_t;\lambda_{r_t})$,allowing equation (2.4.44) to be formulated solely in terms of the transverse electric fields at the interface.In this form the eigenvalue equation may then be solved,for example,by Galerkin's method,identifying a set of eigenvalues $\{cot\alpha_v(\lambda_{r_t})\}$ and eigenvectors $\{\underline{E}_v(x,0;\lambda_{r_t})\}$.

In a discretised form,it is possible to combine the properties of matrices and the physical interpretation introduced above to prove that these solutions are linearly independent and satisfy the required biorthogonality relationship.

2.4.6) Integration of the Transverse Characteristic Green's function in the complex λ_{r_t} plane.

To recover the transverse electric eigensolutions of the structure,the transverse characteristic Green's function derived above,must be integrated around a contour in the complex λ_{r_t} plane that encloses all of its singularities,ie;

$$\frac{1}{2\pi j}\int_{C_{\lambda_{r_t}}} d\lambda_{r_t}\, \underline{\underline{G}}_E(\underline{r}_t,\underline{r}_t',\lambda_{r_t}) = \sum_p \underline{\phi}_p(\underline{r}_t;k_{tp})\underline{\phi}_p^{\Lambda}(\underline{r}_t';k_{tp}) + \int_0^{\infty} dk_t \sum_v \underline{\phi}_v(\underline{r}_t;k_t)\underline{\phi}_v^{\Lambda}(\underline{r}_t';k_t) \qquad (2.4.45)$$

where $\lambda_{r_t} = k_t^2$.

To determine the contour of integration,$C_{\lambda_{r_t}}$,the properties of the transverse characteristic Green's function must be examined.

The lamellar part has been left in a form such that its integral around any closed contour in the λ_{r_t} plane,just recovers the lamellar part of the completeness relationship.This is not a problem as it shall be shown later that the lamellar part of the Green's function,$\underline{\underline{G_E}}(\underline{r},\underline{r})$,may be succinctly derived by an alternative approach.

The solenoidal part of $\underline{\underline{G_E}}(\underline{r}_t,\underline{r}_t';\lambda_{r_t})$ is constructed from solutions of the homogeneous Helmholtz equation in each of the separable regions.Assuming that the nonseparable interface lies in the x-z plane,the solutions in the open region may be written in the form;

$$\underline{\Phi}(k_x,x)e^{-jk_y y} \quad : \quad k_x^2+k_y^2=k_t^2 \quad : \quad 0\le k_x\le\infty \tag{2.4.46}$$

Due to its dependence upon k_y,and not just k_y^2,the solenoidal part of the transverse characteristic Green's function is a multivalued function of λ_{r_t},necessitating the introduction of a branch cut in the complex λ_{r_t} plane.To ensure that the fields are bounded at infinity,the imaginary part of k_y must be negative.Therefore writing $\lambda_{r_t}=\hat{\lambda}_{r_t}e^{j\theta}$ with $\sqrt{\lambda_{r_t}}=\sqrt{\hat{\lambda}_{r_t}}\,e^{j\frac{\theta}{2}}$,restricts θ to the range $-2\pi\le\theta\le 0$,and requires a branch cut along the positive real axis,as illustrated in figure (2.4.3).

Therefore,the contour integration will consist of residues from the isolated singularities and the integral around the branch cut.As observed above,the singularities occur when the source at the nonseparable interface is zero.If λ_{r_t} is complex,then propagating waves exist in the open region.Clearly this implies a source at the interface and therefore $\underline{\underline{G_E}}(\underline{r}_t,\underline{r}_t';\lambda_{r_t})$ cannot be singular.Consequently the singularities are restricted to the negative real axis.

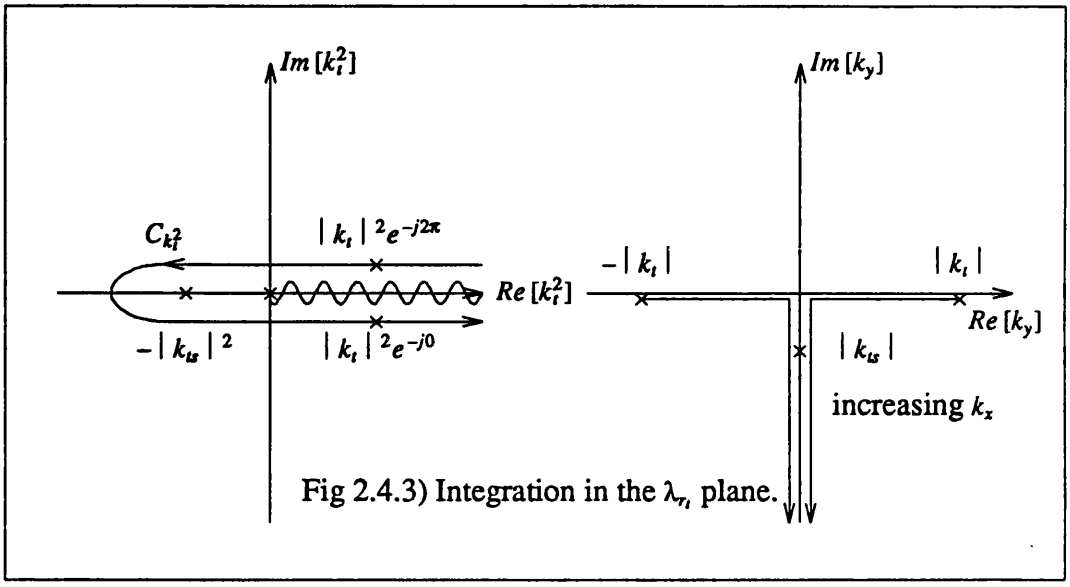

Fig 2.4.3) Integration in the λ_{r_t} plane.

The integral around the branch cut may be determined as follows.

In the lossless case,the dependence of the transverse characteristic Green's function upon the sign of k_y,is manifested in the term $P_v(\lambda_{r_t})$ in equation (2.4.43).On either side of the branch cut this term is of opposite sign.Thus the transverse characteristic Green's function immediately on one side of the branch cut,is the complex conjugate of its value immediately on the other side,ie;

$$\underline{\underline{G}}^s_E(\underline{r}_t,\underline{r}_t';\hat{\lambda}_{r_t}e^{-j2\pi}) = \left(\underline{\underline{G}}^s_E(\underline{r}_t,\underline{r}_t';\hat{\lambda}_{r_t}e^{-j0})\right)^* \tag{2.4.47}$$

Consequently the complete contour integral may be evaluated as;

$$\frac{1}{2\pi j}\int_{C_{\lambda_{r_t}}} \underline{\underline{G}}^s_E(\underline{r}_t,\underline{r}_t';\lambda_{r_t}) = \sum_p res\left[\underline{\underline{G}}^s_E(\underline{r}_t,\underline{r}_t';\lambda_{r_{tp}})\right] + \frac{2}{\pi}\int_0^\infty dk_t\, k_t \mathrm{Im}\left[\underline{\underline{G}}^s_E(\underline{r}_t,\underline{r}_t';\hat{\lambda}_{r_t}e^{-j0})\right]$$

$$= \sum_p \underline{\phi}^s_p(\underline{r}_t;k_{tp})(\underline{\phi}^s_p(\underline{r}_t';k_{tp}))^A + \int_0^\infty dk_t \sum_v \underline{\phi}^s_v(\underline{r}_t;k_t)(\underline{\phi}^s_v(\underline{r}_t';k_t))^A \tag{2.4.48}$$

Clearly,as previously discussed,the singularities of the transverse characteristic Green's function correspond to the point spectrum and the branch cut integral to

the continuous spectrum.

If the specific form of $\underline{\underline{G}}_E^s(\underline{r}_t,\underline{r}_t';\lambda_{\tau_t})$ is introduced,it can be seen that the discrete eigenfunctions are given by;

$$\underline{\phi}_p^s(\underline{r}_t;k_{tp})(\underline{\phi}_p^s(\underline{r}_t';k_{tp}))^A = res\left[\frac{\underline{E}_p(\underline{r}_t;k_{tp})\underline{E}_p^A(\underline{r}_t';k_{tp})}{-j\omega\mu\int_{-\infty}^{\infty}dx\left[R\underline{E}_p(\underline{r}_t;k_{tp})\times\underline{H}_p(\underline{r}_t;k_{tp}).\hat{y}\right]_{y=y'-0}^{y=y'+0}}\right]$$

$$= \frac{\underline{E}_p(\underline{r}_t;\lambda_{\tau_t})\underline{E}_p^A(\underline{r}_t';\lambda_{\tau_t})}{N_p^2}$$

$$N_p^2 = -j\omega\mu\int_{-\infty}^{\infty}dx\,\frac{\partial}{\partial k_t^2}\left[R\underline{E}_p(\underline{r}_t;k_{tp})\times\underline{H}_p(\underline{r}_t;k_{tp}).\hat{y}\right]_{y=y'-0}^{y=y'+0} \qquad (2.4.49)$$

and hence;

$$\underline{\phi}_p^s(\underline{r}_t;k_{tp}) = \frac{\underline{E}_p^+(\underline{r}_t;k_{tp})}{N_p} \quad :y>y' \qquad = \frac{\underline{E}_p^-(\underline{r}_t;k_{tp})}{N_p} \quad :y<y' \qquad (2.4.50)$$

Similar expressions may be identified for the adjoint eigenfunctions.The continuum eigenfunctions may be identified from equation (2.4.48) as;

$$k_t\mathrm{Im}\left[\frac{\underline{E}_v(\underline{r}_t;k_t)\underline{E}_v^A(\underline{r}_t';k_t)}{-jP_v(k_t)(1-j\cot\alpha_v(k_t))}\right] = \underline{\phi}_v(\underline{r}_t;k_t)\underline{\phi}_v^A(\underline{r}_t';k_t) \qquad (2.4.51)$$

where the eigenvalue notation introduced above has been adopted.

In the open region the vector,$\underline{E}_v^+(\underline{r}_t,k_t)$,may be expressed as;

$$\underline{E}_v^+(\underline{r}_t;k_t) = \int_0^{\infty}dk_x\,\tilde{\underline{e}}_v(k_x)\underline{\phi}(k_x,x)e^{-jk_yy} \qquad \tilde{\underline{e}}_v = \int_0^{\infty}dx\,\underline{E}_v(x,0;k_t),\underline{\phi}(k_x,x) \qquad (2.4.52)$$

and,if it is assumed that the other region is bounded,the vector $\underline{E}_v^-(\underline{r}_t;k_t)$ may be written as;

$$\underline{E}_v^-(\underline{r}_t;k_t) = \sum_n \underline{e}_{vn}(k_x)\underline{\phi}_n(x)\chi(k_{y_n}y) \qquad \underline{e}_{vn} = \int_0^\infty dx\, \underline{E}_v(x,0;k_t),\underline{\phi}_n(x) \tag{2.4.53}$$

Because in the lossless case,the dyadic $\underline{E}_v(x,0;k_t)\underline{E}_v^{\wedge}(x'0;k_t)$ is common to $\underline{\underline{G}}_E(\underline{r}_t,\underline{r}_t';\lambda_{r_t})$ on both sides of the branch cut,this term may be taken outside the 'Im' operator in (2.4.51).Therefore using the following identities;

$$\mathrm{Im}\left[\frac{e^{-jk_y y}}{-jP_v(k_t)(1-jcot\alpha_v(k_t))}\right] = \frac{\sin(k_y y+\alpha_v(k_t))\sin\alpha_v(k_t)}{P_v(k_t)} \quad : k_y \textit{ real}$$

$$= \frac{e^{-jk_y y}\sin^2\alpha_v(k_t)}{P_v(k_t)} \quad : k_y \textit{ imaginary}$$

$$\mathrm{Im}\left[\frac{\chi(k_{yn};y)}{-jP_v(k_t)(1-jcot\alpha_v(k_t))}\right] = \chi(k_{yn};y)\sin^2\alpha_v(k_t)P_v(k_t) \tag{2.4.54}$$

permits the continuous eigenfunctions to be identified as;

$$\underline{\phi}_v(\underline{r}_t;k_t) = \left(\frac{2k_t}{\pi P_v(k_t)}\right)^{\frac{1}{2}} \int_0^{k_t} dk_x\, \underline{\tilde{e}}_v(k_x)\underline{\phi}(k_x,x)\sin(k_y y+\alpha_v(k_t))$$

$$+ \left(\frac{2k_t}{\pi P_v(k_t)}\right)^{\frac{1}{2}} \int_{k_t}^\infty dk_x\, \underline{\tilde{e}}_v(k_x)\underline{\phi}(k_x,x)e^{-|k_y|y}\sin\alpha_v(k_t) \qquad :y>y' \tag{2.4.55}$$

$$\underline{\phi}_v(\underline{r}_t;k_t)\left(\frac{2k_t}{\pi P_v(k_t)}\right)^{\frac{1}{2}} \sum_n \underline{e}_{vn}\underline{\phi}_n(x)\chi(k_{y_n};y)\sin(\alpha_v(k_t)) \qquad :y<y' \tag{2.4.56}$$

and similarly for the adjoint quantities.

2.5) The Inversion Operator to Maxwell's Equations:The Green's Function.

2.5.1) Guided Mode Representation of the Green's Function.

Having identified the solenoidal eigensolutions of the operator $(\nabla\times\nabla\times-\varepsilon\mu\partial t^2-\underline{\lambda}_r)$,it is possible to construct the Green's function of the structure and hence define the inverse operator to Maxwell's equations.

The part of the Green's function constructed from the solenoidal eigenfunctions is given by equation (2.1.15) as;

$$\underline{\underline{G}}_E(\underline{r},\underline{r}',t,t') = \int_{-\infty}^{\infty} d\omega \int_{-\infty}^{\infty} d\beta \left[\sum_p \frac{\underline{\phi}_p^s(\underline{r}_t)(\underline{\phi}_p^s(\underline{r}_t'))^A}{k^2-k_{tp}^2-\beta^2} + \int_0^{\infty} dk_t \frac{\underline{\phi}^s(\underline{r}_t;k_t)(\underline{\phi}^s(\underline{r}_t';k_t))^A}{k^2-k_t^2-\beta^2} \right]$$

$$\frac{e^{-j\beta|z-z'|}e^{j\omega|t-t'|}}{(2\pi)^2} \qquad (2.5.1)$$

The integration w.r.t. β may be performed by applying Cauchy's theorem to the contour C_β in figure 2.5.1,giving;

$$\underline{\underline{G}}_E(\underline{r},\underline{r}',t,t') = \int_{-\infty}^{\infty} d\omega \left[\sum_p \frac{\underline{\phi}_p^s(\underline{r}_t)(\underline{\phi}_p^s(\underline{r}_t'))^A}{-2j\beta} e^{-j\beta_p|z-z'|} + \int_0^{\infty} dk_t \frac{\underline{\phi}^s(\underline{r}_t;k_t)(\underline{\phi}^s(\underline{r}_t';k_t))^A}{-2j\beta} e^{-j\beta|z-z'|} \right]$$

$$\frac{e^{j\omega|t-t'|}}{(2\pi)} \quad :with \ \$\beta^2 = k^2 - k_t^{2\$}. \qquad (2.5.2)$$

It is clear that this part of the Green's function may be expressed solely in terms of the eigenfunctions with an eigenvalue,λ,of zero,ie $k^2-\beta^2-k_t^2=0$.If the structure is homogeneous,then these eigenfunctions are the conventional,source free,guided modes and are functionally equal to the transverse eigenfunctions developed above;

$$\underline{\phi}(\underline{r}_t;k_t)\frac{e^{-j\beta z}}{\sqrt{-2j\beta}}\frac{e^{+j\omega t}}{\sqrt{2\pi}} \qquad (2.5.3)$$

However,if the structure is inhomogeneous then the dependence of β upon k,and hence the permeability and permittivity,precludes the possibility of a separable mode of the form equation (2.5.3) being identified.Although this does not invalidate the representation of the Green's function given in equation (2.5.2),it prevents the use of network models as a means of analysing problems.Section 2.6 shall show that a slight modification of the transverse characteristic Green's

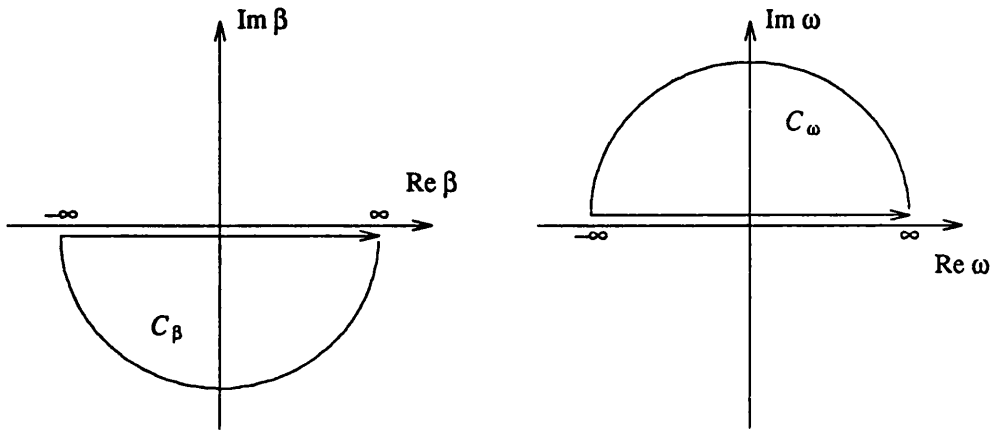

Figure 2.5.1) Integration paths in the complex β and ω planes.

function derived above,allows guided modes to be found for inhomogeneous structures and,in addition,considers some of the effects of lossy materials.

The representation of the Green's function in terms of guided modes is not unique,in fact an alternative representation may be immediately derived by performing the integration w.r.t. ω in (2.5.1) around the contour C_ω in figure 2.5.1,to give;

$$\underline{\underline{G}}_E(\underline{r},\underline{r}') = \int_{-\infty}^{\infty} d\beta \left[\sum_p \frac{\underline{\phi}_p^s(r_t)(\underline{\phi}_p^s(r_t'))^A}{-2j\omega\varepsilon\mu} e^{j\omega_p |z-z'|} + \int_0^{\infty} dk_t \frac{\underline{\phi}^s(r_t;k_t)(\underline{\phi}^s(r_t';k_t))^A}{-2j\omega\varepsilon\mu} e^{j\omega |z-z'|} \right]$$

$$\frac{e^{-j\beta|z-z'|}}{(2\pi)} \qquad (2.5.4)$$

again with $\beta^2 = k^2 - k_t^2$.In certain circumstances,such as determining transient effects,this representation may be more useful.

However,returning to the guided mode representation,it may be shown that the general biorthogonality relationship satisfied by these modes can be re-expressed.

The eigenfunctions with $\lambda = 0$ are solutions to the homogeneous operator equation;

$$\begin{pmatrix} -\partial t\varepsilon(\underline{r}_t) & \nabla \times \\ -\nabla \times & -\partial t\mu(\underline{r}_t) \end{pmatrix} \begin{pmatrix} \underline{E}(\underline{r}) \\ \underline{H}(\underline{r}) \end{pmatrix} = \begin{pmatrix} \underline{0} \\ \underline{0} \end{pmatrix} \tag{2.5.5}$$

which if a guided mode representation is sought,may be rewritten as,[5];

$$\begin{pmatrix} -\partial t\varepsilon(\underline{r}_t) & \nabla_t \times \\ -\nabla_t \times & -\partial t\mu(\underline{r}_t) \end{pmatrix} \begin{pmatrix} \underline{E}(\underline{r}) \\ \underline{H}(\underline{r}) \end{pmatrix} = -\partial z \begin{pmatrix} 0 & \hat{z} \times \\ -\hat{z} \times & 0 \end{pmatrix} \begin{pmatrix} \underline{E}(\underline{r}) \\ \underline{H}(\underline{r}) \end{pmatrix} \tag{2.5.6}$$

where;

$$(\nabla_t + \partial z\, \hat{z}) \times \underline{E}(\underline{r}) = \nabla \times \underline{E}(\underline{r}) \tag{2.5.7}$$

As it is already known that the z dependence of the fields and their adjoints is of form $e^{-j\beta z}$ and $e^{+j\beta z}$,equation (2.5.6) becomes an eigenvalue equation with eigenvalue β;

$$\begin{pmatrix} -\partial t\varepsilon(\underline{r}_t) & \nabla_t \times \\ -\nabla_t \times & -\partial t\mu(\underline{r}_t) \end{pmatrix} \begin{pmatrix} \underline{E}(\underline{r}) \\ \underline{H}(\underline{r}) \end{pmatrix} = j\beta \begin{pmatrix} 0 & \hat{z} \times \\ -\hat{z} \times & 0 \end{pmatrix} \begin{pmatrix} \underline{E}(\underline{r}) \\ \underline{H}(\underline{r}) \end{pmatrix} \tag{2.5.8}$$

Using this equation,it is possible to demonstrate that,if the media possesses particular properties,such as losslessness or isotropic symmetry,then the biorthogonality relationship satisfied by the modes may be simplified to a form that does not involve the adjoint fields.For example,the modes of a structure containing gyrotropic media,ie most common waveguides,satisfy;

$$\int_{-\infty}^{\infty} dx \int_{-\infty}^{\infty} dy\, \underline{E}(\underline{r}_t;\beta_m) \times \underline{H}(\underline{r}_t;\beta_n).\hat{z} = \delta_{mn} \tag{2.5.9}$$

and the transverse completeness relationship;

$$\sum_n \underline{E}_t(\underline{r}_t;\beta_n)\,\underline{H}(\underline{r}_t';\beta_n)\times\hat{z} = (\hat{x}\hat{x}+\hat{y}\hat{y})\delta(\underline{r}_t-\underline{r}_t') \qquad (2.5.10)$$

noting that the summation sign is symbolic,not necessarily literal.

The eigenfunctions developed in section 2.4,are normalised as $\int_{-\infty}^{\infty} dx \int_{-\infty}^{\infty} dy\, \underline{RE}(\underline{r}_t;k_{tn}) \cdot \underline{E}(\underline{r}_t;k_{tm}) = \delta_{mn}$.It is easy to show,that the only difference between this and the normalisation of (2.5.9) is a factor, $\frac{\omega\mu_o}{\beta}$,which can be simply absorbed into the mode functions if the more conventional normalisation of (2.5.9) is required.In fact this convention shall be adopted for the remainder of this thesis.

2.5.2) Completeness of the Green's Function;Validity in the Source Region.

The expression for the Green's function presented above,has been constructed solely from solenoidal eigenfunctions and then reduced to a guided mode representation.To be complete,it is necessary to determine the contribution made by the lamellar eigenfunctions.In fact,it shall be shown that an explicit derivation of the lamellar eigenfunctions is unnecessary and that their contribution to the Green's function may be expressed in a more convenient form.

There has been much discussion,[10-13],upon the validity of electric dyadic Green's functions at the source point.The problem arises because the classical expansion of the Green's function using only the solenoidal modes of a structure,cannot completely represent the lamellar part of the excited field.

It must be noted,that the Green's function constructed from the solenoidal modes is not,in fact,solenoidal at the source point and therefore does contribute a lamellar term.

Pathak,[10],has shown that the complete Green's function may be recovered by augmenting the classical Green's function,ie equation (2.5.2),with an

extra term,specified below.Although the proof of this result is relatively straightforward,it is fairly lengthy and only a general outline shall be given here.

The magnetic field Green's function is purely solenoidal and given a similar guided mode representation to that discussed above,valid at all points of the structure.The electric and magnetic field Green's functions are related by;

$$\partial t \varepsilon \underline{\underline{G_E}}(\underline{r},\underline{r}') = \nabla \times \underline{\underline{G_M}}(\underline{r},\underline{r}') - \underline{\underline{I}}\delta(\underline{r}-\underline{r}') \tag{2.5.11}$$

If the expression for $\underline{\underline{G_M}}(\underline{r},\underline{r}')$ is substituted into equation (2.5.11),it can be shown that,in addition to the guided mode expansion,the electric field Green's function contains an extra term;

$$\underline{\underline{G_E}}(\underline{r},\underline{r}') = \int_{-\infty}^{\infty} d\omega \left[\sum_P \frac{\underline{\phi_P^s}(r_t)(\underline{\phi_P^s}(r_t'))^A}{-2} e^{-j\beta|z-z'|} + \int_0^{\infty} dk_t \frac{\underline{\phi^s}(r_t;k_t)(\underline{\phi^s}(r_t';k_t))^A}{-2} e^{-j\beta|z-z'|} - \hat{z}\hat{z}\frac{\delta(\underline{r}-\underline{r}')}{j\omega\varepsilon} \right] \frac{e^{j\omega|t-t'|}}{(2\pi)} \tag{2.5.12}$$

where the guided modes have been normalised w.r.t. equation (2.5.9).

The extra term is a consequence of the discontinuous nature of the transverse magnetic fields at z=z'.Performing the curl operation results in a term that is proportional to the product of a singularity,$\delta(z-z')$,and a term which is identified by the transverse completeness relationship as $\delta(\underline{r}_t-\underline{r}_t')$.

Unfortunately in practice,the Green's function in the form of equation (2.5.11) is difficult to apply.The difficulty arises due to the numerical accuracy with which the mode vectors may be determined and the behaviour of the integral over k_t.It is often found that both the integral over k_t and the term $\hat{z}\hat{z}\frac{\delta(\underline{r}-\underline{r}')}{j\omega\varepsilon}$ result in unbounded terms and,although theoretically,they have a well behaved,bounded,difference,it is impossible to numerical ascertain.Therefore it is

necessary to somehow express the term $\hat{z}\hat{z}\frac{\delta(r-r')}{j\omega\varepsilon}$ as an integral over k_t,allowing the difference to be taken between the integrands rather than the total integrals.

It is demonstrated in appendix A2 at the end of this chapter,that the longitudinal field components also satisfy a biorthogonality relationship of the form;

$$\int_{-\infty}^{\infty} dx \int_{-\infty}^{\infty} dy\, E_{zn}(\underline{r}_t)E_{zm}(\underline{r}_t) + k_o^2 H_{zn}(\underline{r}_t)H_{zm}(\underline{r}_t) = -\frac{k_t^2}{\omega\varepsilon\beta}\delta_{nm} \tag{2.5.13}$$

As $\hat{z}\hat{z}\frac{\delta(r-r')}{j\omega\varepsilon}$ must satisfy the boundary conditions of $E_z(\underline{r}_t)$ and $E_z^A(\underline{r}_t)$,it may now be expressed as;

$$\hat{z}\hat{z}\frac{\delta(r-r')}{j\omega\varepsilon} = \hat{z}\hat{z}\frac{\beta}{k_t^2}\delta(z-z')\left[\sum_p \phi_{pz}^e(\underline{r}_t;k_{tp})(\phi_{pz}^e(\underline{r}_t';k_{tp}))^A + \int_0^{\infty} dk_t\, \phi_z^e(\underline{r}_t;k_t)(\phi_z^e(\underline{r}_t';k_t))^A\right] \tag{2.5.14}$$

Using this expansion in equation (2.5.12) recasts the Green's function into a form that is convenient to apply in practice.

2.6) Inhomogeneous Structures.

This section shall discuss a slight reformulation of the transverse characteristic Green's function,that allows the guided modes of an inhomogeneous structure to be found.

It has been demonstrated,that to construct the solenoidal part of the Green's function,it is only necessary to determine the eigenfunctions with an eigenvalue of zero.Further,to allow network modelling of the guide,it is advantageous to seek guided mode solutions.Modes satisfying both these criteria are solutions to;

$$(\nabla_t^2 + k^2 - \beta^2)\underline{\phi}(\underline{r}_t;\beta)e^{-j\beta z}e^{j\omega t} = \underline{0} \tag{2.6.1}$$

To permit solutions to be found for piecewise inhomogeneous structures,the transverse mode vectors are defined as solutions to;

$$(\nabla_t^2 + (\varepsilon_r\mu_r - 1)k_o^2 + k_o^2 - \beta^2)\underline{\phi}_t(\underline{r}_t;\beta) = \underline{0} \qquad (2.6.2)$$

ie,

$$(\nabla_t^2 + (\varepsilon_r\mu_r - 1)k_o^2 + k_t^2)\underline{\phi}_t(\underline{r}_t;\beta) = \underline{0} \qquad (2.6.3)$$

where;

$$k_t^2 = k_o^2 - \beta^2 \quad ; \quad \varepsilon = \varepsilon_r\varepsilon_o \quad ; \quad \mu = \mu_r\mu_o \quad ; \quad k_o^2 = \varepsilon_o\mu_o\omega^2$$

k_t^2 may be regarded as the eigenvalue of the position dependent operator $\nabla_t^2 + (\varepsilon_r\mu_r - 1)k_o^2$.A transverse characteristic Green's function for this operator may be developed exactly as before,except that now the vectors $\underline{E}_v^+(\underline{r}_t;\lambda_{r_t})$ and $\underline{E}_v^-(\underline{r}_t;\lambda_{r_t})$ are now defined by;

$$(\nabla_t^2 + (\varepsilon_r^+\mu_r^+ - 1)k_o^2 + k_t^2)\underline{E}_v^+(\underline{r}_t;\lambda_{r_t}) = \underline{0}$$

$$(\nabla_t^2 + (\varepsilon_r^-\mu_r^- - 1)k_o^2 + k_t^2)\underline{E}_v^-(\underline{r}_t;\lambda_{r_t}) = \underline{0} \qquad (2.6.4)$$

The eigenfunctions determined from this transverse characteristic Green's function,will automatically be in the form of guided waves.The integration of the transverse characteristic Green's function in the complex k_t plane still requires a branch cut along the positive real axis,although the position of the poles,and therefore the propagation constants of the discrete modes will change.

2.6.1) Lossy Structures.

The transverse characteristic Green's function developed above,is still valid if the structure contains lossy media.It is possible to make a few observations concerning the effect of various types of losses upon the mode spectrum.Three loss effects shall be discussed,media losses in the open region,media losses in the

bound region and conduction losses.

For comparison purposes figure (2.6.1) shows the positions of the branch cut and typical poles in both the k_t^2 and β planes for the lossless case.

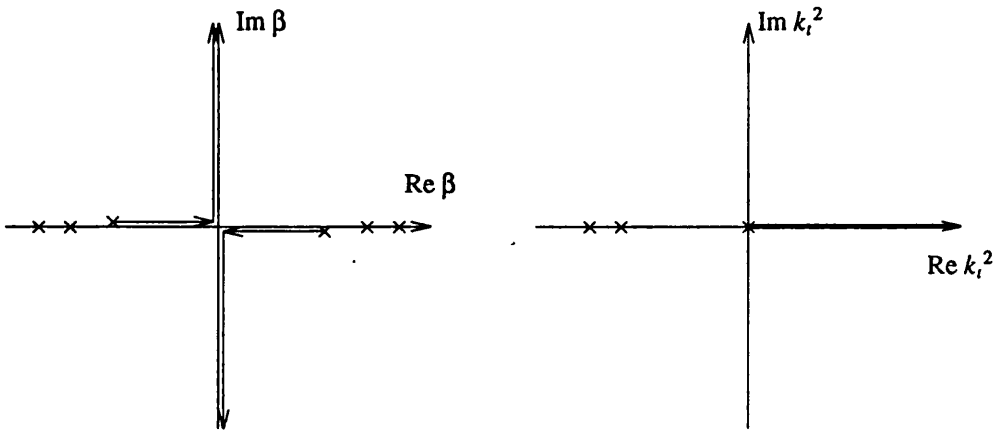

Figure 2.6.1) The β and k_t^2 planes for lossless structures.
× Singularities

If the media in the bound region is lossy and/or the conductivity of the metal walls is finite,then it is well known,[7],that the discrete poles are displaced from the real axis in the β plane,the branch cut however,remains unchanged,figure (2.6.2).

If the media in the open region is also lossy,then due to the dependence of β upon the value of k in the open region,the position of the branch cut in the β plane is displaced,even though the branch cut in the k_t^2 plane is unchanged,figure (2.6.3).

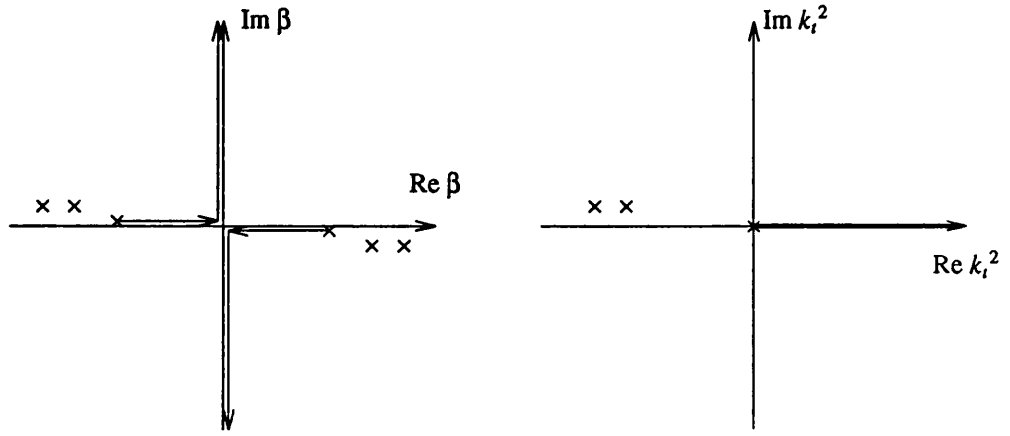

Figure 2.6.2) The β and k_t^2 planes for structures with lossy bound regions.

× Singularities

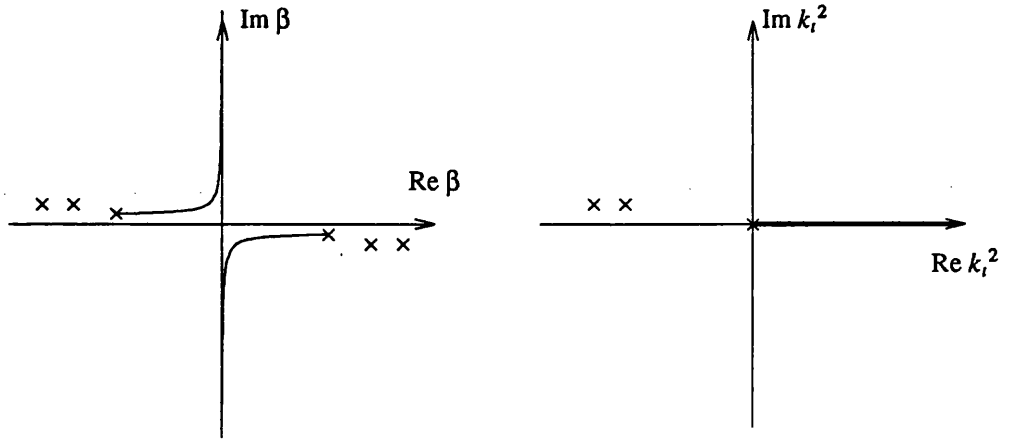

Figure 2.6.3) The β and k_t^2 planes for general,lossy structures.

× Singularities

Naturally,in addition to the changes to the propagation constants,the functional form of the modes will also change in the presence of losses.

2.7) References.

1) V.Hutson and J.Pym,"Applications of Functional Analysis",Academic Press,1980.

2) R.Curtain and A.Pritchard,"Functional Analysis in Modern Applied Mathematics",Academic Press,1977.

3) B.Friedman,"Principles and Techniques of Applied Mathematics",Wiley,1956.

4) D.Jones,"Methods of Electromagnetic Wave Propagation",vol 1,Oxford,1987.

5) L.Felsen and N.Marcuvitz,"Radiation and Scattering of Waves",Prentice Hall,1973. 6) V.Shevchenko,"Continuous Transitions in Open Waveguides",The Golem Press,1971.

7) R.Collin,"Field Theory of Guided Waves",McGraw Hill,1960.

8) S.Saad,"Review of Numerical Methods for the Analysis of Arbitrarily-Shaped Microwave and Optical Dielectric Waveguides",IEEE trans. microwave theory and techniques,vol MTT-33,no 10,Oct 85,pp894-899.

9) S-T.Peng and A.Oliner,"Guidance and Leakage Properties of a Class of Open Dielectric Waveguides:Part 1-Mathematical Formulations",IEEE trans. microwave theory and techniques,vol MTT-29,no 9,Sept 1981,pp843-854.

10) P.Pathak,"On the Eigenfunction Expansion of Electromagnetic Dyadic Green's Functions",IEEE trans. antennas and prop.,vol AP-31,no 6,Nov 83,pp837-846.

11) A.Yaghjian,"Electric Dyadic Green's Functions in the Source Region",proc IEEE,vol 68,no 2,1980,pp248-263.

12) S-W.Lee,J.Boersma,C-L.Law and G.Deschamps,"Singularity in Green's Functions and its Numerical Evaluation",IEEE trans. antennas and prop.,vol AP-28,no 3,May 1980,pp311-317.

13) R.Collin,"On the Incompleteness of E and H Modes in Waveguides",Canadian J. Physics,vol 51,pp1135-1140.

Appendix A2.

This appendix shall prove the result quoted as equation (2.5.13) in the text.

Consider the following integral over the guide cross-section;

$$\int dx \int dy \, \underline{E}_{tm}(\underline{r}_t) \cdot \underline{E}_{tn}(\underline{r}_t) = \int dx \int dy \, \hat{z} \times \underline{E}_m(\underline{r}_t) \cdot \frac{\hat{z} \times \nabla \times \underline{H}_n(\underline{r}_t)}{j\omega\varepsilon} \tag{A2.1}$$

Using a sequence of vector identities allows the following steps to made;

$$\int dx \int dy \, \underline{E}_{tm}(\underline{r}_t) \cdot \underline{E}_{tn}(\underline{r}_t) = \int dx \int dy \, \frac{\hat{z} \times E_m(\underline{r}_t)}{j\omega\varepsilon} \cdot (\nabla H_{zn}(\underline{r}_t) - \partial z \underline{H}_n(\underline{r}_t))$$

$$= \int dx \int dy \, \frac{\beta}{\omega\varepsilon} \hat{z} \times \underline{E}_m(\underline{r}_t) \cdot \underline{H}_n(\underline{r}_t) + \frac{\nabla \cdot [H_{zn}(\underline{r}_t)\, \hat{z} \times \underline{E}_m(\underline{r}_t)] - H_{zn}(\underline{r}_t)\, \nabla \cdot (\hat{z} \times \underline{E}_m(\underline{r}_t))}{j\omega\varepsilon} \tag{A2.2}$$

$$= \frac{\beta}{\omega\varepsilon}\delta_{mn} + \frac{\int dy \left[-H_{zn}(\underline{r}_t) E_{yn}(\underline{r}_t) \right]_{x2}^{x1} + \int dx \left[H_{zn}(\underline{r}_t) E_{xn}(\underline{r}_t) \right]_{y2}^{y1} + \int dx \int dy H_{zn}\, \hat{z} \cdot \nabla \times \underline{E}_m(\underline{r}_t)}{j\omega\varepsilon}$$

$$= \frac{\beta}{\omega\varepsilon}\delta_{mn} - \int dx \int dy \frac{\mu}{\varepsilon} H_{zn}(\underline{r}_t) H_{zm}(\underline{r}_t) \tag{A2.3}$$

In addition,the electric fields of the modes satisfy;

$$\int dx \int dy \, E_m(\underline{r}_t) \times H_n(\underline{r}_t) \cdot \hat{z} = \delta_{mn} = \int dx \int dy \frac{\beta}{\omega\mu} R \underline{E}_m(\underline{r}_t) \cdot \underline{E}_n(\underline{r}_t) \tag{A2.4}$$

Substituting in equation (A2.3) gives;

$$\delta_{mn} = \frac{\beta^2}{k_o^2}\delta_{mn} - \frac{\beta}{\omega\mu}\int dx\int dy E_{zm}(\underline{r}_t)E_{zn}(\underline{r}_t) - \frac{\beta}{\omega\varepsilon}\int dx\int dy H_{zm}(\underline{r}_t)H_{zn}(\underline{r}_t) \qquad \text{(A2.5)}$$

ie,

$$-\int dx\int dy\, E_{zm}(\underline{r}_t)E_{zn}(\underline{r}_t) + k_o^2 H_{zm}(\underline{r}_t)H_{zn}(\underline{r}_t) = \delta_{mn}\frac{\omega\mu}{\beta}\left(1 - \frac{\beta^2}{k_o^2}\right) \qquad \text{(A2.6)}$$

CHAPTER 3.

THE CONTINUOUS SPECTRA OF SEPARABLE OPEN STRUCTURES.

3.1) Introduction.

The previous chapter discussed the spectral approach to electromagnetic problems,demonstrating that the fields excited by a source current may be evaluated by means of a Green's function constructed from the modes of the guide.

A characteristic Green's function method was presented that permits the complete mode spectrum to be derived.The method is applicable to a wide variety of structures including open nonseparable ones.

The first section of this chapter shall consider the mode spectra of a few simple open separable structures within the context of the method presented above.The subsequent section shall then show that it is possible to develop the mode spectra of nonseparable open structures from a conceptually simpler,field matching,approach,albeit lacking as yet the proof of built in completeness and normalisation available from the characteristic Green's function method.

3.2) Separable open Waveguides.

This section shall consider the continuous spectra of open separable structures.It shall be shown that the continuous modes,which for these structures may be found from the separation of variables,may also be derived using the characteristic Green's function method.Although the strength of the latter lies in its ability to tackle nonseparable open structures,it is useful to illustrate its application to structures for which known,analytic,modes are available.

3.2.1) The Grounded Half Space.

As a simple first example,consider the grounded half space illustrated below.

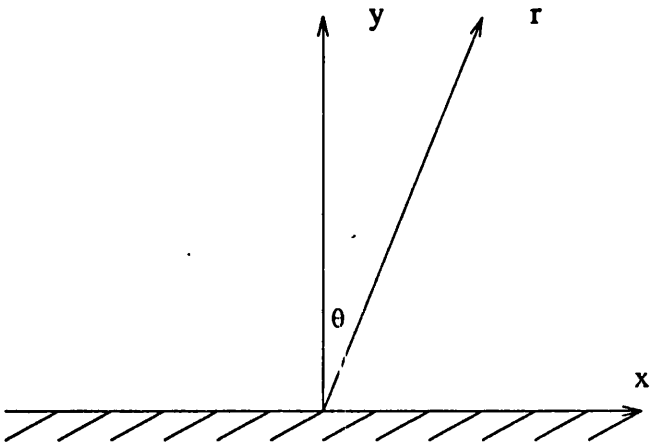

Figure 3.2.1) The Grounded Half Space.

It is interesting to observe that this structure is separable in both rectangular and cylindrical coordinates,permitting two equivalent representations for the continuous modes to be derived.

The position of the interface assumed by the method is arbitrary and may be taken as the ground plane without any difficulty.

The transverse characteristic Green's function for this structure is given by equation (2.4.41);

$$\underline{\underline{G}}_E(\underline{r}_t,\underline{r}_t';k_t^2) = \frac{\underline{E}_v(\underline{r}_t;k_t)\underline{E}_v^{\wedge}(\underline{r}_t';k_t)}{-j\omega\mu_o \int_{-\infty}^{\infty} dx \underline{R}\underline{E}_v(x,0;k_t)\times \underline{H}_v(x,0;k_t).\hat{y}} \qquad (3.2.1)$$

with the vectors $\underline{E}_v(\underline{r}_t;k_t) = \begin{pmatrix} E_{vx}(\underline{r}_t;k_t) \\ E_{vz}(\underline{r}_t;k_t) \end{pmatrix}$ defined by the orthogonality condition;

$$-j\omega\mu \int_{-\infty}^{\infty} dx \underline{R}\underline{E}_\mu(x,0;k_t) \times \underline{H}_v(x,0;k_t).\hat{y} = -j\delta_{\mu v} P_v(1 - jcot\alpha_v(k_t)) \qquad (3.2.2)$$

and;

$$(\nabla_t^2 + k_t^2)\underline{E}_v(\underline{r}_t;k_t) = \underline{0} \qquad : y > 0$$

The electric fields may be expressed as a superposition of a plane waves;

$$\underline{E}_v(\underline{r}_t;k_t) = \int_0^{\infty} dk_x \underline{\underline{\phi}}(k_x,x) e^{-jk_y y} \underline{\tilde{e}}_v(k_x) \qquad : k_y^2 = k_t^2 - k_x^2 \qquad (3.2.3)$$

The odd and even modes,w.r.t. x,may be analysed separately.For the even modes;

$$\underline{\underline{\phi}}(k_x,x) = \left(\frac{2}{\pi}\right)^{\frac{1}{2}} \begin{pmatrix} \cos k_x x & 0 \\ 0 & \sin k_x x \end{pmatrix} \qquad (3.2.4)$$

It is a simple task to show that the magnetic fields transverse to y may be derived in terms of the Fourier amplitudes,$\underline{\tilde{e}}_v(k_x)$,in equation (3.2.3).

$$-\begin{pmatrix} H_{vz}(\underline{r}_t;k_t) \\ H_{vx}(\underline{r}_t;k_t) \end{pmatrix} = \int_0^{\infty} dk_x \underline{\underline{\phi}}(k_x,x) \frac{e^{-jk_y y}}{\omega\mu_o} \underline{\underline{Y}}(k_x) \underline{\tilde{e}}_v(k_x) \qquad (3.2.5)$$

where;

$$k_y \underline{\underline{Y}}(k_x) = \begin{pmatrix} k_t^2 & -j\beta k_x \\ j\beta k_x & k_o^2 - k_x^2 \end{pmatrix} \qquad (3.2.6)$$

This derivation and further observations upon the form of $\underline{\underline{Y}}(k_x)$ shall be considered in more detail in the chapter concerning the inset dielectric guide.

The amplitude vectors,$\underline{\tilde{e}}_v(k_x)$,are determined from the interface fields by;

$$\underline{\tilde{e}}_v(k_x) = \int_{-\infty}^{\infty} dx\, \underline{\underline{\phi}}(k_x,x)\underline{E}_v(x,0;k_t) \tag{3.2.7}$$

Although it is obvious that for the modes,the electric fields transverse to y are zero at the ground plane,it is recalled that this boundary condition has not yet been imposed.

Substituting equations (3.2.5) and (3.2.7) into equation (3.2.2) permits the orthogonality condition to be written as;

$$-j\omega\mu_o \int_{-\infty}^{\infty} dx R\underline{E}_\mu(x,0;k_t) \times \underline{H}_v(x,0;k_t).\hat{y} = -j\int_{-\infty}^{\infty} dx \int_{-\infty}^{\infty} dx' R\underline{E}_\mu(x,0;k_t) \int_0^{\infty} dk_x\, \underline{\underline{\phi}}(k_x,x)\underline{\underline{Y}}(k_x)\underline{\underline{\phi}}(k_x,x')\underline{E}_v(x',0;k_t)$$

$$= -j\delta_{\mu v} P_v(k_t)(1 - jcot\alpha_v(k_t)) \tag{3.2.8}$$

For the lossless case the the application of the similarity transformation that redefines both $R\underline{E}_\mu(\underline{r}_t;k_t)$ and $\underline{E}_v(\underline{r}_t;k_t)$ to be of the form $\begin{pmatrix} E_{vx}(\underline{r}_t;k_t) \\ \partial z E_{vz}(\underline{r}_t;k_t) \end{pmatrix}$ reduces the admittance matrices to a real symmetric form.This allows the observation that the terms $R\underline{E}_\mu(x,0;k_t)\underline{\underline{\phi}}(k_x)\underline{\underline{Y}}(k_x)\underline{\underline{\phi}}(k_x)\underline{E}_v(x,0;k_t)$ are purely real or imaginary,dependent solely upon the phase of k_y,to be made.The eigenvalue equation may therefore be written as;

$$cot\alpha_v(k_t) \int_{-\infty}^{\infty} dx \int_{-\infty}^{\infty} dx' R\underline{E}_\mu(x,0;k_t) \int_0^{k_t} dk_x\, \underline{\underline{\phi}}(k_x,x)\underline{\underline{Y}}(k_x)\underline{\underline{\phi}}(k_x,x')\underline{E}_v(x',0;k_t)$$

$$= -\int_{-\infty}^{\infty} dx \int_{-\infty}^{\infty} dx' R\underline{E}_\mu(x,0;k_t) \int_{k_t}^{\infty} dk_x\, \underline{\underline{\phi}}(k_x,x)\underline{\underline{Y}}(k_x)\underline{\underline{\phi}}(k_x,x')\underline{E}_v(x',0;k_t) \tag{3.2.9}$$

In general this eigenvalue equation must be solved by means of a numerical technique such as Galerkin's method.However the separable nature of this particular example permits analytical solutions to be found.

If the eigenvalue equation,(3.2.8),is re-expressed in terms of the vectors,$\tilde{\underline{e}}_v(k_x)$,we obtain;

$$\cot\alpha_v(k_t)\int_0^{k_t} dk_x R\tilde{\underline{e}}_\mu(k_x)\underline{\underline{Y}}(k_x)\tilde{\underline{e}}_v(k_x) = -\int_{k_t}^{\infty} dk_x R\tilde{\underline{e}}_\mu(k_x)\underline{\underline{Y}}(k_x)\tilde{\underline{e}}_v(k_x) \qquad (3.2.10)$$

and two features may then be observed.

i) The matrix $\underline{\underline{Y}}(k_x)$,given by (3.2.6),has eigenvalues k_o^2 and k_y^2 corresponding to the eigenvectors;

$$\frac{\begin{pmatrix} k_x \\ -j\beta \end{pmatrix}}{(k_x^2+\beta^2)^{\frac{1}{2}}} \qquad \frac{\begin{pmatrix} -j\beta \\ k_x \end{pmatrix}}{(k_x^2+\beta^2)^{\frac{1}{2}}}$$

and adjoint eigenvectors;

$$\frac{\begin{pmatrix} k_x \\ j\beta \end{pmatrix}}{(k_x^2+\beta^2)^{\frac{1}{2}}} \qquad \frac{\begin{pmatrix} j\beta \\ k_x \end{pmatrix}}{(k_x^2+\beta^2)^{\frac{1}{2}}} \qquad (3.2.11)$$

ii) Secondly the 1st and 2nd kind of Chebyshev polynomials;

$$\tilde{g}_n(k_x) = \frac{2}{\sqrt{\pi}} T_{2n}\left(\frac{k_x}{k_t}\right) \quad : \quad \tilde{f}_n(k_x) = \frac{2}{\sqrt{\pi}} U_{2n+1}\left(\frac{k_x}{k_t}\right) \qquad (3.2.12)$$

are the solutions to;

$$\int_0^{k_t} dk_x \frac{\tilde{g}_n(k_x)\tilde{g}_m(k_x)}{k_y} = \delta_{nm} \quad : \quad \int_0^{k_t} dk_x \tilde{f}_n(k_x)\tilde{f}_m(k_x)k_y = \delta_{nm} \qquad (3.2.13)$$

The first observation is a statement of the fact that an arbitrary field may be expressed as the sum of an L.S.E. and an L.S.M. component.This property is independent of the structure involved,although in general it is not possible for purely L.S.E and L.S.M. modes to exist.However for the simple grounded half

space the second observation suggests that it is possible to derive analytic expressions,based upon the L.S.E/L.S.M. decomposition.

Naturally,any two linearly independent combinations of the L.S.E and L.S.M. vectors may be taken as a basis for the interface fields in the k_x domain,and upon consideration of (3.2.12),we form the combinations;

$$\underline{\tilde{e}}^{h}_{v}(k_x)=\frac{k_x T_{2v}(\frac{k_x}{k_t})}{k_t(k_x^2+\beta^2)^{\frac{1}{2}}}\left[\begin{pmatrix}k_x\\-j\beta\end{pmatrix}+j\frac{\beta}{k_x}\begin{pmatrix}-j\beta\\k_x\end{pmatrix}\right] \qquad :k_x\le k_t \qquad :T.E. \qquad (3.2.14)$$

$$\underline{\tilde{e}}^{e}_{v}(k_x)=\frac{j\beta k_y^2 U_{2v+1}(\frac{k_x}{k_t})}{k_t k_o(k_x^2+\beta^2)^{\frac{1}{2}}}\left[\begin{pmatrix}k_x\\-j\beta\end{pmatrix}+\frac{k_x^2 k_o^2}{j\beta k_y^2}\begin{pmatrix}-j\beta\\k_x\end{pmatrix}\right] \qquad :k_x\le k_t \qquad :T.M. \qquad (3.2.15)$$

As indicated,these combinations give rise to $T.E^z$ and $T.M^z$ fields respectively.It is a simple task to demonstrate that $\underline{\tilde{e}}^{e}(k_x)$ and $\underline{\tilde{e}}^{m}(k_x)$ are orthogonal,w.r.t. $\underline{\underline{Y}}(k_x)$ for all values of k_x and,in addition,equation (3.2.12) guarantees the orthogonality between functions of the same type.

The interface fields in the space domain may be recovered by inverting equation (3.2.7),although in this case it is possible to use equation (2.4.55) to identify the modes in a closed form for all $\underline{r}_t$.

It is well known that the fields of the T.E. and T.M. modes may be completely specified by the H_z and E_z components respectively,which in this case are given in the k_x domain by;

$$\tilde{h}^{h}_{vz}(k_x)=k_t^{\frac{1}{2}}T_{2v}(\frac{k_x}{k_t}) \qquad :k_x\le k_t \qquad :T.E. \qquad (3.2.16)$$

$$\tilde{e}^{e}_{vz}(k_x)=\frac{k_t^{\frac{1}{2}}}{k_o}U_{2v+1}(\frac{k_x}{k_t}) \qquad :k_x\le k_t \qquad :T.M. \qquad (3.2.17)$$

Equation (2.4.55) subsequently identifies the fields in the space domain to be;

$$H^h_{vz}(\underline{r}_t;k_t) = k_t(\frac{2}{\pi})^{\frac{1}{2}}\int_0^{k_t} dk_x(\frac{2}{\pi})^{\frac{1}{2}}\cos k_x x\ \cos k_y y\ T_{2v}(\frac{k_x}{k_t}) \qquad :T.E. \qquad (3.2.18)$$

$$E^e_{vz}(\underline{r}_t;k_t) = k_t(\frac{2}{\pi})^{\frac{1}{2}}\int_0^{k_t} dk_x(\frac{2}{\pi})^{\frac{1}{2}}\sin k_x x\ \sin k_y y\ U_{2v+1}(\frac{k_x}{k_t}) \qquad :T.M. \qquad (3.2.19)$$

which may be shown to be equivalent to;

$$H^h_{vz}(\underline{r}_t;k_t) = k_t^2(-1)^v \sin v\theta J_{2v}(k_t r) \qquad :T.E. \qquad (3.2.20)$$

$$E^e_{vz}(\underline{r}_t;k_t) = k_t^2(-1)^v \sin(v+1)\theta J_{2v+1}(k_t r) \qquad :T.M. \qquad (3.2.21)$$

The order of Chebyshev polynomials has been chosen so as to satisfy the boundary conditions on the ground plane.

Equations (3.2.20) and (3.2.21) are the familiar expressions for the grounded half space,although it is noted that the modes are not normalised in a scalar sense,rather in a vector sense as previously discussed.

It was mentioned that there exists two alternative representations for the continuous modes of the ground plane.The second,rectangular coordinate representation,is developed from the identity;

$$\int_0^{\infty} dk_x \delta(k_x - k_x')\delta(k_x - k_x'') = \delta(k_x' - k_x'') \qquad (3.2.22)$$

as an alternative to equation (3.2.13).Using equation (3.2.22),leads to the following,alternative,set of modes for the grounded half space;

$$\underline{E}^h(\underline{r}_t;k_t,k_x) = \frac{\begin{pmatrix} -j\beta \\ k_x \end{pmatrix}}{(k_x^2 + \beta^2)^{\frac{1}{2}}}(k_t\frac{2}{\pi})^{\frac{1}{2}}\underline{\underline{\phi}}(k_x,x)\sin k_y y \qquad :L.S.E. \qquad (3.2.23)$$

$$\underline{E}^e(\underline{r}_t;k_t,k_x) = \frac{\begin{pmatrix} k_x \\ j\beta \end{pmatrix}}{(k_x^2+\beta^2)^{\frac{1}{2}}}(k_t\frac{2}{\pi})^{\frac{1}{2}}\underline{\underline{\phi}}(k_x,x)\sin k_y y \qquad :L.S.M. \qquad (3.2.24)$$

3.2.2) The Grounded Dielectric Slab.

As a second separable example,consider the grounded dielectric slab illustrated in figure (3.2.2);

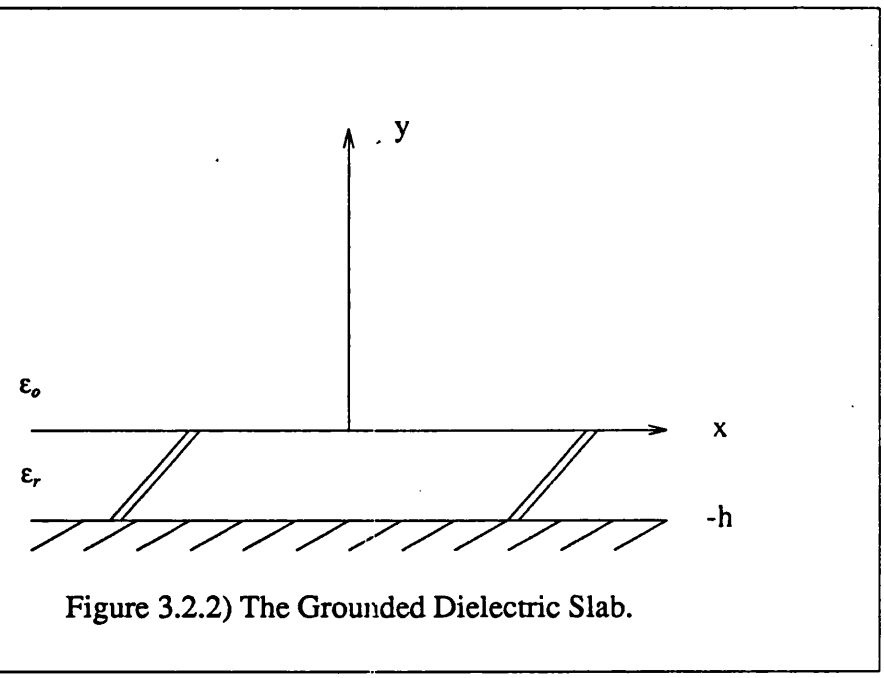

Figure 3.2.2) The Grounded Dielectric Slab.

Unlike the previous example,this structure is inhomogeneous and is is only separable in rectangular coordinates.

As before,the fields in the open region may be expressed by a superposition of plane waves;

$$\underline{E}_v^+(\underline{r}_t;k_t) = \int_0^\infty dk_x \underline{\underline{\phi}}(k_x,x)e^{-jk_y y}\underline{\tilde{e}}(k_x) \qquad :k_y^2 = k_t^2 - k_x^2 \qquad (3.2.25)$$

with $\underline{\underline{\phi}}(k_x,x)$ defined as above,and;

$$\underline{\tilde{e}}(k_x) = \int_{-\infty}^{\infty} \underline{\underline{\phi}}(k_x,x)\underline{E}_v(x,0;k_t) \tag{3.2.26}$$

The fields in the dielectric slab may be expressed as a superposition of standing waves;

$$\underline{E}_v^-(\underline{r}_t;k_t) = \int_0^{\infty} dk_x \underline{\underline{\phi}}(k_x,x)\frac{\sin(q(y+h))}{\sin(qh)}\underline{\tilde{e}}(k_x) \qquad :q^2 = k_t^2(\varepsilon_r-1)k_o^2-k_x^2 \tag{3.2.27}$$

Clearly,as required; $\underline{E}_v^+(x,0,k_t) = \underline{E}_v^-(x,0;k_t)$.

The magnetic fields transverse to $\hat{y}$ in each region,may be written in the form;

$$\underline{H}_v^+(\underline{r}_t;k_t)\times\hat{y} = \int_0^{\infty} dk_x \underline{\underline{\phi}}(k_x,x)e^{-jk_y y}\underline{\underline{Y}}^+(k_x)\frac{\tilde{e}_v(k_x)}{\omega\mu_o} \tag{3.2.28}$$

$$\underline{H}_v^-(\underline{r}_t;k_t)\times\hat{y} = \int_0^{\infty} dk_x \underline{\underline{\phi}}(k_x,x)\frac{\sin(q(y+h))}{\sin(qh)}\underline{\underline{Y}}^-(k_x)\frac{\tilde{e}_v(k_x)}{\omega\mu_o} \tag{3.2.29}$$

with $\underline{\underline{Y}}^+(k_x)$ defined in equation (3.2.6) and $\underline{\underline{Y}}^-(k_x)$ given by;

$$\underline{\underline{Y}}^-(k_x) = \begin{pmatrix} k_t^2+(\varepsilon_r-1)k_o^2 & -j\beta k_x \\ j\beta k_x & \varepsilon_r k_o^2-k_x^2 \end{pmatrix}\frac{cotqh}{q} \tag{3.2.30}$$

For the lossless case,the discussion in the previous section concerning the similarity transform still applies,and noting that $\frac{cotqh}{q}$ is real if q is either real or imaginary,allows the eigenvalue equation to be formulated as;

$$cot\alpha_v(k_t)\int_{-\infty}^{\infty} dx \int_{-\infty}^{\infty} dx' R\underline{E}_\mu(x,0;k_t)\int_0^{k_t} \underline{\underline{\phi}}(k_x,x)\underline{\underline{Y}}^+(k_x)\underline{\underline{\phi}}(k_x,x')\underline{E}_v(x',0;k_t)$$

$$= \int_{-\infty}^{\infty} dx \int_{-\infty}^{\infty} dx' R\underline{E}_\mu(x,0;k_t)\int_0^{\infty} \underline{\underline{\phi}}(k_x,x)\underline{\underline{Y}}^-(k_x)cot(qh)\underline{\underline{\phi}}(k_x,x')\underline{E}_v(x',0;k_t)$$

$$-\int_{-\infty}^{\infty} dx \int_{-\infty}^{\infty} dx' R \underline{E}_{\mu}(x,0;k_t) \int_{k_t}^{\infty} \underline{\underline{\phi}}(k_x,x) \underline{\underline{Y}}^{+}(k_x) \underline{\underline{\phi}}(k_x,x') \underline{E}_{\nu}(x,'0;k_t) \qquad (3.2.31)$$

The separable nature of the interface again allows analytic solutions to be found,most simply if the eigenvalue equation is re-expressed in terms of $\underline{\tilde{e}}_{\nu}(k_x)$;

$$cot\alpha_{\nu}(k_t) \int_{0}^{k_t} dk_x R \underline{\tilde{e}}_{\mu}(k_x) \underline{\underline{Y}}^{+}(k_x) \underline{\tilde{e}}_{\nu}(k_x) = \int_{0}^{\infty} dk_x R \underline{\tilde{e}}_{\mu}(k_x) \underline{\underline{Y}}^{-}(k_x) \underline{\tilde{e}}_{\nu}(k_x)$$

$$-\int_{k_t}^{\infty} dk_x R \underline{\tilde{e}}_{\mu}(k_x) \underline{\underline{Y}}^{+}(k_x) \underline{\tilde{e}}_{\nu}(k_x) = P_{\nu}(k_t) cot\alpha_{\nu}(k_t) \qquad (3.2.32)$$

Although the eigenvectors of the matrix $\underline{\underline{Y}}^{-}(k_x)$ are the same as those of $\underline{\underline{Y}}^{+}(k_x)$,the eigenvalues differ,$\varepsilon_r k_o^2$ and q^2 for $\underline{\underline{Y}}^{-}(k_x)$ corresponding to k_o^2 and k_y^2 for $\underline{\underline{Y}}^{+}(k_x)$.The common eigenvectors suggests that pure L.S.E. and L.S.M. modes may exist and it shall now be shown that this is indeed the case.

Consider letting;

$$\underline{\tilde{e}}_{\nu}^{e}(k_x) = \delta(k_x - \nu) \frac{\begin{pmatrix} k_x \\ -j\beta \end{pmatrix}}{(k_x^2+\beta^2)^{\frac{1}{2}}} \qquad :L.S.M. \qquad (3.2.33)$$

$$\underline{\tilde{e}}_{\nu}^{h}(k_x) = \delta(k_x - \nu) \frac{\begin{pmatrix} -j\beta \\ k_x \end{pmatrix}}{(k_x^2+\beta^2)^{\frac{1}{2}}} \qquad :L.S.E. \qquad (3.2.34)$$

If $\nu \leq k_t$,then substituting these expressions into equation (3.2.32) gives;

$$cot\alpha_{\nu}^{e}(k_t) \frac{k_o^2}{k_y} = \frac{\varepsilon_r k_o^2}{q} cotqh \qquad :L.S.M. \qquad (3.2.35)$$

$$cot\alpha_{\nu}^{h}(k_t) \frac{k_y^2}{k_y} = \frac{q^2}{q} cotqh \qquad :L.S.E. \qquad (3.2.36)$$

ie;

$$\varepsilon_r k_y(\nu;k_t)\tan\alpha_\nu^e(k_t) = q(\nu;k_t)\tan q(\nu;k_t)h \quad ;P_\nu^e(k_t) = \frac{k_o^2}{k_y}\delta(\nu-\nu') \quad :L.S.M. \tag{3.2.37}$$

$$k_y(\nu;k_t)\cot\alpha_\nu^h(k_t) = q(\nu;k_t)\cot q(\nu;k_t)h \quad ;P_\nu^h(k_t) = k_y\delta(\nu-\nu') \quad :L.S.E. \tag{3.2.38}$$

Clearly for all positive real values of k_t there exists a continuous distribution of solutions characterised by $\nu, 0 \le \nu \le k_t$.These solutions constitute the continuum of the structure.

The continuous eigenfunctions may be identified from equation (2.4.55) as;

$$\underline{E}_\nu^e(\underline{r}_t;k_t) = \left(\frac{2k_tk_y}{k_o\pi}\right)^{\frac{1}{2}}\begin{pmatrix}k_x\\-j\beta\end{pmatrix}\underline{\underline{\phi}}(\nu,x)\sin(k_ty+\alpha_\nu^e(k_t)) \qquad :L.S.M.\ ,\ y\ge 0$$

$$\underline{E}_\nu^e(\underline{r}_t;k_t) = \left(\frac{2k_tk_y}{k_o\pi}\right)^{\frac{1}{2}}\begin{pmatrix}k_x\\-j\beta\end{pmatrix}\underline{\underline{\phi}}(\nu,x)\frac{\sin(q(y+h))}{\sin(qh)}\sin\alpha_\nu^e(k_t) \qquad :L.S.M.\ ,\ y\le 0 \tag{3.2.39}$$

$$\underline{E}_\nu^h(\underline{r}_t;k_t) = \left(\frac{2k_t}{k_y\pi}\right)^{\frac{1}{2}}\begin{pmatrix}-j\beta\\k_x\end{pmatrix}\underline{\underline{\phi}}(\nu,x)\sin(k_ty+\alpha_\nu^h(k_t)) \qquad :L.S.E.\ ,\ y\ge 0$$

$$\underline{E}_\nu^h(\underline{r}_t;k_t) = \left(\frac{2k_t}{k_y\pi}\right)^{\frac{1}{2}}\begin{pmatrix}-j\beta\\k_x\end{pmatrix}\underline{\underline{\phi}}(\nu,x)\frac{\sin(q(y+h))}{\sin(qh)}\sin\alpha_\nu^h(k_t) \qquad :L.S.E.\ ,\ y\le 0 \tag{3.2.40}$$

In addition to the continuous spectrum,there also exists the possibility of a discrete spectrum.A point in the discrete spectrum is characterised by the vanishing of both sides of equation (3.2.32).Consider letting;

$$\underline{\tilde{e}}_s^e(k_x) = \delta(k_x-s)\frac{\begin{pmatrix}k_x\\-j\beta\end{pmatrix}}{(k_x^2+\beta^2)^{\frac{1}{2}}} \qquad :L.S.M. \tag{3.2.41}$$

$$\underline{\tilde{e}}_s^h(k_x) = \delta(k_x - s)\frac{\begin{pmatrix} -j\beta \\ k_x \end{pmatrix}}{(k_x^2+\beta^2)^{\frac{1}{2}}} \qquad :L.S.E. \tag{3.2.42}$$

with $s>k_t$.Clearly the L.H.S of equation (3.2.32) vanishes identically,and the R.H.S. will also vanish if;

$$\frac{\varepsilon_r cot(qh)}{q} = \frac{1}{|k_y|} \qquad :L.S.M. \tag{3.2.43}$$

$$qcot(qh) = |k_y| \qquad :L.S.E. \tag{3.2.44}$$

As expected,these conditions will only be satisfied by a discrete set of values of k_t for each value of s.The solution of these equations has been discussed by many authors,for example [1].

Equation (2.4.50) shows that the normalisation of the discrete surface modes requires the evaluation of;

$$-j\omega\mu_o \int_{-\infty}^{\infty} dx \frac{\partial}{\partial k_t^2}\left[\underline{RE}_s(\underline{r}_t;k_t) \times \underline{H}_s(\underline{r}_t;k_t).\hat{y}\right]_{y=0-}^{y=0+} \tag{3.2.45}$$

This is quite simple to perform,although somewhat lengthy,and the result shall just be quoted as it has been presented elsewhere,[2].

Equation (2.4.50) allows the discrete eigenfunctions to be identified as;

$$\underline{E}_s^e(\underline{r}_t;k_t) = \frac{\begin{pmatrix} k_x \\ -j\beta \end{pmatrix}\underline{\underline{\phi}}(k_x,x)e^{-|k_y|}}{\left(\frac{k_o^2}{2k_y^3} - \frac{\varepsilon_r k_o^2}{2q^3}(qsec(qh) - cot(qh))\right)^{\frac{1}{2}}} \qquad :L.S.M. \quad ,y\geq 0$$

$$\underline{E}_s^e(\underline{r}_t;k_t) = \frac{\begin{pmatrix} k_x \\ -j\beta \end{pmatrix}\underline{\underline{\phi}}(k_x,x)\frac{sin(q(y+h))}{sin(qh}}{\left(\frac{k_o^2}{2k_y^3} - \frac{\varepsilon_r k_o^2}{2q^3}(qsec(qh) - cot(qh))\right)^{\frac{1}{2}}} \qquad :L.S.M. \quad ,y\leq 0 \tag{3.2.46}$$

$$\underline{E}_s^h(\underline{r}_t;k_t)=\frac{\begin{pmatrix}-j\beta\\ k_x\end{pmatrix}\underline{\underline{\phi}}(k_x,x)e^{-|k_y|}}{\left(\frac{1}{2k_y}-\frac{1}{2q}(q\sec(qh)-\cot(qh))\right)^{\frac{1}{2}}} \qquad :L.S.E. \quad ,y\geq 0$$

$$\underline{E}_s^h(\underline{r}_t;k_t)=\frac{\begin{pmatrix}-j\beta\\ k_x\end{pmatrix}\underline{\underline{\phi}}(k_x,x)\frac{\sin(q(y+h))}{\sin(qh}}{\left(\frac{1}{2k_y}-\frac{1}{2q}(q\sec(qh)-\cot(qh))\right)^{\frac{1}{2}}} \qquad :L.S.E. \quad ,y\leq 0 \qquad (3.2.47)$$

3.3) A field Matching approach to the Continuous Spectrum.

This section shall discuss an alternative field matching approach that may be used to determine the continuous mode functions.Although the mode functions recovered are identical to those obtained from the characteristic Green's function method,the approach is conceptually simpler and,in certain circumstances,such as for lossy structures,may be easier to formulate.The field matching approach cannot strictly be regarded as independent from the characteristic Green's function as it assumes 'a priori' some results so far only proved by the characteristic Green's function method.For example it is assumed that the continuous eigenfunctions are characterised by k_t lying in the range $0 \leq k_t \leq \infty$.In fact the proof of orthogonality and the correct normalisation using the field matching approach,may so far,only be achieved by integrating the Poynting vector over the guide cross-section,which is a cumbersome process.

The field matching approach may be succinctly summarised by stating that the modes must satisfy the homogeneous wave equation and have electric and magnetic fields that are transversally continuous at any interface.Therefore the electric fields transverse to y are expanded in each region by a superposition of solutions to the homogeneous wave equation and continuity applied at the interface.

For example consider the grounded dielectric slab discussed in the previous section.In the open region the source free nature of the modes requires that the electric fields must be represented by a superposition of standing and exponentially damped waves,ie;

$$\underline{E}_v^+(\underline{r}_t;k_t) = \int_0^{k_t} dk_x \underline{\underline{\phi}}(k_x,x)\sin(k_y y+\alpha_v(k_t))\tilde{\underline{e}}_v(k_x)$$

$$+ \int_{k_t}^{\infty} dk_x \underline{\underline{\phi}}(k_x,x)e^{-|k_y|}\sin\alpha_v(k_t)\tilde{\underline{e}}_v(k_x) \qquad (3.3.1)$$

The connection with the characteristic Green's function method is immediately apparent if equation (3.3.1) is compared with equations (3.1.39) and (3.1.40).The fields in the dielectric are similarly expanded as;

$$\underline{E}_v^-(\underline{r}_t;k_t) = \int_0^{\infty} dk_x \underline{\underline{\phi}}(k_x,x)\frac{\sin(q(y+h))}{\sin(qh)}\sin\alpha_v(k_t)\tilde{\underline{e}}_v(k_x) \qquad (3.3.2)$$

and clearly the electric fields transverse to y are continuous across the interface.Exactly as before,the transverse to y magnetic fields in each region may be written in terms of admittance operators acting upon the electric fields.The admittance operator for the dielectric region will be identical to that given in equation (3.1.30),whereas that for the open region at the interface will be given by;

$$k_y \underline{\underline{Y}}^+(k_x) = \begin{pmatrix} k_t^2 & -j\beta k_x \\ j\beta k_x & k_o^2-k_x^2 \end{pmatrix} cot\alpha_v(k_t) \qquad :k_x \le k_t$$

$$|k_y| \underline{\underline{Y}}^+(k_x) = \begin{pmatrix} k_t^2 & -j\beta k_x \\ j\beta k_x & k_o^2-k_x^2 \end{pmatrix} \qquad :k_x \ge k_t \qquad (3.3.3)$$

Clearly if the continuity of the magnetic fields transverse to y is enforced,then the same eigenvalue equation,derived by the characteristic Green's

function method,defining $cot\alpha_v(k_t)$ and $\underline{E}_v(k_t)$ will be obtained.

Besides conceptual simplicity,the field matching method may be simpler to apply to lossy structures.It is recalled that $cot\alpha_v(k_t)$ is defined by the characteristic Green's function method as a real quantity and that the modes are constructed from contributions from either side of a branch cut,which in the lossless case are conjugates.Additionally,the lossless case always leads to admittance matrices which may be transformed into real symmetric forms,therefore allowing the real and imaginary parts of the orthogonality condition to be separated by inspection.However,for the lossy case this is not so and it may be difficult to formulate the eigenvalue equation.Also the contributions from either side of the branch cut are not conjugates which complicates the identification of the mode functions.

Consider the lossy case from a field matching point of view.The eigenvalue equation would be formulated exactly as before,except that now the eigenvalues,$cot\alpha_v(k_t)$,will be complex.With this in mind,it is possible to redefine $cot\alpha_v(k_t)$ in the characteristic Green's function method to allow lossy structures to be tackled more straightforwardly.It is recalled that $cot\alpha_v(k_t)$ has been defined in section 2.6 by;

$$-j\omega\mu_o \int_{-\infty}^{\infty} dx \left[R\underline{E}_\mu(\underline{r}_t;k_t) \times \underline{H}_v(\underline{r}_t;k_t).\hat{y} \right]_{y=0-}^{y=0+} = -j\delta_{\mu v} P_v(k_t)(1 - jcot\alpha_v(k_t))$$

$$= -j\delta_{\mu v}(P_v(k_t) - jQ_v(k_t)) \qquad (3.3.4)$$

In the lossless case,$P_v(k_t) - jQ_v(k_t)$ consists of three terms,a real term due to propagating plane waves in the open region,an imaginary term due to non-propagating plane waves in the open region and an imaginary term due to standing waves in the bound region.Clearly $P_v(k_t)$ is given solely by the plane waves in the

open region.However in the lossy case all plane waves in the open region and standing waves in the bound region contribute to both the real and imaginary parts.The ability to formulate the eigenvalue equation by inspection in the lossless case,relies on the dependence of $P_v(k_t)$ solely upon the propagating plane waves in the open region.If $P_v(k_t)$ is redefined as the contribution from the propagating plane waves,rather than the real part,and $-jP_v(k_t)cot\alpha_v(k_t)$ as the contribution from the non-propagating plane waves and the standing waves in the bound region,then the eigenvalue equation may again be formulated by inspection and the characteristic Green's function is conjugated on either side of the branch cut.However $cot\alpha_v(k_t)$ is now complex,as observed in the field matching approach.

3.4) Pure Polarisation.

The two separable examples that have been examined both exhibited an L.S.E./L.S.M. or a T.E./T.M. decomposition of the modes.This is a common feature of separable structures and it is reasonable to assume such a decomposition from the outset.This reduces the eigenvalue equation to a scalar form which is easier to handle than the more general matrix form.

In general,inhomogeneous,nonseparable structures may not possess modes with pure L.S.E./L.S.M. or T.E./T.M. polarisations,however it shall be shown that even for nonseparable structures the hybrid modes are divided into L.S.E. and L.S.M. dominated modes.It may be the case that pure L.S.E. and L.S.M. approximations to the modes may prove adequate in certain circumstances,in which case these approximations may also be developed from the simpler scalar eigenvalue equation.

3.5) References.

1) R.Collin,"Field Theory of Guided Waves",McGraw Hill,1960.

2) T.Rozzi and L.Ma,"Mode completeness,Normalisation and Green's Function of the Inset Dielectric Guide",IEEE trans. microwave theory and techniques,vol MTT-36,no 3,Mar 88,pp542-551.

CHAPTER 4.

THE CONTINUOUS SPECTRUM OF THE INSET DIELECTRIC GUIDE.

4.1) Introduction.

The Inset Dielectric Guide,(I.D.G.),was introduced in chapter 1 as a dielectric waveguide possessing excellent potential for both millimeter wave propagation and leaky-wave antenna applications.

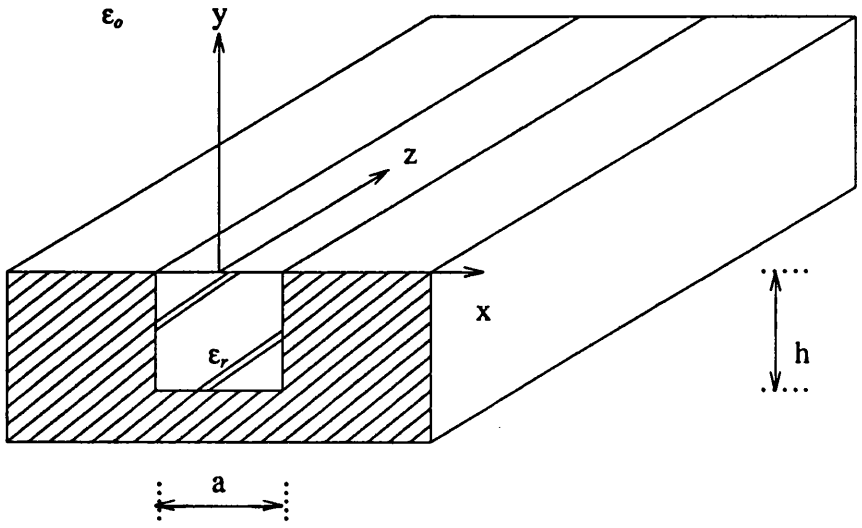

Figure 4.1) The Inset Dielectric Guide.

The objective of this chapter is to construct the transverse characteristic Green's function of the I.D.G. using the method presented in chapter 2 and to

identify its continuous modes.The following two chapters shall then use these modes to analyse rectangular waveguide to I.D.G. transitions and radiating antenna elements respectively.

In common with most open dielectric waveguides,the I.D.G. is nonseparable in the transverse plane.This ensures that the modes of the I.D.G. are hybrid and therefore not amenable to identification by the separation of variables.Transverse resonance has successfully recovered the discrete surface modes,[1],although to date,the continuous modes have not been rigorously determined.Previously a partial wave expansion of the continuous modes was proposed and subsequently used to analyse radiating strips on the I.D.G.,[2-5].However it shall now be demonstrated that this expansion is *fundamentally inconsistent with the boundary conditions.*

The partial wave expansion assumed that each continuous mode comprised of a single,purely polarised,standing wave in the open region.This standing wave,expressed in the form of a y-directed Hertzian potential proportional to $\hat{y}\phi_h(k_x,x)\sin(k_y y+\alpha(k_x,k_y))$,was coupled by continuity at the nonseparable interface to a summation of standing waves in the slot.A scalar transverse characteristic Green's function was constructed,containing the net complex power leaving the interface in the denominator.

This last step is indeed similar to the method presented in chapter 2.However,recall that the transverse characteristic Green's function is required to be the solution of the transverse wave equation with a point source at the interface.As the standing wave in the open region and those in the slot are local solutions of the transverse wave equation and the transverse characteristic Green's function,$G_E(\underline{r}_t,\underline{r}_t';k_t)$,has a discontinuous derivative w.r.t. y at the interface,this reduces to the requirement that;

$$\left[\partial y G_E(\underline{r}_t,\underline{r}_t';k_t)\right]_{y=y-0}^{y=y+0} = -\delta(x-x') \qquad (4.1.1)$$

(for a scalar transverse characteristic Green's function.)

As stressed in chapter 2,this is not an identity,rather a necessary condition on $G_E(\underline{r}_t,\underline{r}_t';k_t)$,if it is indeed the correct transverse characteristic Green's function.However,the form proposed for $G_E(\underline{r}_t,\underline{r}_t';k_t)$,cannot actually satisfy equation (4.1.1).This was not realised and it was believed that integrating equation (4.1.1) w.r.t x' would recover the phase shift of the standing wave in the open region.In fact,upon examination of the orthonormalisation by direct integration of the modes over the guide cross-section,given in [4],the Fourier transform of (4.1.1) was recovered,which again could not be rigorously satisfied.

This is basically due to the fact that the partial wave expansion does not satisfy all the boundary conditions of the guide,specifically that of the ground plane into which the slot is recessed,although in [5] this boundary condition was imposed upon the field as a whole.

It is necessary to note at this stage,that although the earlier method is similar in some aspects to that presented in chapter 2,the latter not only treats the analogous equation to (4.1.1.) correctly,but is also a dyadic method that yields the rigorous hybrid modes of the guide.

The next section shall derive the rigorous hybrid modes of the I.D.G. by constructing the correct dyadic transverse characteristic Green's function.

4.2) Formulation of the Transverse Characteristic Green's Function for the Inset Dielectric Guide.

4.2.1) The fields in the Open Region.

The two examples given in chapter 3 have shown that the fields in the open

region of an open waveguide may be expressed by a superposition of plane waves.In both examples the magnetic and electric fields transverse to y,were linked by means of admittance operators.The derivation of these admittance operators shall be shown in more detail in this section.

It is possible to derive the admittance operators by two different approaches.Clearly Maxwell's equations may be used to relate the electric and magnetic fields,but it is also possible to derive the relationship by the introduction of Hertzian Potentials.The latter method is interesting as it shows that the hybrid fields may be expressed by a superpostion of purely L.S.E. and L.S.M. polarised fields,rotated about the y axis.

Without loss of generality,the electric and magnetic fields may be derived from the following pair of y directed Hertzian potentials;

$$\underline{\Pi}_e^+(\underline{r}_t;k_t) = \hat{y}\int_0^\infty dk_x \frac{\phi_e(k_x,x)e^{-jk_y y}}{j\omega\varepsilon(k_x^2+\beta^2)^{\frac{1}{2}}}\tilde{I}(k_x) \quad : \quad \phi_e(k_x,x) = (\frac{2}{\pi})^{\frac{1}{2}}\cos(k_x x) \tag{4.2.1}$$

$$\underline{\Pi}_h^+(\underline{r}_t;k_t) = \hat{y}\int_0^\infty dk_x \frac{\phi_h(k_x,x)e^{-jk_y y}}{j\omega\mu(k_x^2+\beta^2)^{\frac{1}{2}}}\tilde{V}(k_x) \quad : \quad \phi_h(k_x,x) = (\frac{2}{\pi})^{\frac{1}{2}}\sin(k_x x) \tag{4.2.2}$$

where $\underline{\Pi}_e^+(\underline{r}_t;k_t)$ and $\underline{\Pi}_h^+(\underline{r}_t;k_t)$ are electric and magnetic type Hertzian potentials respectively.The functions $\phi_e(k_x,x)$ and $\phi_h(k_x,x)$ have been chosen to give E_x components that are odd w.r.t. x.

The electric and magnetic fields are given by;

$$\underline{E}^+(\underline{r}_t;k_t) = -j\omega\mu\nabla\times\underline{\Pi}_h^+(\underline{r}_t;k_t) + (k^2 + \nabla\nabla.)\underline{\Pi}_e^+(\underline{r}_t;k_t)$$

$$\underline{H}^+(\underline{r}_t;k_t) = j\omega\varepsilon\nabla\times\underline{\Pi}_e^+(\underline{r}_t;k_t) + (k^2 + \nabla\nabla.)\underline{\Pi}_h^+(\underline{r}_t;k_t) \tag{4.2.3}$$

Substituting equations (4.2.1) and (4.2.2) into equation (4.2.3) gives;

$$\begin{pmatrix} E_x(\underline{r}_t;k_t) \\ -E_z(\underline{r}_t;k_t) \end{pmatrix} = \int_0^{\infty} \frac{dk_x}{(k_x^2+\beta^2)^{\frac{1}{2}}} \begin{pmatrix} \phi_h(k_x,x) & 0 \\ 0 & \phi_e(k_x,x) \end{pmatrix} \begin{pmatrix} k_x & -j\beta \\ -j\beta & k_x \end{pmatrix} \begin{pmatrix} \frac{k_y}{\omega\varepsilon} & 0 \\ 0 & 1 \end{pmatrix} \begin{pmatrix} \tilde{I}(k_x) \\ \tilde{V}(k_x) \end{pmatrix}$$

$$-\begin{pmatrix} H_z(\underline{r}_t;k_t) \\ H_x(\underline{r}_t;k_t) \end{pmatrix} = \int_0^{\infty} \frac{dk_x}{(k_x^2+\beta^2)^{\frac{1}{2}}} \begin{pmatrix} \phi_h(k_x,x) & 0 \\ 0 & \phi_e(k_x,x) \end{pmatrix} \begin{pmatrix} k_x & -j\beta \\ -j\beta & k_x \end{pmatrix} \begin{pmatrix} 1 & 0 \\ 0 & \frac{k_y}{\omega\mu} \end{pmatrix} \begin{pmatrix} \tilde{I}(k_x) \\ \tilde{V}(k_x) \end{pmatrix} \quad (4.2.4)$$

The terms $\frac{k_y}{\omega\varepsilon}$ and $\frac{k_y}{\omega\mu}$ are recognised as the characteristic impedance and admittance, $z_e(k_x)$ and $y_h(k_x)$, of purely polarised L.S.M. and L.S.E. fields propagating in the y direction. The matrix $\underline{\underline{T}}(k_x)$, defined by;

$$\underline{\underline{T}}(k_x) = \frac{\begin{pmatrix} k_x & -j\beta \\ -j\beta & k_x \end{pmatrix}}{(k_x^2+\beta^2)^{\frac{1}{2}}} = \begin{pmatrix} \cos\theta & -j\sin\theta \\ -j\sin\theta & \cos\theta \end{pmatrix} \quad (4.2.5)$$

performs a coordinate rotation about the y axis in the k_x domain. Using these two notations, the electric and magnetic fields, transverse to y, may be linked by an admittance operator of the form;

$$-\begin{pmatrix} H_z(\underline{r}_t;k_t) \\ H_x(\underline{r}_t;k_t) \end{pmatrix} = \int_{-\infty}^{\infty} dx' \, \underline{\underline{Y}}(x,x';k_t) \begin{pmatrix} E_z(\underline{r}_t;k_t) \\ -E_z(\underline{r}_t;k_t) \end{pmatrix} \quad (4.2.6)$$

with the kernel, $\underline{\underline{Y}}(x,x';k_t)$ given by;

$$\underline{\underline{Y}}(x,x';k_t) = \int_0^{\infty} dk_x \begin{pmatrix} \phi_h(k_x,x) & 0 \\ 0 & \phi_e(k_x,x) \end{pmatrix} \underline{\underline{T}}(k_x) \begin{pmatrix} y_e(k_x) & 0 \\ 0 & y_h(k_x) \end{pmatrix} \underline{\underline{T}}^{-1}(k_x) \begin{pmatrix} \phi_h(k_x,x') & 0 \\ 0 & \phi_e(k_x,x') \end{pmatrix} \quad (4.2.7)$$

and;

$$\underline{\underline{T}}^{-1}(k_x) = \begin{pmatrix} \cos\theta & j\sin\theta \\ j\sin\theta & \cos\theta \end{pmatrix} \quad (4.2.8)$$

The kernel acts upon the electric fields as follows. The integration w.r.t. x' of the product of $\begin{pmatrix} \phi_h(k_x,x') & 0 \\ 0 & \phi_e(k_x,x') \end{pmatrix}$ and the electric field vector, transforms the

latter from the space domain to the k_x domain.The matrix $\underline{\underline{T}}^{-1}(k_x)$ determines from the amplitudes of the electric fields in the k_x domain,the amplitudes of its L.S.E. and L.S.M. components.The matrix $\begin{pmatrix} y_e(k_x) & 0 \\ 0 & y_h(k_x) \end{pmatrix}$ subsequently determines the amplitudes of the transverse magnetic fields for each polarisation separately,which are then recombined into the hybrid form by the matrix $\underline{\underline{T}}(k_x)$.Finally the magnetic fields are transformed back to the space domain.

The interesting step in the process is the decomposition by the matrix $\underline{\underline{T}}^{-1}(k_x)$ of the hybrid field into its L.S.E. and L.S.M. components.This may be viewed in two ways.It was shown in chapter 3 that the transverse electric fields for L.S.M. and L.S.E. polarisations are proportional to the vectors;

$$\frac{\begin{pmatrix} k_x \\ -j\beta \end{pmatrix}}{(k_x^2+\beta^2)^{\frac{1}{2}}} \quad :L.S.M. \qquad \frac{\begin{pmatrix} -j\beta \\ k_x \end{pmatrix}}{(k_x^2+\beta^2)^{\frac{1}{2}}} \quad :L.S.E. \tag{4.2.9}$$

It is therefore not surprising that a matrix whose columns are the adjoint vectors to those of equation (4.2.9),ie $\underline{\underline{T}}^{-1}(k_x)$,identifies the amplitudes of the L.S.E. and L.S.M. components of a hybrid field.

An alternative view is to consider the geometrical notation introduced in equation (4.2.5),[6].The two vectors given in equation (4.2.9) define a coordinate system for the plane perpendicular to y,in the k_x domain and upon which the transverse electric fields may be mapped.In general this coordinate system will not coincide with the x-z coordinate system used to characterise the structure.The matrix $\underline{\underline{T}}^{-1}(k_x)$ transforms a vector given in the x-z coordinate system to its equivalent representation in the L.S.E./L.S.M. coordinate system by performing a rotation about the y axis,as illustrated in figure (4.2).

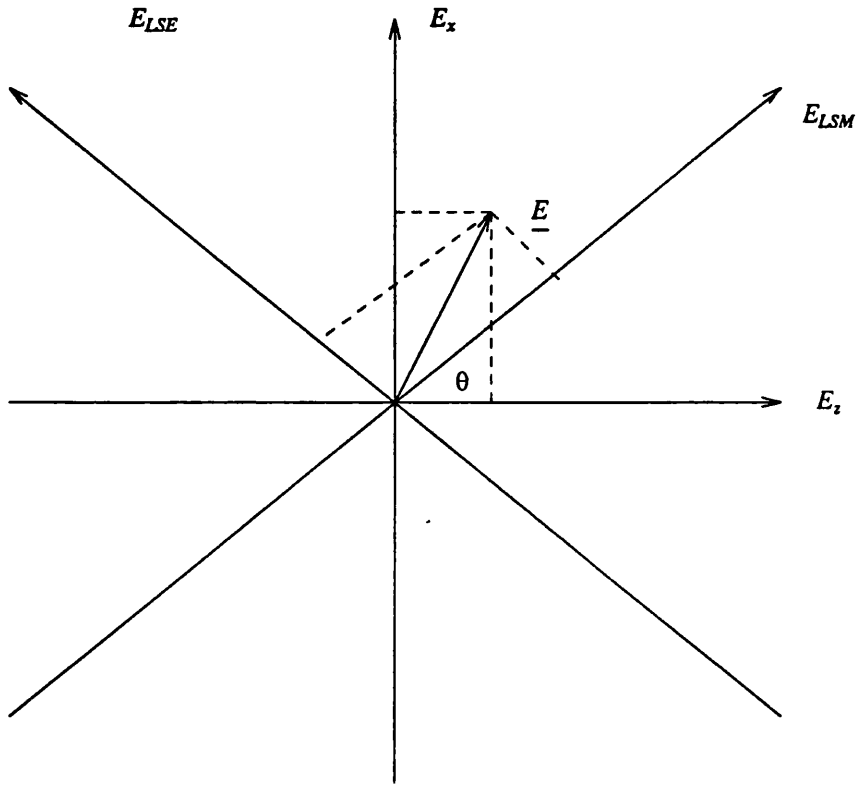

Fig 4.2) Coordinate rotation about the y axis in the k_x domain

Formulation of the transverse characteristic Green's function requires the evaluation of the quantity;

$$-j\omega\mu \int_{-\infty}^{\infty} dx \left[R\underline{E}_{\mu}(\underline{r}_t;k_t) \times \underline{H}_{v}(\underline{r}_t;k_t) \cdot \hat{y} \right]_{y=0+}$$

$$= -j\omega\mu_o \int_{-\infty}^{\infty} dx \begin{pmatrix} E_{\mu x}(x,0^+;k_t) & -E_{\mu z}(x,0^+;k_t) \end{pmatrix} \begin{pmatrix} -H_{vz}(x,0^+;k_t) \\ H_{vx}(x,0^+;k_t) \end{pmatrix} \qquad (4.2.10)$$

It is convenient to deal with quantities that are all of the same parity,ie odd or even,w.r.t. x,and therefore equation (4.2.10) shall be expressed in the form;

$$-j\omega\mu\int_{-\infty}^{\infty}dx\left[R\underline{E}_{\mu}(\underline{r}_t;k_t)\times\underline{H}_{v}(\underline{r}_t;k_t)\,.\,\hat{y}\right]_{y=0+}$$

$$=j\omega\mu_o\int_{-\infty}^{\infty}dx\begin{pmatrix}E_{\mu x}(x,0^+;k_t) & -\partial xE_{\mu z}(x,0^+;k_t)\end{pmatrix}\begin{pmatrix}H_{vz}(x,0^+;k_t)\\ \int dxH_{vx}(x,0^+;k_t)\end{pmatrix} \qquad (4.2.11)$$

With this in mind,the expression for $H_x(\underline{r}_t;k_t)$ in equation (4.2.6) is integrated w.r.t. x and the integration w.r.t. x' of $\phi_e(k_x,x)E_z(\underline{r}_t,k_t)$ is performed by parts to give;

$$-\begin{pmatrix}H_{vz}(\underline{r}_t;k_t)\\ \int dxH_{vz}(\underline{r}_t;k_t)\end{pmatrix}=\int_{-\infty}^{\infty}dx'\int_{0}^{\infty}dk_x\phi_h(k_x,x)\begin{pmatrix}1 & 0\\ 0 & \frac{1}{k_x}\end{pmatrix}\underline{\underline{T}}(k_x)\begin{pmatrix}y_e(k_x) & 0\\ 0 & y_h(k_x)\end{pmatrix}$$

$$\underline{\underline{T}}^{-1}(k_x)\begin{pmatrix}1 & 0\\ 0 & \frac{1}{k_x}\end{pmatrix}\phi_h(k_x,x')\begin{pmatrix}E_{vx}(\underline{r}_t',k_t)\\ \partial x'E_{vz}(\underline{r}_t',k_t)\end{pmatrix} \qquad (4.2.12)$$

thus allowing equation (4.2.11) to be written as;

$$-j\omega\mu\int_{-\infty}^{\infty}dx\left[R\underline{E}_{\mu}(\underline{r}_t;k_t)\times\underline{H}_{v}(\underline{r}_t;k_t)\,.\,\hat{y}\right]_{y=0+}=-j\omega\mu_o\int_{-\infty}^{\infty}dx\int_{-\infty}^{\infty}dx'\begin{pmatrix}E_{\mu x}(x,0^+;k_t) & \partial xE_{\mu z}(x,0^+;k_t)\end{pmatrix}\begin{pmatrix}1 & 0\\ 0 & -1\end{pmatrix}$$

$$\int_{0}^{\infty}dk_x\phi_h(k_x,x)\begin{pmatrix}1 & 0\\ 0 & \frac{1}{k_x}\end{pmatrix}\underline{\underline{T}}(k_x)\begin{pmatrix}y_e(k_x) & 0\\ 0 & y_h(k_x)\end{pmatrix}\underline{\underline{T}}^{-1}(k_x)\phi_h(k_x,x')\begin{pmatrix}E_{vx}(x',0^+,k_t)\\ \partial x'E_{vz}(x',0^+,k_t)\end{pmatrix} \qquad (4.2.13)$$

Noting that the reflection operator,R,has been included as the term $\begin{pmatrix}1 & 0\\ 0 & -1\end{pmatrix}$Equation (4.2.13) may be expressed more succinctly as;

$$-j\omega\mu\int_{-\infty}^{\infty}dx\left[R\underline{E}_{\mu}(\underline{r}_t;k_t)\times\underline{H}_{v}(\underline{r}_t;k_t)\,.\,\hat{y}\right]_{y=0+}=-j\int_{-\infty}^{\infty}dx\int_{-\infty}^{\infty}dx'\begin{pmatrix}E_{\mu x}(x,0^+;k_t) & \partial xE_{\mu z}(x,0^+;k_t)\end{pmatrix}$$

$$\left[\int_{0}^{k_t}dk_x\phi_h(k_x,x)\underline{\underline{Y}}(k_x)\phi_h(k_x,x')+j\int_{k_t}^{\infty}dk_x\phi_h(k_x,x)\underline{\underline{Y}}(k_x)\phi_h(k_x,x')\right]\begin{pmatrix}E_{vx}(x',0^+,k_t)\\ \partial x'E_{vz}(x',0^+,k_t)\end{pmatrix} \qquad (4.2.14)$$

where $\underline{\underline{Y}}(k_x)$ is given by;

$$\frac{k_y}{|k_y|}\underline{\underline{Y}}(k_x)=\omega\mu_o\begin{pmatrix} y_e(k_x)\cos^2\theta+y_h\sin^2\theta & j\cos\theta\sin\theta\dfrac{(y_e-y_h)}{k_x} \\ j\cos\theta\sin\theta\dfrac{(y_e-y_h)}{k_x} & \dfrac{-(y_e\sin^2\theta+y_h\cos^2\theta)}{k_x^2}\end{pmatrix} \tag{4.2.15}$$

ie;

$$|k_y|\underline{\underline{Y}}(k_x)=\begin{pmatrix} k_t^2 & j\beta \\ j\beta & \dfrac{-(k_o^2-k_x^2)}{k_x^2}\end{pmatrix} \tag{4.2.16}$$

4.2.2) The fields in the Slot region.

The fields in the slot region may similarly be developed from the y directed electric and magnetic Hertzian potentials;

$$\underline{\Pi}_e^-(\underline{r}_t;k_t)=\hat{y}\sum_{n=1,3,\ldots}^{\infty}\frac{\phi_{en}(x)\cos(q_n(y+h))}{j\omega\varepsilon(k_x^2+\beta^2)^{\frac{1}{2}}\cos(q_nh)}I_n \quad ; \quad \phi_{en}(x)=\frac{2}{\sqrt{a}}\cos(\frac{n\pi}{a}x) \tag{4.2.17}$$

$$\underline{\Pi}_h^-(\underline{r}_t;k_t)=\hat{y}\sum_{n=1,3,\ldots}^{\infty}\frac{\phi_{hn}(x)\sin(q_n(y+h))}{j\omega\mu(k_x^2+\beta^2)^{\frac{1}{2}}\sin(q_nh)}V_n \quad ; \quad \phi_{hn}(x)=\frac{2}{\sqrt{a}}\sin(\frac{n\pi}{a}x) \tag{4.2.18}$$

where $q_n^2=k^2-(\frac{n\pi}{a})^2-\beta^2=(\varepsilon_r-1)k_o^2+k_t^2-(\frac{n\pi}{a})^2$.

As before the magnetic fields,transverse to y, may be expressed by means of an admittance operator;

$$-\begin{pmatrix} H_{vz}(\underline{r}_t;k_t) \\ \int dx H_{vx}(\underline{r}_t;k_t)\end{pmatrix}=\int_{-\infty}^{\infty}dx'\sum_{n=1,3\ldots}^{\infty}\phi_{hn}(x)\begin{pmatrix}1 & 0\\ 0 & \dfrac{1}{\frac{n\pi}{a}}\end{pmatrix}\underline{\underline{T}}_n\begin{pmatrix}y_{en} & 0\\ 0 & y_{hn}\end{pmatrix}\underline{\underline{T}}_n^{-1}\begin{pmatrix}1 & 0\\ 0 & \dfrac{1}{\frac{n\pi}{a}}\end{pmatrix}$$

$$\phi_{hn}(k_x,x')\begin{pmatrix}E_{vx}(\underline{r}_t',k_t)\\ \partial x' E_{vz}(\underline{r}_t';k_t)\end{pmatrix} \tag{4.2.19}$$

where;

$$\underline{\underline{T}}_n = \begin{pmatrix} \frac{n\pi}{a} & -j\beta \\ -j\beta & \frac{n\pi}{a} \end{pmatrix} = \begin{pmatrix} \cos\theta' & -j\sin\theta' \\ -j\sin\theta' & \cos\theta' \end{pmatrix} \tag{4.2.20}$$

and

$$\begin{pmatrix} y_{en} & 0 \\ 0 & y_{hn} \end{pmatrix} = \begin{pmatrix} j\frac{\omega\varepsilon}{q_n} & 0 \\ 0 & j\frac{q_n}{\omega\mu} \end{pmatrix} cot(q_n(y+h)) \tag{4.2.21}$$

Two observations are immediately apparent.Firstly the matrix $\underline{\underline{T}}_n^{-1}$,that decomposes the hybrid slot fields into their L.S.E. and L.S.M. parts,is different to the matrix $\underline{\underline{T}}^{-1}(k_x)$ performing the same operation in the open region.Although this may be seen as stating the obvious,as the fields in the two regions exist over different x domains,it highlights the fact that purely polarised L.S.E. or L.S.M. modes can not exist.It is recalled that the existence of purely polarised modes on the structures discussed in chapter 3,is dependent upon the proportionality of the L.S.E. and L.S.M. eigenvectors in both regions.Alternatively,it may be argued that if a purely polarised field exists in one region then,as $\theta \neq \theta'$,fields of both polarisations must exist in the other region to ensure continuity at the interface,again precluding the possibility of purely polarised modes.

Secondly it is observed that the standing wave nature of the fields in the slot region is manifested by both the dependence upon y of the characteristic admittances of the L.S.E and L.S.M. fields and the time quadrature,in the lossless case,of the electric and magnetic fields.

In a similar manner to that used before,it is possible to write;

$$-j\omega\mu\int_{-\infty}^{\infty} dx\left[R\underline{E}_\mu(\underline{r}_t;k_t)\times\underline{H}_v(\underline{r}_t;k_t)\,.\,\hat{y}\right]_{y=0_-} = -j\int_{-\infty}^{\infty} dx\int_{-\infty}^{\infty} dx' \sum_{n=1,3...}^{\infty} (E_{\mu x}(x,0^-;k_t)\quad \partial x E_{\mu z}(x,0^-;k_t))$$

$$\phi_{hn}(x)j\underline{\underline{Y}}_n\phi_{hn}(x')\begin{pmatrix} E_{vx}(x',0^-;k_t) \\ \partial x' E_{vz}(x',0^-;k_t)\end{pmatrix} \tag{4.2.22}$$

where;

$$q_n\underline{\underline{Y}}_n = -j\omega\mu_o\begin{pmatrix} y_{en}\cos^2\theta'+y_{hn}\sin^2\theta' & j\dfrac{\cos\theta'\sin\theta'}{(\frac{n\pi}{a})}(y_{en}-y_{hn}) \\ j\dfrac{\cos\theta'\sin\theta'}{(\frac{n\pi}{a})}(y_{en}-y_{hn}) & \dfrac{-(y_{en}\sin^2\theta'+y_{hn}\cos^2\theta')}{(\frac{n\pi}{a})^2}\end{pmatrix} cot(q_nh)$$

$$= \begin{pmatrix} k_t^2+(\varepsilon_r-1)k_o^2 & j\beta \\ j\beta & -\dfrac{(k^2-(\frac{n\pi}{a})^2)}{(\frac{n\pi}{a})^2}\end{pmatrix} cot(q_nh) \tag{4.2.23}$$

4.2.3) Formulation of the Eigenvalue Equation.

Equations (4.2.14) and (4.2.22) permit the eigenvalue equation characterising the modes of the I.D.G. to be written as;

$$\omega\mu_o\int_{-\infty}^{\infty}dx\left[R\underline{E}_\mu(\underline{r}_t;k_t)\times\underline{H}_v(\underline{r}_t;k_t)\cdot\hat{y}\right]_{y=0-}^{y=0+} = P_v(k_t)(1-jcot\alpha_v(k_t))$$

$$= \int_{-\infty}^{\infty}dx\int_{-\infty}^{\infty}dx'(E_{\mu x}(x,0;k_t)\quad \partial xE_{\mu z}(x,0;k_t))$$

$$\left[\int_0^{k_t}dk_x\phi_h(k_x,x)\underline{\underline{Y}}(k_x)\phi_h(k_x,x') + j\int_{k_t}^{\infty}dk_x\phi_h(k_x,x)\underline{\underline{Y}}(k_x)\phi_h(k_x,x') - j\sum_{n=1,3...}^{\infty}\phi_{hn}(x)\underline{\underline{Y}}_n(k_x)\phi_{hn}(x')\right]$$

$$\begin{pmatrix} E_{vx}(x',0;k_t) \\ \partial x' E_{vz}(x',0;k_t)\end{pmatrix} \tag{4.2.24}$$

ie;

$$\cot\alpha_v(k_t)\int_{-\infty}^{\infty}dx\int_{-\infty}^{\infty}dx'(E_{\mu x}(x,0;k_t)\quad \partial xE_{\mu z}(x,0;k_t))\int_0^{k_t}dk_x\phi_h(k_x,x)\underline{\underline{Y}}(k_x)\phi_h(k_x,x')\begin{pmatrix}E_{vx}(x',0;k_t)\\ \partial x'E_{vz}(x',0;k_t)\end{pmatrix}$$

$$=\int_{-\infty}^{\infty}dx\int_{-\infty}^{\infty}dx'(E_{\mu x}(x,0;k_t)\quad \partial xE_{\mu z}(z,0;k_t))\left[\sum_{n=1,3\ldots}^{\infty}\phi_{hn}(x)\underline{\underline{Y}}_n(k_x)\phi_{hn}(x')-\int_{k_t}^{\infty}dk_x\phi_h(k_x,x)\underline{\underline{Y}}(k_x)\phi_h(k_x,x')\right]$$

$$\begin{pmatrix}E_{vx}(x',0;k_t)\\ \partial x'E_{vz}(x',0;k_t)\end{pmatrix} \qquad (4.2.25)$$

with;

$$P_v(k_t)=\int_{-\infty}^{\infty}dx\int_{-\infty}^{\infty}dx'(E_{vx}(x,0;k_t)\quad \partial xE_{vz}(x,0;k_t))\int_0^{k_t}dk_x\phi_h(k_x,x)\underline{\underline{Y}}(k_x)\phi_h(k_x,x')$$

$$\begin{pmatrix}E_{vx}(x',0;k_t)\\ \partial x'E_{vz}(x',0;k_t\end{pmatrix} \qquad (4.2.26)$$

4.2.4) Solution of the Eigenvalue Equation.

Unlike the separable examples examined in chapter 3,the nonseparable nature of the I.D.G. necessitates the solution of the eigenvalue equation,equation (4.2.25),by numerical means.Using Galerkin's method,the transverse electric fields at the interface are expanded by a complete set of basis functions,$\{f_p(x)\}$,and a weight function $W(x)$;

$$\begin{pmatrix}E_{vx}(x,0;k_t)\\ \partial xE_{vz}(x,0;k_t)\end{pmatrix}=W(x)\sum_{p=1}^{N}f_p(x)\underline{E}_{vp}(k_t) \qquad (4.2.27)$$

The choice of basis and weight functions shall be discussed later.If the terms $Q_p(k_x)$ and Q_{pn} are defined as;

$$Q_p(k_x)=\int_{-\infty}^{\infty}dx\phi_h(k_x,x)f_p(x)W(x)$$

$$Q_{pn} = \int_{-\infty}^{\infty} dx \phi_{kn}(x) f_p(x) W(x) \tag{4.2.28}$$

then the eigenvalue equation may be written in the discrete form;

$$cot\alpha_v(k_t)\underline{E}_\mu(k_t)\int_0^{k_t} dk_x \underline{\underline{Q}}(k_x)\underline{\underline{Y}}(k_x)\underline{\underline{Q}}^T(k_x)\underline{E}_v(k_t)$$

$$= \underline{E}_\mu(k_t)\left[\sum_{n=1,3...}^{\infty} \underline{\underline{Q}}_n \underline{\underline{Y}}_n \underline{\underline{Q}}_n^T - \int_{k_t}^{\infty} dk_x \underline{\underline{Q}}(k_x)\underline{\underline{Y}}(k_x)\underline{\underline{Q}}^T(k_x)\underline{E}_v(k_t)\right]\underline{E}_v(k_t) \tag{4.2.29}$$

with;

$$P_v(k_t) = \underline{E}_v(k_t)\int_0^{k_t} dk_x \underline{\underline{Q}}(k_x)\underline{\underline{Y}}(k_x)\underline{\underline{Q}}^T(k_x)\underline{E}_v(k_t) \tag{4.2.30}$$

Equation (4.2.29) is a pencil of quadratics,(often referred to as a generalised eigenvalue equation),of the form;

$$\underline{E}_\mu(k_t) \cdot \underline{\underline{B}} \cdot \underline{E}_v(k_t) = cot\alpha_v(k_t)\underline{E}_\mu(k_t) \cdot \underline{\underline{G}} \cdot \underline{E}_v(k_t) \tag{4.2.31}$$

It is necessary and appropriate at this stage,to consider certain results concerning the solution of such matrix equations.The observations may be divided into two catagories,those concerning the theoretical properties of the solutions and those concerning their numerical determination.

Theoretically,the generalised eigenvalue equation of order N,does not neccessarily possess N eigenvalues.This will only be the case if the matrix $\underline{\underline{G}}$ is of full rank.If $\underline{\underline{G}}$ is rank deficient there may exist a finite,an infinite,or an empty set of eigenvalues [7].Additionally if the matrices $\underline{\underline{G}}$ and $\underline{\underline{B}}$ are self adjoint,ie hermitian or real and symmetric,and either of the two is positive,or negative,definite,then it can be shown that the eigenvalues are purely real.With these points in mind the properties of the matrices $\underline{\underline{B}}$ and $\underline{\underline{G}}$ as defined by equation (4.2.29) shall be

examined.

In the lossless case,as observed in chapter 3,a similarity transform may be applied,redefining $\underline{\underline{B}}$ and $\underline{\underline{G}}$ as real symmetric matrices.Further,again in the lossless case,it may be shown that $\underline{\underline{G}}$ is positive (negative) semi-definite for outgoing (incoming) plane waves in the open region.Obviously $\underline{E}_{\mu}(k_t) \cdot \underline{\underline{G}} \cdot \underline{E}_{\nu}(k_t)$ is only zero if k_t corresponds to a discrete mode.For all values of k_t comprising the continuous spectrum $\underline{\underline{G}}$ is a positive (negative) definite matrix.Thus in the lossless case the matrices $\underline{\underline{G}}$ and $\underline{\underline{B}}$ have the neccessary properties to ensure that the eigenvalue equation of order N will possess N real eigenvalues.

Even though it has been demonstrated that the eigenvalue equation of order N theoretically possesses N eigenvalues,their accurate numerical determination must be carefully considered.It shall be shown later that for a given value of k_t,,the eigenvalues roughly fall into two classes,those of finite amplitude and those tending towards infinity.This appears to be a common feature of nonseparable open structures and highlights a numerical difficulty.The problem is that,whilst the matrix $\underline{\underline{B}}$ is theoretically positive (negative) definite,numerically it is significantly rank deficient,causing the eigenvalue equation to be very ill conditioned.Consequently there are three questions that must be answered.Firstly,how accurately is it actually neccessary to calculate the very large eigenvalues,in other words,can they be regarded as infinite?Secondly,given that these eigenvalues may be ill determined,can the values of the finite amplitude eigenvalues still be trusted?Finally what numerical algorithms are available to tackle such an ill conditioned problem?

The physical interpretation of a very large eigenvalue,is that the interface between the two regions of the structure is effectively behaving as a ground plane,fields only existing in the open region.The relative amplitudes of the

interface fields of these modes,compared to those associated with a finite sized eigenvalue is insignificant,and in most applications may be approximated to zero without any problem.Therefore very large eigenvalues may be treated as infinite.However this still leaves the corresponding eigenvectors,which contribute to the far field,to be determined.This is somewhat more difficult.For the I.D.G. it is observed that the eigenvectors associated with moderately sized eigenvalues are amenable to a fairly simple approximation,which does not deteriorate in validity as the size of the eigenvalue increases.It seems reasonable to assume that this approximation is equally valid for quasi-infinite eigenvalues.

The numerical solution of the generalised eigenvalue equation has received much attention recently as it is a commonly occuring problem in many disciplines,[8].The treatment of ill conditioned problems has also generated much interest,[9-12].It is not proposed to discuss the techniques available in any detail,rather to briefly state the method that has been used and its relevance to the second question posed above.

The numerical rank deficiency of the matrix $\underline{\underline{B}}$ precludes the use of any routine,such as the Cholesky-Housholder-QL algorithm,that requires that $\underline{\underline{B}}$ is positive definite.The method that has been used is a commercially available implementation of the QZ algorithm.This algorithm yields a set of pairs of values,the ratios of which are the required eigenvalues.It is stated,[13],that if the divisor tends towards zero,and thus the eigenvalue towards infinity,no particular problem is presented.However if both values of one pair tend towards zero,then no reliance may be placed in any of the eigenvalues obtained.Fortunately,it is found that this does not occur for the examples examined in this thesis and,with reference to the second question posed above,the finite eigenvalues can be accurately determined.Further confirmation of this may be obtained by varying the

order of the matrix equation.For example,it is observed that if a problem of order N yields M eigenvalues of finite size,then the matrix $\underline{\underline{B}}$ is approximately of numerical rank M.Progressively reducing the order of the problem towards M,thus improving the conditioning of $\underline{\underline{B}}$,does not significantly affect the M finite sized eigenvalues.

Although it has been demonstrated that the eigenvalue equation may be numerically solved with sufficient accuracy to render it a viable proposition,there is certainly scope for further investigation of the numerical techniques used.

4.2.5) Choice of the Interface Field expansion Basis.

The expansion basis used to expand the transverse electric fields at the interface,theoretically defines a functional space of infinite dimension.Obviously in practice,this space must be approximated by one of finite dimension.The rate of convergence of the approximate eigenfunctions towards the true eigenfunctions,as the order of approximation is increased,is significantly affected by the choice of basis functions.Previous work has shown that a basis set that intrinsically incorporates any dominant features known to exist in the modal fields,will converge more rapidly than will an arbitrary basis set,[1].The surface modes of the I.D.G. have been developed by the transverse resonance technique,using the weighted Gegenbauer polynomials as a basis.These were employed because the weight function can be chosen to be of the same order of singularity at the corners of the interface,as that predicted for the electric fields,[14].This choice proved very successful and converged excellently with just a few terms.However analysis of the continuous modes introduces a few complications that do not,in general,arise for the surface modes.

The dimensions of guides analysed for transmission purposes,are usually such that only a small number of surface modes exist at the frequencies of

interest.Consequently the gradient of the fields w.r.t. x,apart from in the region of any singularities,tends to be quite low and the singularities are a prominent feature.However,the continuous modes encompass a wide range of field gradients and it is observed that although the singularities are still present,they are no longer the dominant feature.Obviously,although not as significant as for the surface modes,it should improve the convergence to incorporate the singularities in the basis functions.Whichever basis set is used it is neccessary to use a far larger order of expansion for the continuous modes as used for the surface modes.For example,if it were possible to find a basis set such that each continuum mode may be adequately modelled by a single basis term,(which it is not!),then clearly if M significant modes exist for a given value of k_t,then at least M basis terms must be used.Analysis of discontinuity problems at x-band has shown that M may be of the order of 50 for reasonable accuracy.Although a matrix problem of such an order presents no particular difficulty for the matrix eigenvalue routines,the evaluation of the matrix elements is a time consuming process,Therefore it is attractive to use a basis set that simplifies the computation of the matrix elements.Not surprisingly it is the evaluation of the integrals w.r.t. k_x in equation (4.2.29) that is the bottleneck,as these must be evaluated numerically.If weighted Gegenbauer polynomials are used then the elements of $\underline{Q}(k_x)$ involve Bessel functions,which themselves must be determined numerically.It is apparent that a basis set that optimises computational efficiency and rate of convergence must be used.

Consider using the set $\{\phi_{hp}\}$.Clearly the summation over n in equation (4.2.29) is replaced by a single term,in effect diagonalising the matrix due to the slot terms.The elements of $\underline{Q}(k_x)$ are given by;

$$Q_p(k_x)=2\left(\frac{2}{\pi a}\right)^{\frac{1}{2}}(-1)^{\frac{p-1}{2}}\frac{k_x\cos(\frac{k_x a}{2}x)}{(\frac{p\pi}{a})^2-k_x{}^2} \tag{4.2.32}$$

which are relatively simple to evaluate.A further saving in computational effort may be made by realising that;

$$Q_p(k_x)Q_q(k_x)=2\left(\frac{2}{\pi a}\right)^{\frac{1}{2}}k_x\cos(\frac{k_x a}{2}x)\left[\frac{(-1)^{\frac{q-1}{2}}}{(\frac{q\pi}{a})^2-k_x{}^2}Q_p(k_x)+\frac{(-1)^{\frac{p-1}{2}}}{(\frac{p\pi}{a})^2-k_x{}^2}Q_q(k_x)\right] \tag{4.2.33}$$

which reduces the number of numerical integrations that must be evaluated approximately by a factor of N.This last observation allows the solution of the eigenvalue equation to be obtained reasonably quickly,even though the unspectacular rate of convergence requires the use of a relatively large of expansion terms.Roughly speaking,the number of terms needs to be twice the number of modes sought.

It is interesting to note that the partial diagonalisation of the eigenvalue equation that motivated the use of $\{\phi_{hp}(x)\}$,would be complete if the two regions of the structure shared a common x domain.In fact,this is the spectral domain approach to such problems,[6],that has proved popular for the analysis of printed circuit and multilayer structures.

4.3) Discussion of the Modal Properties of the I.D.G. Continuum.

This section shall present and discuss the properties of the continuous modes obtained by solving the eigenvalue equation developed above.To counter the criticism that the numerical nature of these modes renders them unwieldy,it shall be shown that they may be determined with sufficient accuracy to be a viable proposition,without the need for excessive computational effort.In fact,it shall be

demonstrated that many of the modes may be closely approximated by analytic expressions.

Due to the dependence of the mode functions upon frequency,k_t and ν,not to mention the guide dimensions and its electrical properties,it is possible to generate a myriad of graphs describing the behaviour of the modes.Fortunately most of the interesting properties may be observed from the typical examples that shall be presented here.Although these examples are for a shallow slot guide,the general properties observed are also exhibited by the deep slot guide.

These examples are for an X band,shallow slot I.D.G. of width 22.86mm and depth 10.16mm operating at 10Ghz.The structure has been assumed lossless,as for most discontinuity applications,radiation losses far exceed material losses.The permittivity of the dielectric,P.T.F.E.,has been taken as 2.08.

The interface field components have each been expanded by 40 basis terms giving a matrix equation of order 80.This is somewhat more than it proves necessary to use in practice but it allows the numerical convergence to be fully examined.

It is found that there are two distinct classes of modes.The first,which are characterised by finite sized eigenvalues and fields that exist in the slot,shall be referred to as slot region modes.The second class,the open region modes,possess quasi-infinite eigenvalues and fields that exist almost exclusively in the open region.

The existence of two classes of modes may be intuitively explained by noting that at the 90 degree corners of the guide,there is an apparent contradiction between the boundary conditions required on the slot wall and those required on the metal portion of the interface.Physically this results in field singularities which are similarly indeterminate in terms of both magnitude and gradient.However,it

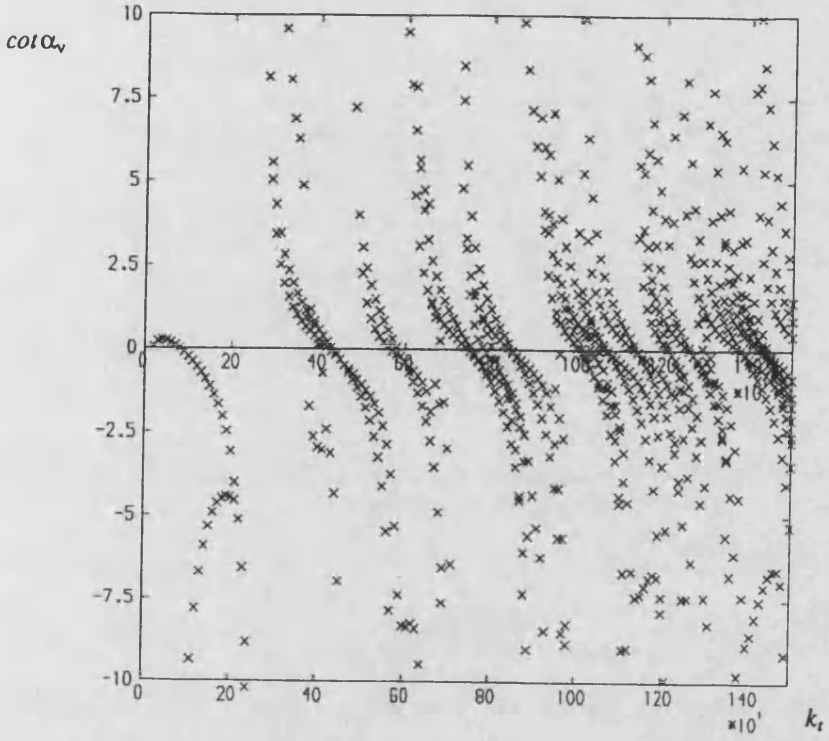

Figure 4.3) Variation of the eigenvalues with k_t.

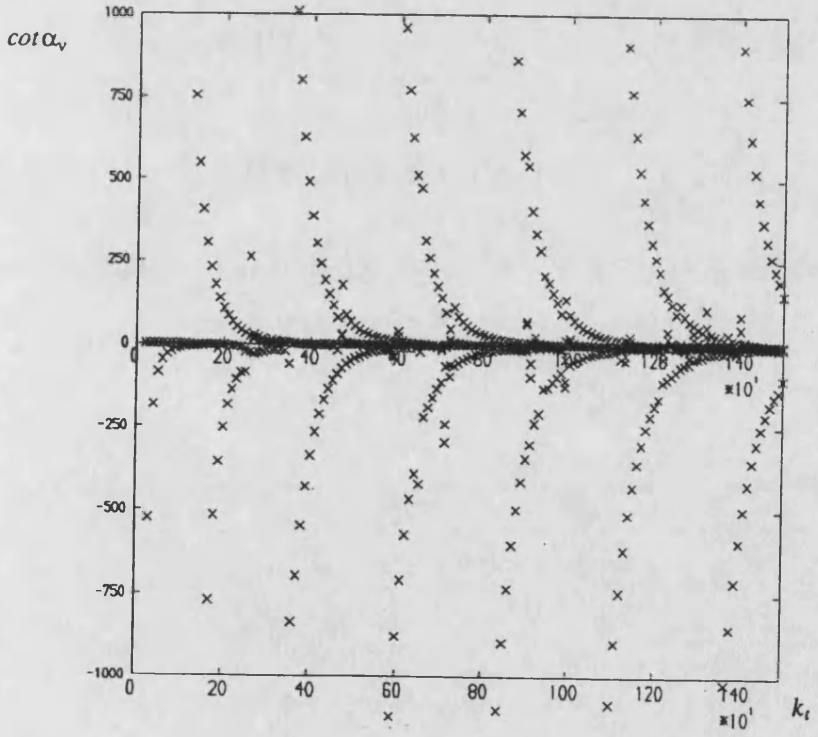

Figure 4.4) Variation of the eigenvalues with k_t.

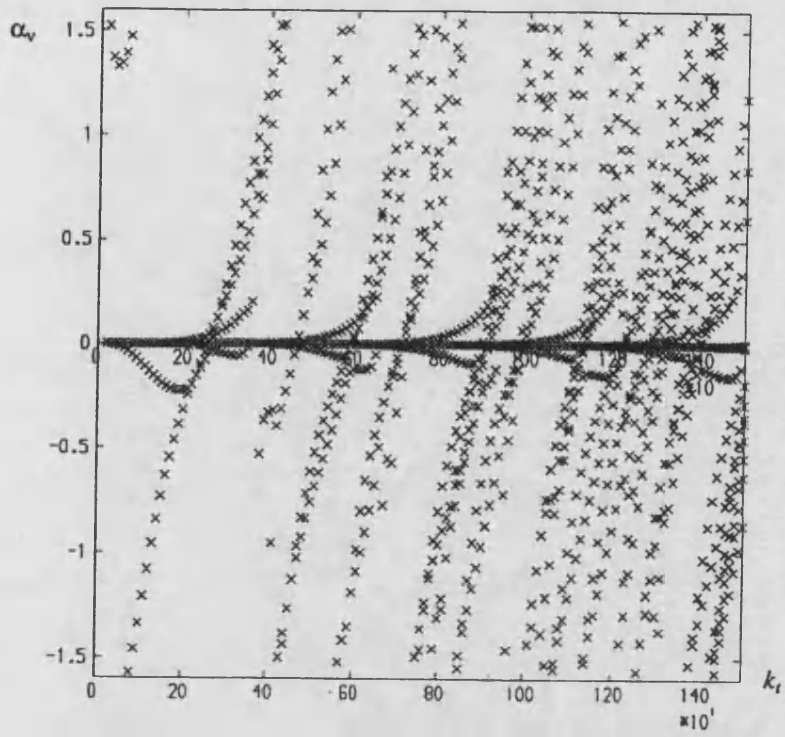

Figure 4.5) Variation of α_v with k_t.

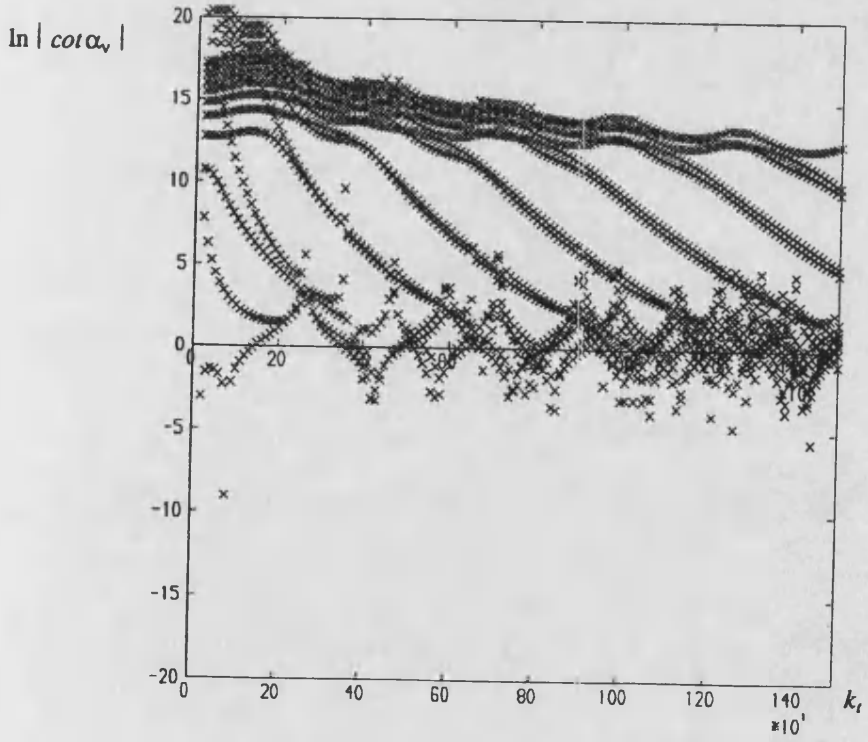

Figure 4.6) Variation of $ln \mid cot\alpha_v \mid$ with k_t.

seems reasonable that one set of boundary conditions could have more influence upon the fields of a mode than the other.This appears to be the case,as,except in the immediate vicinity of the corners,the slot region modes and the open region modes are influenced more by the boundary conditions of the slot and the metal interface respectively.

4.3.1) The slot region modes.

Figure 4.3 shows the variation of the finite magnitude eigenvalues as k_t is varied.It is immediately observed that the number of finite eigenvalues increases with k_t.This feature is even more apparent in figure 4.4,a rescaled version of figure 4.3,in which it can be seen that there appears to be a reasonably well defined 'critical' value of k_t above which each eigenvalue becomes finite.The spacing of these 'critical' values seems to be be very uniform along the k_t axis.It is also observed that the eigenvalues are grouped in pairs of opposite sign,suggesting the existence of L.S.E. and L.S.M. dominated modes.Once finite,each eigenvalue appears to vary approximately as the cotangent of k_t.This would suggest that α_v is proportional to k_t,a supposition confirmed by figure 4.5.

Plots of the interface fields corresponding to the ten lowest eigenvalues with kt=500,are given in appendix A4.1.For convenience two examples are repeated in figures 4.7 and 4.8.These show the two lowest order modes.The phrase 'lowest order' refers to the dominant slot term used to represent the modes,rather than the magnitude of the eigenvalues.In fact,it may seen from the remaining figures in appendix A4.1,that the first six modes all have one basis term that is significantly larger than the rest,and that a pair of modes have the same dominant term.These are examples of the slot region modes and shall be represented by $H.E._n(k_t)$ and $E.H._n(k_t)$,the value of n being odd and identifying the dominant slot term.The dominance of the slot region modes by a single slot term may be clearly

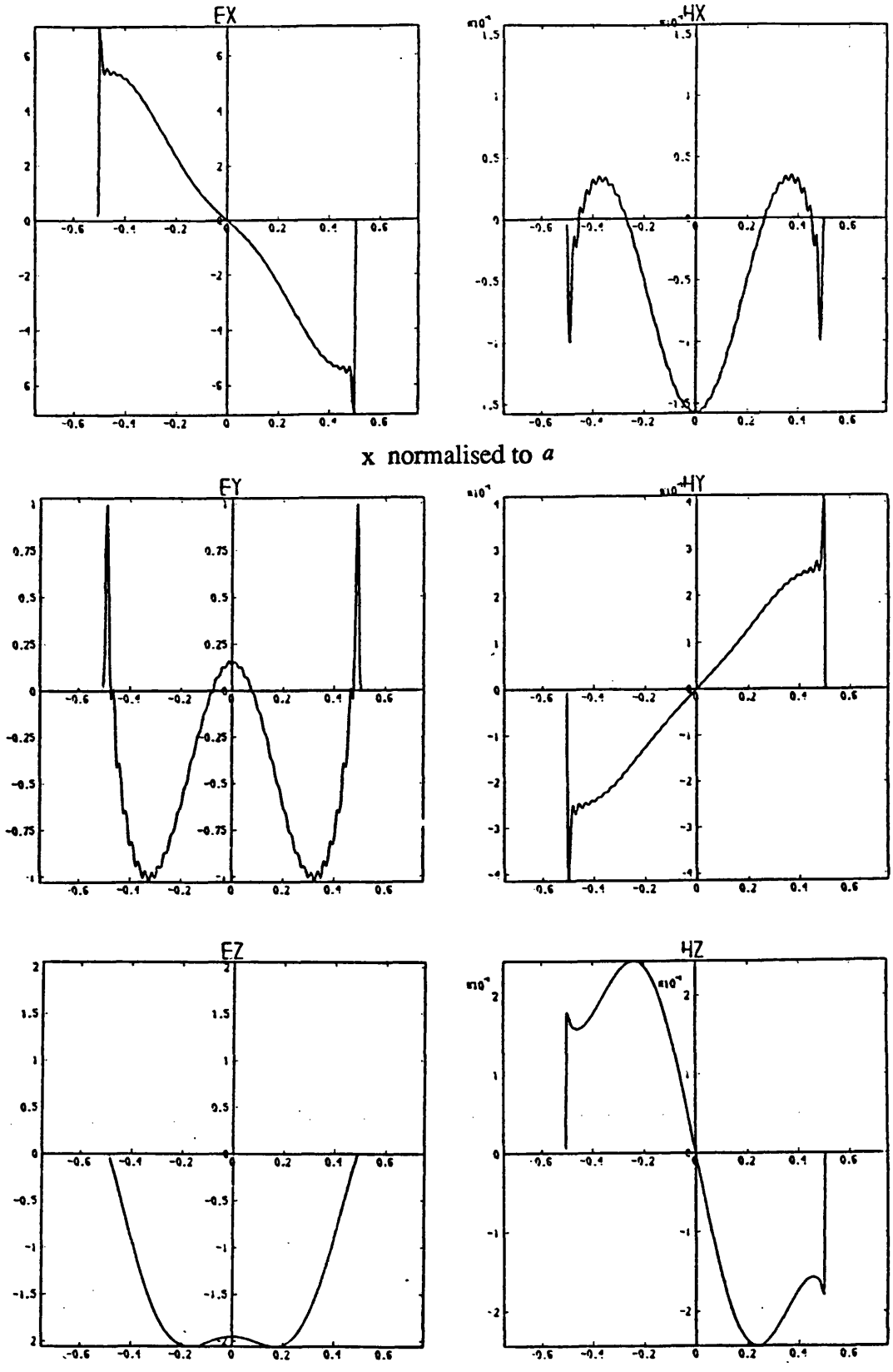

Figure 4.7) The Interface fields of the $HE_{.1}$ mode.

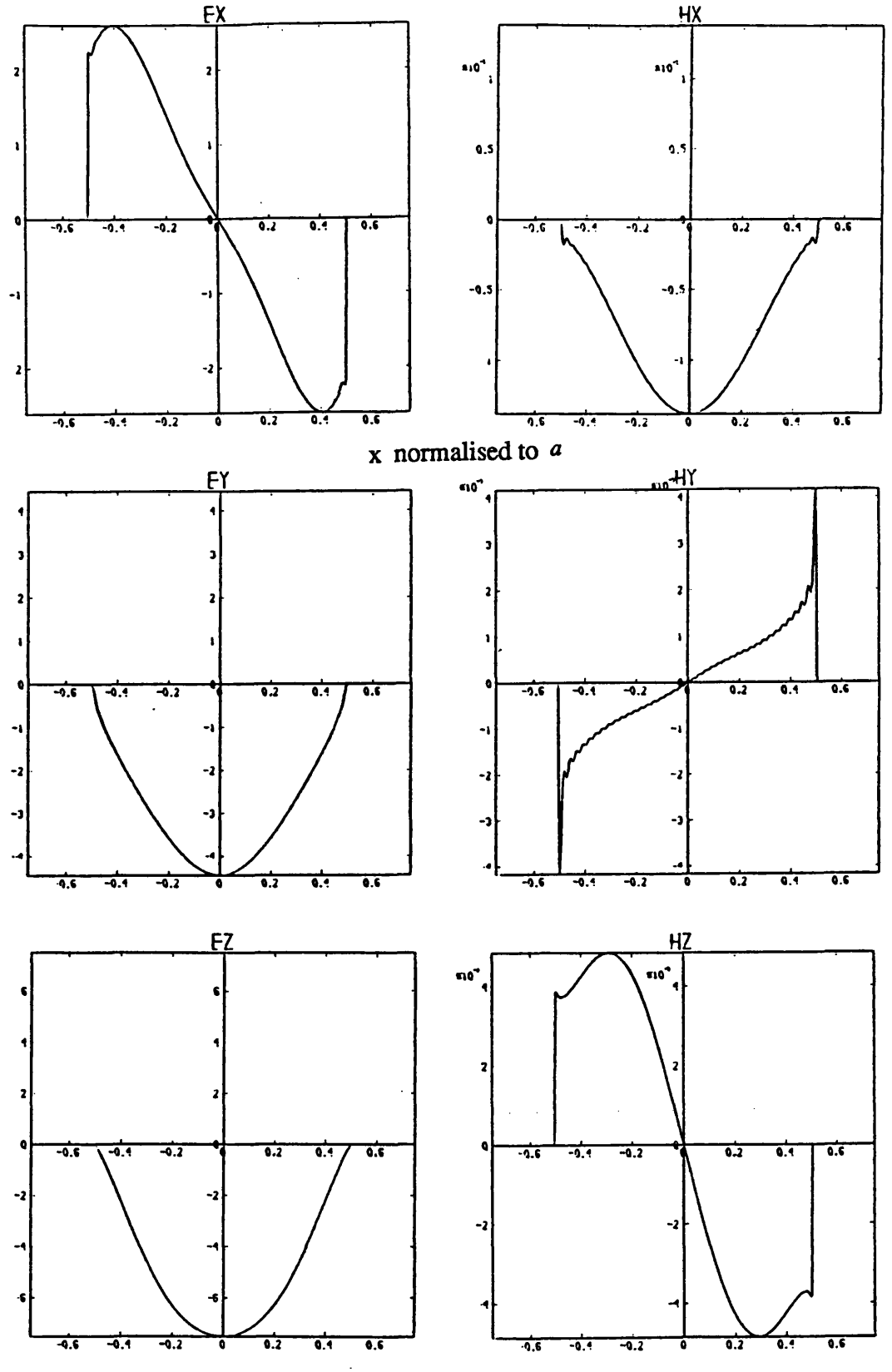

Figure 4.8) The Interface fields of the $E.H._1$ mode.

seen in the figures in appendix A4.2,showing the basis amplitudes for each mode.

The characterisation of a pair of modes by their dominant slot term does not imply that representing them by this single term is acceptable.Even the lowest order pair differ enough from the dominant term to necessitate the use of a moderate number of basis terms.Unfortunately this is a consequence of using a numerically expedient basis.However,when in spite of the significant increase in computational effort,Gegenbauer polynomials were tried as the basis,surprisingly the convergence was not significantly improved.This may be explained by noting that the field singularities occuring at the corners of the guide are very localised and over the slot,the true fields differ significantly from the weighted Gegenbauer polynomials.

The notation introduced above tacitly assumes that the existence of a pair of modes for each value of n indicates the presence of L.S.E.- and L.S.M.-dominated modes.This may be substantiated by examining the relative amplitudes of the field components of such a pair,for example those given in figures 4.7 and 4.8.It is observed that,although the modes may be regarded as L.S.E.- and L.S.M.-dominated,they are still too hybrid to entertain the possibility of using purely polarised approximations to them.In fact 'dominated' may be too strong a word to use in this context.

Although a single term approximation to the slot region modes is not in general an acceptable proposition,it is still necessary to justify the presence of a dominant term and additionally the existence of quasi-L.S.E. and quasi-L.S.M. modes.

The admittance matrices appearing in the eigenvalue equation are of the form $\underline{Q}(k_x)\underline{\underline{Y}}(k_x)\underline{Q}^T(k_x)$.The distinction between the slot region and open region modes may be traced to the properties of the vector $\underline{Q}(k_x)$ characterising the

nonseparable interface.The existence of quasi-L.S.E. and -L.S.M. polarisations for each class of mode is dependent upon both the matrix $\underline{\underline{Y}}(k_x)$ and the vector $\underline{Q}(k_x)$.

The eigensolutions of the matrices $\underline{\underline{Y}}(k_x)$ and $\underline{\underline{Y}}_n$ are no longer purely L.S.E. and L.S.M. solutions.However the L.S.E. and L.S.M. vectors are still orthogonal w.r.t. $\underline{\underline{Y}}(k_x)$ and $\underline{\underline{Y}}_n$ and may be shown to satisfy;

L.S.E.

$$\underline{\underline{Y}}(k_x)\begin{pmatrix}\beta\\ -k_x^2\end{pmatrix}=k_y\begin{pmatrix}\beta\\ -1\end{pmatrix}$$

$$\underline{\underline{Y}}_n\begin{pmatrix}\beta\\ -(\frac{n\pi}{a})^2\end{pmatrix}=q_n\begin{pmatrix}\beta\\ -1\end{pmatrix} \qquad (4.34)$$

L.S.M.

$$\underline{\underline{Y}}(k_x)\begin{pmatrix}1\\ \beta\end{pmatrix}=\frac{k_o^2}{k_y}\begin{pmatrix}1\\ \frac{\beta}{k_x^2}\end{pmatrix}$$

$$\underline{\underline{Y}}_n\begin{pmatrix}1\\ \beta\end{pmatrix}=\frac{\varepsilon_r k_o^2}{q_n}\begin{pmatrix}1\\ \frac{\beta}{(\frac{n\pi}{a})^2}\end{pmatrix} \qquad (4.35)$$

Even though this decomposition is valid for all structures,the existence of quasi-L.S.E. and -L.S.M. modes is not ensured.It is also necessary for the vector $\underline{Q}(k_x)$ to possess certain properties.

The functions $Q_n(k_x)$ are strictly orthogonal from 0 to ∞ in the k_x domain.However they are sufficiently localised about the maximum value,which occurs at $k_x=\frac{n\pi}{a}$,that for $k_t \gg \frac{n\pi}{a}$;

$$\int_0^{k_t} dk_x \frac{Q_n(k_x)Q_m(k_x)}{k_y} \approx \frac{\delta_{mn}}{k_{yn}} \quad ; \quad \int_0^{k_t} dk_x Q_n(k_x)Q_m(k_x)\frac{k_y}{k_x^2} \approx \delta_{mn}\frac{k_{yn}}{(\frac{n\pi}{a})^2}$$

$$\int_{k_t}^{\infty} dk_x \frac{Q_n(k_x)Q_m(k_x)}{k_y} \approx 0 \quad ; \quad \int_{k_t}^{\infty} dk_x Q_n(k_x)Q_m(k_x)\frac{k_y}{k_x^2} \approx 0 \qquad (4.36)$$

where $k_{yn}^2 = k_t^2 - (\frac{n\pi}{a})^2$.

These approximations,combined with equations (4.34) and (4.35),suggest the following modes as approximations to the solutions of the eigenvalue equation;

Quasi-L.S.E.

$$\underline{E}_{vn}^h = \delta_{vn}\begin{pmatrix}\beta\\ -(\frac{v\pi}{a})^2\end{pmatrix}\frac{1}{(k_{yv}(\beta^2+(\frac{v\pi}{a})^2))^{1/2}} \quad ; \quad \underline{\tilde{E}}_v^h(k_x) = Q_v(k_x)\begin{pmatrix}\beta\\ -k_x^2\end{pmatrix}\frac{1}{(k_{yv}(\beta^2+k_x^2))^{1/2}} \qquad (4.37)$$

with $k_{yv}cot\alpha_v = q_v cot q_v h$

Quasi-L.S.M.

$$\underline{E}_{vn}^e = \frac{\delta_{vn}}{k_o}\begin{pmatrix}1\\ \beta\end{pmatrix}\frac{k_{yv}}{(\beta^2+1)^{1/2}} \quad ; \quad \underline{\tilde{E}}_v^e(k_x) = \frac{Q_v(k_x)}{k_o}\begin{pmatrix}1\\ \beta\end{pmatrix}\frac{k_{yv}}{(\beta^2+1)^{1/2}} \qquad (4.38)$$

with $\varepsilon_r k_{yv}\tan\alpha_v = q_v \tan q_v h$

These approximations allow the following observations to be made;

i) Clearly equations (4.37) and (4.38) are only valid if $k_t \gg \frac{v\pi}{a}$.This explains the appearance of critical values of k_t defining the range of existence of the slot region modes.As a first approximation,the critical values may be taken as $k_t \approx \frac{v\pi}{a}$ which is reasonably consistent with figure 4.4.

ii) The modes of equations (4.37) and (4.38) are very close to the modes of a dielectric bar in an infinite height trough,the distinguishing feature is the spreading that occurs in the open region caused by diffraction at the guide corners.This is shown in the figures in appendix A4.3.

4.3.2) The open region Modes.

Below its critical value of k_t a slot region mode changes into an open region mode.In figure 4.4 the eigenvalues of these modes appear to vary exponentially with k_t.Figure 4.6 shows the variation of $\ln | cot\alpha_v(k_t) |$ against k_t and clearly exhibits a reasonable degree of linear behaviour.(The curves level off due to the numerical range of the computer.)

Besides their quasi-infinite eigenvalues,there is a further major difference between the open region modes and the slot region modes.Superficially the interface fields of the open region modes,typified by those shown in figures 4.9 and 4.10,still appear to be dominated by a single slot term.However closer examination reveals that the fields are dominated by $\sin(\frac{m\pi}{a}x)$ and $\cos(\frac{m\pi}{a}x)$ behaviour where m is even,rather than an odd value indicative of a slot term.

It is possible to model the interface fields of the open region modes very easily by making the following observations.

i) The normalised coefficients,E_{xn} and ∂xE_{zn} have an almost identical variation with n,as illustrated in figure 4.11.(Each term has been scaled by $(-1)^n$ for convenience.)Thus each mode is characterised by a scalar function of n and a vector that is independent of n.

ii) The ratios $\frac{E_{vxn}}{\partial xE_{vzn}}$ and $\frac{H_{vxn}}{\partial xH_{vzn}}$,which are independent of n as observed in i),are plotted against v in figure 4.12.For the open region modes,not only are these

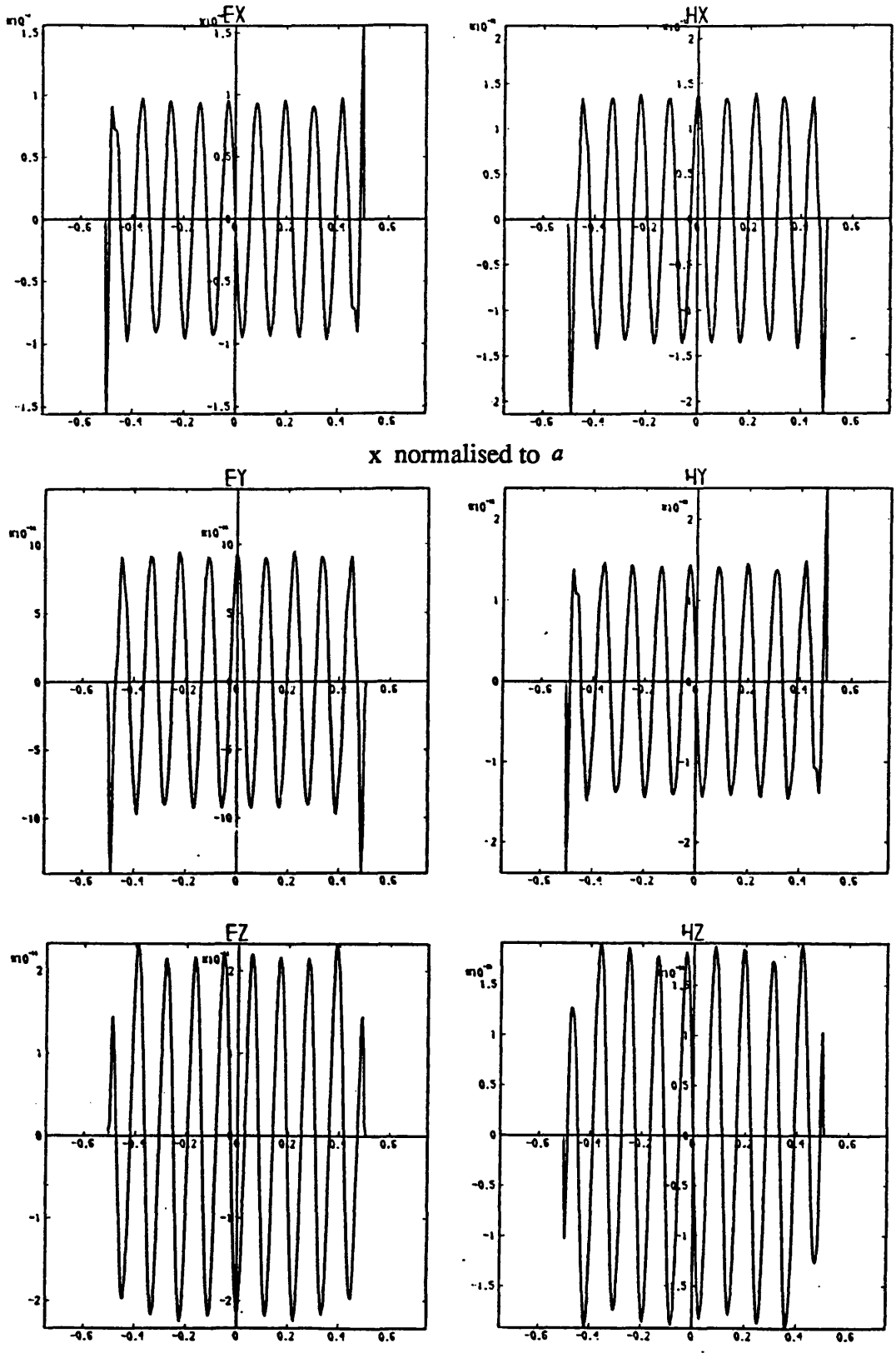

Figure 4.9) The interface fields of the open region mode with $cot\alpha_v = 9.15\times10^6$.

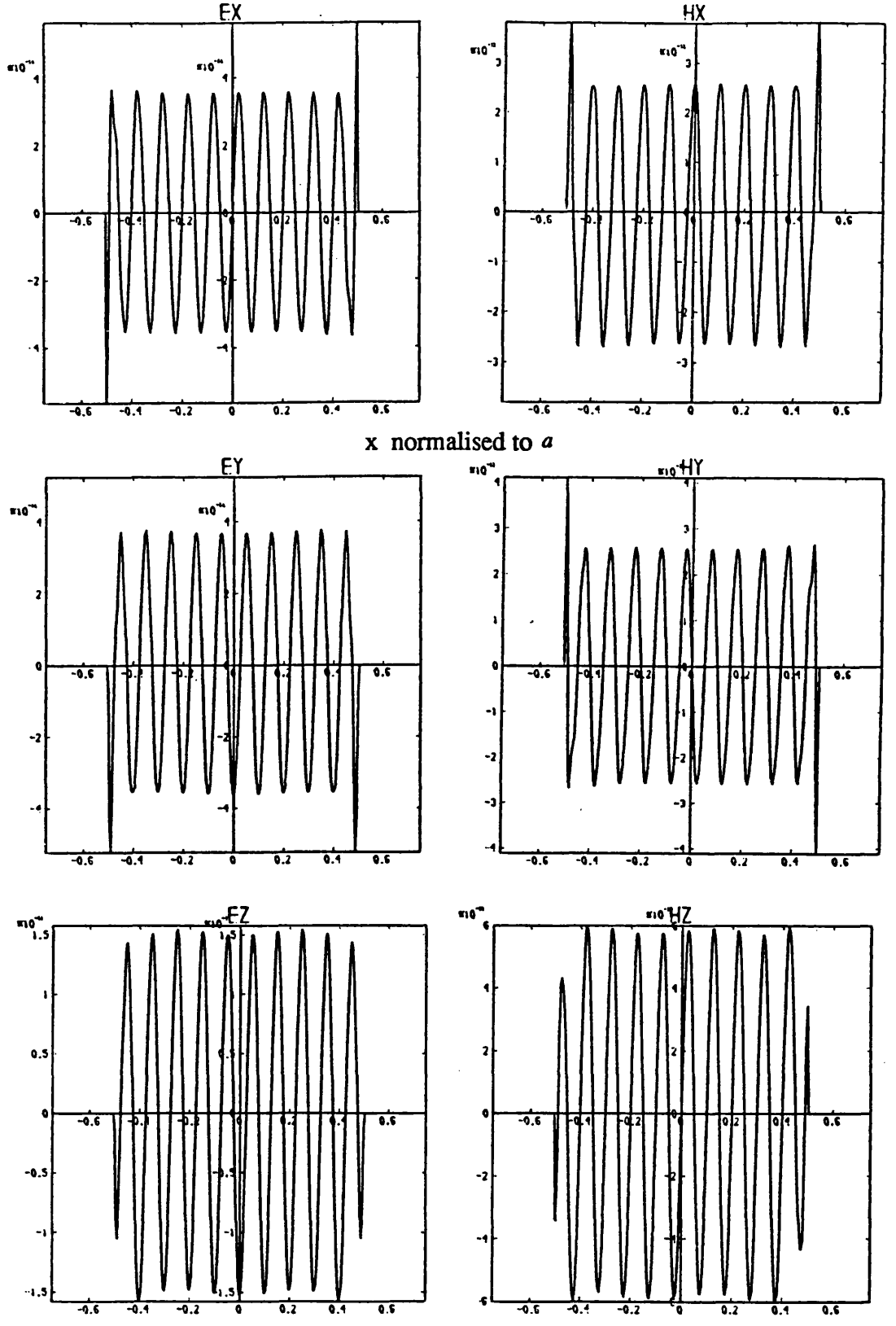

Figure 4.10) The interface fields of the open region mode with $cot\alpha_v = -1.06\times10^8$.

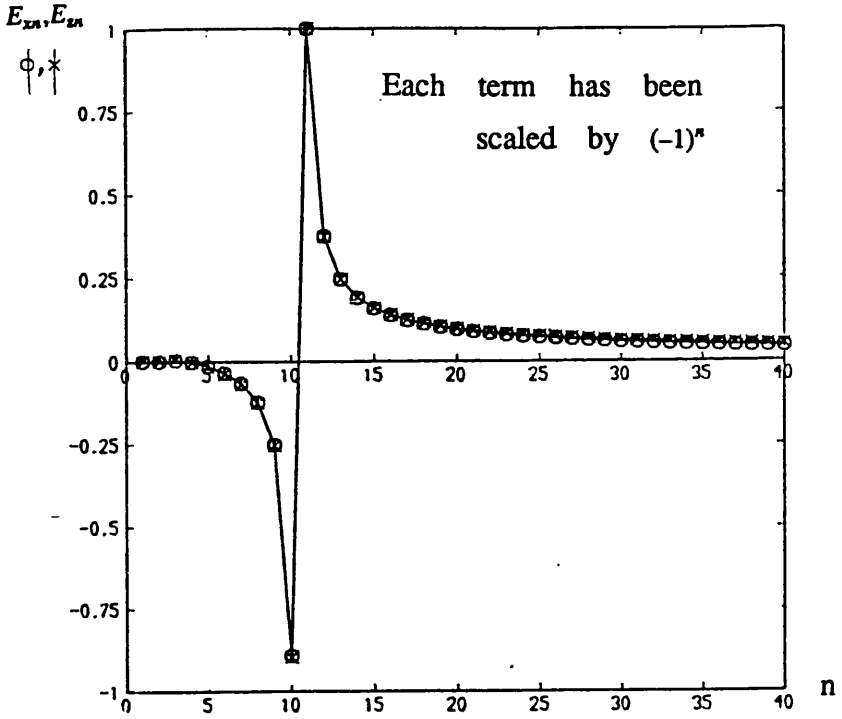

Figure 4.11) Basis amplitudes, E_{xn} and E_{zn}, for the mode of figure 4.9).

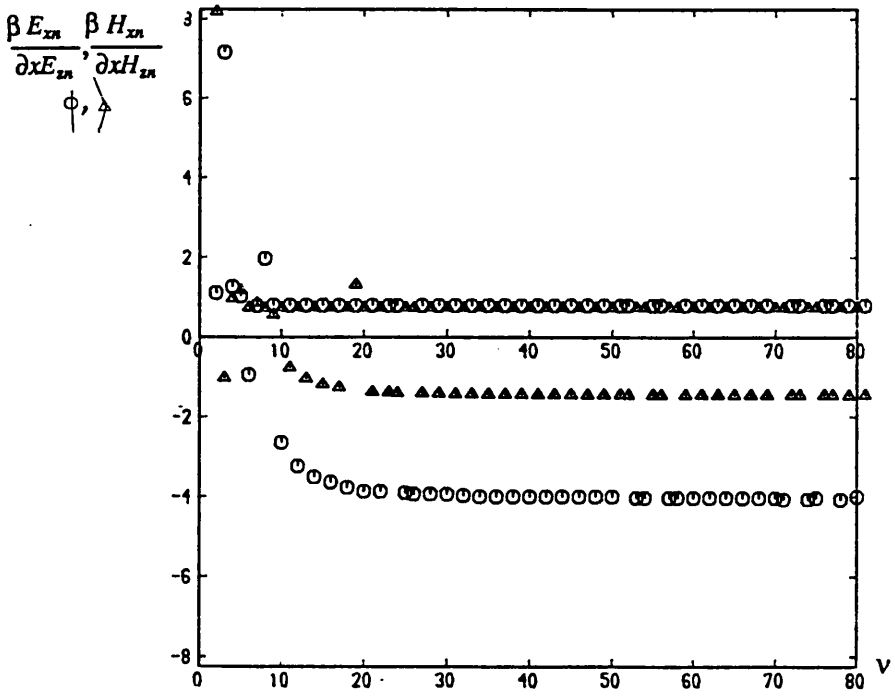

Figure 4.12) $\frac{\beta E_{xn}}{\partial x E_{zn}}$ and $\frac{\beta H_{xn}}{\partial x H_{zn}}$ versus ν.

ratios constant for all the modes,but it can be seen that each mode has either $\beta E_{zn} \approx \partial x E_{zn}$ or $\beta H_{zn} \approx \partial H_{zn}$,confirming the existence of L.S.E. and L.S.M. dominated modes.

iii) In the k_x domain the open region modes predominantly exist in the range $k_x \gg k_t$.As shown in figures 4.13 an excellent approximation to the fourier transform of the interface fields is;

$$\tilde{F}(k_x) = \frac{k_x \sin(\frac{k_x a}{2})}{(\frac{m\pi}{a}) - k_x} \quad : \quad m \text{ even} \tag{4.39}$$

This is the transform of the function;

$$F(x) = (-1)^{\frac{n}{2}} \cos(\frac{n\pi}{a}x)\left[ci(\frac{n\pi}{a} \mid x - \frac{a}{2} \mid) - ci(\frac{n\pi}{a} \mid x + \frac{a}{2} \mid) \right]$$

$$+ (-1)^{\frac{n}{2}} \sin(\frac{n\pi}{a}x)\left[\pi + si(\frac{n\pi}{a} \mid x - \frac{a}{2} \mid) - si(\frac{n\pi}{a} \mid x + \frac{a}{2} \mid) \right] \quad : \quad \mid x \mid \leq \frac{a}{2}$$

$$= (-1)^{\frac{n}{2}} \cos(\frac{n\pi}{a}x)\left[ci(\frac{n\pi}{a} \mid x - \frac{a}{2} \mid) - ci(\frac{n\pi}{a} \mid x + \frac{a}{2} \mid) \right]$$

$$+ (-1)^{\frac{n}{2}} \sin(\frac{n\pi}{a}x)\left[si(\frac{n\pi}{a} \mid x - \frac{a}{2} \mid) - si(\frac{n\pi}{a} \mid x + \frac{a}{2} \mid) \right] \quad : \quad \mid x \mid \geq \frac{a}{2} \tag{4.40}$$

This function is very close to $\pi(-1)^{\frac{n}{2}} \sin(\frac{m\pi}{a}x)$ over the majority of the dielectric interface and also possesses very localised singularities,($\approx_{x \to 0} \ln x$),at the guide corners.The function is not identically zero on the metal interface but decays very rapidly away from the corners,as shown in figure 4.14.

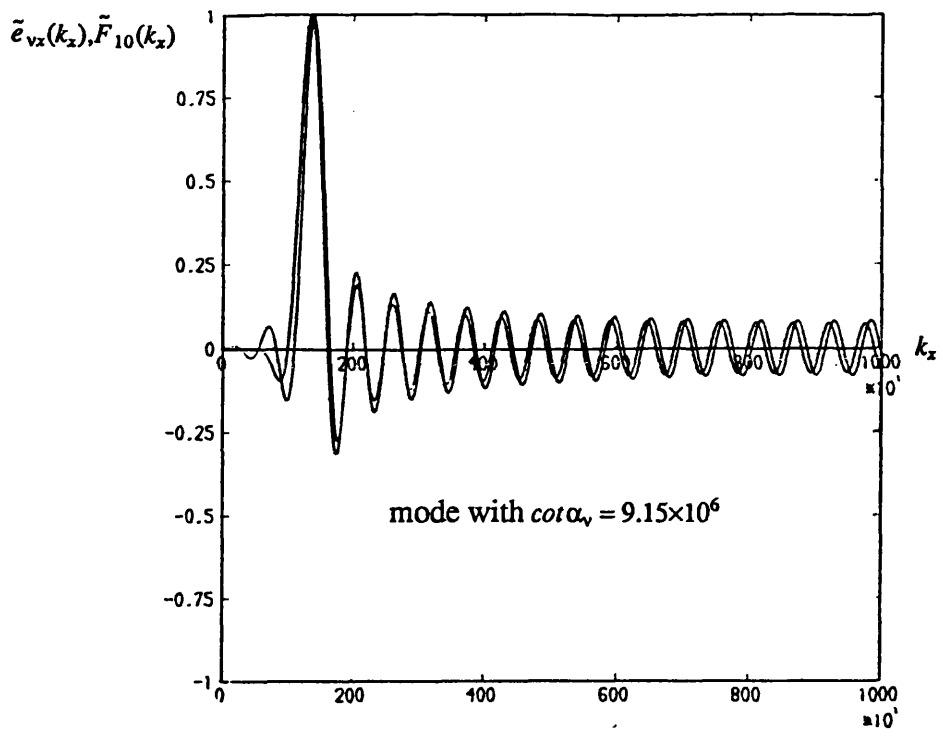

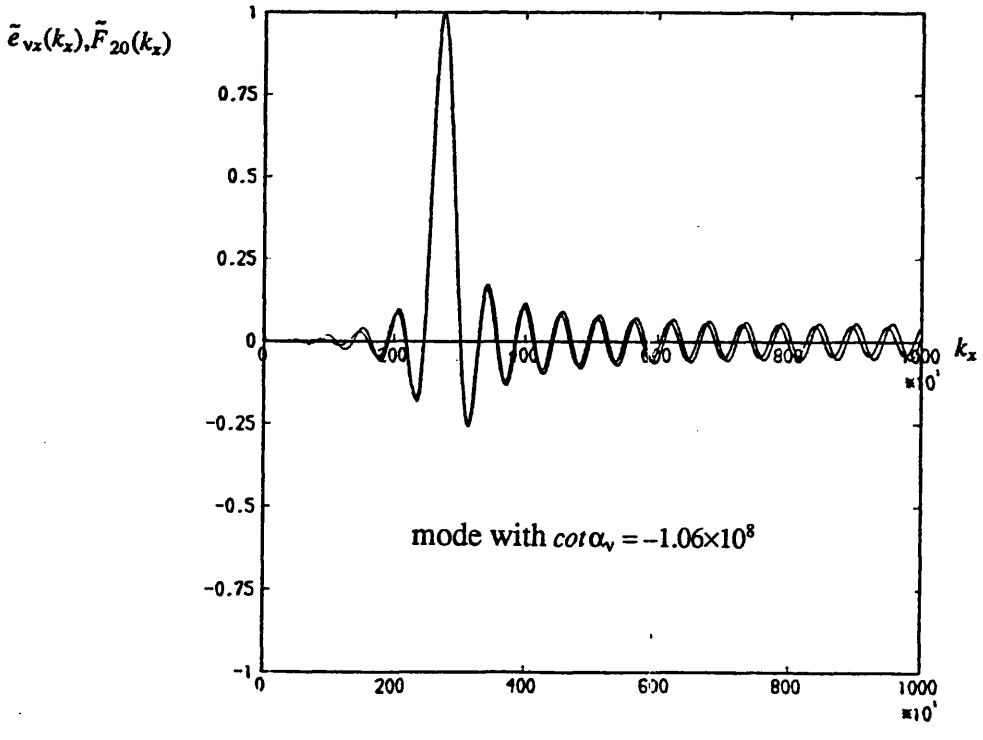

Figure 4.13) $\tilde{e}_{vx}(k_x)$ and its approximation,$\tilde{F}_m(k_x)$ for the open region modes.

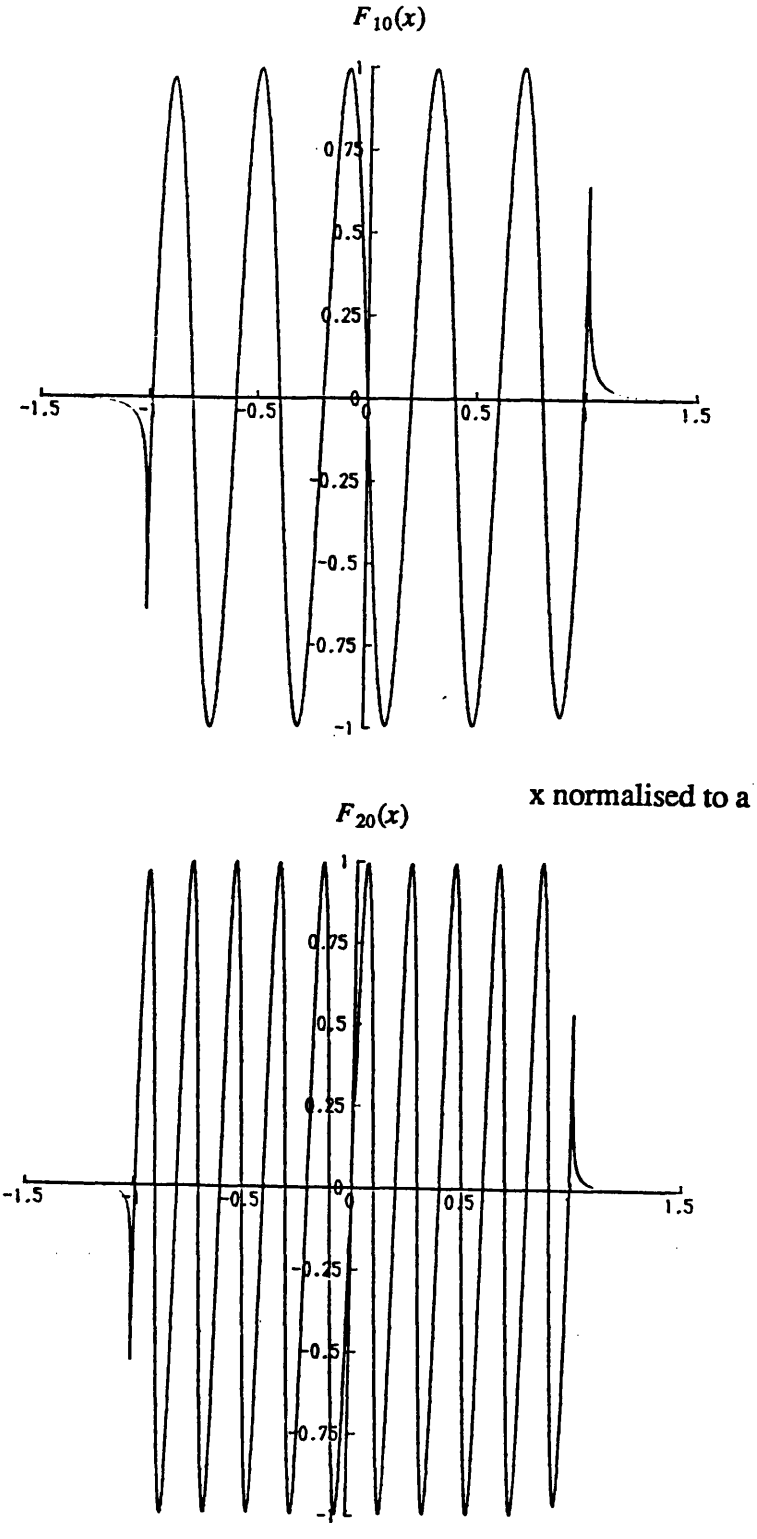

Figure 4.14) $F_m(x)$ approximation to the near fields of the open region modes.

Unfortunately,although this approximation is excellent for the near field it is inadequate for the far field.For network modelling of discontinuities this does not present a problem,but to determine the radiation pattern of antenna elements,the full numerical process must be undertaken to determine the modal fields.The far fields of some open region modes are shown in A4.4 and clearly illustrate the diffraction caused by the guide corners.

In general,it is suggested that the slot region modes be numerically determined from a moderate order eigenvalue equation as the single term approximation is not particularly good and,if it is necessary to use large numbers of open region modes,that these may be excellently modelled by the approximation discussed above.

Now that the continuous modes of the I.D.G. have identified,it is possible to rigorously analyse discontinuities in I.D.G.The next chapter shall consider the transition from rectangular metallic waveguide to I.D.G. and chapter 6,radiating metallic strips on the surface of the I.D.G.

4.4) References.

1) T.Rozzi and S.Hedges,"Rigorous Analysis and Network Modelling of the Inset Dielectric Guide",IEEE trans. microwave theory and techniques,vol MTT-35,no 9,Sept 87,pp823-834.

2) T.Rozzi,L.Ma,R de Leo and A.Morini,"Equivalent Network of Transverse Dipoles on Inset Dielectric Guide:Application to Linear Arrays",IEEE trans antennas and prop.,vol AP-38,no 3,Mar 90,pp380-385.

3) T.Rozzi and L.Ma,"Scattering by Dipoles in I.D.G. and Application to Millimeter Antennas",proc 17th European microwave conf.,Rome,Sept 87,pp543-548

4) T.Rozzi and L.Ma,"Mode Completeness,Normalisation and Green's Function of the Inset Dielectric Guide",IEEE trans. microwave theory and techniques,vol MTT-36,no 3,Mar 88,pp542-551.

5) P.Sewell and T.Rozzi,"Rigorous Analysis of a Longitudinal Strip on the Surface of Inset Dielectric Guide",1990 MTT-S digest,pp1059-1062.

6) T.Itoh,"Spectral Domain Immitance Approach for Dispersion Characteristics of Generalised Printed Transmission Lines",IEEE trans. microwave theory and techniques,vol MTT-28,no 7,July 1980,pp733-736.

7) J.Wilkinson,"The Algebraic Eigenvalue Problem",Clarendon Press,1965.

8) G.Peters and J.Wilkinson,"$AX = \lambda BX$ and the Generalised Eigenproblem",SIAM J. Numer. Anal. 10,Dec 1970,pp479-492.

9) A.Ruhe,"Properties of a Matrix with a very Ill-conditioned Eigenproblem",Num. Math. 15,1970,pp57-60.

10) G.Stewart,"On the Sensitivity of the Eigenvalue $AX = \lambda BX$",SIAM J. Numer. Anal.,9,1972,pp669-686.

11) G.Golub and J.Wilkinson,"Ill-conditioned Eigensystem and the Computation of the Jordan Canonical form",SIAM J. rev. 18,Oct 1976,pp578-619.

12) J.Wilkinson,"Notes on Matrices with a very Ill-Conditioned Eigenproblem",Num. Math. 19,1971

13) J.Wilkinson and C.Reinsch,"Handbook for Automatic Computation.Vol II,Linear Algebra,Springer-Verlag,1971.

14) R.Collin,"Field Theory of Guided Waves",McGraw Hill,1960.

APPENDIX A4.1) THE INTERFACE FIELDS.

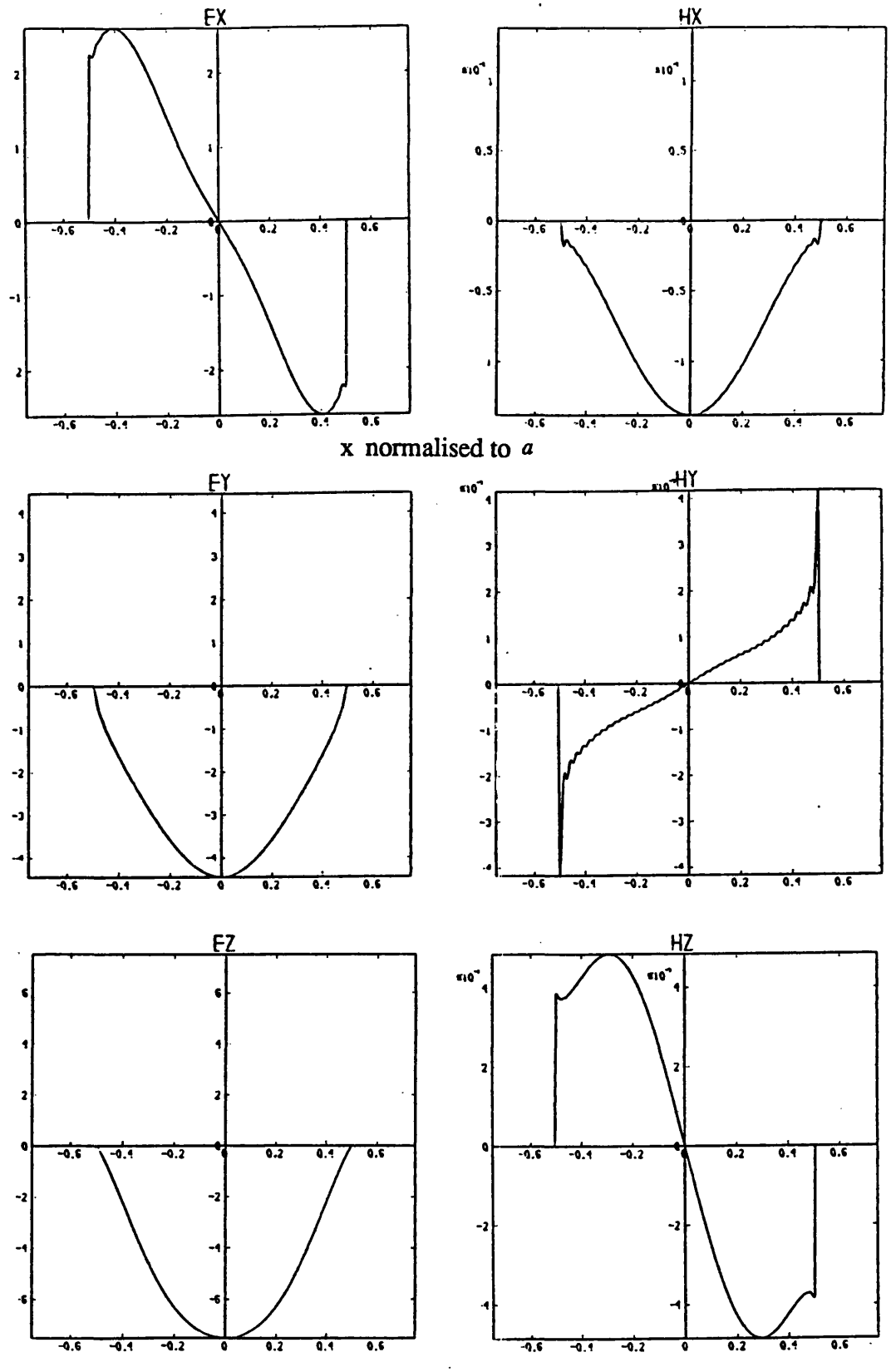

Figure 4.15 a) Interface fields for the mode with $cot\alpha_v = -1.43$.

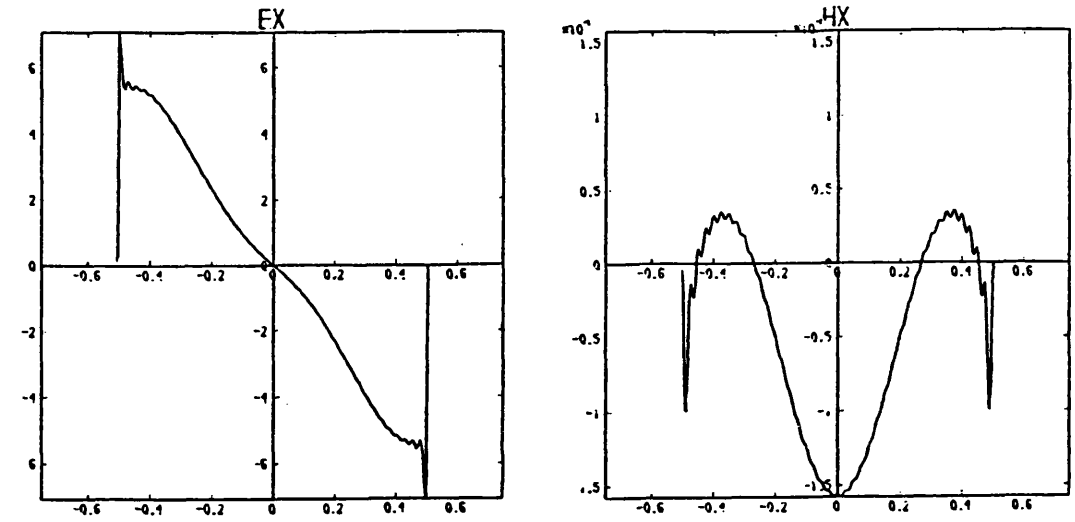

x normalised to a

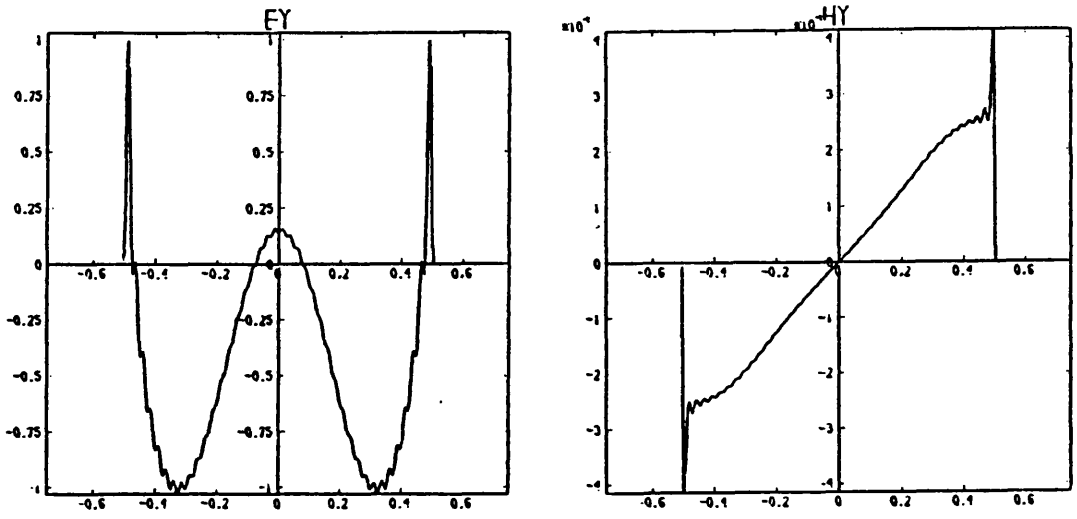

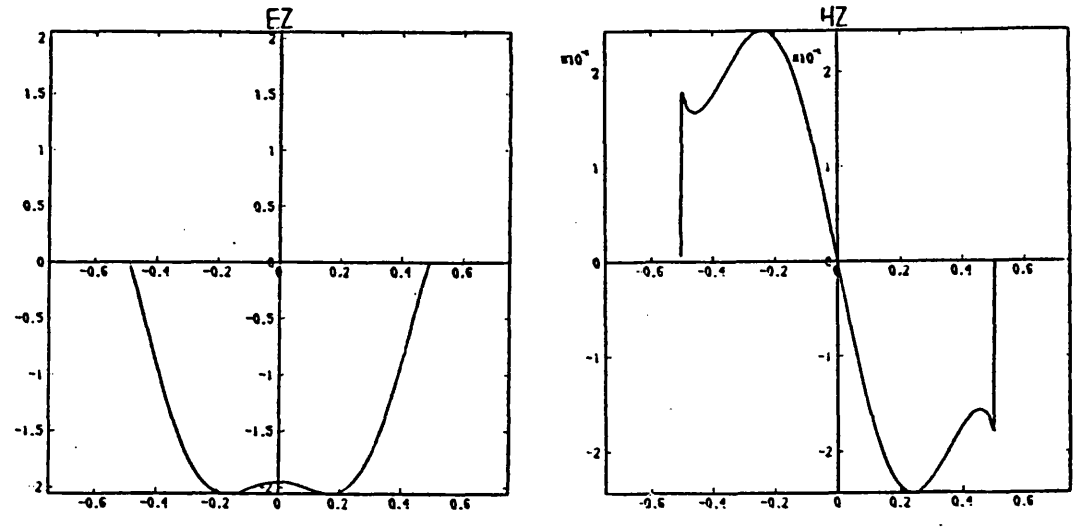

Figure 4.15 b) Interface fields for the mode with $cot\alpha_v = -1.06$.

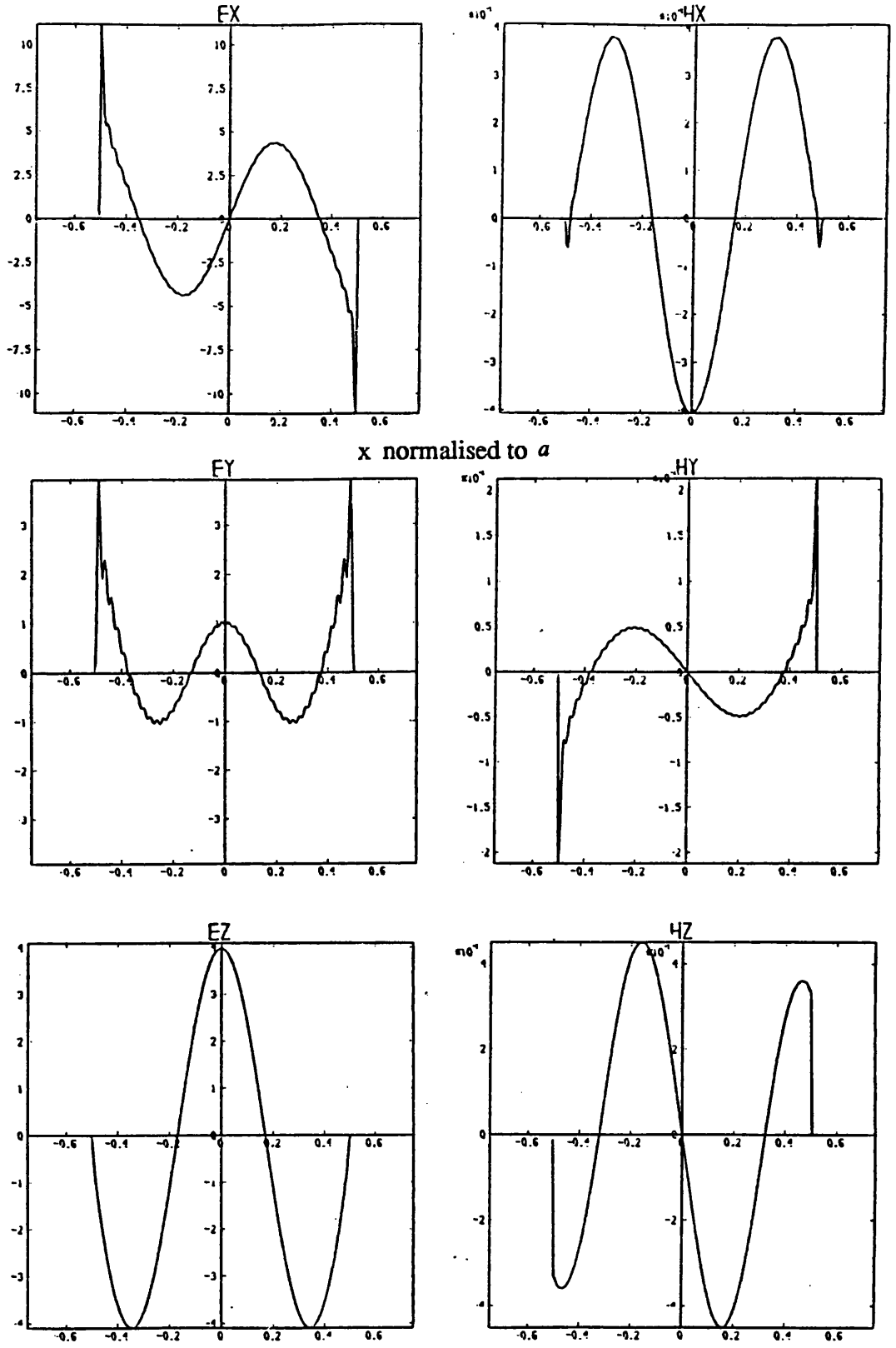

Figure 4.15 c) Interface fields for the mode with $cot\alpha_v = 2.29$.

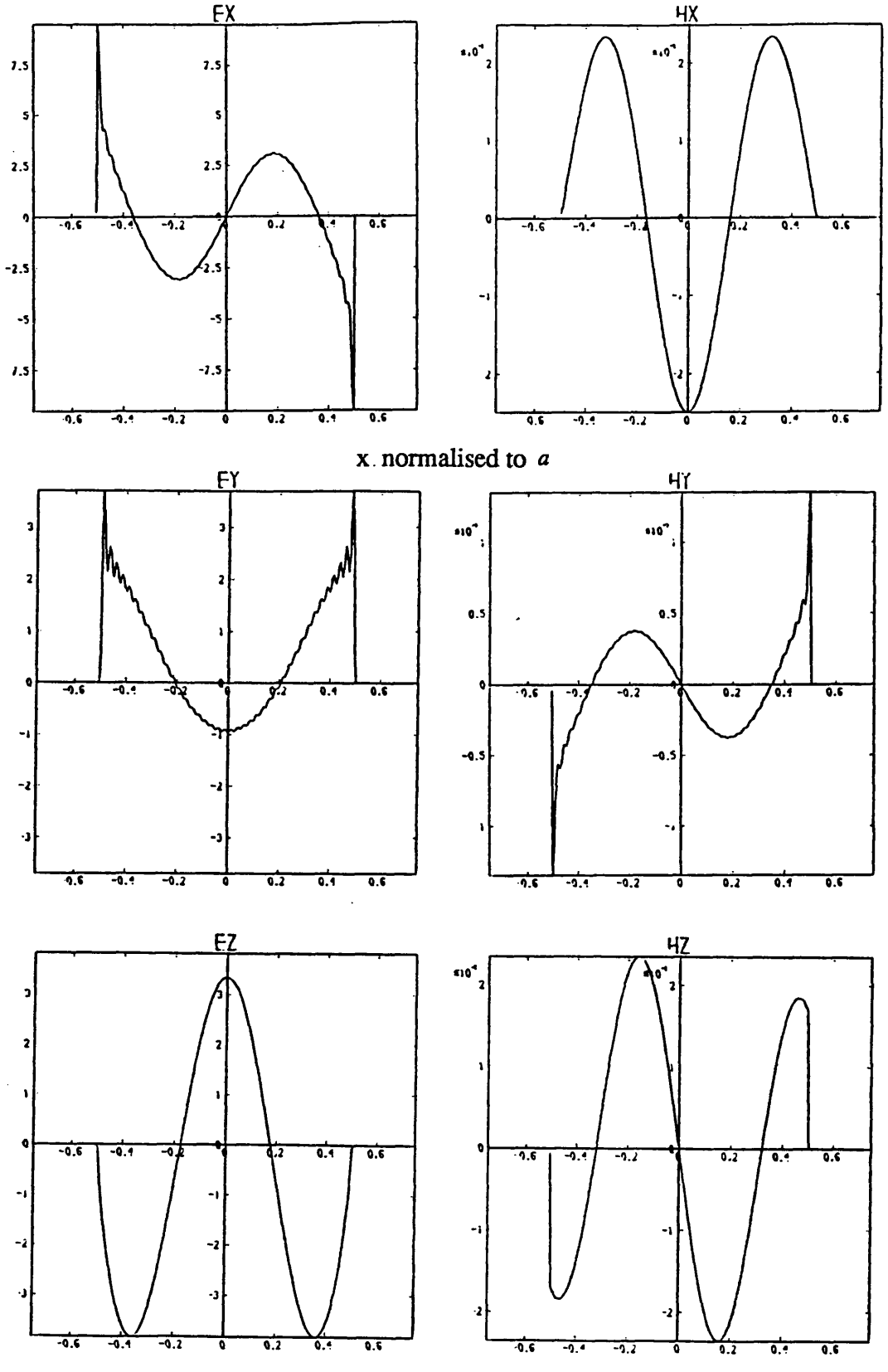

Figure 4.15 d) Interface fields for the mode with $cot\alpha_v = 3.03$.

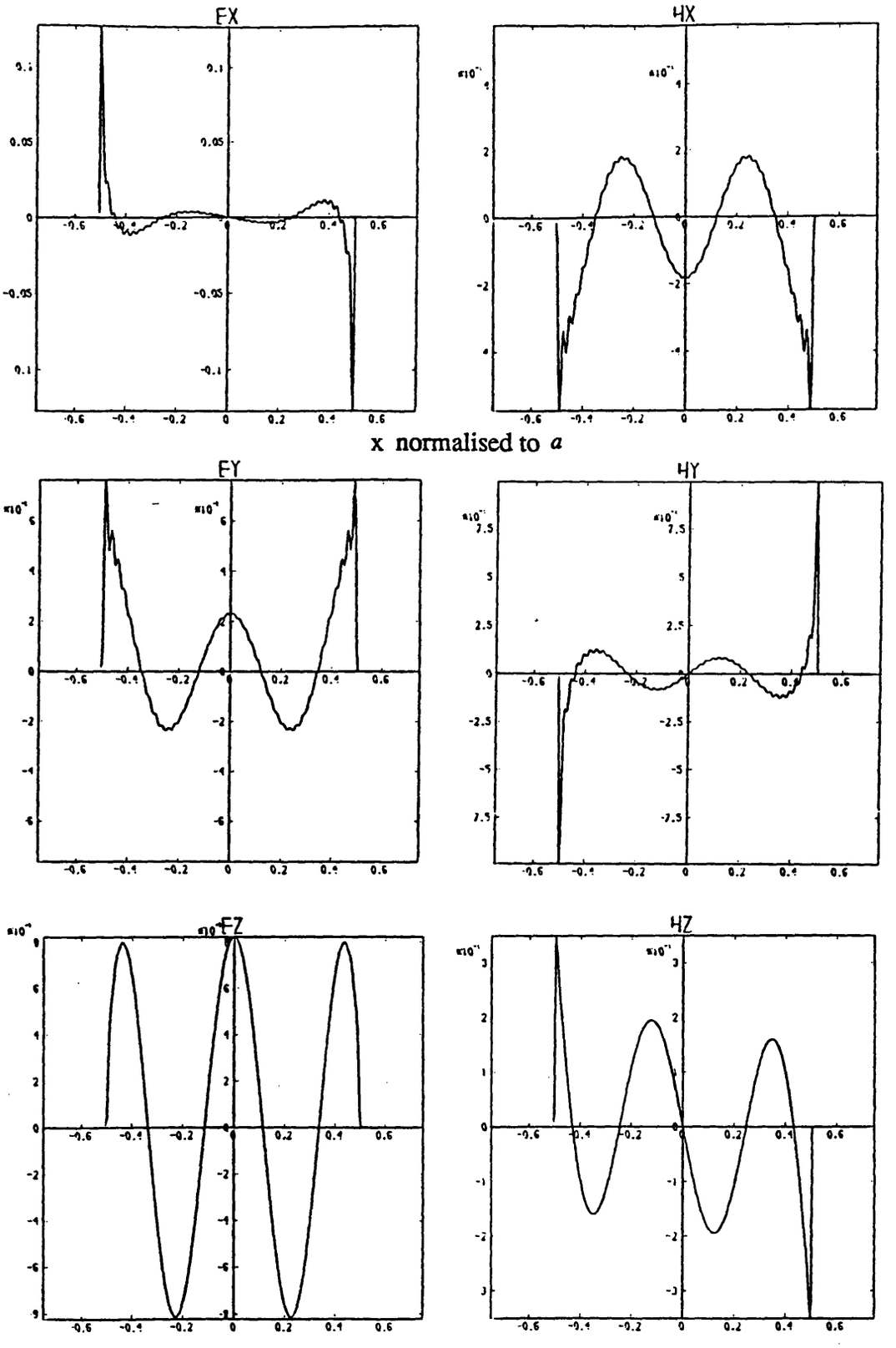

Figure 4.15 e) Interface fields for the mode with $cot\alpha_v = -39.9$.

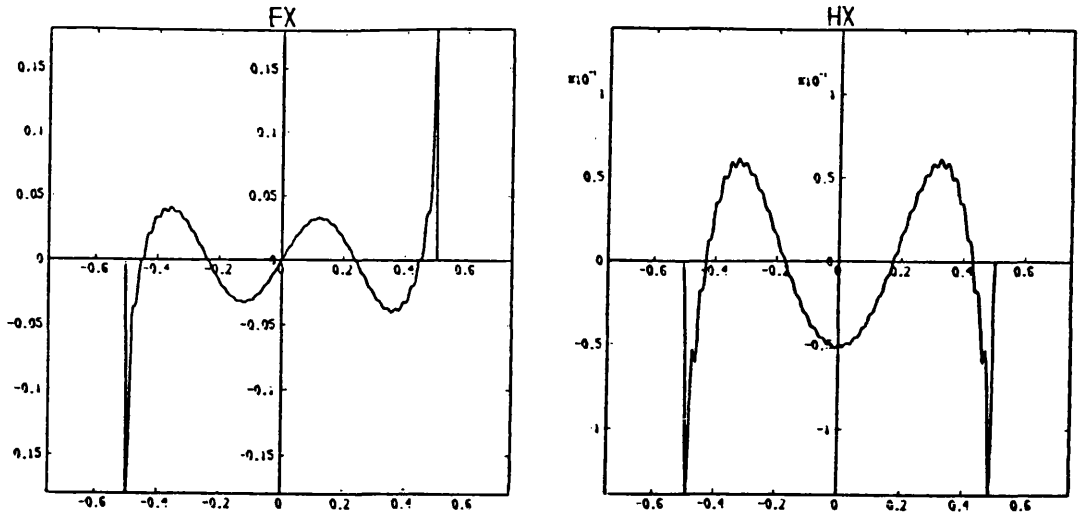

x normalised to a

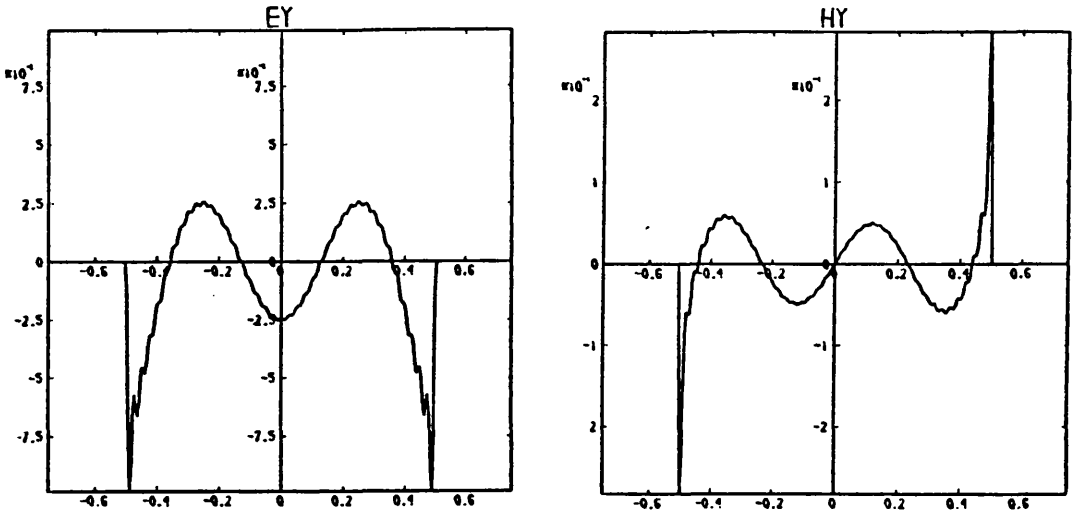

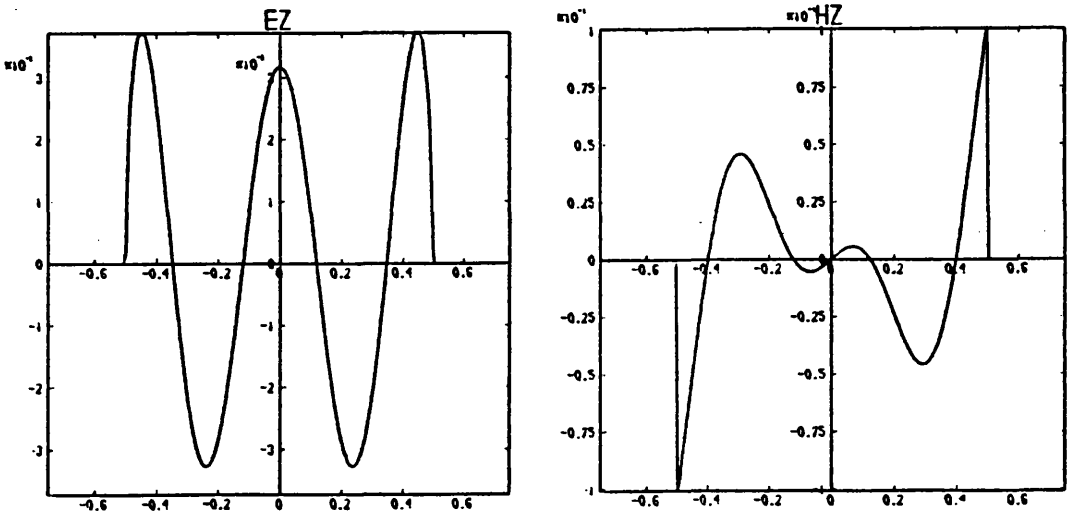

Figure 4.15 f) Interface fields for the mode with $cot\alpha_v = 52.7$.

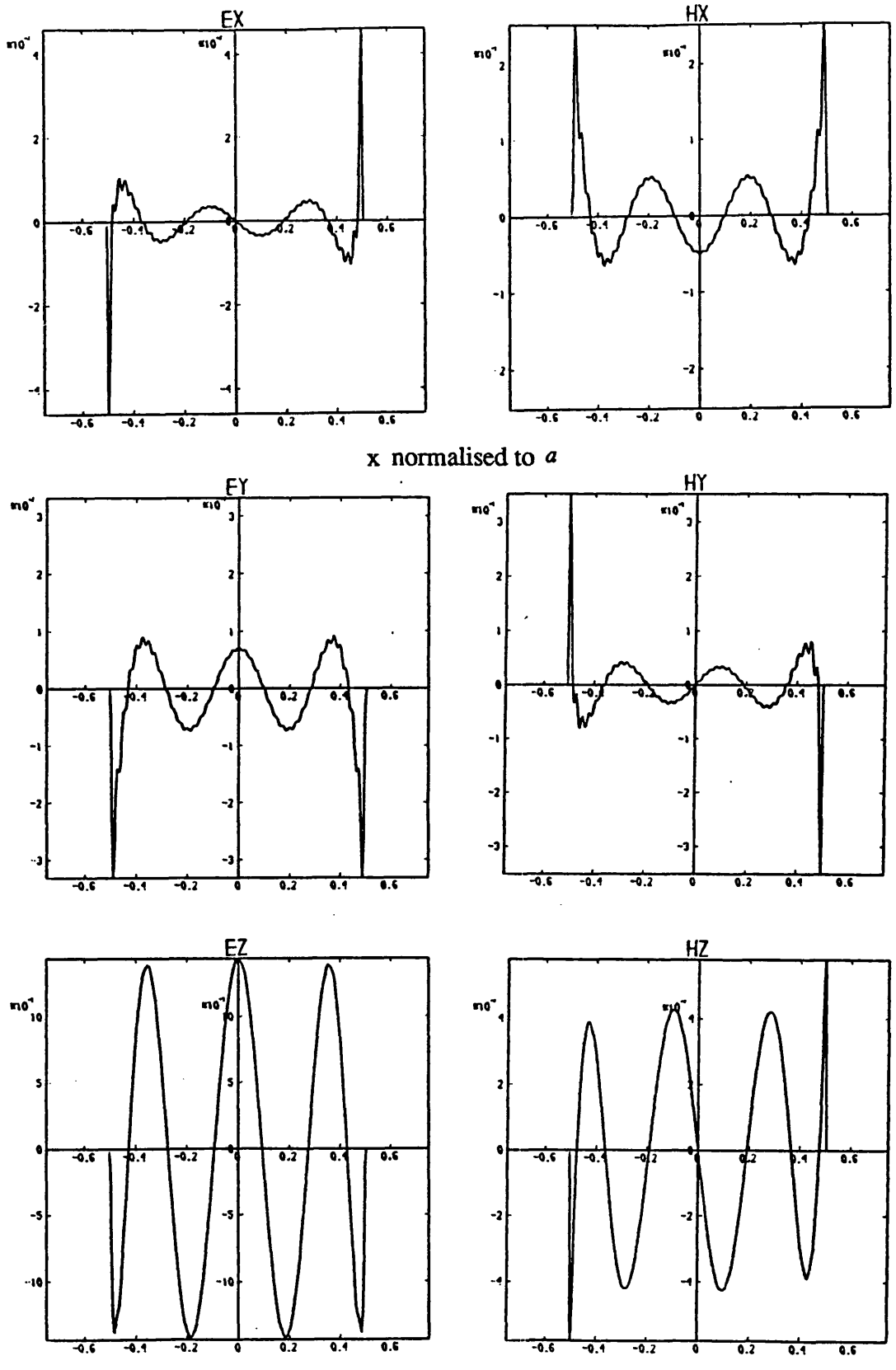

Figure 4.15 g) Interface fields for the mode with $cot\alpha_v = -9.3\times10^3$.

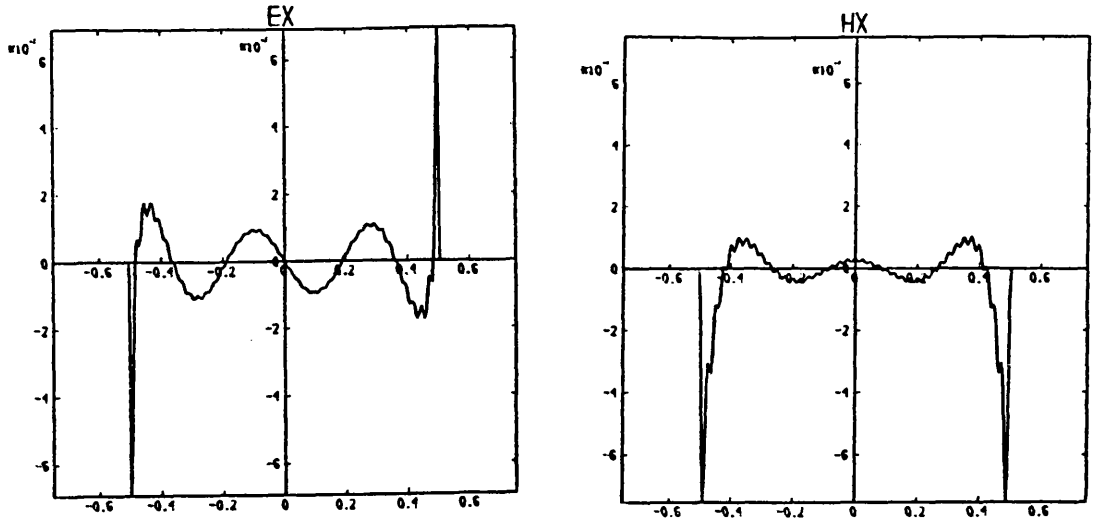

x normalised to a

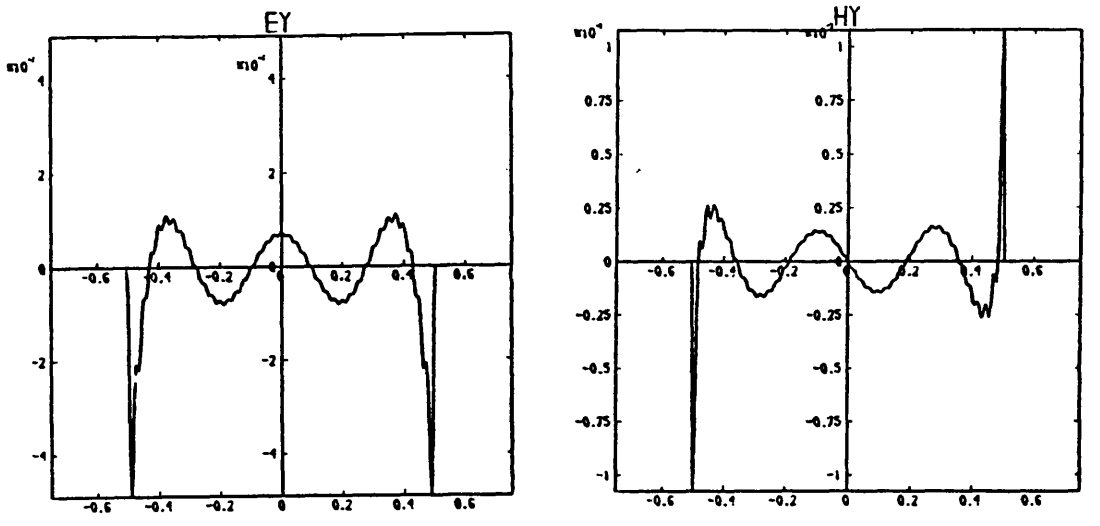

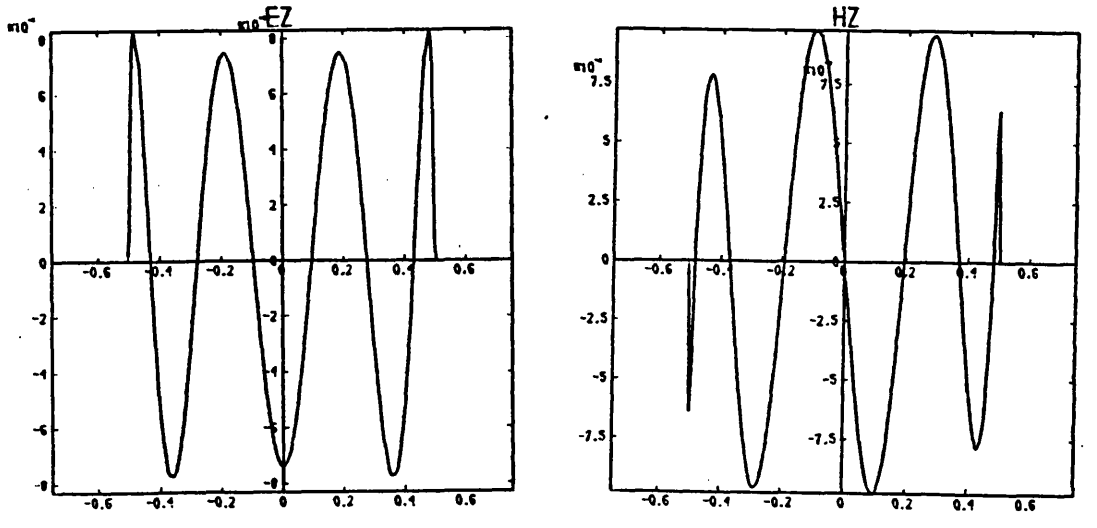

Figure 4.15 h) Interface fields for the mode with $cot\alpha_v = 1.21\times10^4$.

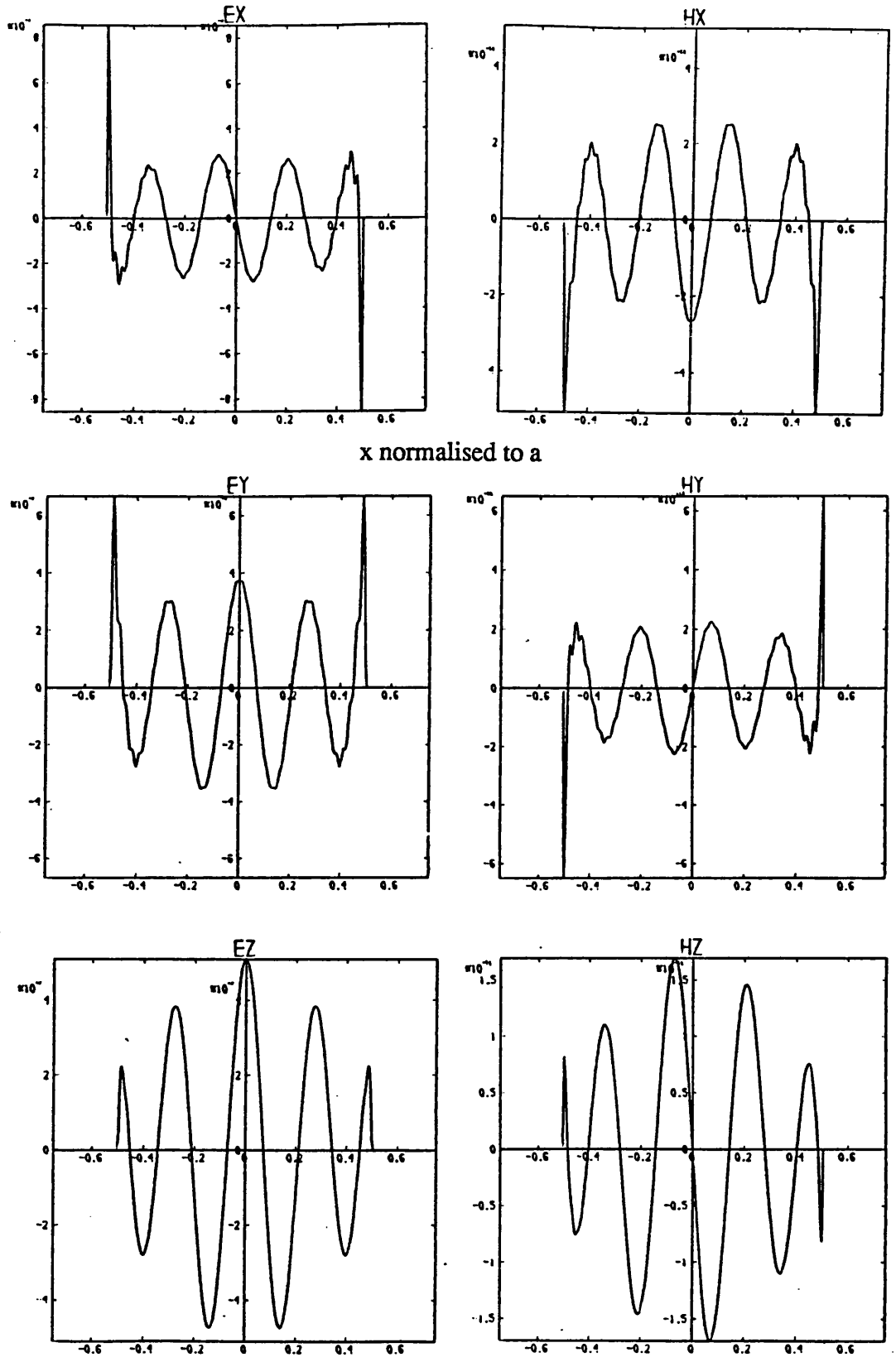

Figure 4.15 i) Interface fields for the mode with $cot\alpha_v = -4.05\times10^5$.

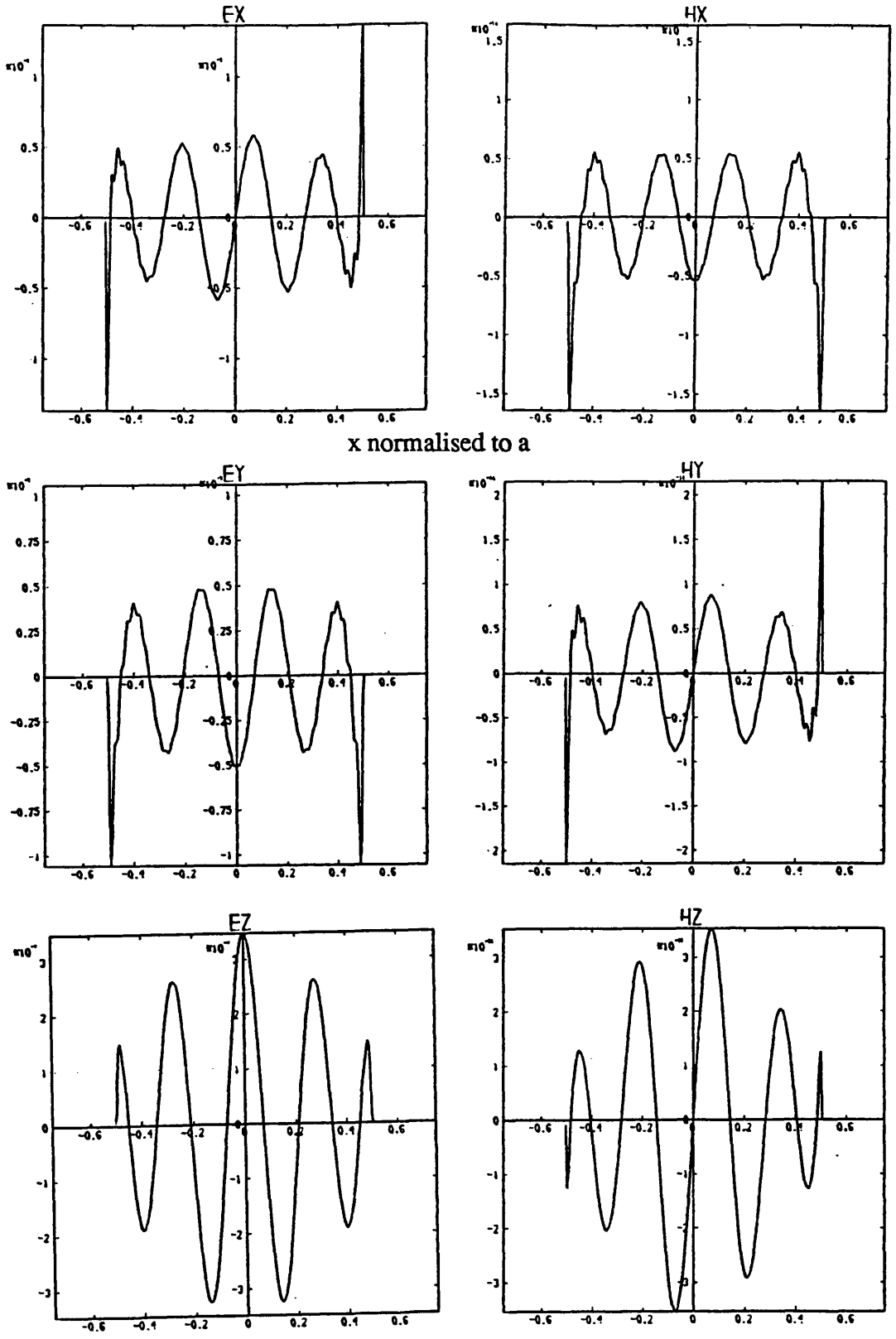

Figure 4.15 j) Interface fields for the mode with $cot\alpha_v = 5.01\times10^5$.

APPENDIX A4.2) THE BASIS AMPLITUDES.

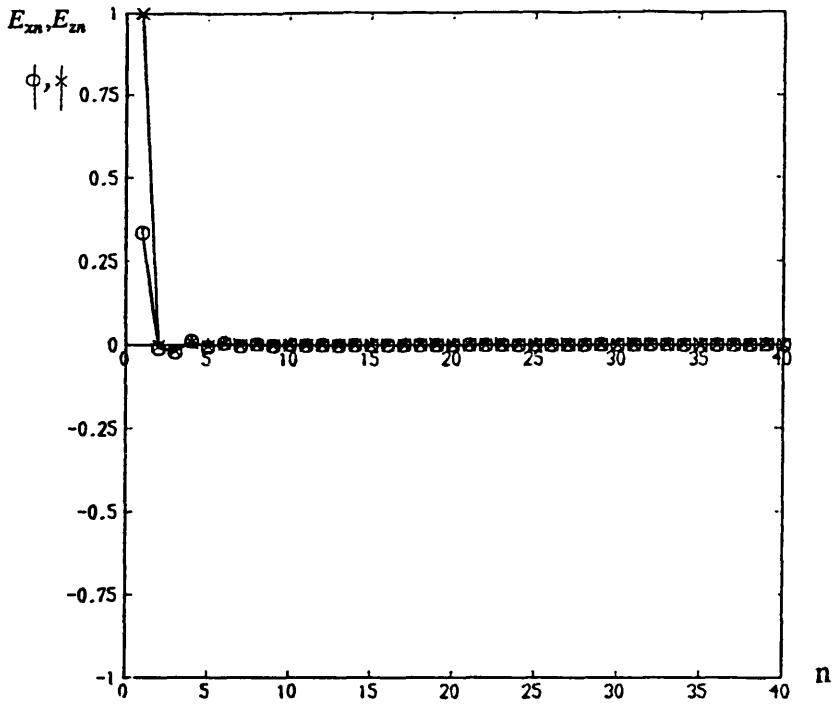

Figure 4.16 a) Basis amplitudes for the mode with $cot\alpha_v = -1.43$.

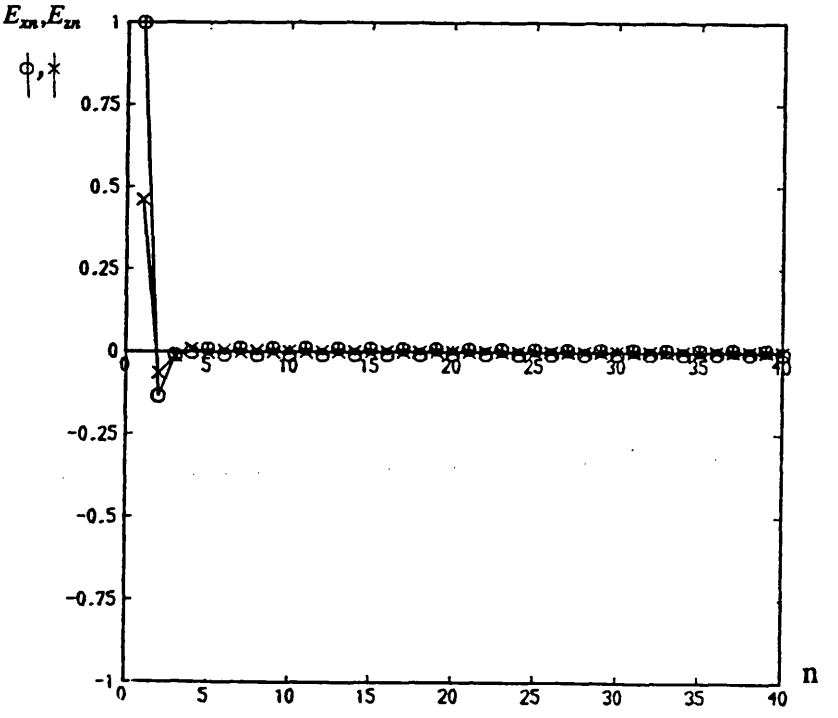

Figure 4.16 b) Basis amplitudes for the mode with $cot\alpha_v = -1.06$.

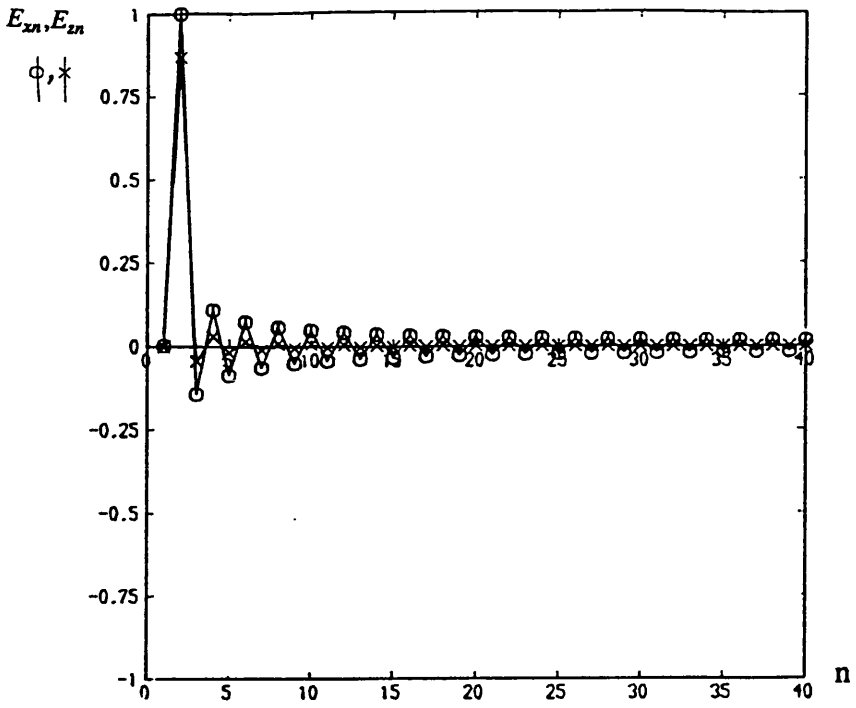

Figure 4.16 c) Basis amplitudes for the mode with $cot\alpha_v = 2.29$.

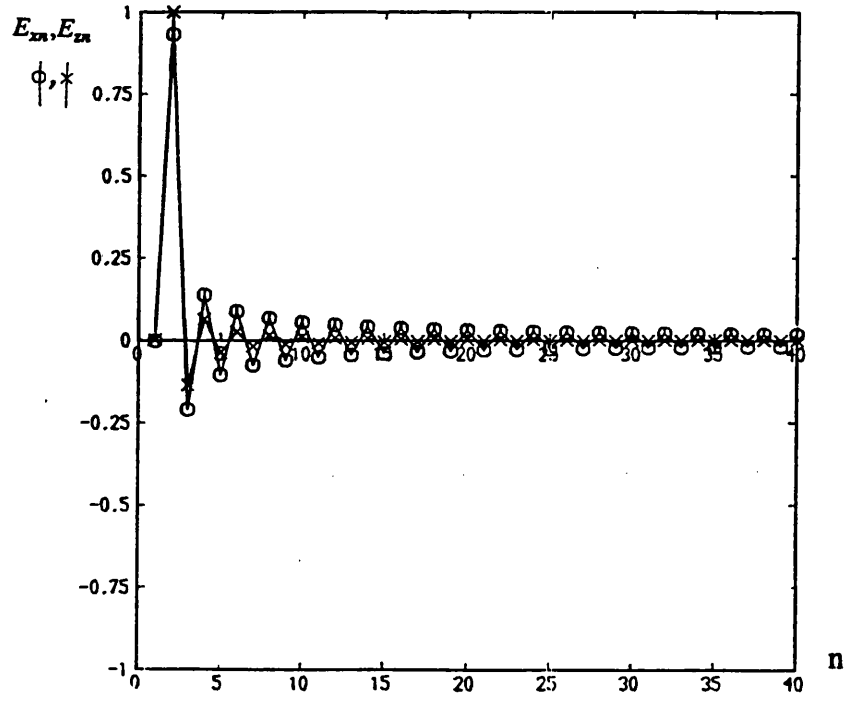

Figure 4.16 d) Basis amplitudes for the mode with $cot\alpha_v = 3.03$.

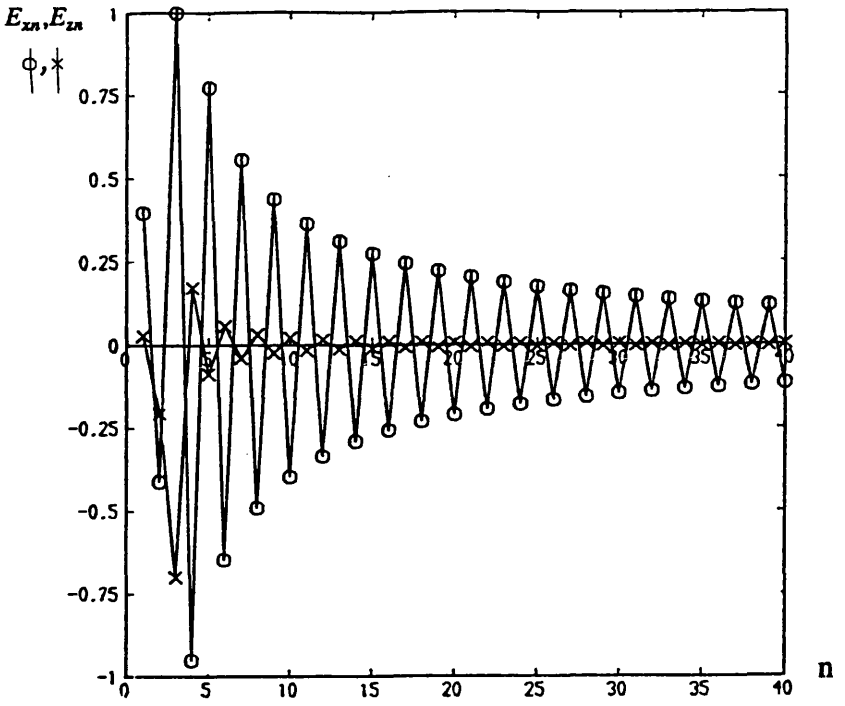

Figure 4.16 e) Basis amplitudes for the mode with $cot\alpha_v = -39.9$.

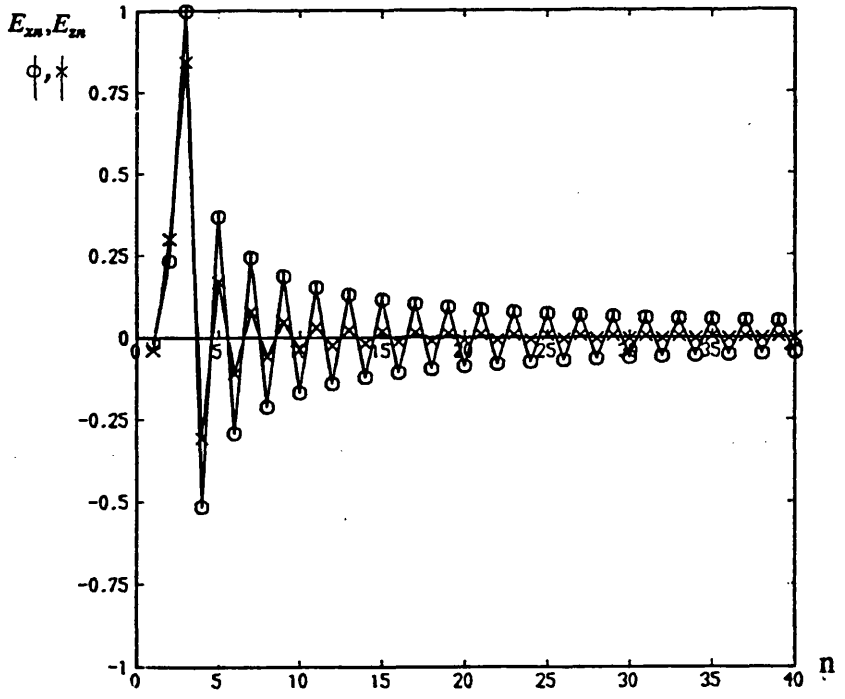

Figure 4.16 f) Basis amplitudes for the mode with $cot\alpha_v = 52.7$.

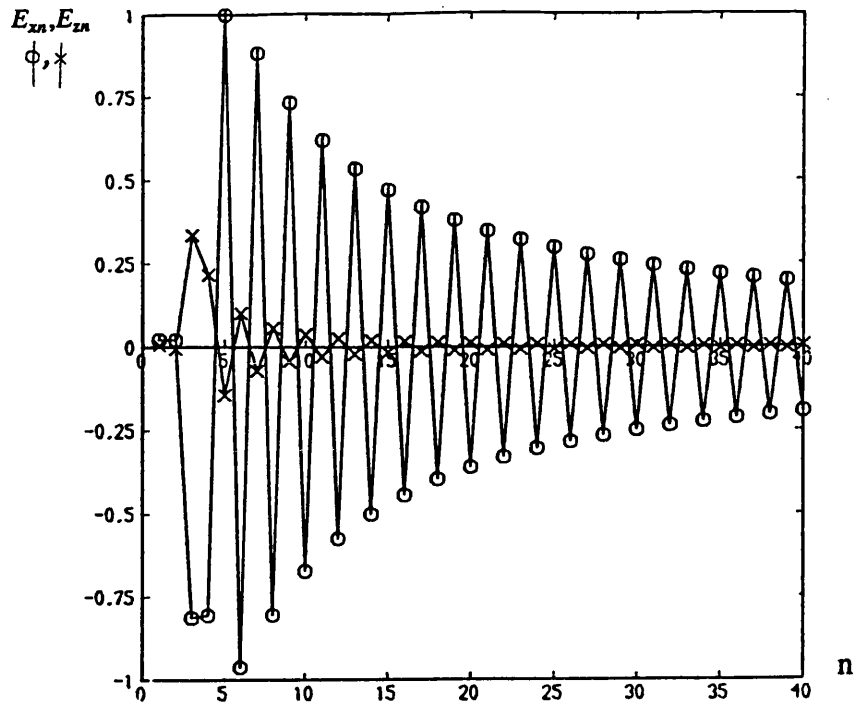

Figure 4.16 g) Basis amplitudes for the mode with $cot\alpha_v = -9.3\times10^3$.

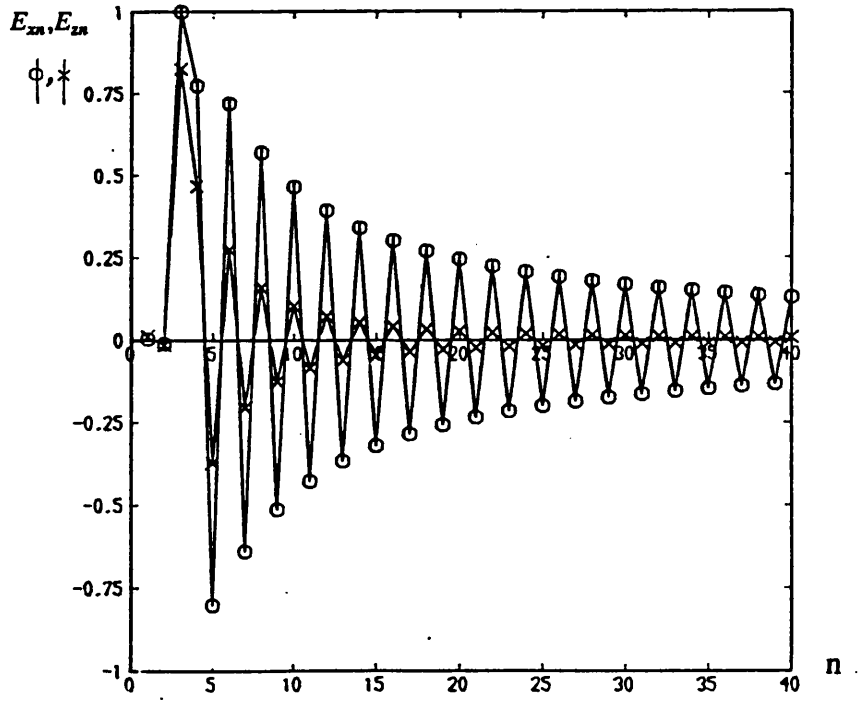

Figure 4.16 h) Basis amplitudes for the mode with $cot\alpha_v = 1.21\times10^4$.

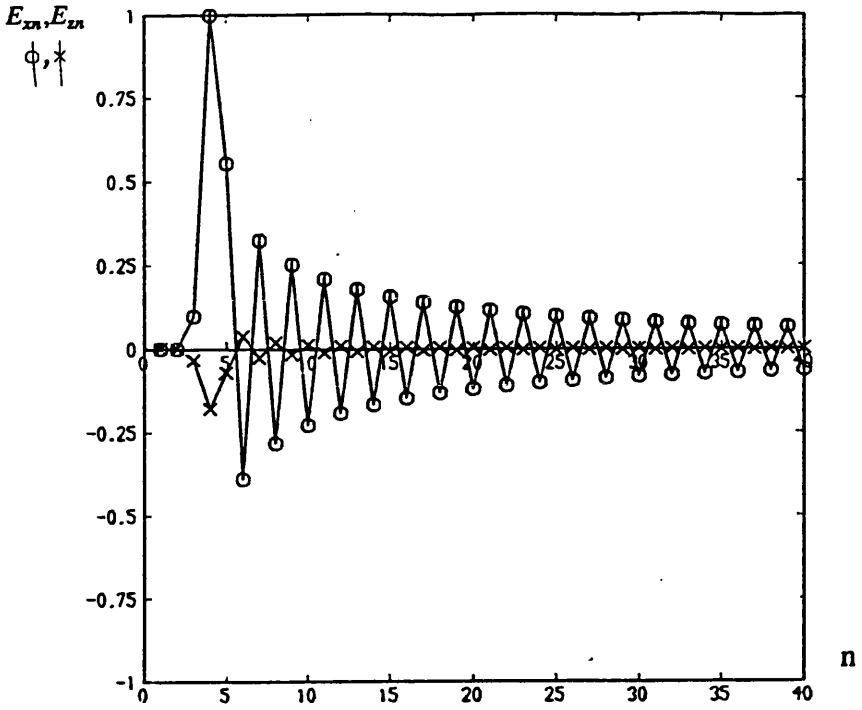

Figure 4.16 i) Basis amplitudes for the mode with $cot\alpha_v = -4.05\times10^5$.

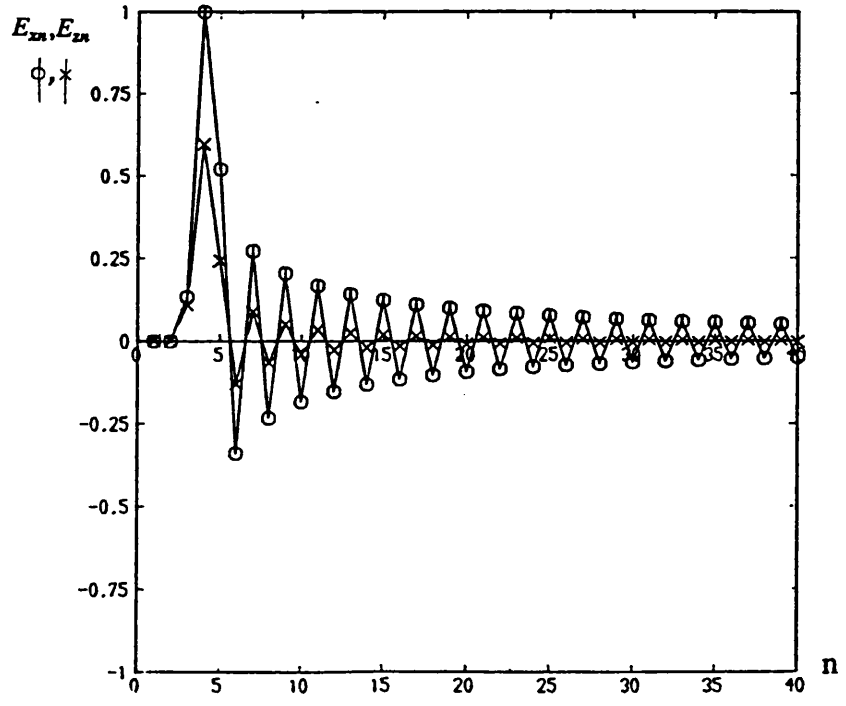

Figure 4.16 j) Basis amplitudes for the mode with $cot\alpha_v = 5.01\times10^5$.

APPENDIX A4.3) THE FAR FIELDS.

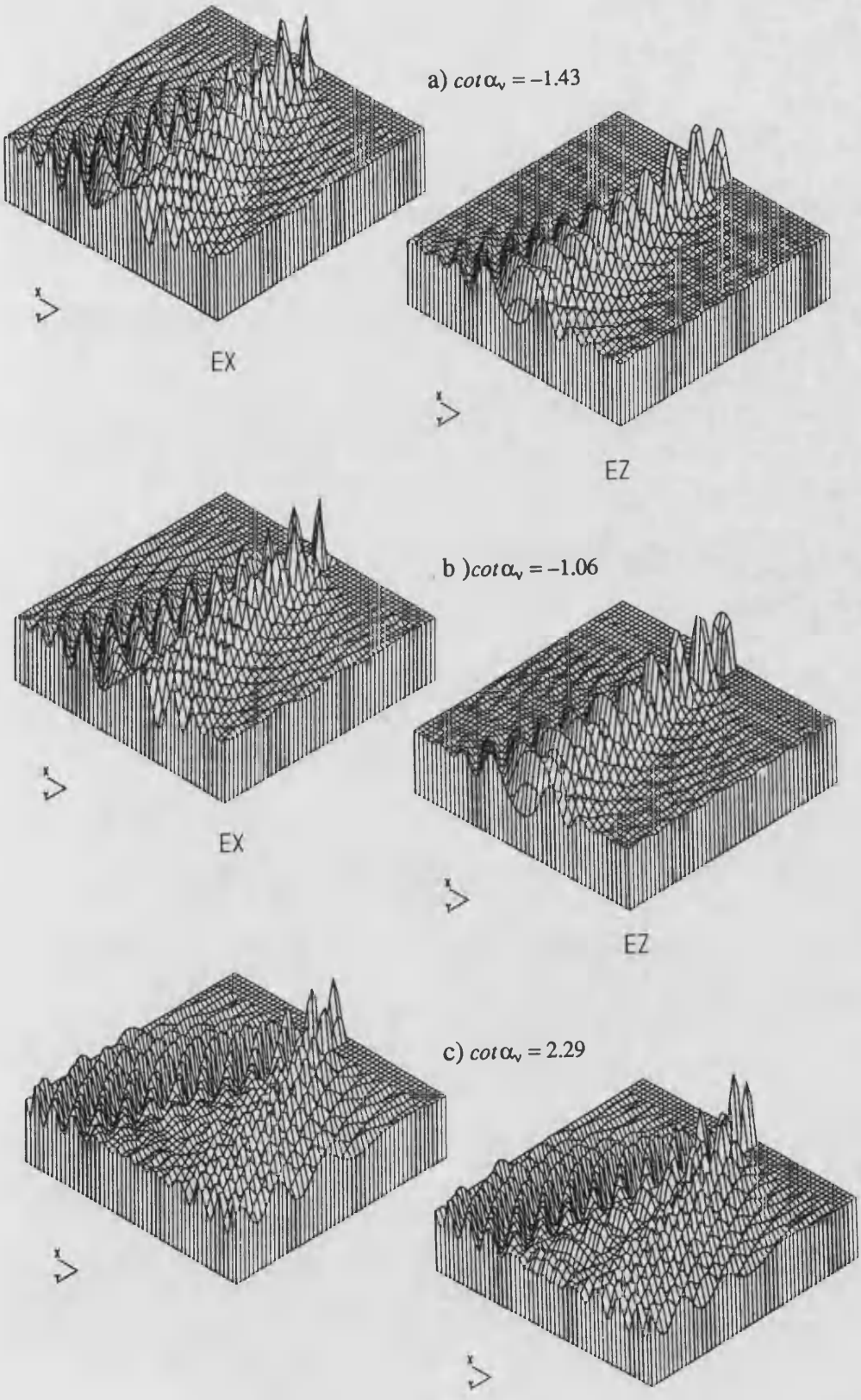

Figure 4.17) Far fields of the modes.

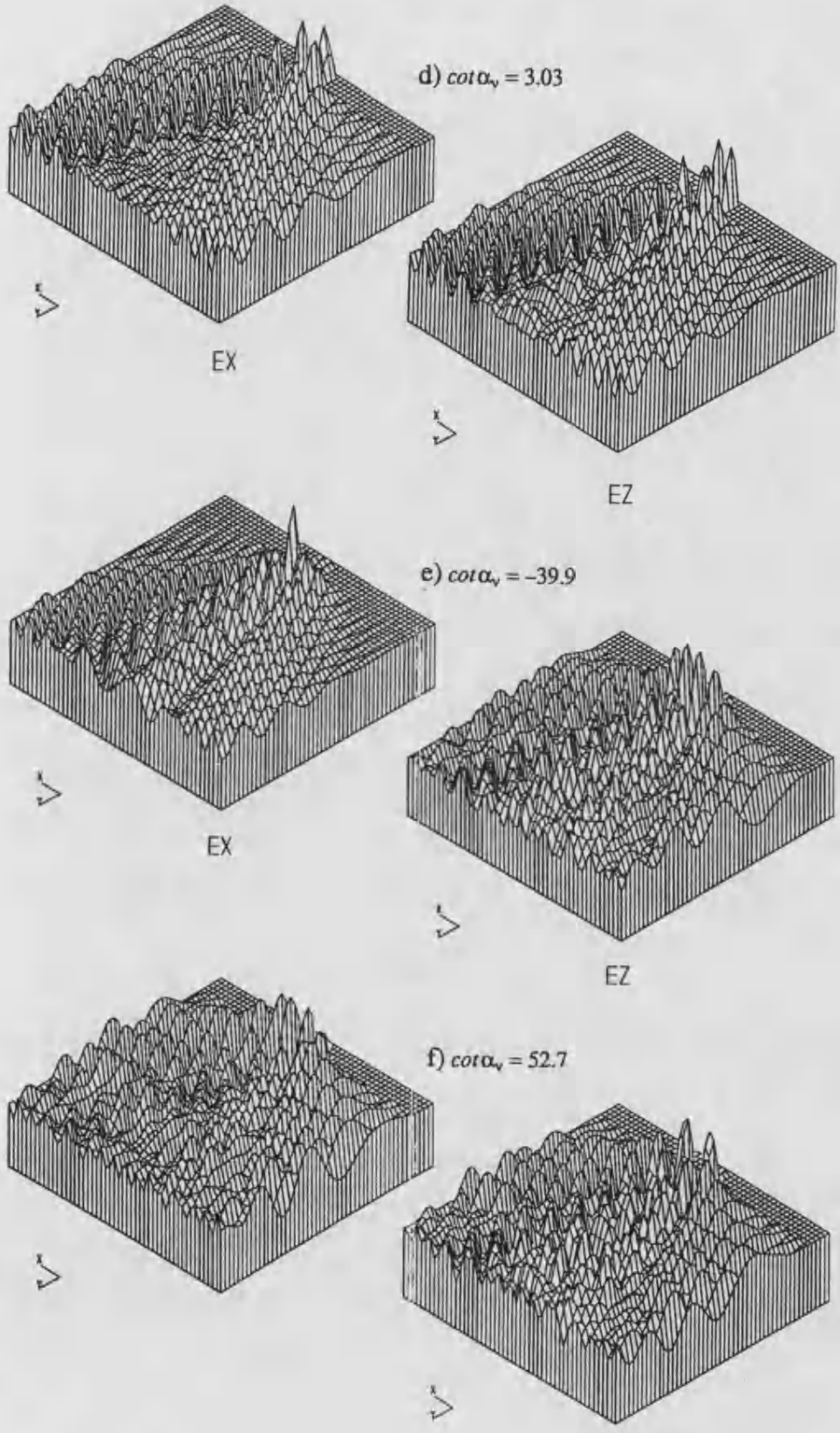

Figure 4.17) Far fields of the modes.

CHAPTER 5.

RECTANGULAR WAVEGUIDE TO I.D.G. TRANSITIONS.

5.1) Introduction.

This chapter shall present an analysis of direct transitions between rectangular waveguide and the I.D.G.

Direct transitions from closed waveguide to I.D.G. are practically important,being,to date the simplest way to excite this type of guide.These transitions,however,are known to involve a significant contribution from the I.D.G. continuum and require future attention with a view to improve their efficiency,[1].

The non trivial contribution of the continuous spectrum suggests that these transitions are suitable candidates for the verification of the complete mode spectrum developed in chapter 4.Additionally,it is relatively simple to obtain a set of experimental values for comparison.Two examples shall discussed,the transition between rectangular waveguide and both the deep slot and the shallow slot I.D.G.

Due to the similarity between the fields of the fundamental $T.E._{10}$ mode of the rectangular waveguide and the $H.E._{10}$ surface mode of the deep slot I.D.G.,this transition is expected,and indeed proves to be,the more transparent of the two configurations.In fact,if a dielectric taper is introduced into the rectangular waveguide and the height of the I.D.G. is reduced,then the V.S.W.R. of the transition may be reduced to less than 1.1 over the x-band,[2].However the $E.H._{11}$ surface mode of the shallow slot I.D.G. radically differs from the $T.E._{10}$ mode of

the rectangular waveguide.This results in significant excitation of the continuum of the I.D.G.Introduction of a taper does improve the situation,although not to the same extent as for the deep slot I.D.G.

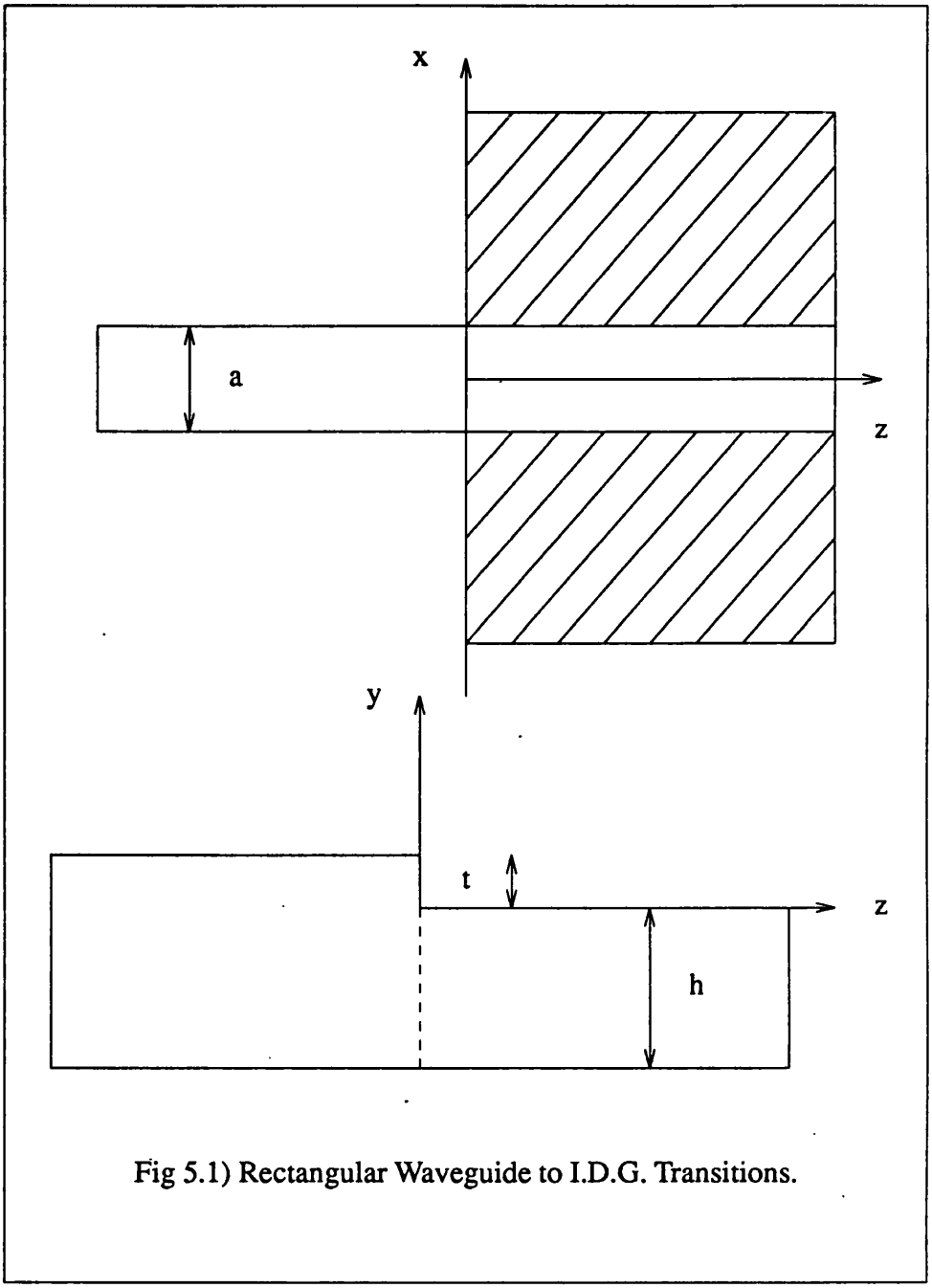

Fig 5.1) Rectangular Waveguide to I.D.G. Transitions.

In order to simplify the analysis,a semi-infinite metal screen is included in the structures.This has two advantages,firstly it excludes from the analysis the open region above the rectangular waveguide and secondly it results in a bounded aperture between the two guides.The two structures under consideration are shown in figure (5.1).

5.2) Formulation of the Problem.

The analysis follows a conventional approach [3].The unknown transverse electric fields in the aperture are expanded by the mode functions of both the rectangular waveguide and the I.D.G.Continuity of the transverse magnetic fields in the aperture results in an integral equation which may be solved for the aperture electric fields.

A $T.E._{10}$ rectangular waveguide mode of unit amplitude excites the transition.The transverse electric fields in the aperture,$\underline{\varepsilon}(r_t)$,may be expressed as;

$$\underline{\varepsilon}(r_t) = \sum_{n}^{\infty}\sum_{m}^{\infty}\sum_{\rho=e,h} <\underline{\varepsilon}(r_t'),\underline{H}^{\rho}_{mn}(r_t')> \underline{E}^{\rho}_{mn}(r_t)$$

$$= \sum_{s}^{N} <\underline{\varepsilon}(r_t'),\underline{H}_s(r_t')> \underline{E}_s(r_t) + \int_0^{\infty} dk_t \sum_{v}^{\infty} <\underline{\varepsilon}(r_t'),\underline{H}_v(r_t';k_t)> \underline{E}_v(r_t;k_t) \qquad (5.1)$$

where:

i) e=T.M.,h=T.E.

ii) $\underline{E}^{\rho}_{mn}(r_t)$ is a transverse mode vector of the rectangular waveguide,n and m being the two transverse wavenumbers and ρ=T.E.,T.M.,its polarisation.

In order to be consistent with the modes of the I.D.G.,the rectangular waveguide modes have also been normalised as;

$$\int_{-a/2}^{a/2}\int_{-h}^{t} dx\,dy\ \underline{E}^{\rho}_{nm}(r_t)\times\underline{H}^{\kappa}_{n'm'}(r_t)\,.\,\hat{z}=\delta_{nn'}\delta_{mm'}\delta_{\rho\kappa}\quad:\quad \rho,\kappa=e,h$$

iii) $\underline{E}_s(r_t)$ is the transverse mode vector of an I.D.G. surface mode.

iv) $\underline{E}_v(r_t;k_t)$ is a transverse mode vector of the I.D.G. continuum.

v) $<\underline{a}(r_t),\underline{b}(r_t)>=\int_{-a/2}^{a/2}\int_{-h}^{t} dx\,dy\ \underline{a}(r_t)\times\underline{b}(r_t)\,.\,\hat{z}$

If the electric field amplitude of the $T.E._{10}$ rectangular waveguide mode at the aperture is written as (1+R),where R is the reflection coefficient,then the amplitude of the corresponding magnetic field is (1-R) = 2-(1+R).Thus the requirement for continuity of the transverse magnetic fields at the aperture may be written as;

$$\left[2H_{h10}(r_t)-\sum_{n}^{\infty}\sum_{m}^{\infty}\sum_{\rho}<\underline{\varepsilon}(r_t'),\underline{H}^{\rho}_{mn}(r_t')>\underline{H}^{\rho}_{mn}(r_t)\right]\times\hat{z}$$

$$=\left[\sum_{s}^{N}<\underline{\varepsilon}(r_t'),\underline{H}_s(r_t')>\underline{H}_s(r_t)+\int_0^{\infty}dk_t\sum_{v}^{\infty}<\underline{\varepsilon}(r_t),\underline{H}_v(r_t;k_t)>\underline{H}_v(r_t;k_t)\right]\times\hat{z}\qquad(5.2)$$

This equation may be solved for the aperture electric field using Galerkin's method.The transverse electric fields in the aperture are expanded with an appropriate basis;

$$\underline{\varepsilon}(r_t)=\sum_{i}^{I}\underline{\Phi}(r_t)X_i\qquad(5.3)$$

and then tested with the same basis,resulting in the following matrix equation;

$$\underline{A}=\underline{\underline{G}}\,\underline{X}\qquad(5.4)$$

Where;

$$\underline{\underline{G}}^{ij} = \left[\sum_{n}\sum_{m}\sum_{\rho} \langle \underline{\Phi}_i(\underline{r}_t), \underline{H}^{\rho}_{mn}(\underline{r}_t) \rangle \langle \underline{\Phi}_j(\underline{r}_t), \underline{H}^{\rho}_{mn}(\underline{r}_t) \rangle \right] + \sum_{s}^{N} \langle \underline{\Phi}_i(\underline{r}_t), \underline{H}_s(\underline{r}_t) \rangle \langle \underline{\Phi}_j(\underline{r}_t), \underline{H}_s(\underline{r}_t) \rangle$$

$$+ \int_0^{\infty} dk_t \sum_{v} \langle \underline{\Phi}_i(\underline{r}_t), \underline{H}_v(k_t;\underline{r}_t) \rangle \langle \underline{\Phi}_j(\underline{r}_t), \underline{H}_v(k_t;\underline{r}_t) \rangle \qquad (5.5)$$

$$A_i = 2\langle \underline{\Phi}_i(\underline{rt}), \underline{H}_{h10}(\underline{r}_t) \rangle \qquad (5.6)$$

Equation (5.4) may be solved for the coefficient vector $\underline{X}$.The reflection coefficient,S_{11},is subsequently given by;

$$(1 + S_{11}) = \sum_{i}^{I} \langle X_i \underline{\Phi}_i(r_t), \underline{H}_{h10}(r_t) \rangle \qquad (5.7)$$

and the transmission coefficient,S_{21},by;

$$S_{21} = \sum_{i}^{I} \langle X_i \underline{\Phi}_i(r_t), \underline{H}_1(r_t) \rangle \qquad (5.8)$$

5.3) Choice of the basis set.

As discussed before,in the context of determining the I.D.G. modes,there are two criteria to be considered when choosing the basis set used to expand the interface fields,convergence and numerical expediency.If a basis that intrinsically models the expected field singularities is used,then Galerkin's method will converge rapidly.However for this analysis,use of the appropriate basis,the Gegenbauer polynomials,significantly increases the computational effort required to achieve sufficient accuracy.The alternative is to use a simple basis that is numerically convenient,albeit at the expense of convergence.The present analysis involves an integral and a summation of the numerically defined continuous modes,which is a reasonably lengthy process,and in order to minimise the overall analysis time the latter type of basis has been chosen.

The simplest basis that can be used is the following double fourier series;

$$\begin{pmatrix} \varepsilon_x(\underline{r}_t) \\ \varepsilon_y(\underline{r}_t) \end{pmatrix} = \sum_{p=1,3..} \sum_{q=1,2..} \frac{4}{\sqrt{ah}} \begin{pmatrix} \sin(\frac{p\pi}{a}x)\sin(\frac{q\pi}{h}y) & 0 \\ 0 & \cos(\frac{p\pi}{a}x)\cos(\frac{q\pi}{h}y) \end{pmatrix} \begin{pmatrix} X_x^{pq} \\ X_y^{pq} \end{pmatrix} \tag{5.9}$$

This could be decomposed into the T.E. and T.M. modes of the rectangular waveguide although if,in order to improve the matching,the height of the rectangular waveguide is different to that of the slot of the I.D.G.,as in the case of the deep slot I.D.G. in figure (5.1),this would not be possible,and so the form of equation (5.9) shall be retained.

5.4) Transition to the shallow Slot I.D.G.

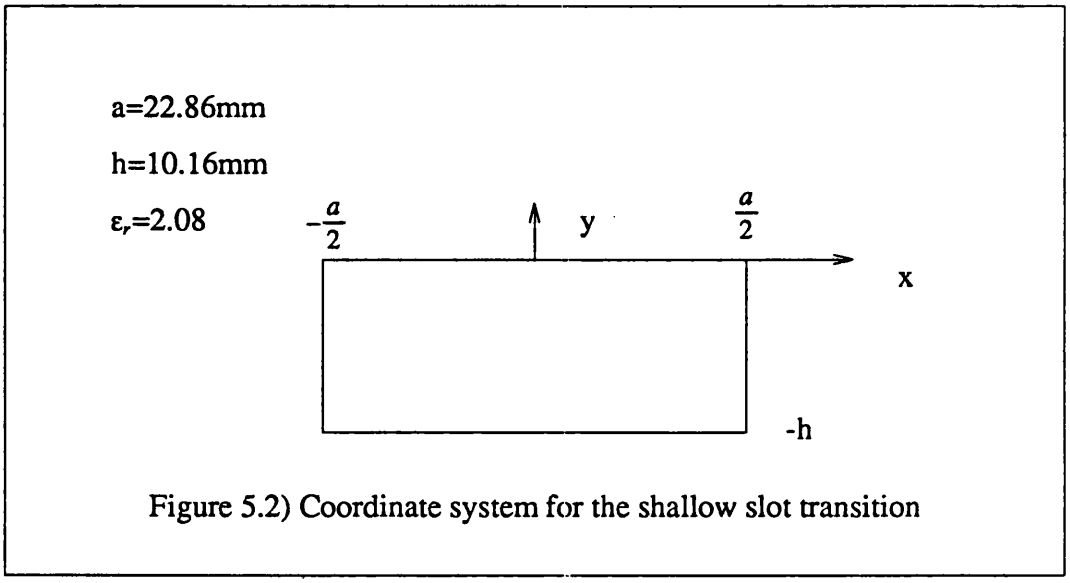

Figure 5.2) Coordinate system for the shallow slot transition

In the coordinate system shown in figure (5.2),the $T.E._{10}$ rectangular waveguide mode has an E_y component and no E_x component.

The appropriately normalised components of the rectangular waveguide modes may be written as;

T.E.

$$H_x^{nm}(\underline{r}_t) = -\frac{4}{\sqrt{ah}}\sqrt{y_h^{mn}}\cos(\theta_{mn})\cos(\frac{n\pi}{a}x)\cos(\frac{m\pi}{h})$$

$$H_y^{nm}(\underline{r}_t) = \frac{4}{\sqrt{ah}}\sqrt{y_h^{mn}}\sin(\theta_{mn})\sin(\frac{n\pi}{a}x)\sin(\frac{m\pi}{h}) \qquad (5.10)$$

T.M.

$$H_x^{nm}(\underline{r}_t) = \frac{4}{\sqrt{ah}}\sqrt{y_e^{mn}}\sin(\theta_{mn})\cos(\frac{n\pi}{a}x)\cos(\frac{m\pi}{h})$$

$$H_y^{nm}(\underline{r}_t) = -\frac{4}{\sqrt{ah}}\sqrt{y_e^{mn}}\cos(\theta_{mn})\sin(\frac{n\pi}{a}x)\sin(\frac{m\pi}{h}) \qquad (5.11)$$

where,n=1,3,..,m=0,1,2,.. and

$$y_h^{mn} = \frac{\beta_{mn}}{\omega\mu_o} \quad : \quad y_e^{mn} = \frac{\omega\varepsilon}{\beta_{mn}} \quad : \quad \beta_{mn}^2 = k_o^2 - (\frac{n\pi}{a})^2 - (\frac{m\pi}{h})^2$$

$$\sin(\theta_{mn}) = \frac{\frac{m\pi}{h}}{\left((\frac{n\pi}{a})^2 + (\frac{m\pi}{h})^2\right)^{\frac{1}{2}}} \quad : \quad \cos(\theta_{mn}) = \frac{\frac{n\pi}{a}}{\left((\frac{n\pi}{a})^2 + (\frac{m\pi}{h})^2\right)^{\frac{1}{2}}} \qquad (5.12)$$

The I.D.G. field components in the slot are in the form;

$$\begin{pmatrix} H_x^v(\underline{r}_t;k_t) \\ H_y^v(\underline{r}_t;k_t) \end{pmatrix} = \sum_{k=1,3...} \frac{2}{\sqrt{a}} \begin{pmatrix} \sin(\frac{k\pi}{a}x)\frac{\sin(q_k(y+h))}{\sin(q_k h)} & 0 \\ 0 & \cos(\frac{k\pi}{a}x)\frac{\cos(q_k(y+h))}{\cos(q_k h)} \end{pmatrix} \begin{pmatrix} H_{xk}^v \\ H_{yk}^v \end{pmatrix} \qquad (5.13)$$

where $q_k^2 = (\varepsilon_r - 1)k_o^2 - (\frac{k\pi}{a})^2 + k_t^2$.

Therefore the inner products defined in equation (5.5) are given by;

$$<\underline{\phi}_{pq}(\underline{r}_t),\underline{H}^h_{mn}(\underline{r}_t)> = \int_{-\frac{a}{2}}^{\frac{a}{2}} dx \int_{-h}^{0} dy \left(\frac{4}{\sqrt{ah}}\right)^2 \begin{pmatrix} \sin(\frac{p\pi}{a}x)\sin(\frac{q\pi}{h}y) & 0 \\ 0 & \cos(\frac{p\pi}{a}x)\cos(\frac{q\pi}{h}y) \end{pmatrix}$$

$$\begin{pmatrix} \sin(\frac{n\pi}{a}x)\sin(\frac{m\pi}{h}y) & 0 \\ 0 & \cos(\frac{n\pi}{a}x)\cos(\frac{m\pi}{h}y) \end{pmatrix} \begin{pmatrix} \sqrt{y_h^{mn}}\sin(\theta_{mn}) \\ \sqrt{y_h^{mn}}\cos(\theta_{mn}) \end{pmatrix}$$

$$= \delta_{pn}\delta_{qm} \begin{pmatrix} \sqrt{y_h^{mn}}\sin(\theta_{mn}) \\ \sqrt{y_h^{mn}}\cos(\theta_{mn}) \end{pmatrix} \tag{5.14}$$

for a T.E. mode.Similarly for a T.M. mode of the rectangular waveguide;

$$<\underline{\phi}_{pq}(\underline{r}_t),\underline{H}^e_{mn}(\underline{r}_t)> = \delta_{pn}\delta_{qm} \begin{pmatrix} \sqrt{y_e^{mn}}\cos(\theta_{mn}) \\ -\sqrt{y_e^{mn}}\sin(\theta_{mn}) \end{pmatrix} \tag{5.15}$$

Therefore;

$$\sum_n \sum_m \sum_\rho <\underline{\phi}_{pq}(\underline{r}_t),\underline{H}^\rho_{mn}(\underline{r}_t)><\underline{\phi}_{rs}(\underline{r}_t),\underline{H}^\rho_{mn}(\underline{r}_t)> =$$

$$\delta_{pr}\delta_{qs} \begin{pmatrix} y_h\sin^2(\theta_{mn})+y_e\cos^2(\theta_{mn}) & (y_h-y_e)\sin(\theta_{mn})\cos(\theta_{mn}) \\ (y_h-y_e)\sin(\theta_{mn})\cos(\theta_{mn}) & y_h\cos^2(\theta_{mn})+y_e\sin^2(\theta_{mn}) \end{pmatrix} \tag{5.16}$$

The inner products involving the I.D.G. modes are given by;

$$<\phi_{pq}(\underline{r}_t),\underline{H}_v(\underline{r}_t;k_t)> = \int_{-\frac{a}{2}}^{\frac{a}{2}} dx \int_{-h}^{0} dy \frac{2}{\sqrt{ah}} \begin{pmatrix} \sin(\frac{p\pi}{a}x)\sin(\frac{q\pi}{h}y) & 0 \\ 0 & \cos(\frac{p\pi}{a}x)\cos(\frac{q\pi}{h}y) \end{pmatrix}$$

$$\sum_{k=1,3\ldots} \frac{2}{\sqrt{a}} \begin{pmatrix} \sin(\frac{k\pi}{a}x)\dfrac{\sin(q_k(y+h))}{\sin(q_k h)} & 0 \\ 0 & \cos(\frac{n\pi}{a}x)\cos\dfrac{(q_k(y+h))}{\cos(q_k h)} \end{pmatrix} \begin{pmatrix} H^v_{yk}(k_t) \\ -H^v_{xk}(k_t) \end{pmatrix}$$

$$= \begin{pmatrix} S^{pq} H^{v}_{yk}(k_t) \\ -C^{pq} H^{v}_{xk}(k_t) \end{pmatrix} \tag{5.17}$$

where;

$$S^{pq} = \int_{-h}^{0} dy \frac{2}{\sqrt{h}} \sin(\frac{q\pi}{h} y) \frac{\sin(q_k(y+h))}{\sin(q_k h)}$$

$$C^{pq} = \int_{-h}^{0} dy \frac{2}{\sqrt{h}} \cos(\frac{q\pi}{h} y) \frac{\cos(q_k(y+h))}{\cos(q_k h)} \tag{5.18}$$

Therefore;

$$\int_0^{\infty} dk_t \sum_v < \underline{\phi}_{pq}(r_t), \underline{H}_v(r_t;k_t) > < \underline{\phi}_{rs}(r_t), \underline{H}_v(r_t;k_t) >$$

$$= \int_0^{\infty} dk_t \sum_v \begin{pmatrix} S^{pq} S^{rs} H^{v}_{yp}(k_t) H^{v}_{yr}(k_t) & -S^{pq} C^{rs} H^{v}_{yp}(k_t) H^{v}_{xr}(k_t) \\ -C^{pq} S^{rs} H^{v}_{xp}(k_t) H^{v}_{yr}(k_t) & C^{pq} C^{rs} H^{v}_{xp}(k_t) H^{v}_{xr}(k_t) \end{pmatrix} \tag{5.19}$$

The surface mode inner products will give similar terms to those of equation (5.19).

The computed values of S_{11} and S_{21} are given in table 5.1 and figure (5.3).Measurements of S_{11} were made using an HP8510 network analyser calibrated onto the rectangular waveguide.As at present a calibration for the analyser onto the I.D.G. is not available,it was not possible to obtain any measurements of S_{21}.Figure (5.4) compares the theoretical and measured values of both the amplitude and phase of S_{11}.It can be seen that good agreement has been achieved over most of the x band.At the higher frequencies,particularly at 11Ghz,there does appear to be a discrepancy of about 3dB.These points were further examined theoretically,increasing both the number of basis terms and the accuracy of the numerical integrations,although no significant changes were

freq./Ghz	$\|S_{11}\|$	$arg(S_{11})$	$\|S_{21}\|$	$arg(S_{21})$	% loss
8.0	0.399	-157.3	0.637	-12.7	43.5
8.5	0.354	-162.1	0.757	173.1	30.2
9.0	0.300	-161.1	0.828	175.3	22.4
9.5	0.306	-141.5	0.848	178.9	18.6
10.0	0.269	-151.7	0.878	178.7	15.6
10.5	0.288	-155.7	0.877	178.7	14.9
11.0	0.233	-153.2	0.902	178.5	13.2
11.5	0.173	-142.3	0.922	178.1	12.1
12.0	0.207	-154.0	0.934	178.8	8.5

Table 5.1) Rectangular waveguide to shallow slot I.D.G. parameters.

observed.The problem may lie with the experimental results,as in the absence of a matched load for the I.D.G.,it was necessary to use absorbing material to prevent multiple reflections from the far end of the I.D.G.It was observed that the absorber was surprisingly frequency sensitive,its performance generally degrading with frequency.As the experimental values of reflection are slightly higher than the theoretical values,it is possible that a small reflection from the far end of the I.D.G. is constructively interfering at the transition.

Theoretically both the power lost through radiation and the reflection coefficient decrease in magnitude with frequency.This is understandable as,with increasing frequency,the surface mode of the I.D.G. becomes more tightly bound to the guide.The increased concentration of the surface mode fields in the slot results in improved coupling at the aperture with the $T.E._{10}$ mode of the rectangular waveguide.Notwithstanding this,the opposite polarisations of these two modes ensures that a significant continuum field is always excited.

The phase of S_{11} indicates that the transition is basically capacitive.This is consistent with its excitation solely by a y-component of electric field,as this couples most strongly to the L.S.M. dominated modes of the I.D.G.Thus,the

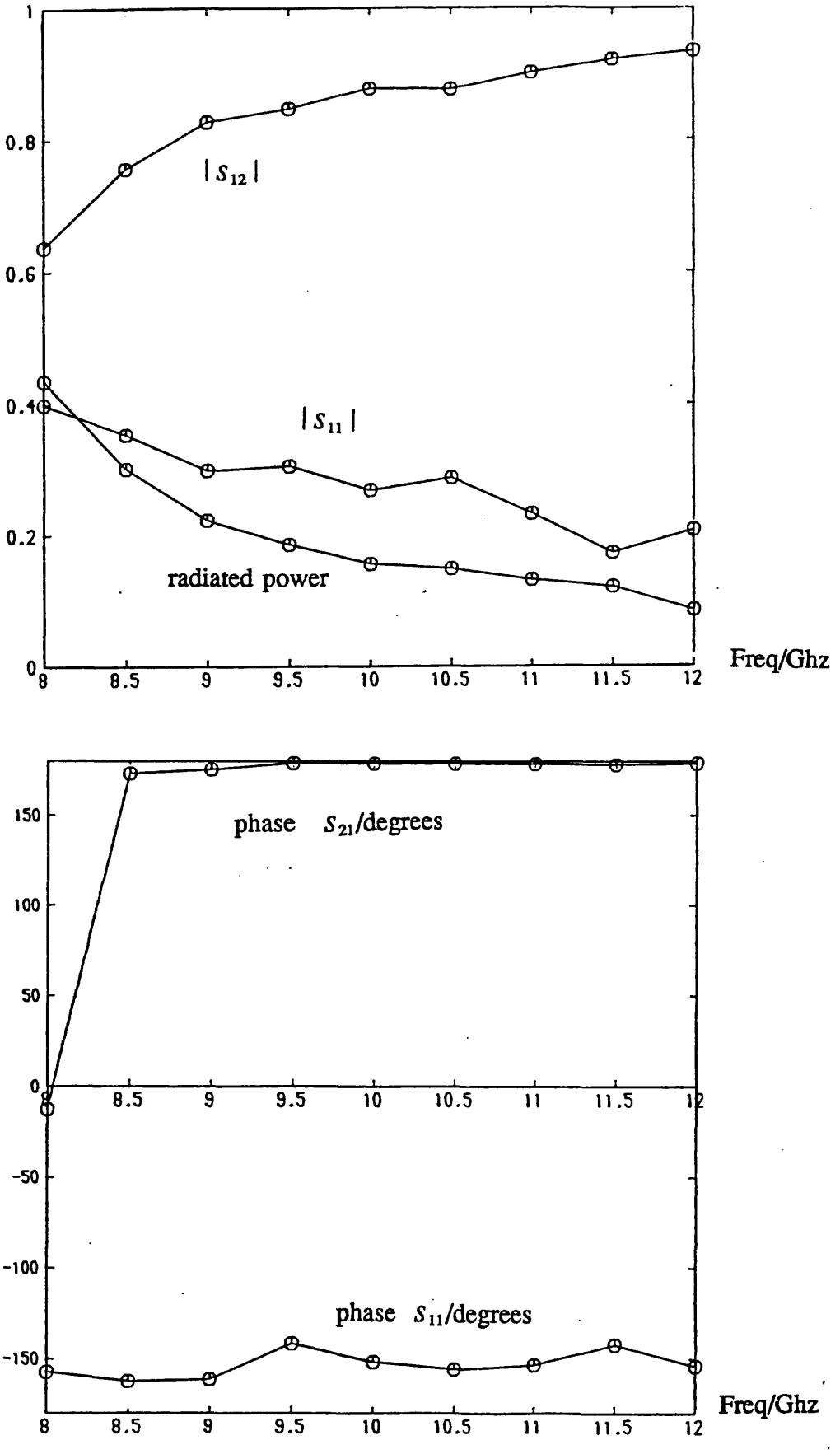

Figure 5.3) Theoretical S-Parameters of the shallow slot I.D.G. transition.

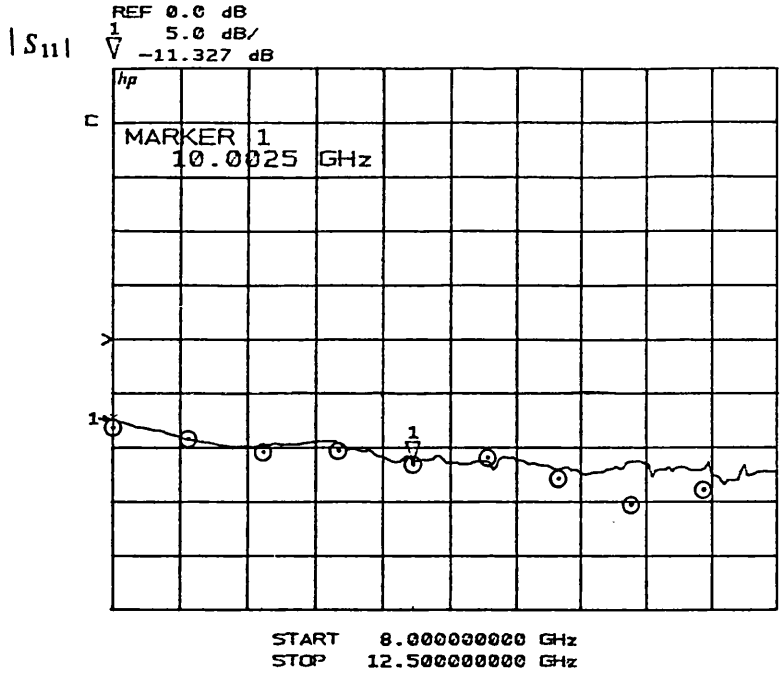

Theoretical points

phase S_{11}/degrees

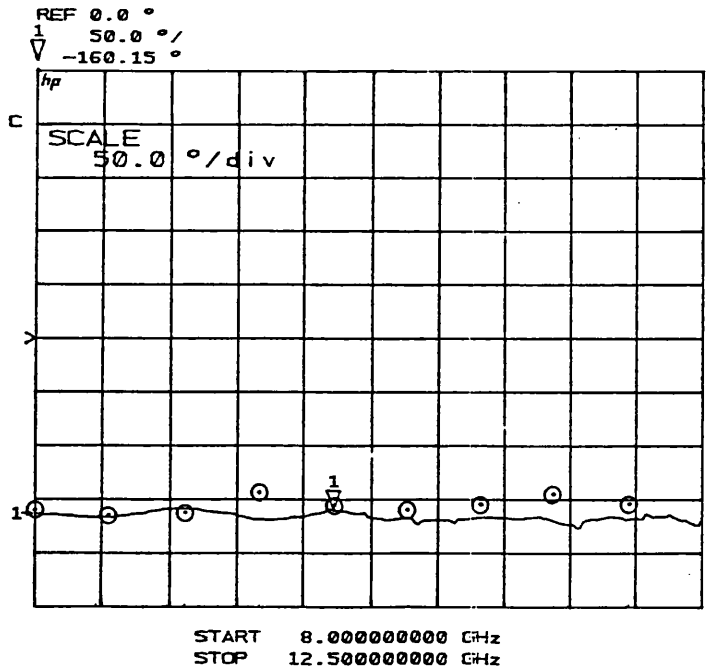

Figure 5.4) Theoretical and experimental values of S_{11} for the shallow slot I.D.G. transition.

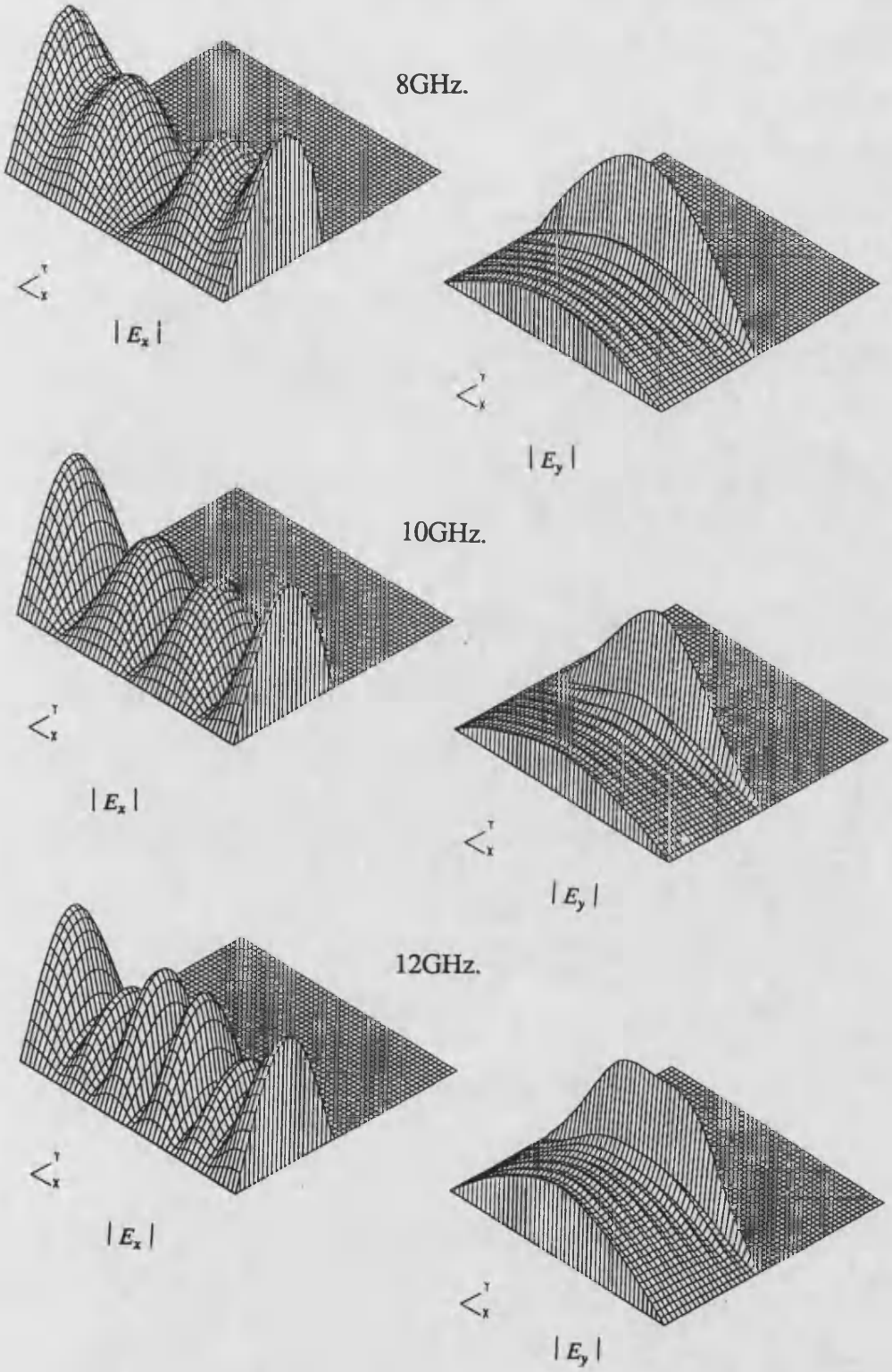

Figure 5.5) Aperture fields for the shallow slot I.D.G. transition.

energy storage in the nonradiating modes is predominantly electric.

Figure (5.5) shows some examples of the transverse electric fields in the aperture.The presence of the $T.E._{10}$ rectangular waveguide mode is clearly visible in the E_y component and,in addition,a singularity caused by the 90 degree corner formed by the top of the rectangular waveguide and the metal screen.The E_x component is tangential to,and is consequently zero at,the 90 degree corner.As it is the minor field component,it is difficult to predict its behaviour,and indeed,it varies significantly with frequency.

5.5) Transition to the deep slot I.D.G.

Although the rectangular waveguide to deep slot I.D.G. transition does not excite the continuum of the I.D.G. to the same extent as the shallow slot transition,it is by no means an ideal transition.The deep slot I.D.G. analysed is not as deep as the rectangular waveguide.Although this improves the performance of the transition,it is offset to some degree by the presence of the infinite metal screen,that causes diffraction.

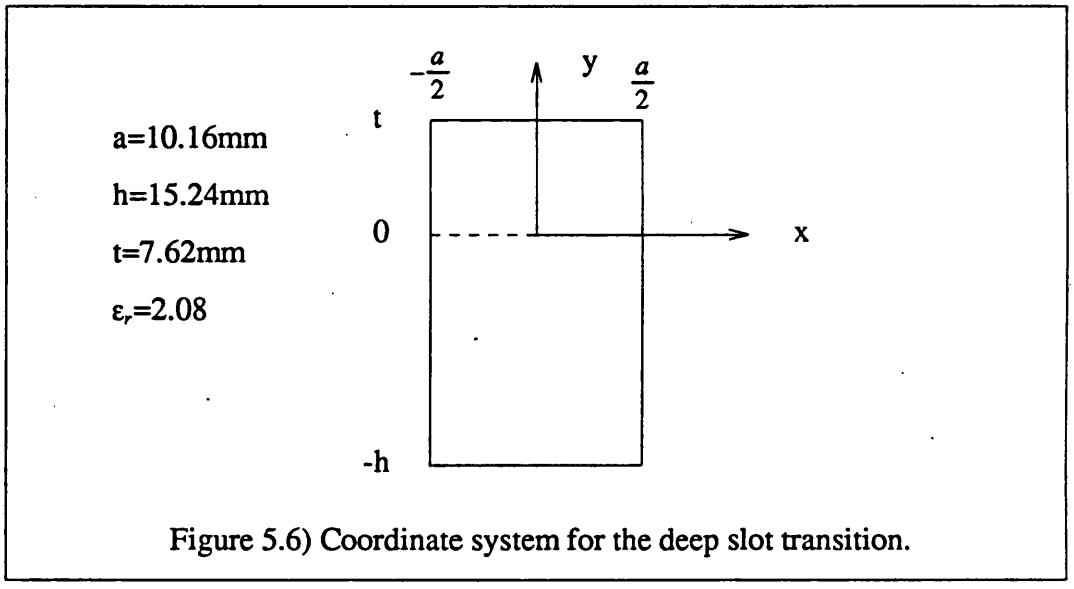

Figure 5.6) Coordinate system for the deep slot transition.

In the coordinate system of figure 5.6 the fundamental $T.E._{10}$ mode of the rectangular waveguide has an E_x component and no E_y component.Due to the polarity of the fundamental mode of the deep slot I.D.G.,the transition fields are now expanded with an even basis w.r.t. x,ie;

$$\begin{pmatrix}\varepsilon_x(\underline{r}_t)\\ \varepsilon_y(\underline{r}_t)\end{pmatrix}=\sum_{p=0,2..}\sum_{q=1,2..}\frac{4}{\sqrt{ah}}\begin{pmatrix}\cos(\frac{p\pi}{a}x)\sin(\frac{q\pi}{h}y) & 0\\ 0 & \sin(\frac{p\pi}{a}x)\cos(\frac{q\pi}{h}y)\end{pmatrix}\begin{pmatrix}X_x^{pq}\\ X_y^{pq}\end{pmatrix} \tag{5.20}$$

The I.D.G. related inner product terms will be identical to those given for the shallow slot guide,except that now k=0,2...,n=0,2,4..,m=1,2,... and obviously the coefficients $H_{xk}^{v}(kt)$ and $H_{yk}^{v}(kt)$ are different.In this coordinate system the rectangular modes are given by;

T.E.

$$H_x^{nm}(\underline{r}_t)=\frac{4}{\sqrt{ah}}\sqrt{y_h^{mn}}\sin(\theta_{mn})\sin(\frac{n\pi}{a}x)\cos(\frac{m\pi}{h})$$

$$H_y^{nm}(\underline{r}_t)=\frac{4}{\sqrt{ah}}\sqrt{y_h^{mn}}\cos(\theta_{mn})\cos(\frac{n\pi}{a}x)\sin(\frac{m\pi}{h}) \tag{5.21}$$

T.M.

$$H_x^{nm}(\underline{r}_t)=\frac{4}{\sqrt{ah}}\sqrt{y_e^{mn}}\cos(\theta_{mn})\sin(\frac{n\pi}{a}x)\cos(\frac{m\pi}{h})$$

$$H_y^{nm}(\underline{r}_t)=-\frac{4}{\sqrt{ah}}\sqrt{y_e^{mn}}\sin(\theta_{mn})\cos(\frac{n\pi}{a}x)\sin(\frac{m\pi}{h}) \tag{5.22}$$

The mismatch between the depth of the I.D.G. and the height of the rectangular waveguide complicates the inner products involving the modes of the latter.These inner products may be evaluated as;

$$\sum_{m}\sum_{n}\sum_{\rho}<\underline{\phi}_{pq},\underline{H}_{mn}^{\rho}><\underline{\phi}_{rs},\underline{H}_{mn}^{\rho}>=$$

$$\delta_{pr}\sum_{m}\begin{pmatrix} S_1^{qm}S_1^{sm}(y_h\cos^2(\theta_{mn})+y_e\sin^2(\theta_{mn})) & (y_e-y_h)S_1^{qm}C_1^{sm}\sin(\theta_{mn})\cos(\theta_{mn}) \\ (y_e-y_h)C_1^{qm}S_1^{sm}\sin(\theta_{mn})\cos(\theta_{mn}) & C_1^{qm}C_1^{ms}(y_h\sin^2(\theta_{mn})+y_e\cos^2(\theta_{mn})) \end{pmatrix} \tag{5.23}$$

where;

$$S_1^{qm} = \int_{-h}^{0} dy \frac{4}{\sqrt{h(h+t)}}\sin(\frac{q\pi}{h}y)\sin(\frac{m\pi(y-t)}{h+t}y)$$

$$C_1^{qm} = \int_{-h}^{0} dy \frac{4}{\sqrt{h(h+t)}}\cos(\frac{q\pi}{h}y)\cos(\frac{m\pi(y-t)}{h+t}y) \tag{5.24}$$

freq./Ghz	$\lvert S_{11}\rvert$	$arg(S_{11})$	$\lvert S_{21}\rvert$	$arg(S_{21})$	% loss
8.0	0.557	151.9	0.801	-152.6	4.7
8.5	0.491	151.4	0.840	-157.5	5.3
9.0	0.442	152.5	0.864	-161.4	5.9
9.5	0.408	154.6	0.877	-164.5	6.5
10.0	0.386	157.5	0.881	-167.1	7.4
10.5	0.374	160.6	0.881	-169.2	8.5
11.0	0.373	163.0	0.874	-170.6	9.8
11.5	0.362	164.3	0.884	-171.9	8.9
12.0	0.356	166.0	0.889	-173.0	8.3

Table 5.2) Rectangular waveguide to deep slot I.D.G. parameters.

The computed S-parameters are given in table 5.2 and figure (5.7).Figure (5.8) compares the theoretical and experimental values obtained for S_{11} and it can be seen that the correlation between the two sets of data is even closer than for the shallow slot I.D.G. transition.This is not surprising as the similarity between the fields of the surface mode of the deep slot I.D.G. and the $T.E._{10}$ rectangular waveguide mode improves the numerical convergence of the analysis.It is also noted that as the amplitude of S_{11} is approximately 3dB higher than that of the shallow slot I.D.G.,the effect of the reflections from the imperfect end-absorber is reduced.This increased amplitude is a consequence of the mismatch in the height

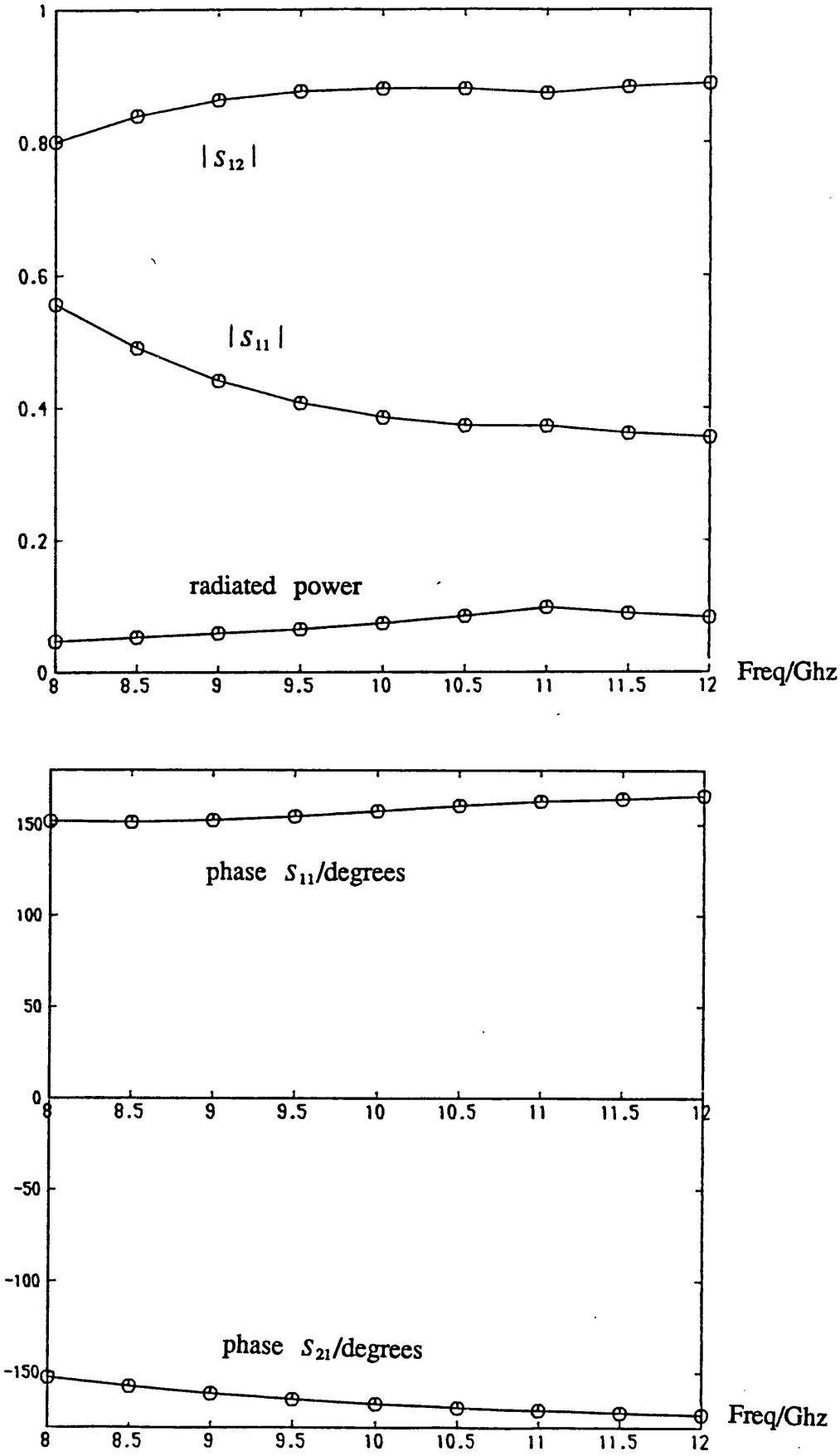

Figure 5.7) Theoretical S-Parameters of the deep slot I.D.G. transition.

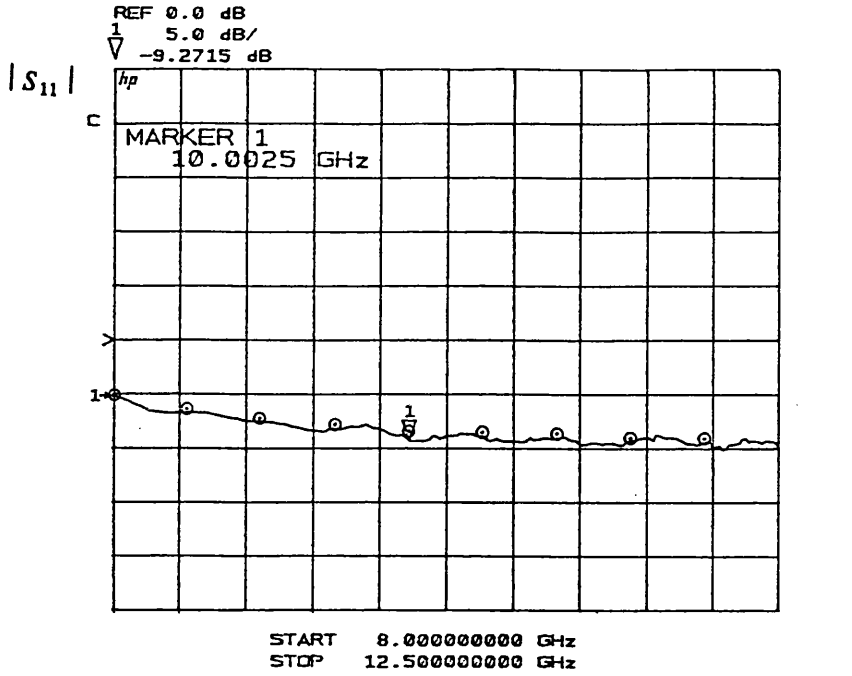

phase S_{11}/degrees

Theoretical points

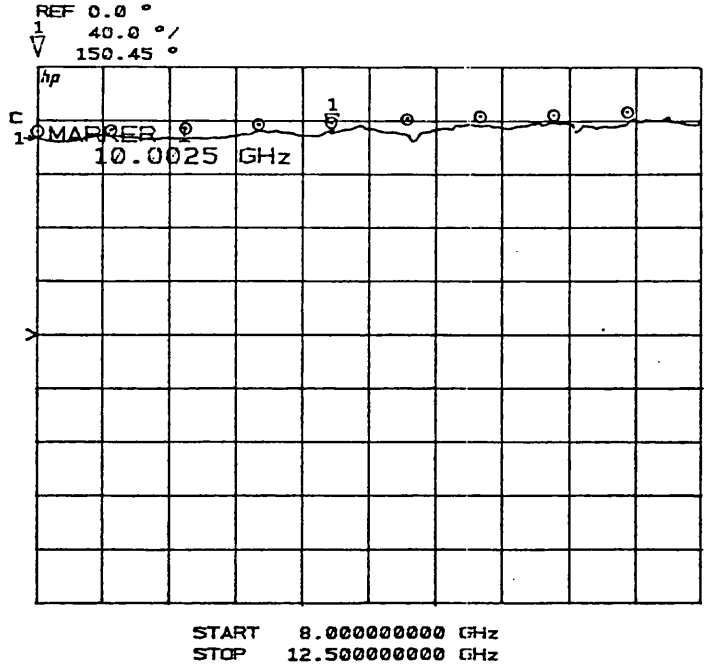

Figure 5.8) Theoretical and experimental values of S_{11} for the deep slot I.D.G. transition.

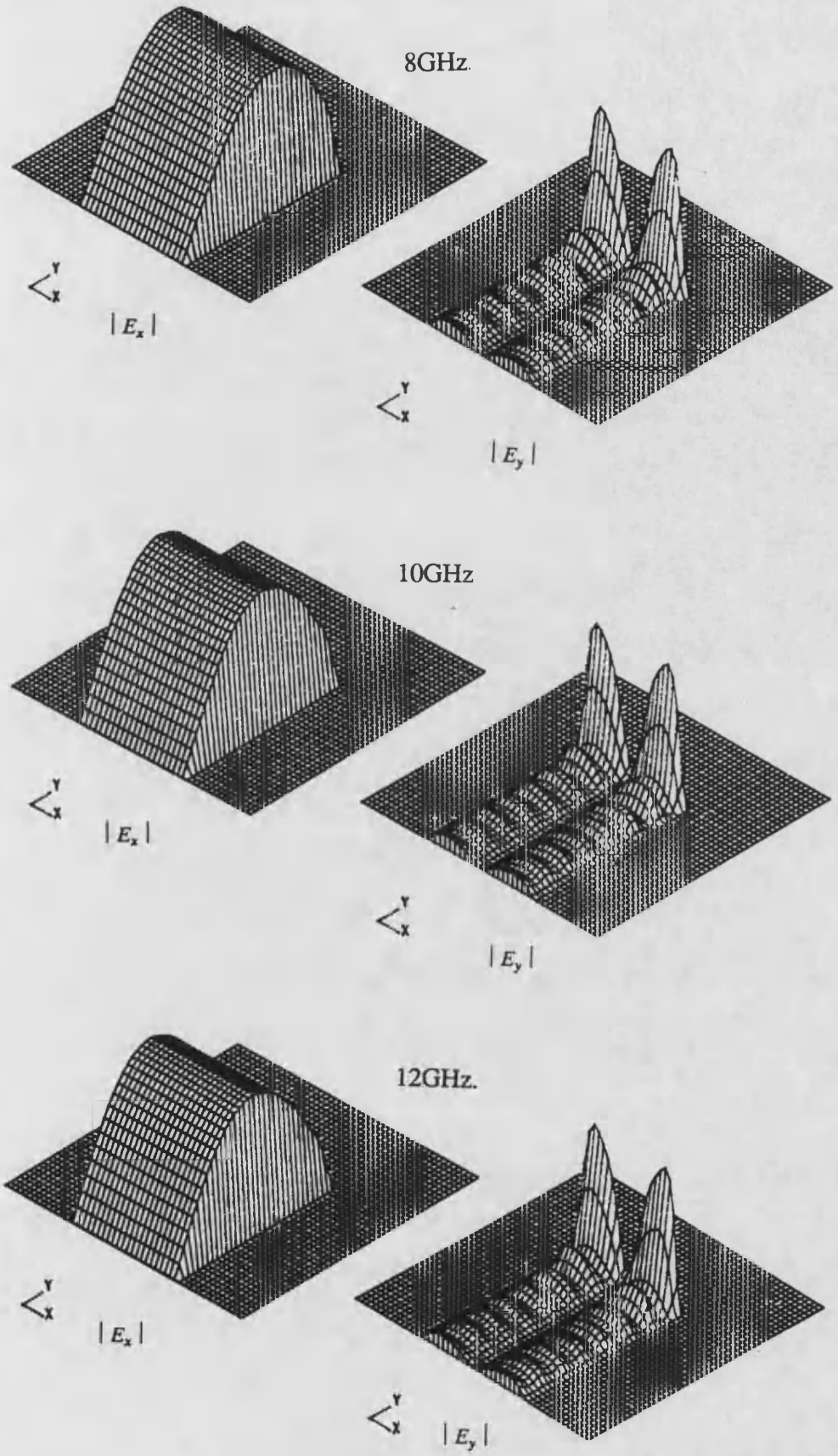

Figure 5.9) Aperture fields for the deep slot I.D.G. transition.

of the rectangular waveguide and the depth of the I.D.G. slot,causing the bottom of the metal screen to act as an inductive iris in the former.In fact,this iris is responsible for most of the behaviour of the transition,its inductive nature clearly indicated by the phase of S_{11}.It is also observed that the power lost to radiation is significantly smaller than that of the shallow slot I.D.G.This confirms the reduced involvement of the I.D.G continuum for this transition.

The aperture fields shown in figure (5.9) demonstrate both the singularity in the E_y component,due to the bottom of the screen,and the dominance of the E_x component by the $T.E._{10}$ rectangular waveguide mode.

The good correlation that has been achieved between theoretical and experimental values for these transitions,confirms,not only the validity of the I.D.G. continuous modes developed in the previous chapter,but also demonstrates that they may be successfully used to analyse practical discontinuity problems.The next chapter shall further use the modes in the form of the Green's function of the I.D.G.,to develop network models for metallic strips and patches on the air-dielectric interface of the I.D.G.,that are the basis of I.D.G. leaky wave antennas.

5.6) References.

1) T.Rozzi and L.Ma,"An efficient Mode Launcher for Arrays of Longitudinal Dipoles in I.D.G.",1990 IEEE MTT-S digest,pp1243-1246.

2) S.Hedges and T.Rozzi,"The Loss Analysis of Inset Dielectric Guide Including Bending Loss and a Comparison with Image Line,17th European microwave conf.,Rome,Sept 1987,pp933-938.

3) R.Collin,"Field Theory of Waves",McGraw Hill,1960.

CHAPTER 6.

ANALYSIS OF RADIATING STRIPS AND PATCHES ON THE I.D.G.

6.1) Introduction.

As discussed in chapter 1,the I.D.G. provides an excellent basis for the construction of leaky wave antennas,[1-4].These antennas are simple to manufacture,compact,lightweight and may be electrically scanned in two dimensions.As shown in figure 6.1,the radiating elements are simply strips or

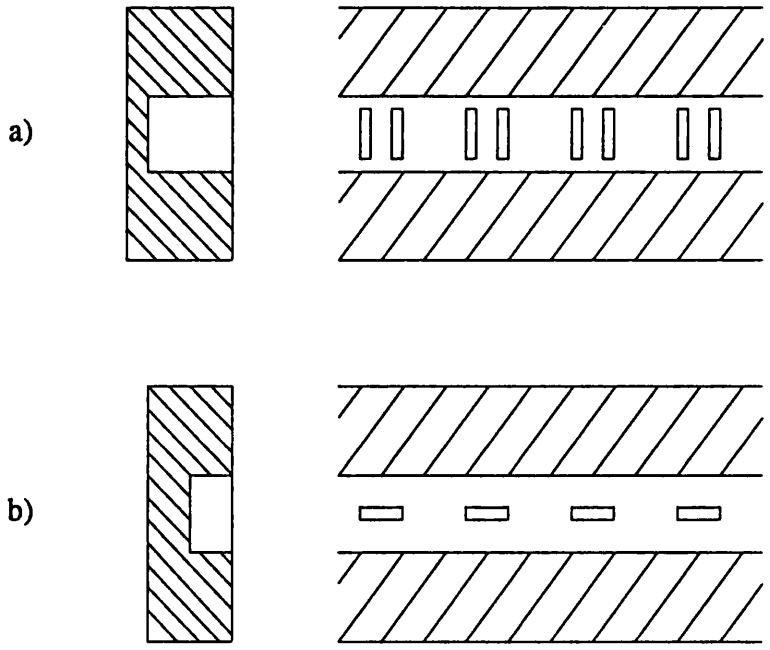

Figure 6.1) Linear Arrays in I.D.G.;a) vertically,b) horizontally polarised.

patches of metal placed upon the air-dielectric interface of the I.D.G.,exciting radiation with good polarisation properties.

Due to the good degree of isolation that exists between I.D.G.'s in close proximity,planar arrays may be formed by placing linear arrays in parallel and scanned by means of phase controlled feed networks and frequency,[5,6].

The practical implementation of I.D.G. leaky wave arrays necessitates that they be accurately designed without excessive recourse to experimentation.Ultimately an ability to design and simulate these arrays using computer aided design techniques is desired.To develop such a facility,it is necessary to provide accurate models of the behaviour of the arrays,both in terms of their radiation characteristics,network parameters and frequency dependence.In particular it is necessary to consider;

i) The element sizes and orientation.

ii) The interelement spacing and overall array length.

iii) The radiation patterns;beamwidth,purity of polarisation

and the existence of blind spots and side lobes.

iv) The bandwidth.

v) The frequency dependence of the beam direction.

vi) The input impedance to the array.

vii) Methods of exciting the array.

viii) The gain and efficiency.

The analysis of the linear arrays may be undertaken in two ways.Firstly,if the array is uniform and long enough to prevent reflections from the far end,then it is possible to consider the structure as a whole.This approach treats the array as a

periodic structure supporting a leaky wave with a complex propagation constant along the guide,[7].Many examples of this method may be found in the literature,[8-15],including an application to the I.D.G.,[16].Before discussing the latter,it is necessary to comment upon the method in general.Its attraction is that it can be relatively simple to undertake and allows for mutual coupling effects between the elements.The leaky wave pole may be identified by transverse resonance,[7],requiring only that a transverse equivalent network be developed.However the major limitation is that it is only applicable to uniform arrays,which is clearly restrictive.In addition,whilst the array may be correctly terminated to prevent reflections,it is not possible to totally eliminate radiation from the transition from the feed network.In fact for I.D.G. arrays,this is a nontrivial source of radiation,which cannot easily be accounted for by the leaky wave approach.

The recent paper concerning the I.D.G.,[16],considered transverse strips placed periodically upon the surface of a deep slot I.D.G.The top of the dielectric is recessed into the slot,indicative of the method rather than any design advantage.In addition to the general limitations,there are some further restrictions in the applicability of the method presented.The method models the transverse network as shorted transmission lines in the dielectric,coupled to each other and a parallel plate waveguide radiating into free space,by a transformer characterising the strips.The parallel plate to free space transition is modelled by a lumped admittance assuming monomodal propagation in the parallel plate waveguide.It is assumed that as the other modes are below cut off,that their contribution to the fields at the open end of the parallel plate waveguide is negligible.Of course this is only acceptable if the dielectric height is reduced substantially into the slot of the I.D.G.Therefore the method is not applicable to the I.D.G. proper,only its reduced height variant.

The alternative to assuming a periodic structure,is to analyse each radiating element individually.This approach is more involved but it does permit nonuniform arrays,such as Taylor and Chebyshev arrays,to be developed.Naturally,as the elements are being investigated in isolation it is necessary to account for mutual coupling effects when combining elements into an array environment.This problem shall be discussed at the end of the chapter in the light of the behaviour of the individual elements.

In this chapter radiating strips and patches producing radiation of both polarisations shall be characterised both in terms of their network parameters and their radiation patterns.

6.2) Formulation of the Integral Equation.

This section shall demonstrate that the parameters characterising these elements may be derived from the solution to an integral equation for the current on the patch.This integral equation is a consequence of requiring that the tangential electric fields are zero on the patch.

Naturally strips may be regarded as particular cases of patches,upon which only one component of current exists,and therefore the general analysis shall assume a patch of arbitrary dimensions.

The patch is excited by an incident field $\underline{E}_i(\underline{r})$.A current,$\underline{J}(\underline{r})$,flows on the on the patch resulting in a scattered field,$\underline{E}_s(\underline{r})$.The sum of the incident and the scattered fields must satisfy the boundary conditions of both the empty guide and the patch.The boundary conditions of the empty guide will automatically be satisfied if both the incident and the scattered fields are expressed in terms of the modes of the guide,leaving the satisfaction of the boundary conditions of the patch

to be ensured.Thus it is required that:

$$[\underline{E}_i(\underline{r}) + \underline{E}_s(\underline{r})] \times \hat{n} = \underline{0} \quad : \underline{r} \text{ on the patch.} \tag{6.1}$$

where $\hat{n}$ is the normal to the patch.

The scattered electric field may be determined from the patch current using the Green's function of the I.D.G. ,allowing equation (6.1) to be written as;

$$[\underline{E}_i(\underline{r}) + \int_{patch} d\underline{r}' \underline{\underline{G}}_E(\underline{r};\underline{r}') \cdot \underline{J}(\underline{r}')] \times \hat{n} = \underline{0} \quad : \underline{r} \text{ on the patch.} \tag{6.2}$$

The dyadic electric Green's function is given in equations (2.5.15) and (2.5.17) as;

$$\underline{\underline{G}}_E(\underline{r}_t;\underline{r}_t') = -\sum_p \frac{E_p(\underline{r}_t) RE_p(\underline{r}_t')}{2} e^{-j\beta_p |z-z'|} + \hat{z}\hat{z}\frac{\beta_p}{\varepsilon_r k_o^2 - \beta^2}\delta(z-z')E_{zp}(\underline{r}_t)E_{zp}(\underline{r}_t')$$

$$-\int_0^\infty dk_t \frac{\underline{E}(\underline{r}_t;k_t) RE(\underline{r}_t';k_t)}{2} e^{-j\beta|z-z'|} + \hat{z}\hat{z}\frac{\beta}{\varepsilon_r k_o^2 - \beta^2}\delta(z-z')E_z(\underline{r}_t;k_t)E_z(\underline{r}_t';k_t) \tag{6.3}$$

Recalling that the adjoint fields are related to the original fields by the reflection operator,ie $\begin{pmatrix} E_x \\ E_z \end{pmatrix}^A = \begin{pmatrix} E_x \\ -E_z \end{pmatrix}^*$,has allowed the inner product involving the Green's function to be redefined as a real integral.

Equation (6.2) is an integral equation that may be solved for the patch current and subsequently be used to determine the scattered field and hence the equivalent network of the patch.

The integral equation may be solved by Galerkin's method.As the patch has been assumed to be of infinitesimal thickness,the current may be expanded as;

$$\underline{J}(\underline{r}) = \sum_n^N \hat{x} J_{xn}(\underline{r}) X_n + \hat{z} J_{zn}(\underline{r}) Z_n \tag{6.4}$$

resulting in the following matrix equation;

$$-\begin{pmatrix} \int_s \underline{dr}\, E_{ix}(\underline{r})J_x(\underline{r}) \\ \int_s \underline{dr} E_{iz}(\underline{r})J_z(\underline{r}) \end{pmatrix} = \begin{pmatrix} \int_s \underline{dr}\int_s \underline{dr}' J_x(\underline{r})\underline{\underline{G}}_E^{xx}(\underline{r},\underline{r}')J_x^T(\underline{r}') & \int_s \underline{dr}\int_s \underline{dr}' J_x(\underline{r})\underline{\underline{G}}_E^{xz}(\underline{r},\underline{r}')J_z^T(\underline{r}') \\ \int_s \underline{dr}\int_s \underline{dr}' J_z(\underline{r})\underline{\underline{G}}_E^{zx}(\underline{r},\underline{r}')J_x^T(\underline{r}') & \int_s \underline{dr}\int_s \underline{dr}' J_z(\underline{r})\underline{\underline{G}}_E^{zz}(\underline{r},\underline{r}')J_z^T(\underline{r}') \end{pmatrix} \begin{pmatrix} \underline{X} \\ \underline{Z} \end{pmatrix} \qquad (6.5)$$

where s represents the surface of the patch.

Although not strictly necessary for longitudinally symmetric patches,it is convenient to consider separately the cases of odd and even excitation.The advantage of this approach is that,if an N term expansion is used for both the odd and even current components,then solutions are required to two inhomogeneous matrix equations of order N,rather than one of order 2N.Clearly,for a given solution accuracy,this reduces the requirements placed upon the numerical matrix routine.

Naturally in an array environment,the incident field will comprise of many modal components,although it is expected that the dominant contribution will be from the fundamental mode.At present it shall be assumed that the patch is excited solely by the fundamental surface mode of the I.D.G.,without accounting for the mutual coupling affects caused by the interaction of the higher order modes.Under this assumption the patch may be modelled by a two port network,utilising either a Y-parameter or an S-parameter representation.Although the physical symmetry of the patches ensures the reciprocal nature of the two representations,it is necessary to use a full π network to model an arbitrary patch,which only simplifies to a simple shunt element for transverse strips of infinitesimal width.Under odd and even excitation the equivalent admittance networks reduce to those shown in figure 6.2

Once the patch currents have been identified,the reflection coefficients R_o and R_e,under odd and even excitation respectively,may be found using the Green's function,from which the Y- and S-parameters may be identified through;

$$R_o = \frac{Y_o - (Y_{11} - Y_{12})}{Y_o + (Y_{11} - Y_{12})} \quad : \quad R_e = \frac{Y_o - (Y_{11} + Y_{12})}{Y_o + (Y_{11} + Y_{12})}$$

$$S_{11} = \frac{1}{2}(R_e + R_o) \quad : \quad S_{21} = \frac{1}{2}(R_e - R_o) \tag{6.6}$$

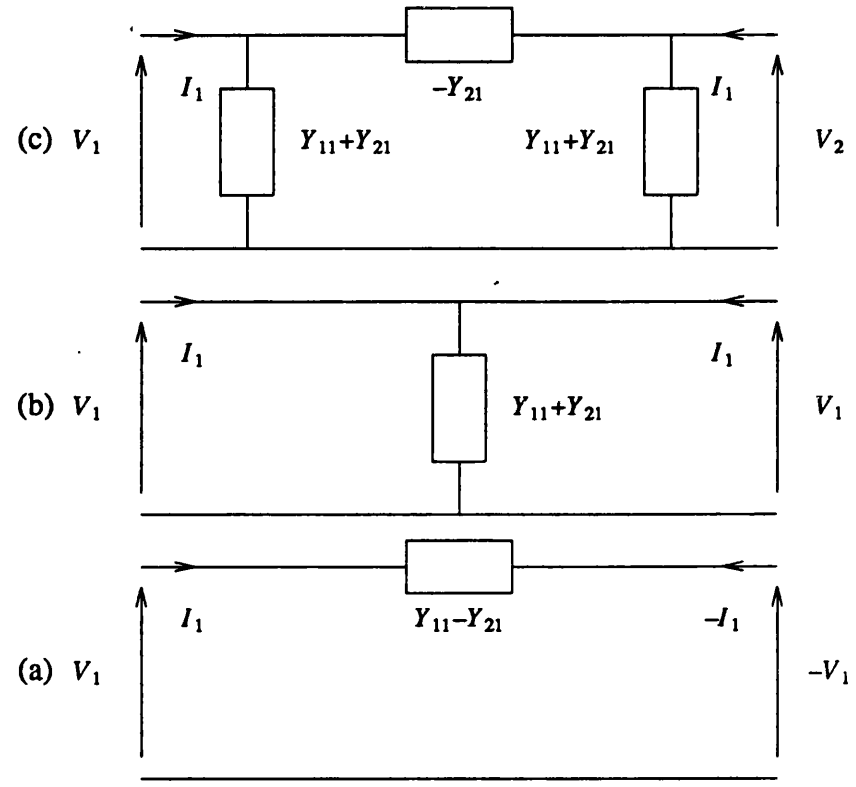

Figure 6.2) Admittance networks under a) general,b) even and c) odd excitation.

6.3) Determination of the Radiation Patterns.

As shall now be demonstrated,it is possible to determine the radiation patterns of the patches using a far field analysis based upon saddle point

integration techniques.

Only the continuous spectrum of the I.D.G. contributes to the far field,which may be consequently identified from the Green's function as;

$$\underline{E}_{rad}(\underline{r}) = \int_0^{\infty} dk_t \sum_{v} \underline{E}_v(\underline{r}_t;k_t) e^{-j\beta z} \int_s d\underline{r}' \frac{R\underline{E}_v(\underline{r}_t';k_t) e^{+j\beta z'} . \underline{J}(\underline{r}')}{-2} \tag{6.7}$$

Substituting in the explicit form of the continuous modes gives;

$$\underline{E}_{rad}(\underline{r}) = \int_0^{\infty} dk_t \sum_{v} \int_0^{\infty} dk_x \phi_h(k_x,x) \sin(k_y y + \alpha_v(k_t)) e^{-j\beta z} \underline{\tilde{e}}_v(k_x) \int_s d\underline{r}' \frac{R\underline{E}_v(\underline{r}_t';k_t) e^{+j\beta z'} . \underline{J}(\underline{r}')}{-2} \tag{6.8}$$

or alternatively;

$$\underline{E}_{rad}(\underline{r}) = \int_{-\infty}^{\infty} dk_t \sum_{v} \int_{-\infty}^{\infty} dk_x \underline{\tilde{A}}_v(k_x,k_t) e^{-j(k_x x + k_y y + \beta z)} \tag{6.9}$$

where;

$$\underline{\tilde{A}}_v(k_x,k_t) = \underline{\tilde{e}}_v(k_x) e^{-j\alpha_v(k_t)} \int_s d\underline{r}' \frac{R\underline{E}_v(\underline{r}_t';k_t) e^{+j\beta z'} . \underline{J}(\underline{r}')}{-2} \tag{6.10}$$

Direct evaluation of equation (6.9) is numerically inefficient and it is possible to use saddle point integration techniques to render a good approximation.For this purpose it is appropriate to transform equation (6.9) into cylindrical coordinates in both the space and wavenumber domains.As illustrated in figure 6.3,this involves the following substitutions;

$$k_t = k_o \sin\eta \quad : k_x = k_t \cos\theta \quad : k_y = k_t \sin\theta \quad : \beta = k_o \cos\eta$$

$$x = R\sin\delta\cos\phi \quad : y = R\sin\delta\sin\phi \quad : z = R\cos\delta \tag{6.11}$$

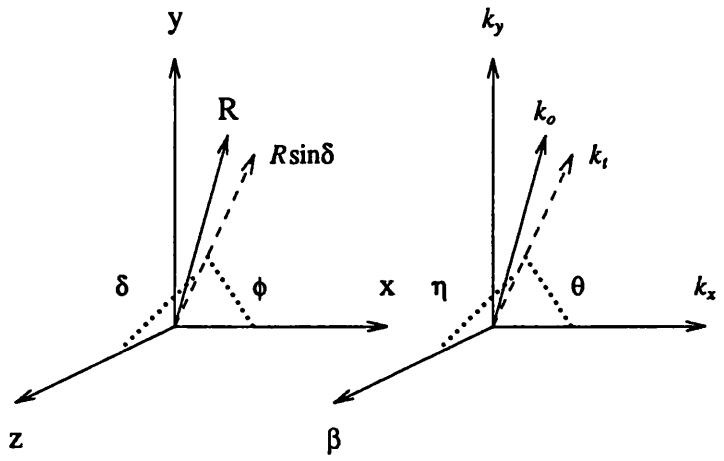

Figure 6.3) Cylindrical Transformations.

The Jacobian associated with this transformation is given by;

$$dk_t dk_x = \begin{vmatrix} \frac{\partial k_t}{\partial \theta} & \frac{\partial k_t}{\partial \eta} \\ \frac{\partial k_x}{\partial \theta} & \frac{\partial k_x}{\partial \eta} \end{vmatrix} d\eta d\theta = k_o^2 \sin\eta\cos\eta\sin\theta d\eta d\theta \qquad (6.12)$$

Using this transformation equation (6.9) becomes;

$$\underline{E}_{rad}(\underline{r}_t) = \sum_{v} \int_{C_\eta} d\eta k_o^2 \sin\eta\cos\eta \int_{C_\theta} d\theta \sin\theta \underline{\tilde{A}}_v(\eta,\theta) e^{-jk_o R(\sin\eta\sin\delta\cos(\theta-\phi) + \cos\delta\cos\eta)} \qquad (6.13)$$

The contours C_η and C_θ are shown in figure 6.4.From Cauchy's theorem the integrals along these contours are equal to the sum of the residues from any poles less the integrals over the steepest descent paths,(S.D.P.'s),also shown.

Consider the integral w.r.t. θ.There are no poles in the integrand which,as it is in the form $p(\theta)e^{-jk_o Rq(\theta)}$,has a saddle point at the point at which $q'(\theta) = 0$,ie in this

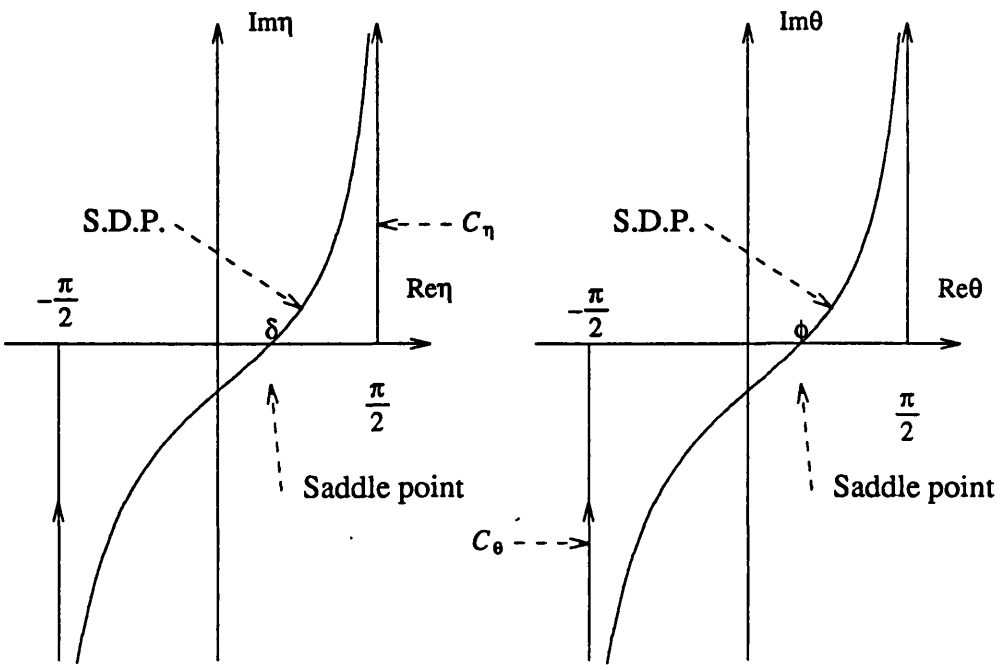

Figure 6.4) Contour paths in the η and θ planes.

case at $\theta = \phi$.From [17],the integral over the S.D.P. is excellently approximated by $p(\phi)e^{-jk_oRq(\phi)}\left(\frac{2\pi}{-q''(\phi)}\right)^{\frac{1}{2}} e^{\pm j\frac{\pi}{4}}$.Using this result in equation (6.13) gives;

$$\underline{E}_{rad}(\underline{r}_t) = -\sum_v k_o^2 \sin\phi \left(\frac{2\pi}{k_oR}\right)^{\frac{1}{2}} e^{\pm j\frac{\pi}{4}} \int_{C_\eta} d\eta \cos\eta \left(\frac{\sin\eta}{\sin\delta}\right)^{\frac{1}{2}} e^{-jk_oR\cos(\eta-\delta)} \underline{\tilde{A}}_v(\eta,\phi) \qquad (6.14)$$

Repeating the process for the integral w.r.t. η gives,within a phase shift,the radiation pattern associated with the patch;

$$\underline{E}_{rad}(\underline{r}_t) = \frac{2\pi k_o}{R} \cos\delta \sin\phi e^{-jk_oR} \sum_v \underline{\tilde{A}}_v(\delta,\phi) \qquad (6.15)$$

6.4) Transverse Strips on a deep Slot I.D.G.

The main electric field component of the fundamental $H.E._{10}$ mode of the deep slot I.D.G. is,x-directed.Transverse metallic strips placed upon the air-dielectric interface couple strongly to the incident field and produce very pure vertically polarised radiation.

Transverse strips of infinitesimal width and thickness only support an x-directed component of current.Therefore the vector integral equation given in equation (6.2) reduces to a scalar equivalent,involving just the $\underline{\underline{G}}_E^{xx}$ part of the Green's function.This scalar integral equation is given by;

$$-\int_{-\frac{L}{2}}^{\frac{L}{2}} dx E_{xx}(x,0)\underline{J}_x(x) = \int_{-\frac{L}{2}}^{\frac{L}{2}} dx \int_{-\frac{L}{2}}^{\frac{L}{2}} dx' \underline{J}_x(x)$$

$$\left(\frac{E_{xx}(x,0)E_{xx}(x',0)}{-2} + \int_0^{\infty} dk_t \sum_v \frac{E_{vx}(x,0;k_t)E_{vx}(x',0;k_t)}{-2} \right) \underline{J}_x^T(x') \qquad (6.16)$$

The choice of the basis functions used to expand $J_x(x)$ again raises the dilemma of numerical expediency and convergence.However,in contrast to modelling the modes of the I.D.G.,which requires a large number of terms to encompass the wide variety of modal fields whichever basis is used,it is expected that the strip current may be modelled with a handful of astutely chosen terms.Theoretically it is known that the current will exhibit a singularity of order $-\frac{1}{2}$ at the ends of the strip and that,away from the guide corners,the E_x component of the incident surface mode is very uniform.This suggests that the Chebychev polynomials are a suitable basis with which to expand the strip current.This choice is further supported by the analytical nature of the integration of the product of these polynomials and the functions $\phi_{hn}(x)$ used to to represent the modes of the

I.D.G.

Strips of various lengths,placed upon a deep slot I.D.G. of dimensions 1.016mm by 1.524mm and containing P.T.F.E.,(ε_R = 2.08),have been analysed at various frequencies.The Y- and S-parameters are plotted in figures 6.5 and 6.6 and tabulated in table 6.1.

Network Parameters at 8.0Ghz							
Width	|s11|	arg(s11)	|s21|	arg(s21)	% loss	re[Y]	im[Y]
1mm	0.015	90.9	1.000	-89.1	0.01	0.0001	-0.029
2mm	0.021	91.4	1.000	-88.6	0.01	0.0001	-0.042
3mm	0.035	92.3	0.999	-87.7	0.03	0.0003	-0.071
4mm	0.060	93.8	0.998	-86.2	0.09	0.0009	-0.120
5mm	0.089	95.7	0.995	-84.3	0.19	0.0019	-0.178
6mm	0.117	97.6	0.991	-82.4	0.33	0.0034	-0.237
7mm	0.140	99.0	0.988	-81.0	0.47	0.0049	-0.283
8mm	0.158	100.2	0.984	-79.8	0.61	0.0063	-0.320
9mm	0.173	101.2	0.981	-78.8	0.75	0.0078	-0.352

Network Parameters at 9.0Ghz							
Width	|s11|	arg(s11)	|s21|	arg(s21)	% loss	re[Y]	im[Y]
1mm	0.013	91.4	1.000	-88.6	0.03	0.0003	-0.025
2mm	0.017	91.8	1.000	-88.2	0.05	0.0005	-0.034
3mm	0.027	92.9	0.999	-87.1	0.13	0.0013	-0.054
4mm	0.043	94.6	0.997	-85.4	0.32	0.0032	-0.087
5mm	0.057	96.1	0.996	-83.9	0.56	0.0056	-0.114
6mm	0.069	97.3	0.994	-82.7	0.81	0.0082	-0.138
7mm	0.078	98.4	0.992	-81.6	1.06	0.0108	-0.158
8mm	0.084	99.1	0.990	-80.9	1.24	0.0127	-0.170
9mm	0.090	99.7	0.989	-80.3	1.41	0.0144	-0.181

Table 6.1) The Network Parameters of Transverse Strips on a Deep Slot I.D.G.

Network Parameters at 10.0Ghz							
Width	|s11|	arg(s11)	|s21|	arg(s21)	% loss	re[Y]	im[Y]
1mm	0.012	92.2	1.000	-87.8	0.06	0.0006	-0.024
2mm	0.016	92.9	0.999	-87.1	0.11	0.0011	-0.032
3mm	0.026	94.6	0.998	-85.4	0.28	0.0028	-0.051
4mm	0.048	98.6	0.994	-81.4	0.98	0.0100	-0.096
5mm	0.070	102.7	0.987	-77.3	2.11	0.0217	-0.141
6mm	0.088	106.0	0.979	-74.0	3.31	0.0346	-0.177
7mm	0.099	108.0	0.974	-72.0	4.17	0.0440	-0.198
8mm	0.105	109.3	0.970	-70.7	4.73	0.0503	-0.211
9mm	0.111	110.5	0.967	-69.5	5.30	0.0567	-0.223

Network Parameters at 11.0Ghz							
Width	|s11|	arg(s11)	|s21|	arg(s21)	% loss	re[Y]	im[Y]
1mm	0.014	93.6	0.999	-86.4	0.14	0.0014	-0.029
2mm	0.020	95.1	0.998	-84.9	0.28	0.0028	-0.041
3mm	0.033	98.2	0.996	-81.8	0.71	0.0072	-0.065
4mm	0.048	102.1	0.991	-77.9	1.54	0.0157	-0.095
5mm	0.060	105.1	0.986	-74.9	2.41	0.0248	-0.119
6mm	0.069	107.6	0.981	-72.4	3.22	0.0335	-0.137
7mm	0.078	109.7	0.977	-70.3	4.03	0.0422	-0.153
8mm	0.084	111.3	0.973	-68.7	4.69	0.0496	-0.165
9mm	0.088	112.5	0.970	-67.5	5.18	0.0551	-0.173

Network Parameters at 12.0Ghz							
Width	|s11|	arg(s11)	|s21|	arg(s21)	% loss	re[Y]	im[Y]
1mm	0.014	93.2	0.999	-86.8	0.12	0.0012	-0.027
2mm	0.019	94.5	0.999	-85.5	0.22	0.0022	-0.038
3mm	0.030	96.9	0.997	-83.1	0.54	0.0054	-0.059
4mm	0.045	100.6	0.993	-79.4	1.26	0.0127	-0.090
5mm	0.060	104.1	0.987	-75.9	2.20	0.0226	-0.119
6mm	0.072	107.1	0.981	-72.9	3.22	0.0334	-0.144
7mm	0.082	109.5	0.976	-70.5	4.12	0.0433	-0.163
8mm	0.091	111.7	0.970	-68.3	5.08	0.0540	-0.180
9mm	0.100	113.8	0.964	-66.2	6.05	0.0650	-0.196

Table 6.1) Continued.

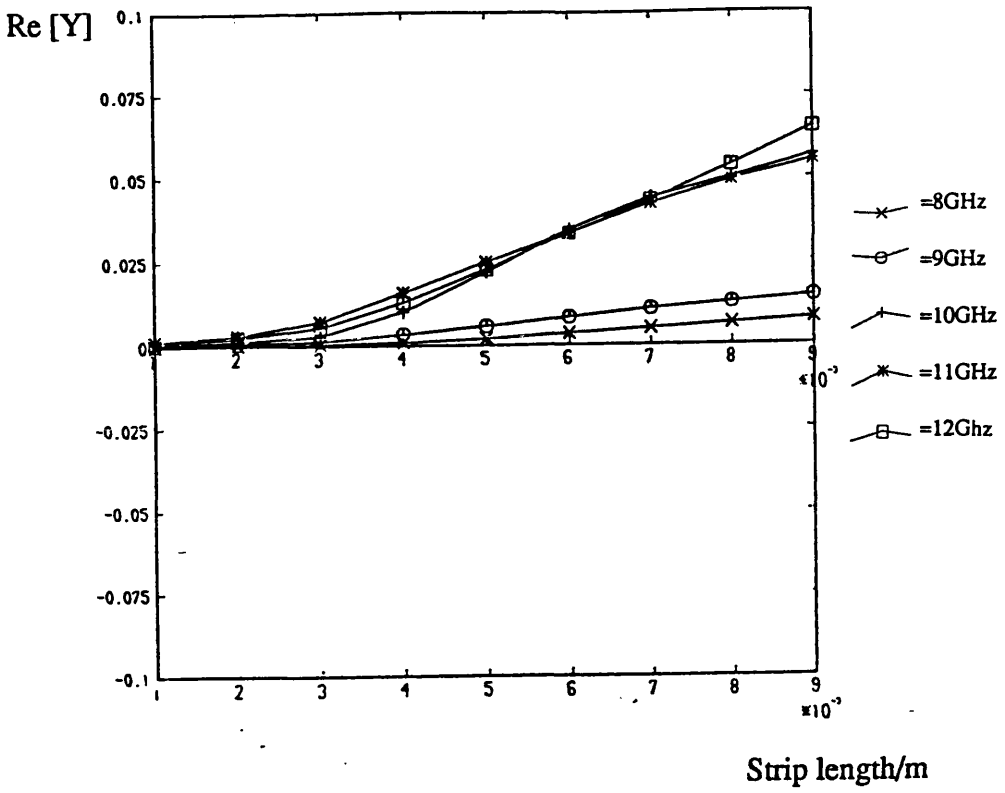

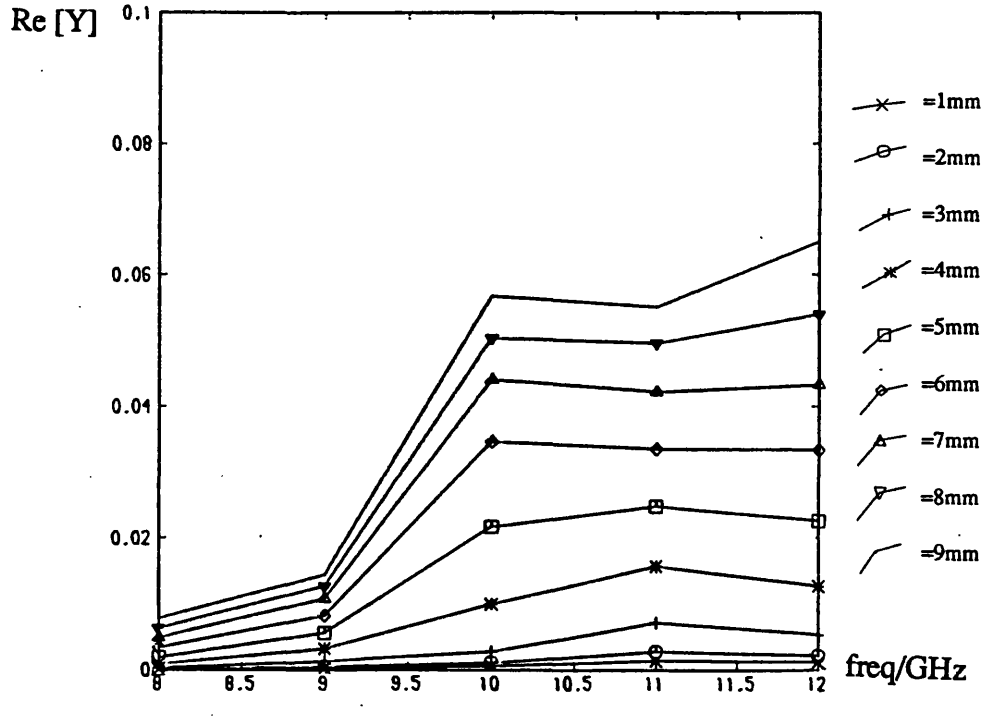

Figure 6.5) Variation of the real part of the equivalent shunt admittance of a transverse strip on a deep slot I.D.G. with a) strip length,b) frequency.

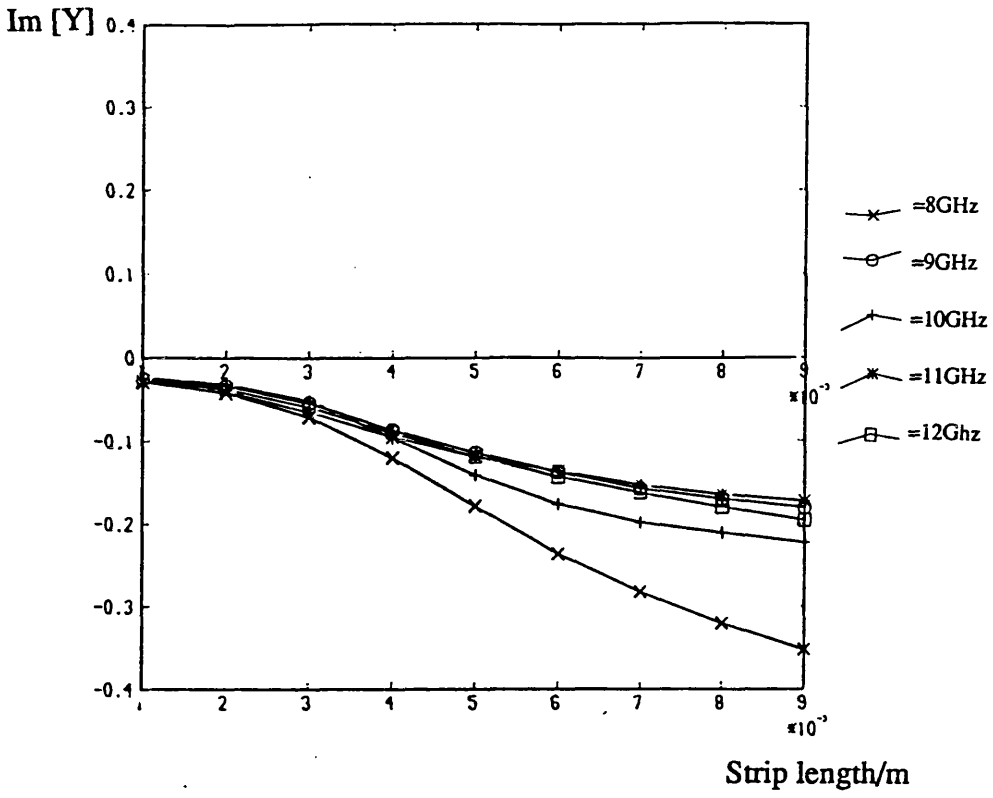

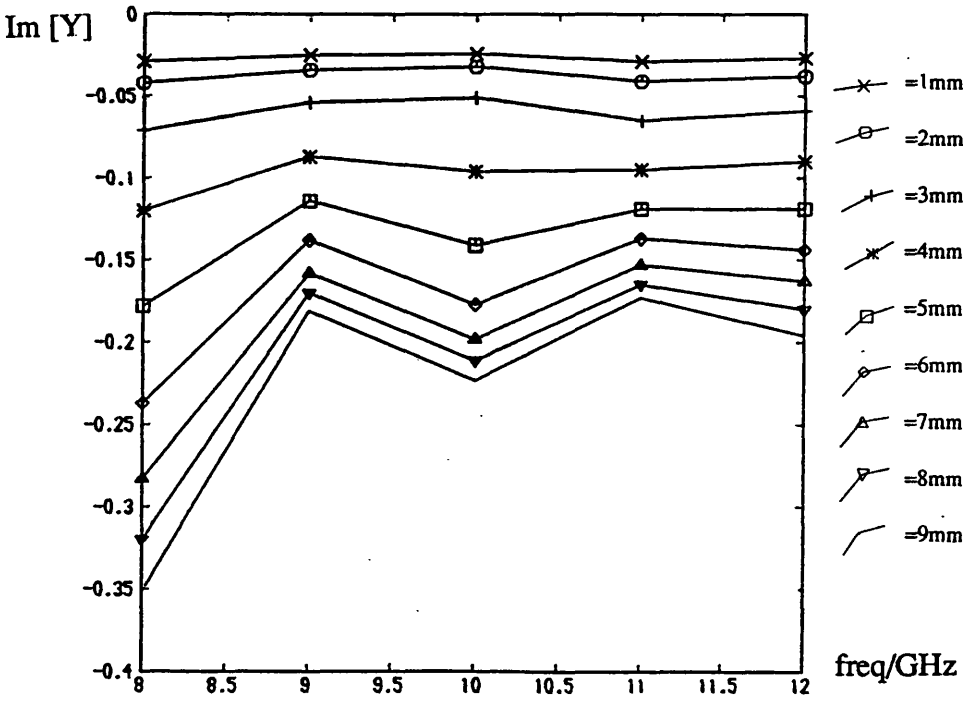

Figure 6.5) Variation of the imaginary part of the equivalent shunt admittance of a transverse strip on a deep slot I.D.G. with c) strip length,d) frequency.

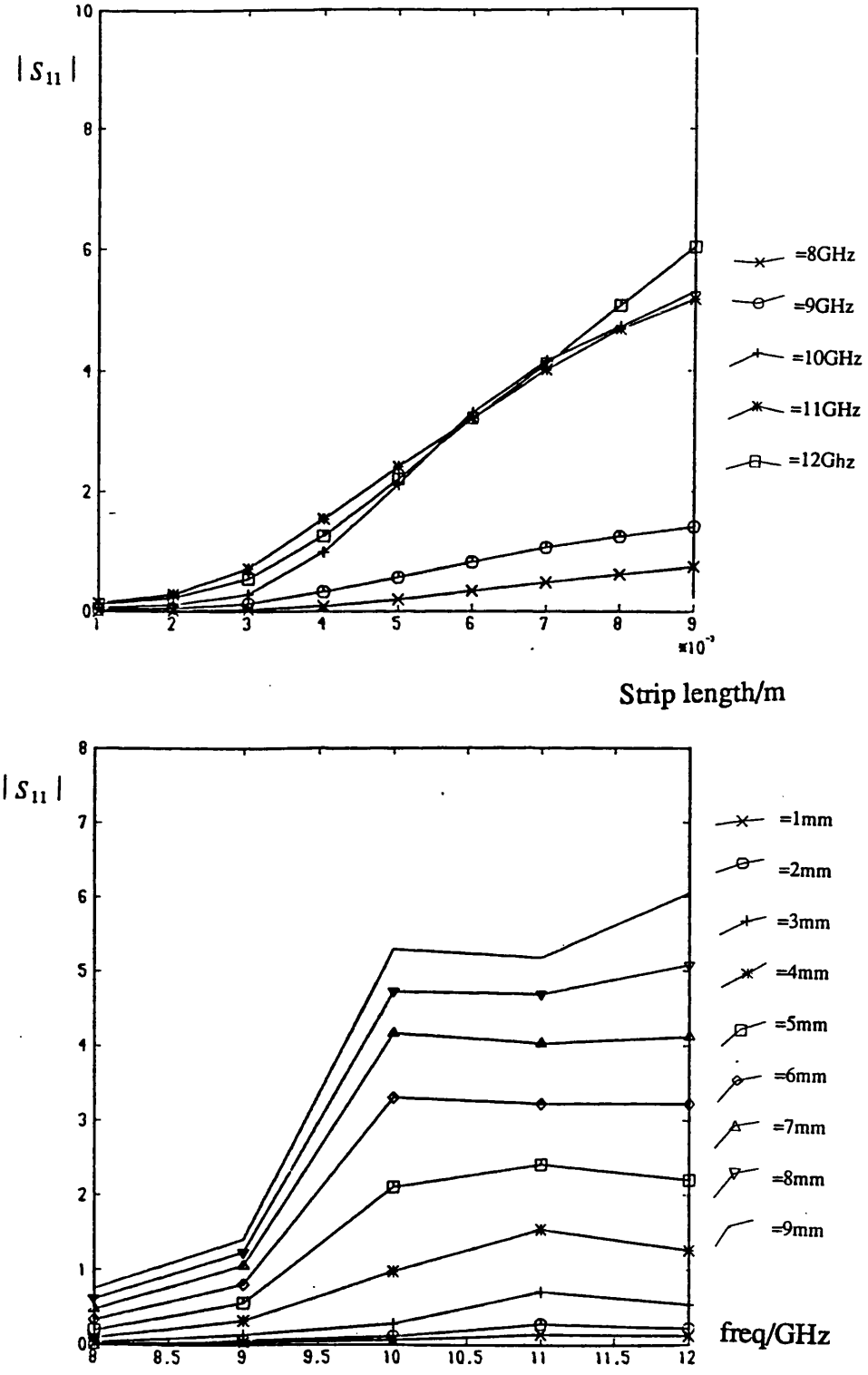

Figure 6.6) Variation of $|S_{11}|$ with a) strip length and b) frequency for the transverse strip.

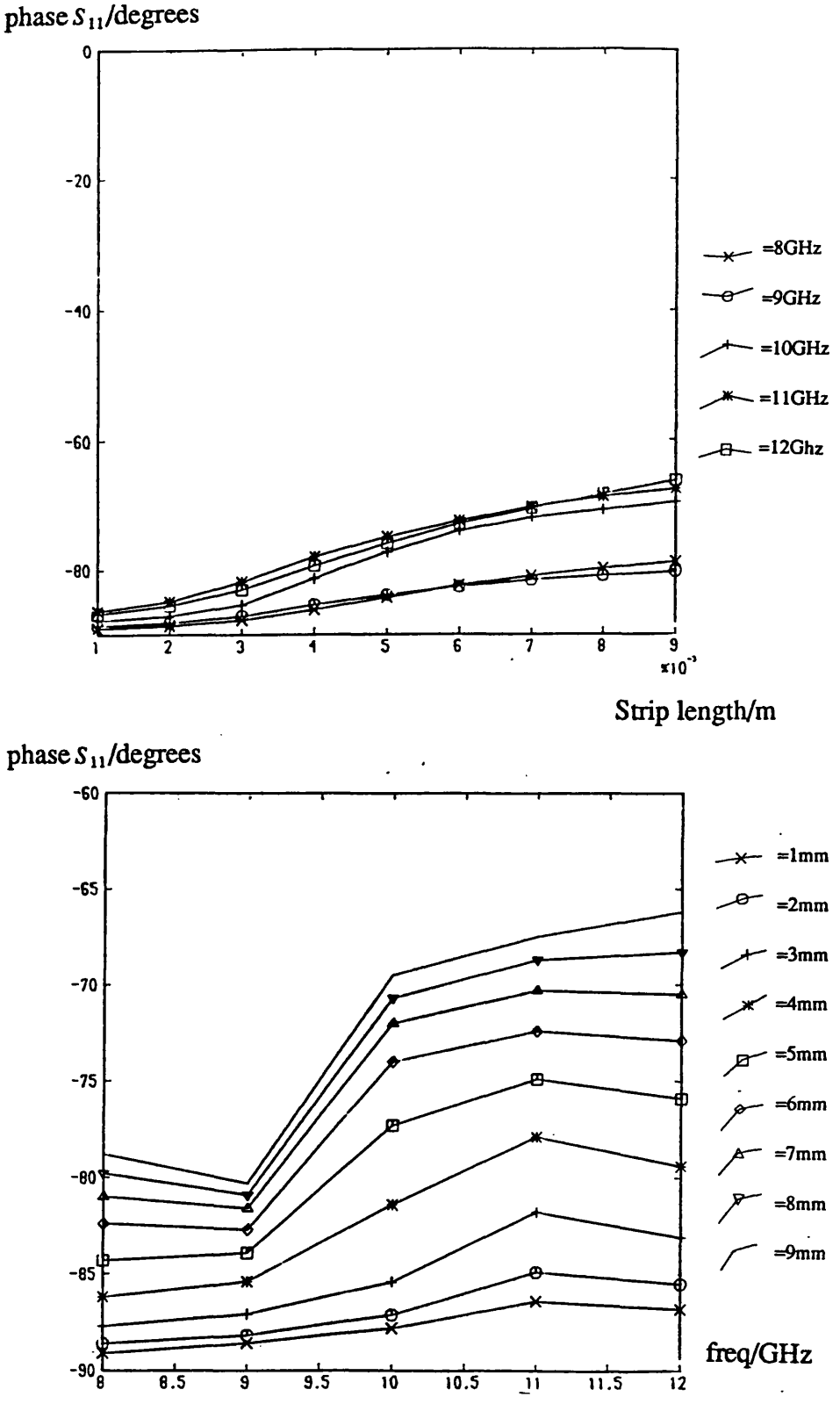

Figure 6.6) Variation of the phase S_{11} with c) strip length and d) frequency for the transverse strip.

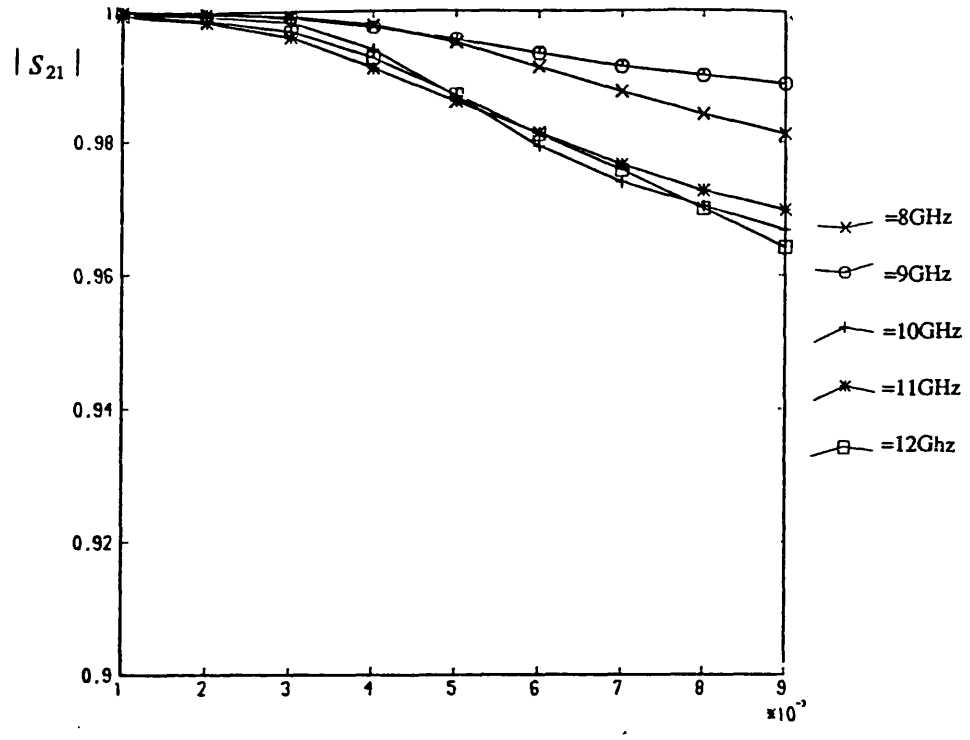

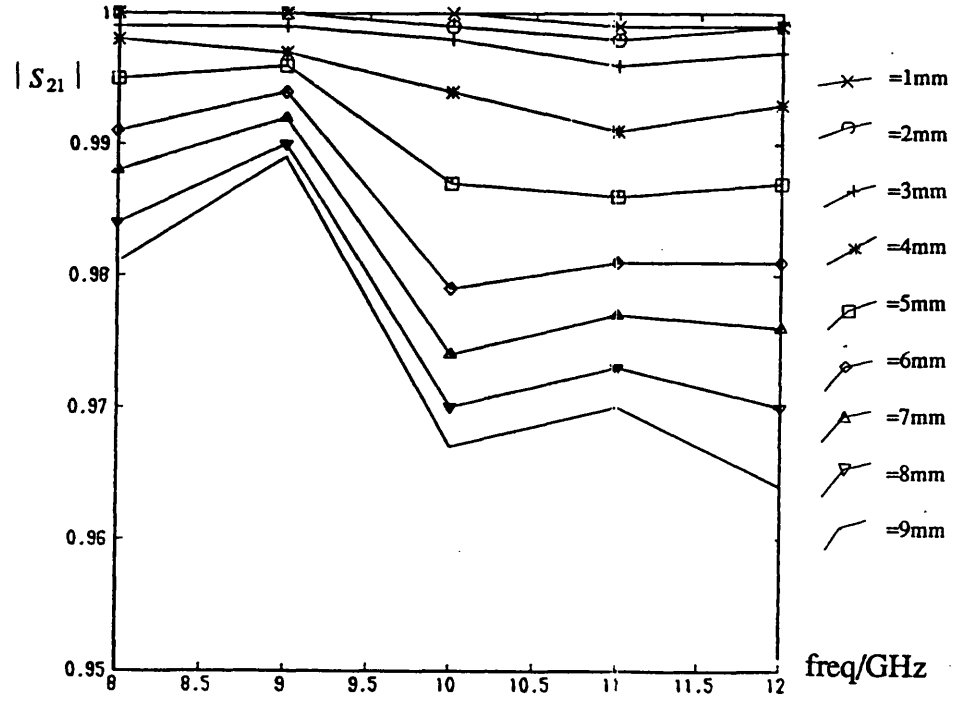

Figure 6.6) Variation of $|S_{21}|$ with e) strip length and f) frequency for the transverse strip.

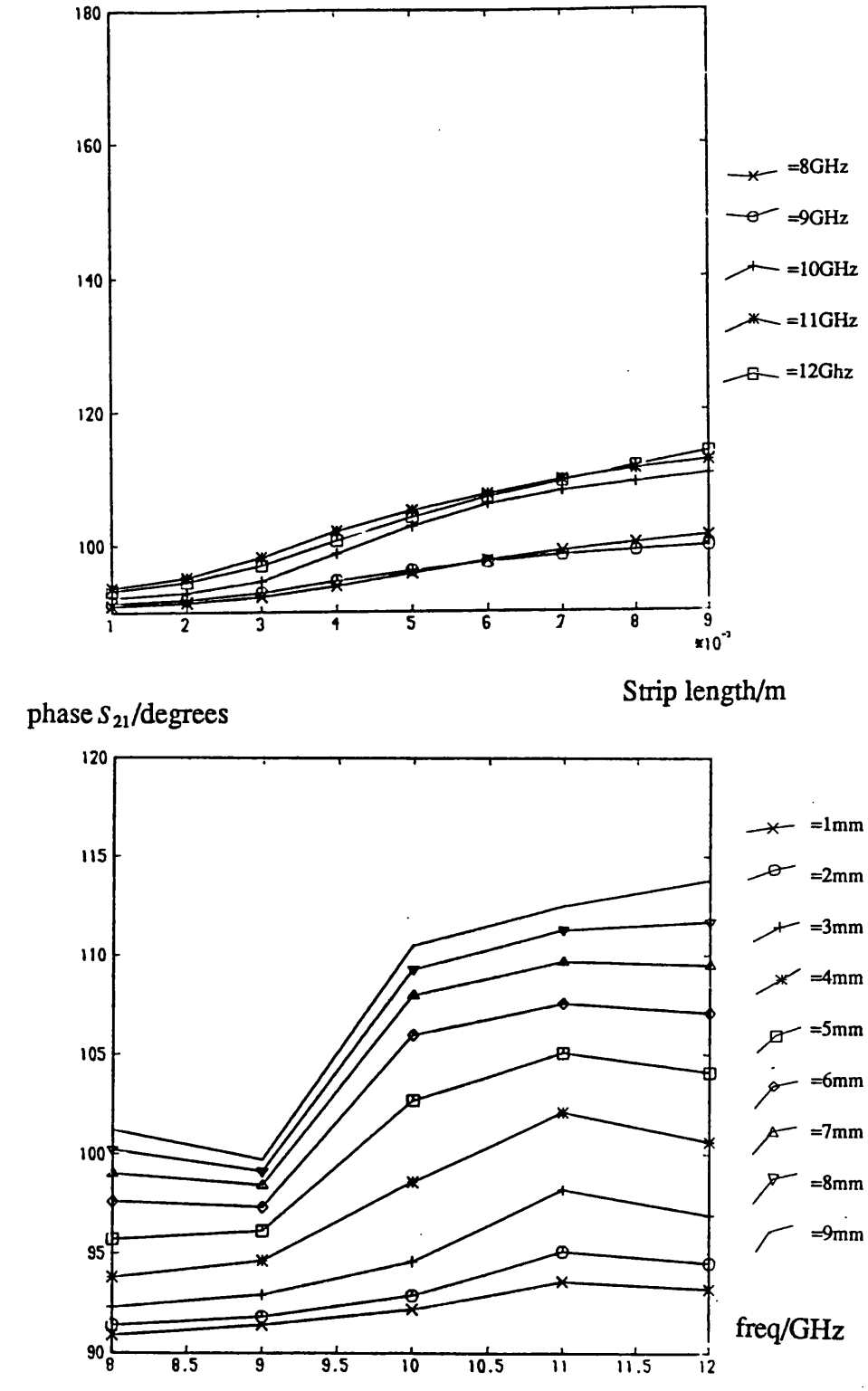

Figure 6.6) Variation of the phase S_{21} with g) strip length and h) frequency for the transverse strip.

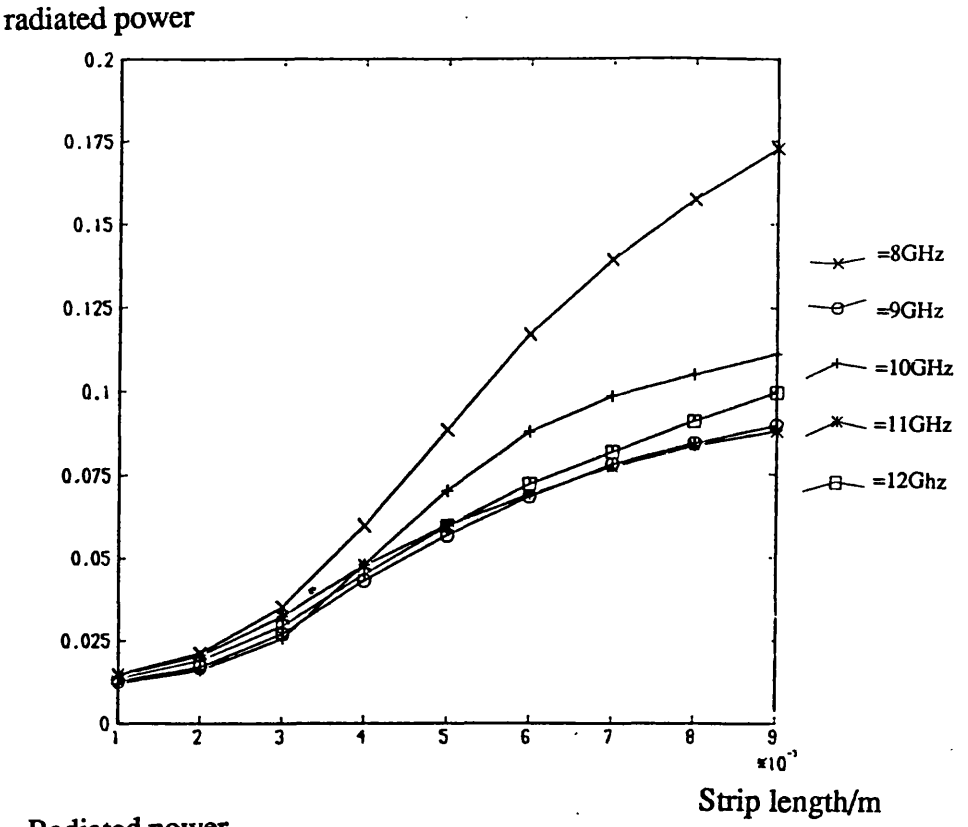

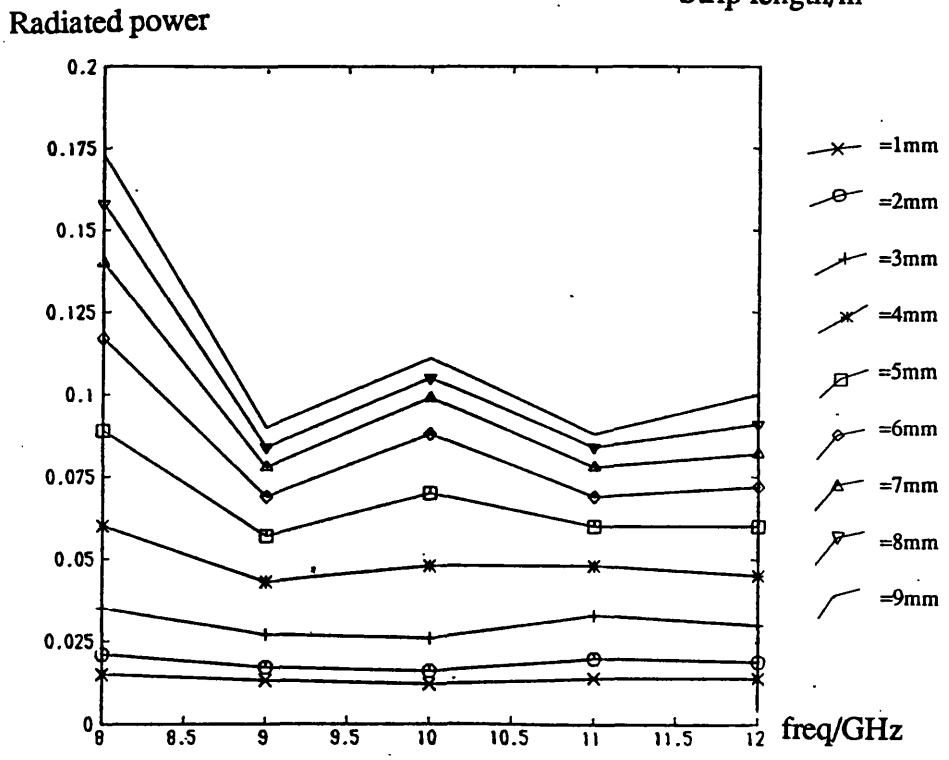

Figure 6.6) Variation of the radiated power with i) strip length and j) frequency for the tranverse strip.

It is observed from figures 6.5a and 6.6i,that the real part of the admittance and consequently the radiated power increase with strip length.Not only is the variation approximately linear,but also virtually independent of frequency above 9GHz.Approximately,the reactive part of the admittance similarly increases with length and is clearly inductive,consistent with the L.S.E. nature of the deep slot I.D.G. surface mode at these frequencies.

The S-parameters also exhibit the same uniform behaviour with length and frequency independence above 9GHz.

So far the parameters suggests that these strips are very promising as array elements.The strength of the radiation may be altered by varying the strip length,without requiring excessive mechanical tolerances,and in addition,the good degree of frequency independence above 9GHz would allow frequency scanning arrays to be designed unhindered by the behaviour of the individual elements.Unfortunately the frequency independence of the network parameters does not extend to the radiation patterns illustrated in figure 6.7.Whilst the beamwidth in the transverse plane is slightly better than that of a free space dipole and insensitive to frequency,there is surprisingly a beam squint in the longitudinal plane.The beam starts to squint between 9 and 10 GHz and moves from broadside to endfire as the frequency increases.Obviously this is somewhat unexpected from just a single element and requires further investigation.Examination of the network parameters also reveals a marked change in behaviour at about 9.5Ghz.

Both the change in behaviour of the network parameters and the beam squint may be explained by considering the strength with which the strip current couples to each mode of the continuum.The degree of coupling depends upon the amplitude of the mode at the strip and the functional forms of the mode and the current.As the incident E_x field component is,to a first approximation,constant

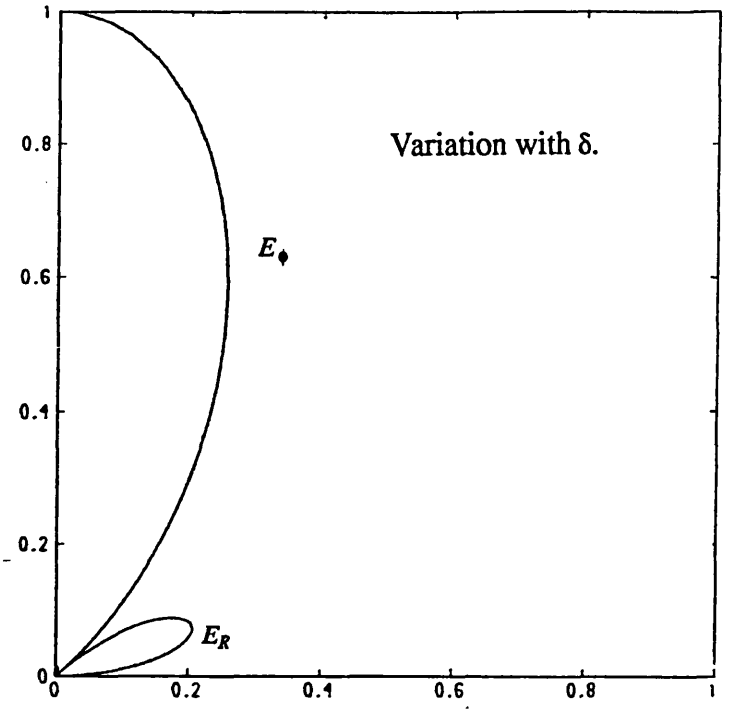

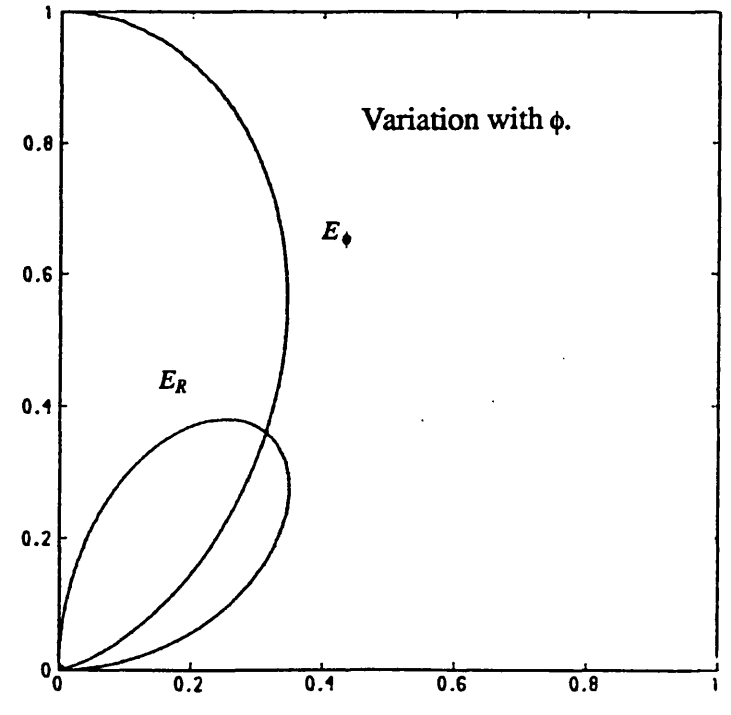

Figure 6.7a) Radiation patterns for a 5mm long strip at 8GHz.

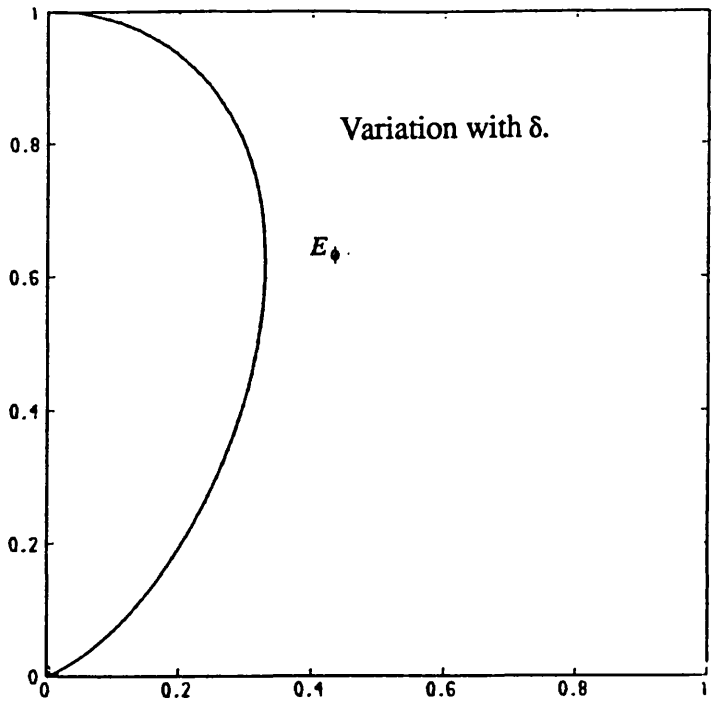

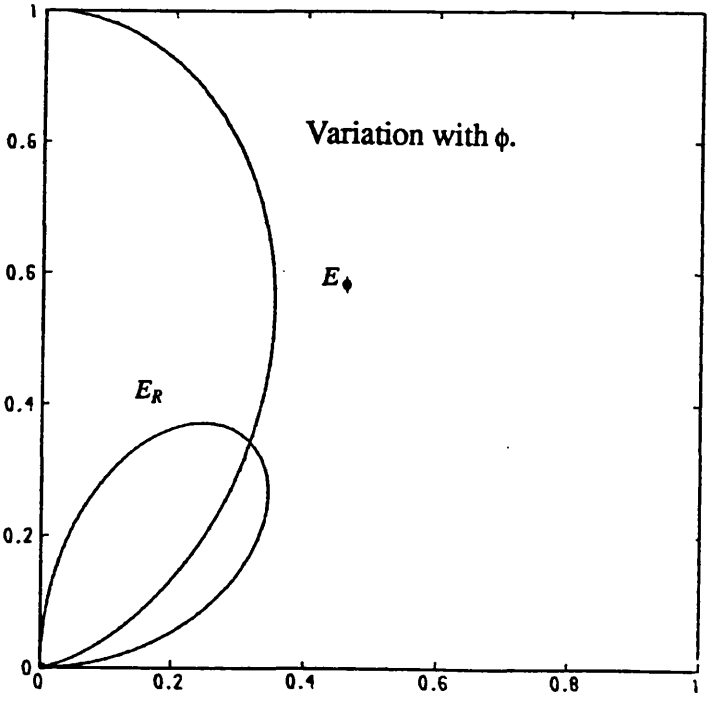

Figure 6.7b) Radiation patterns for a 5mm long strip at 9GHz.

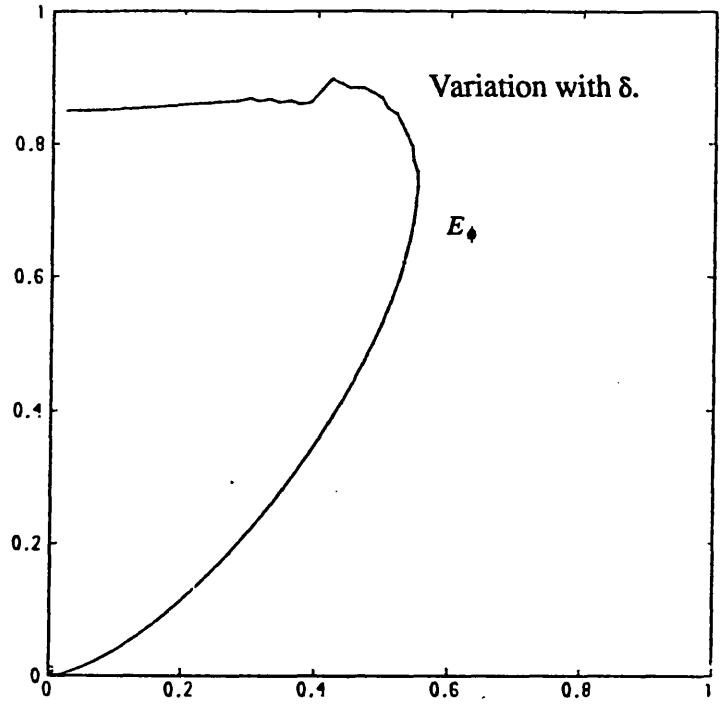

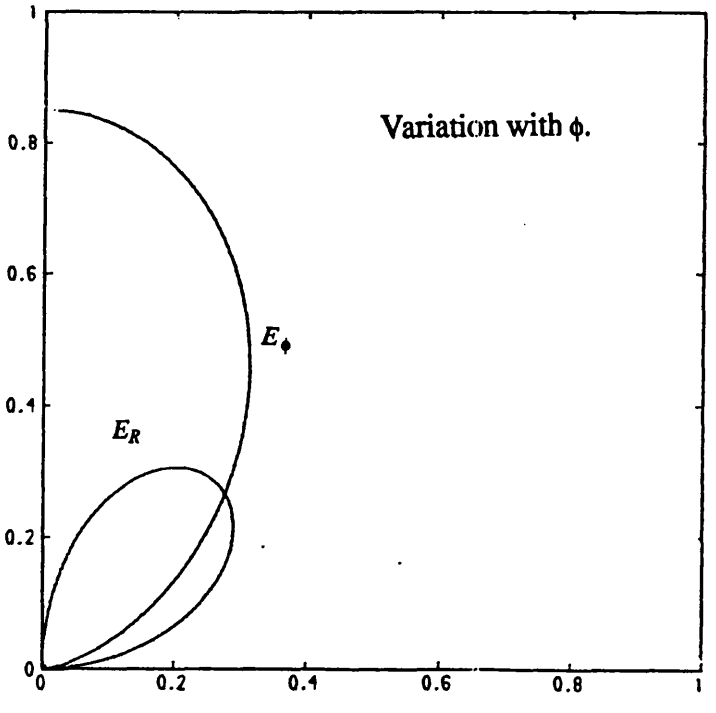

Figure 6.7c) Radiation patterns for a 5mm long strip at 10GHz.

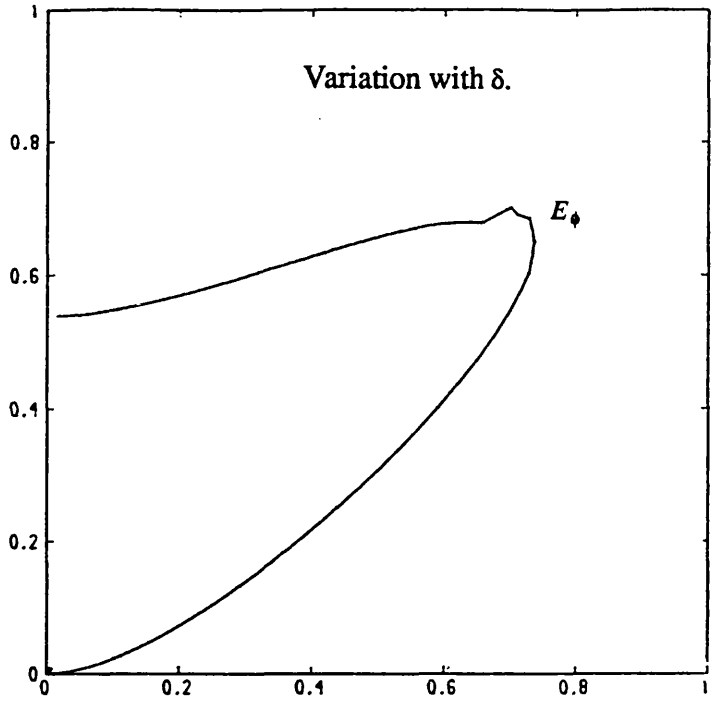

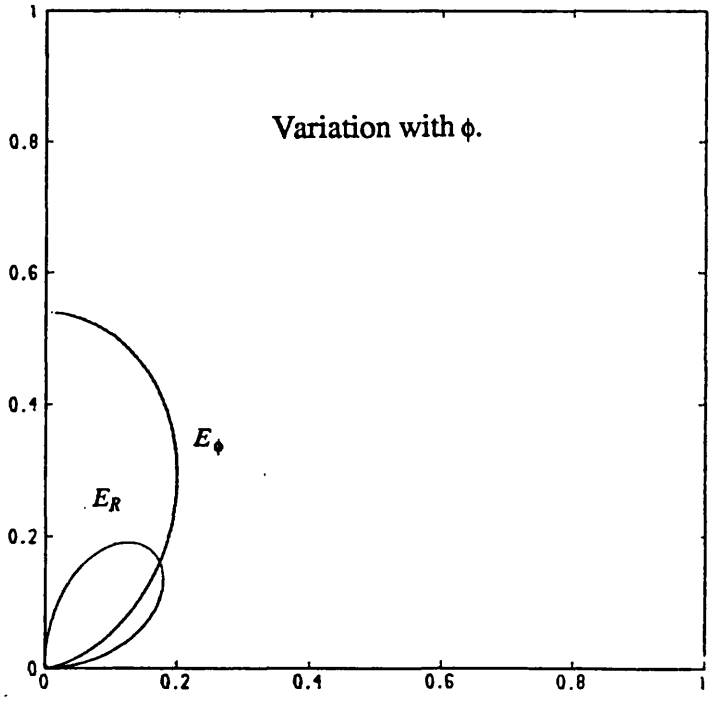

Figure 6.7d) Radiation patterns for a 5mm long strip at 11GHz.

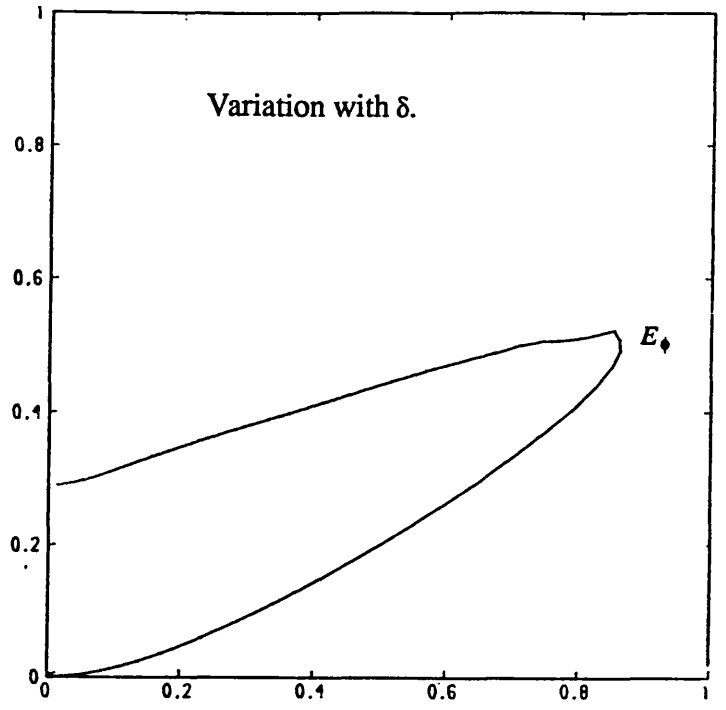

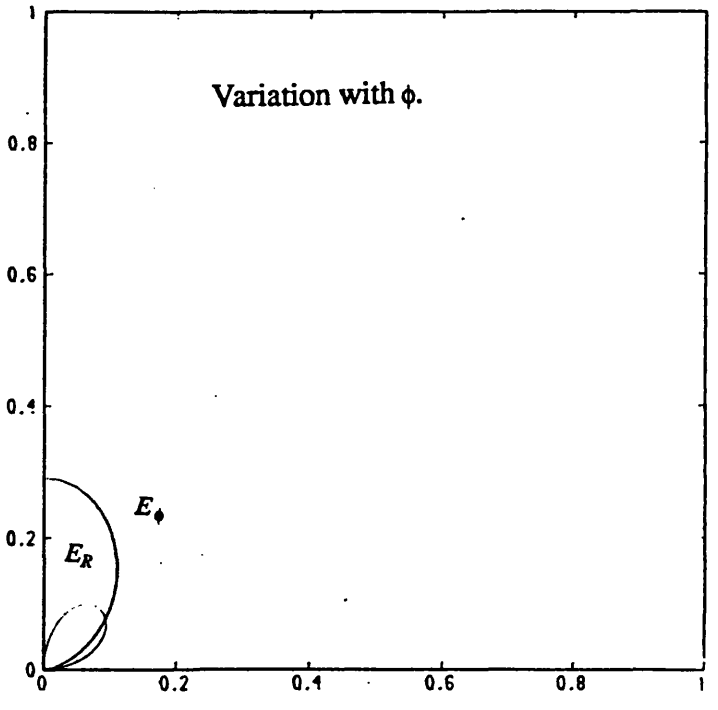

Figure 6.7e) Radiation patterns for a 5mm long strip at 12GHz.

w.r.t. x,it seems reasonable to assume that,except in the immediate vicinity of the ends of the strip,the current will also be independent of x.Therefore the strength of the coupling to a mode depends primarily upon the amplitude of its constant term,ie its $\phi_{ho}(x)$term.Using the approximation discussed in chapter 4,(equation(4.39)),the amplitude of the E_{xo} term at the interface is approximately $\frac{1}{\sqrt{\beta}}\left(\frac{k_t^2}{q_o^2 cot^2 q_o h + k_t^2}\right)^{\frac{1}{2}}$.The broadside radiation is due to those modes with $\beta \approx 0$ and $k_t \approx k_o$ and will clearly be significantly larger than those contributing to the endfire radiation which have $\beta \approx k_o$ and $k_t \approx 0$.However if at some value of k_t,$cotq_o h = 0$,then the coupling to the modes with this value of k_t would exhibit a local maximum.This would indeed result in both an increase in the radiated power and a side lobe,if not the main lobe,in the radiation pattern.Noting that $q_o = 0$ is not a viable solution,the first maximum occurs when $q_o h = \frac{3\pi}{2}$,ie $(\varepsilon_r - 1)k_o^2 + k_t^2 = (\frac{3\pi}{2h})^2$.As only those modes with $0 < k_t < k_o$ contribute to the radiation field,this restricts the frequency range for which a solution exists to 10.2GHz < freq. < 14.2GHz.This is illustrated in figure 6.8 along with the solutions to $q_o h = \frac{5\pi}{2}$.

Direct experimental verification of these results is difficult,due to the fairly small effect of a single strip,in fact comparable to that of the feed transition.In the light of the rather unusual theoretical results,experimental confirmation is certainly required,although this will have to be the subject of further investigation.

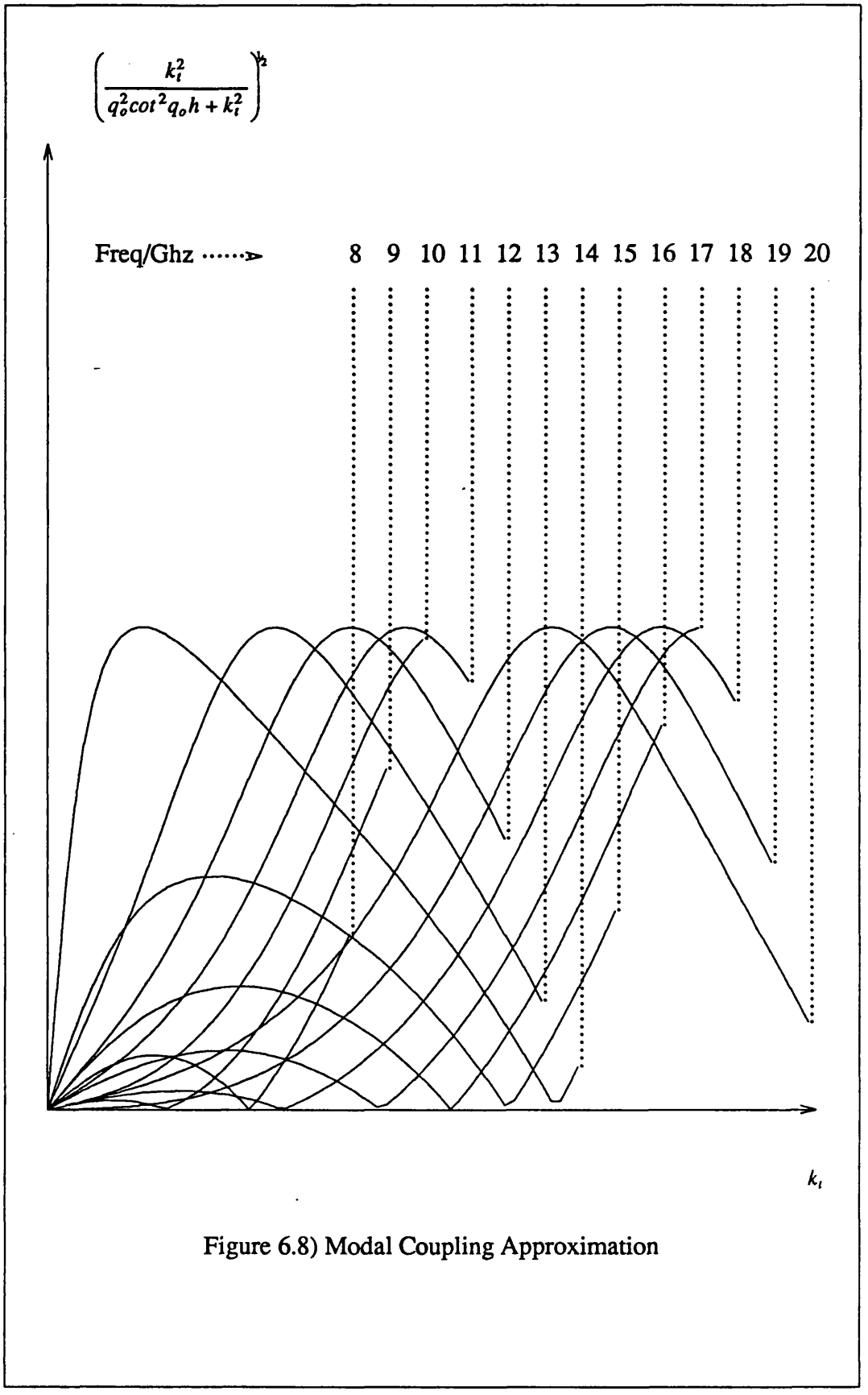

Figure 6.8) Modal Coupling Approximation

6.5) Longitudinal Strips and Patches on a Shallow Slot I.D.G.

The fundamental $E.H._{11}$ mode of the shallow slot I.D.G. contains two main electric field components,E_z and E_y.Longitudinal strips and patches couple to these components exciting radiation with horizontal and radial electric field components.

The ability to produce horizontally polarised radiation,in addition to the vertically polarised radiation of the previous section,is useful for many reasons.The orientation of an array may be constrained by its location,for example on ships and aircraft,and it may be more appropriate to produce vertically polarised radiation by rotating a horizontally polarised array through 90 degrees.Many environments,such as forests,the sea and urban areas,have propagation characteristics that change significantly with polarisation.Also in this context,the ability to produce elliptically polarised radiation by alternating elements of each type,is useful for penetrating certain atmospheric conditions such as rain and fog.Finally,interference from strong sources can be minimised by using an antenna of the opposite polarisation.

This section shall analyse longitudinal strips of infinitesimal width and longitudinal patches with widths up to half that of the guide using a scalar and a vector approach respectively.

The choice of basis functions used to expand the z-dependences of the currents in both cases is limited by the awkward dependence of the Green's function upon z and z'.Unless a very simple basis set is used,the two dimensional integral w.r.t. z and z' must be evaluated numerically.As this integral is itself part of the integrand of the integral over k_t,this is not desirable from either a time or an accuracy point of view.Consequently the z-dependence of the currents has been expanded using simple sine and cosine functions which enable analytic

expressions to be determined for the integration over the z-z' plane.

The x-dependence has been expanded using weighted 1st and 2nd kind Chebychev polynomials that intrinsically model the expected orders of zero and singularity at the edges of the patch.

One final difficulty that arises is the appearance of ε_r in the Green's function given in equation (6.3).The patches are placed on the surface of the dielectric at which point the value of ε_r theoretically changes discontinuously.Initially it was hoped that assuming either value,ie displacing the patch slightly above or below the interface,would give similar results.Unfortunately this is not the case and clearly presents a problem.Examination of a number of papers that analyse strips on the top of dielectric slabs,[18-20] revealed nothing as were primarily concerned with the scattering of plane waves and thus adopted a different approach.However one lead was to allow for the presence of separate currents on the top and bottom of the patch,either both in the air,or both in the dielectric or one in each region.Unfortunately this was not fruitful and just complicated the problem.Therefore,in an attempt to resolve the problem,a slightly different approach was taken.If the length of the patch is extended to infinity,then the microstrip loaded I.D.G. is recovered.(This structure shall be considered in more detail in the next chapter.)The discrete modes of this structure may be identified by applying transverse resonance,[4],in which the ε_r dilemma does not occur.However the Green's function of the I.D.G. may also be used to recover these modes,all that needs to be done is to assume a propagating form for the current,and to solve the homogeneous,ie source free,integral equation,equation (6.5).This was tried with both values of ε_r and it was found that neither value correctly predicted the dispersion equation of the fundamental quasi-T.E.M.

mode.However using the value of ε_r for the dielectric,did model very well the dispersion equation of the first L.S.M. polarised surface mode of the microstrip loaded I.D.G.,(Table 6.2).It is not unreasonable that the first L.S.M. polarised surface mode is most easily recovered by this approach,as the modes of the I.D.G. which couple most strongly to the strip are L.S.M. polarised.Although this can hardly be regarded as a proof,it is at present the best indicator available for solving the ε_r dilemma.

freq./Ghz	k_o	β_1 (*T.R.*)	β_2 (*T.R.*)	β_1 (*G.F.*)	β_2 (*G.F.*)
9.0	188.58	251.9	189.3	271.9	190.5
10.0	209.54	281.6	219.3	302.1	223.2
11.0	230.49	309.7	253.3	332.5	250.1
12.0	251.44	331.5	286.8	362.6	279.2

Table6.2) Shallow Slot MIG Dispersion Characteristics using Transverse Resonance,(T.R.),and the Green's Function,(G.F.),of the I.D.G.

Strips of varying length and width,placed upon a shallow slot I.D.G. of dimensions 22.86mm by 10.16mm and containing P.T.F.E,(ε_r = 2.08),have been analysed at various frequencies.The 2mm wide strip has been analysed using both the scalar and vector approaches.Two basis functions have been used for the x-dependence and ten for the z-dependence.

The computed S-parameters,radiation patterns strip currents are given in figures (6.11) to (6.19) in appendix A6 at the end of this chapter.

In general the S-parameters exhibit two types of behaviour as the length of the strip is changed.There is a 'slow' variation with length which gives maximum radiation for strips with lengths in the vicinity of 30mm.Superimposed upon this,there is a 'fast' variation with a period of about 25mm.What is surprising is the extremely high levels of radiation that are predicted,in some cases over 90% of

the total power.

Unlike the transverse strips,the effect of a longitudinal strip is clearly measurable and consequently experiments were made.The S-parameters of an I.D.G.,fed by a rectangular waveguide with a dielectric taper,were measured using an HP8510 network analyser,with and without the strips in place.For moderate length strips the effect of the waveguide transitions was negligible in comparison with that of the strip and the latter were indeed found to radiate the levels of power theoretically predicted.However the validity of trying to exactly quantify these experiments is suspect for the following reason.If the radiation from the strip is low,the effect of the waveguide transitions masks that of the strip.Whereas if the strip radiation is high then this radiation also couples strongly into the transition,obscuring the measurement of the surface mode levels.Therefore,again,direct measurement of the network parameters is difficult and can only yield the following qualitative observations.

i) The peak radiation levels do reach levels of 80-90%.

ii) The 'slow' variation with strip length is also observed although it peaks between 40-50mm,rather than between 30-40mm as theoretically predicted.

iii) The 'fast' variation with strip length is also present and has a period of about 25mm

Further details of the experimental results shall not be presented as it is not possible to place too much faith in their quantitative behaviour.

The 'fast' variation with strip length of the S-parameters may be attributed to the excitation on the strip of the fundamental,quasi-T.E.M.,mode of a microstrip loaded I.D.G.,(M.I.G.).Strips of lengths equal to multiples of the half wavelength of this mode would be expected to resonate thus giving radiation and

$|S_{11}|$ maxima and $|S_{21}|$ minima.For example,the fundamental wavelength of a M.I.G. with a 2mm wide strip is 22mm at 10GHz and examination the S-parameters clearly proves the consistency of this value with this explanation of the 'fast' variation.

Initially is was thought that the 'slow' variation with strip length could be explained by the excitation of the first L.S.M. polarised surface mode of the M.I.G.,arguing that the interaction between this and the fundamental mode would produce the high radiation levels and the 'slow' variation.For example,if these modes are excited such that they are constructively interfering at one end of the strip,it is possible that for some strip lengths they would be destructively interfering at the other end causing a significant transmission minima to occur.This explanation does not seem too sound as the surface mode cuts off at about 9GHz,whereas the maximum radiation does not significantly diminish with frequency.

A more plausible explanation is simply,that there is very strong coupling between the two ends of the strip by the continuous modes.To substantiate this argument,reference was made to papers concerning interacting steps in dielectric slab waveguide,[21,22],shown in figure 6.9.The theoretical results given in these papers are similar in their general behaviour to those derived here,exhibiting both a 'slow' and a 'fast' variation with the distance between the steps.Additionally replacing the rib between the steps with air,produces S-parameters that just exhibit the 'slow' variation with distance.Consequently it seems reasonable to attribute the 'fast' and 'slow' variations,to coupling between the two discontinuities,ie in this case the ends of the strip and in [21] and [22] the steps,by the fundamental and continuous modes respectively of the intervening medium.

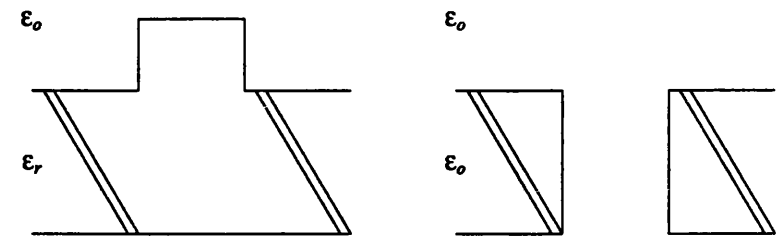

a) Rib. b) Airgap.

Figure 6.9) Interacting Steps in Planar Dielectric Waveguide.

In addition to the general behaviour discussed above,it is also possible to make the following observations on the S-parameters.

i) For short strips,the S-parameters are almost frequency independent.

ii) The variation with strip width is fairly minor at 8Ghz but shows a noticeable variation at 10GHz.It can be seen in figure 6.13 that the 'fast' variation is less prominent as the strip width increases.This is not surprising as the increasing the strip width extenuates the difference between the fundamental modes of the I.D.G. and the M.I.G.,thus reducing the excitation of the latter.

iii) The comparison between the results obtained for the scalar and vector approaches shown in figures 6.14 and 6.15,demonstrates fairly close agreement,although there is sufficient discrepancy to warrant the full vector approach.

A few examples of the strip currents are given in figure 6.16,showing both the presence of the fundamental M.I.G. mode and the singularities on the perimeter of the strip.

Figures 6.17-6.19 show the far field patterns evaluated for a 2mm wide strip using the full vector approach.As expected,the dominant components are the horizontally and radially components.The beamwidth in the transverse plane is good,although it does appear to vary slightly with strip length,as does the relative amplitudes of the two main field components.

The variation in the longitudinal plane is interesting.As for the transverse strips,the beam is squinted from broadside,although in this case the direction does not appear to vary with frequency,rather slightly with strip length.In addition,the radiation levels in the forward and backward beams differ,their ratio varying primarily with strip length and secondly with frequency.Whilst the angle of the beam varies with strip length,it does so by a fairly small amount.This suggests that it may be possible to model the continuum fields on the strip by a single,continuously radiating leaky mode.Such a leaky mode would certainly give rise to a beam squint,although as the strip decreases in length,the contribution from the steepest descent path integral in the saddle point analysis,would increase and lessen the effective beam squint,as observed in figures 6.17-6.19.It is also interesting to note that the 'slow' variation of the S-parameters with strip length,may also be explained by the interaction between the fundamental quasi-T.E.M. mode and a leaky mode,rather than the L.S.M. polarised surface mode as earlier considered.Clearly,identification of this leaky mode of the M.I.G. could prove very useful and is a task for the future.

6.6) Array Design.

Finally it is necessary to consider the effects of mutual coupling between elements in an array environment.

It has been demonstrated that even relatively short longitudinal strips excite high levels of radiation and mutual coupling effects are likely to be very

significant in determining the performance of an array.

It is possible to extend the Green's function approach to analyse multiple strips in close proximity.However this does not seem to be a very efficient method of approaching the problem as each new array design must be analysed from scratch.

A better approach is treat the array as a cascade of alternate sections of empty and microstrip loaded I.D.G.Due to the high levels of radiation,it is unlikely that involving only the fundamental modes of the two structures,as has previously been undertaken,[4],will provide sufficiently accurate results for all purposes.Using in addition to the fundamental modes,the leaky mode of the M.I.G.,may prove adequate even though radiative coupling between strips is still not taken into account,although the non-spectral nature of the leaky mode does cause difficulties in determining its amplitude.

The papers referenced earlier,[21,22],both tackled this problem by discretising the continuum fields in either the space domain,[21], or the spectral domain,[22].Thus following this approach,each section of the array may be modelled by an multiport network,as illustrated in figure 6.10.In the space domain it is simple to see how these networks may be developed using the Green's function analysis above.Instead of considering the excitation of,for example the strip section,by just the surface mode of the I.D.G.,a set of excitations is considered.If the members of this set provide a complete basis for the two transverse planes at either end of the section,a multiport network for each section may be derived.Cascading the appropriate networks together and applying a known excitation at both ends of the array results in a matrix equation which may be solved for the amplitudes of the basis functions at each intersection and hence the array characteristics.

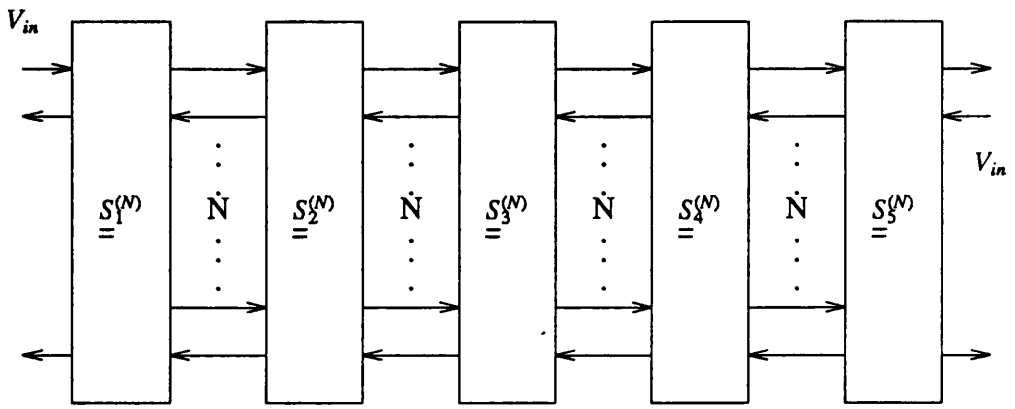

Figure 6.10) Multiport Network Model of a Two Strip Array.

The next chapter shall consider the first stage in this process,the development of the continuous spectrum of the M.I.G.

6.7) References.

1) T.Rozzi,L.Ma,R.de Leo and A.Morini,"Equivalent Network of Transverse Dipoles on Inset Dielectric Guide:Application to Linear Arrays",IEEE trans. Antennas and prop.,Vol AP-38,no3,Mar 90,pp380-385.

2) T.Rozzi and L.Ma,"Scattering by Dipoles in I.D.G. and Application to Millimeter Millimeter Antennas",Proc 17th European microwave conf.,Rome Sept 87,pp543-548.

3) P.Sewell and T.Rozzi,"Rigorous Analysis of a Longitudinal Strip on the Surface of Inset Dielectric Guide",1990 IEEE MTT-S digest,pp1059-1062.

4) T.Rozzi,Rde Leo and A.Morini,"Analysis of the 'Microstrip-Loaded Inset Dielectric Guide",1989 IEEE MTT-S digest,pp923-926.

5) A,Rudge,K.Milne,A.Olver and P.Knight,"The Handbook of Antenna Design",vols 1 and 2,1986 Peregrinus,London.

6) L.Ma,S.Pennock and T.Rozzi,"Design of Multiple Array Flat Millimetric Antennas,proc. 21st European microwave conf.,Stuttgart Sept 91.

7) T.Tamir and A.Oliner,"Guided Complex Waves",parts 1 and 2,Proc I.E.E.,vol 110,no 2,Feb 63,pp310-334.

8) T.Itoh and B.Adelseck,"Trapped Image Guide Leaky-Wave Antennas for Millimeter Wave Applications",IEEE trans. Antennas and prop.,vol AP-30,no 3,May 82,pp505-509.

9) M.Ghomi,H.Baudrand and C.Cavelli,"New Approach for Computing Radiation Patterns of Dielectric Leaky wave Antennas",Electronics letts.,vol 25,no 5,2nd Mar 89,pp345-346.

10) T.Wu,K.Chen and S.Peng,"Spectral Domain Analysis for Dielectric Antennas Loaded with Metallic Strips",1987 IEEE MTT-S digest,p299-301.

11) T.Itoh,"Application of Gratings in a Dielectric Waveguide for Leaky-Wave Antennas and Band-Reject Filters",IEEE trans. microwave theory and techniques,vol MTT-25,no 12,Dec 77,pp1134-1137.

12) R.Collin and F.Zucker,"Antenna Theory",New York McGraw Hill,1969.

13) J.Malherbe,"A Leaky Wave Antenna in Nonradiative Waveguide",IEEE trans antennas and prop.,vol AP-36,no 9,Sept 88,pp1231-1235.

14) D.Jackson and A.Oliner,"A Leaky-Wave Analysis of the High Gain Printed Antenna Configuration",IEEE trans. antennas and prop.,vol AP-36,no 7,Jul 88,pp905-910.

15) L.Brillouin,"Wave Propagation in Periodic Structures",2 ed.,Dover Publications,New York,1953.

16) M.Guglielmi and G.Boccalone,"A Novel Theory for Dielectric-Inset Waveguide Leaky-Wave Antennas",IEEE trans. antennas and prop.,vol AP-39,no 4,Apr 91,pp497-504.

17) L.Felsen and N.Marcuwitz,"Radiation and Scattering of Waves",Prentice-Hall,1973.

18) C.Butler,"Current Induced on a Conducting Strip which resides on the Planar Interface between two Semi-infinite Half-Spaces",IEEE trans. Antennas and prop.,vol AP-32,no 3,Mar 84,pp226-231.

19) C.Butler,"Current Induced on a Conducting Cylinder located near the interface between two Semi-infinite Half-Spaces",IEEE trans. Antennas and prop,vol AP-33,no 6,June 85,pp616-624.

20) X.Xu and C.Butler,"Scattering of TM Excitation by Coupled and Partially buried Cylinders at the Interface between two Media",IEEE trans. Antennas and prop,vol AP-35,no 5,May 87,pp529-538.

21) T.Rozzi and G.In't Veld,"Field and Network Analysis of interacting Step Discontinuities in Planar Dielectric Waveguides",IEEE trans. microwave theory and techniques,vol MTT-27,no 4,Apr 79,pp303-309.

22) H.Shigesawa and M.Tsuji,"A New Equivalent Network Method for analysing Discontinuity Problems of Open Dielectric Waveguides",IEEE trans. microwave theory and techniques,vol MTT-37,no 1,Jan 89,pp3-14.

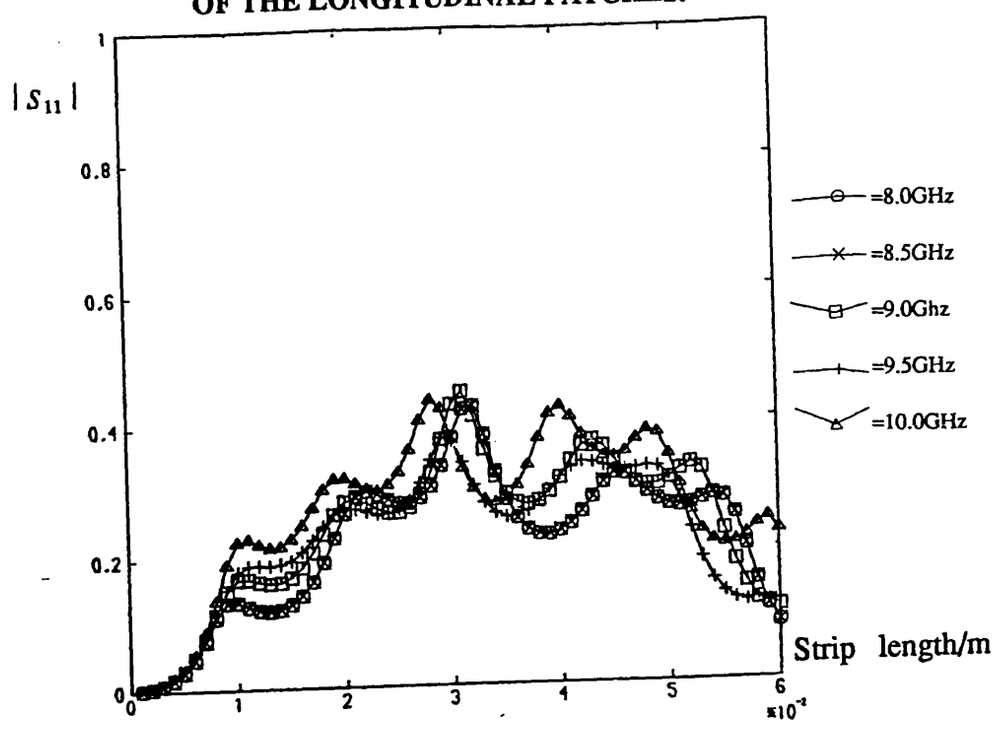

Figure 6.11a) Scalar analysis : $|S_{11}|$ vrs strip length.

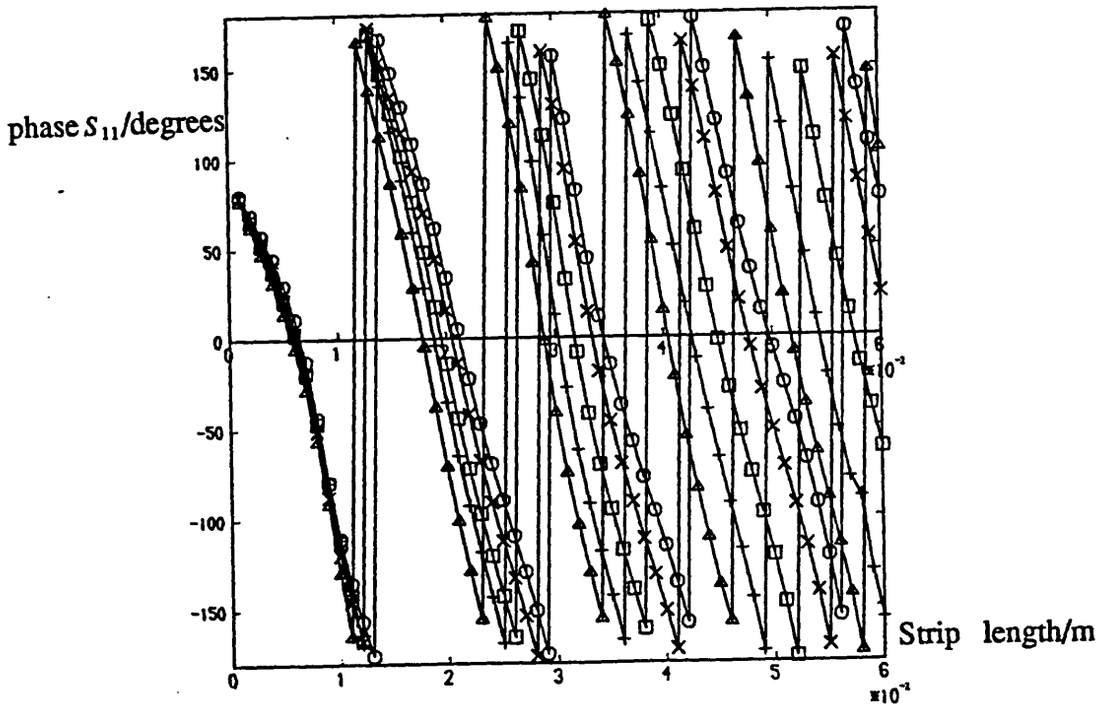

Figure 6.11b) Scalar analysis : phase S_{11} vrs strip length.

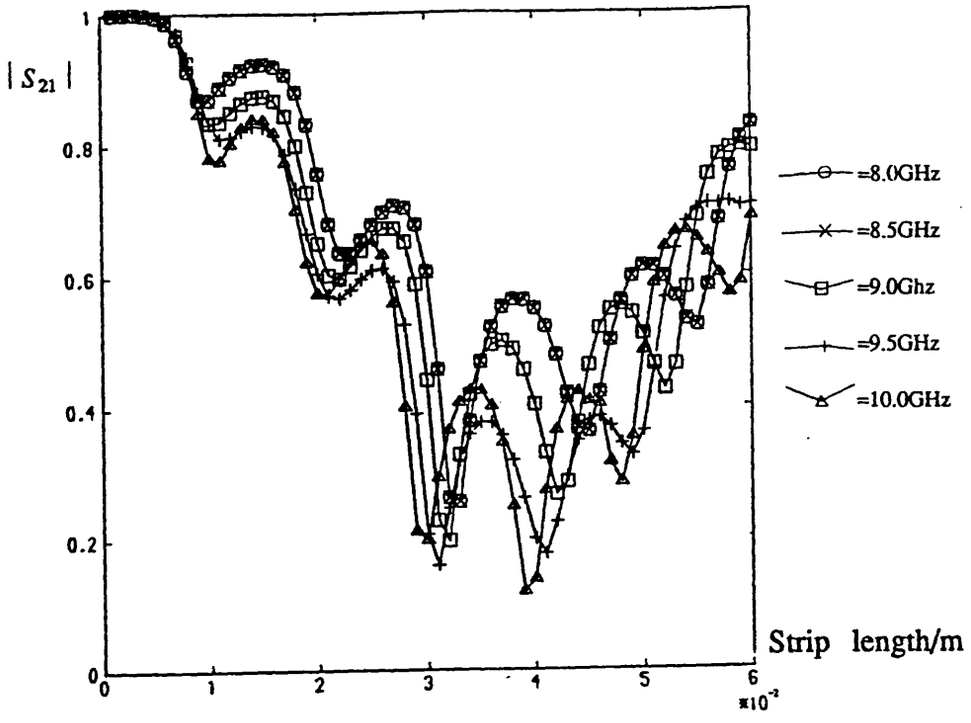

Figure 6.11c) Scalar analysis : $|S_{21}|$ vrs strip length.

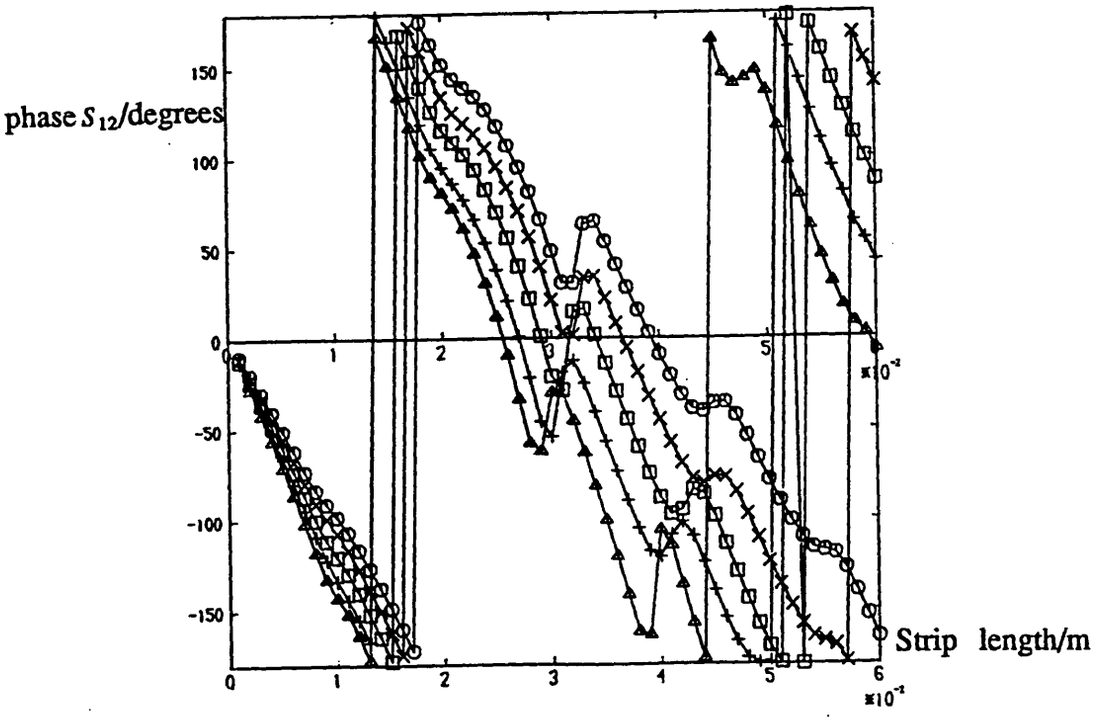

Figure 6.11d) Scalar analysis : phase S_{21} vrs strip length.

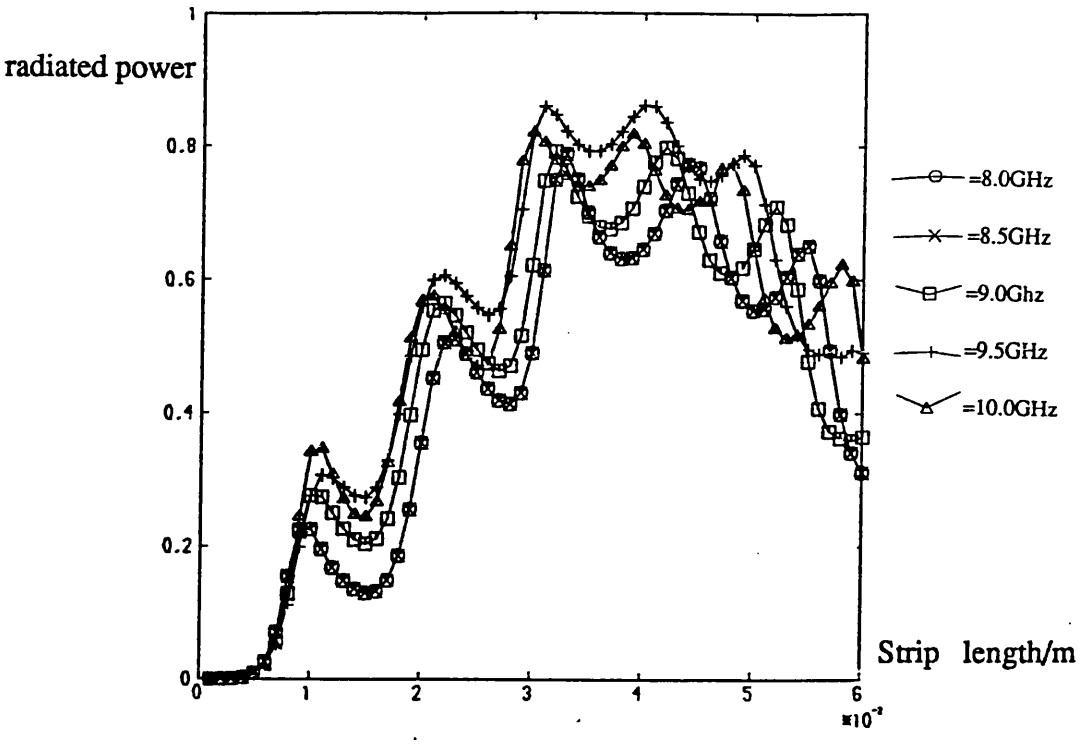

Figure 6.11e) Scalar analysis : radiated power vrs strip length.

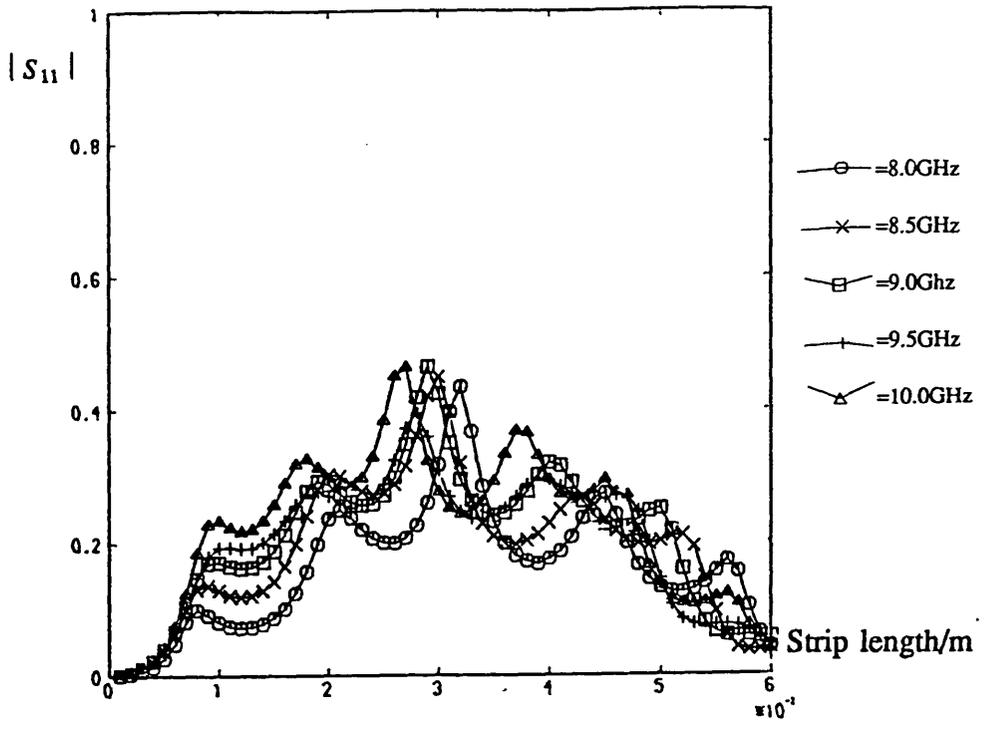

Figure 6.12a) Vector analysis : $|S_{11}|$ vrs strip length,width=2mm.

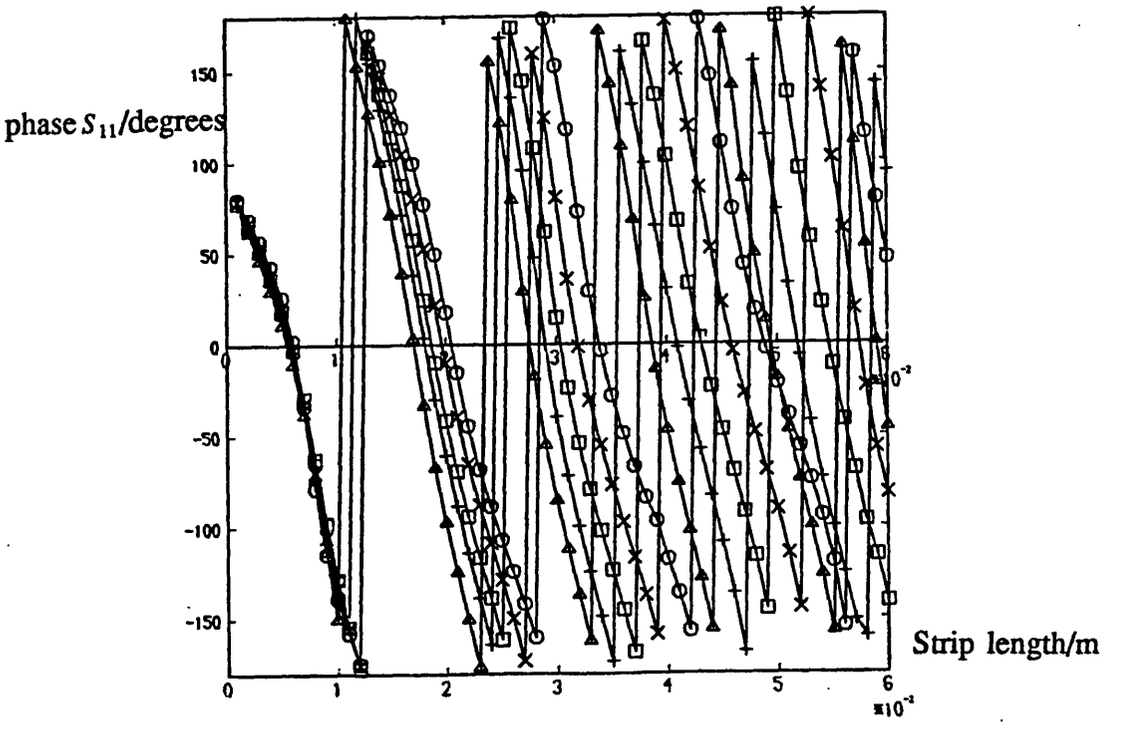

Figure 6.12b) Vector analysis : phase S_{11} vrs strip length,width=2mm.

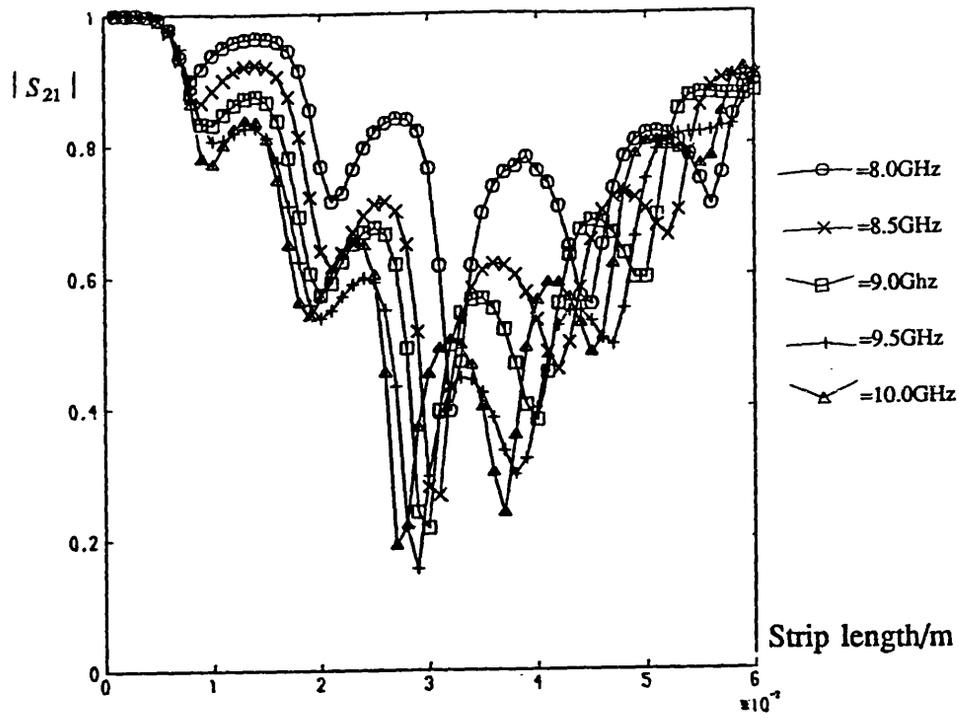

Figure 6.12c) Vector analysis : $|S_{21}|$ vrs strip length,width=2mm.

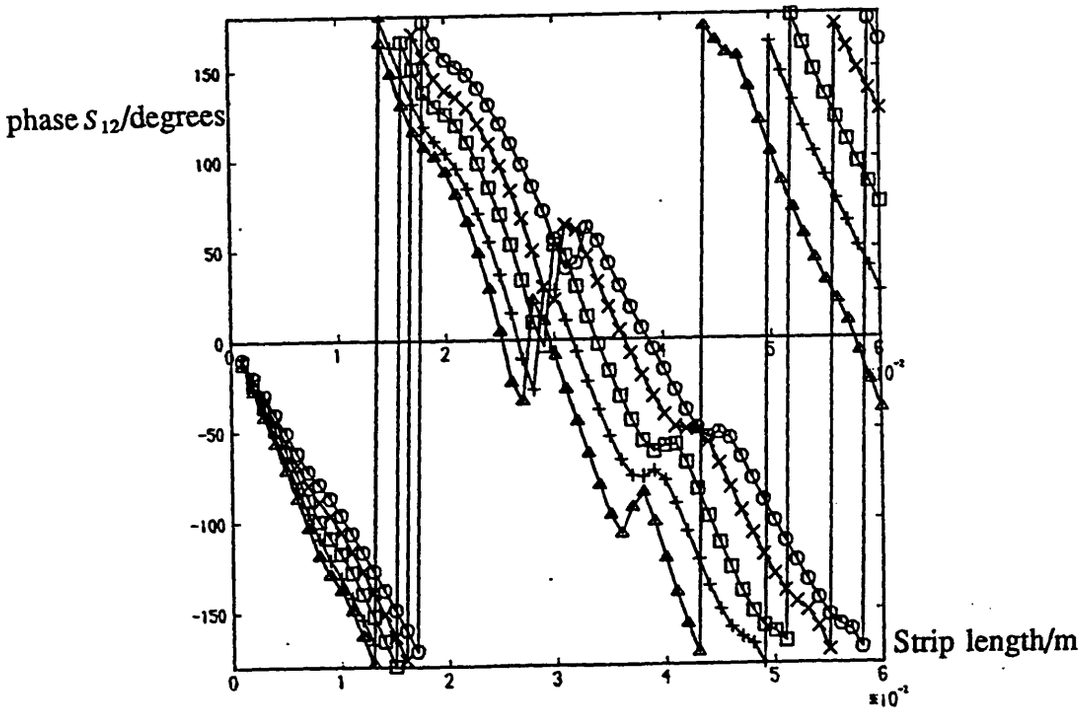

Figure 6.12d) Vector analysis : phase S_{21} vrs strip length,width=2mm.

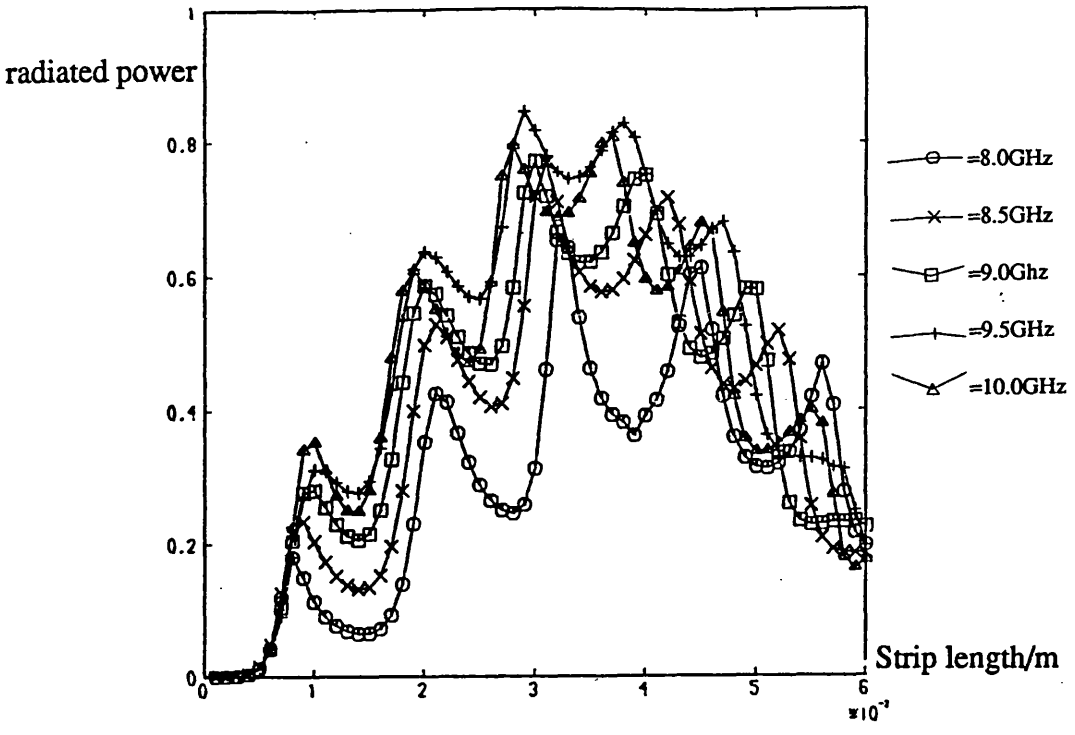

Figure 6.12e) Vector analysis : radiated power vrs strip length,width=2mm.

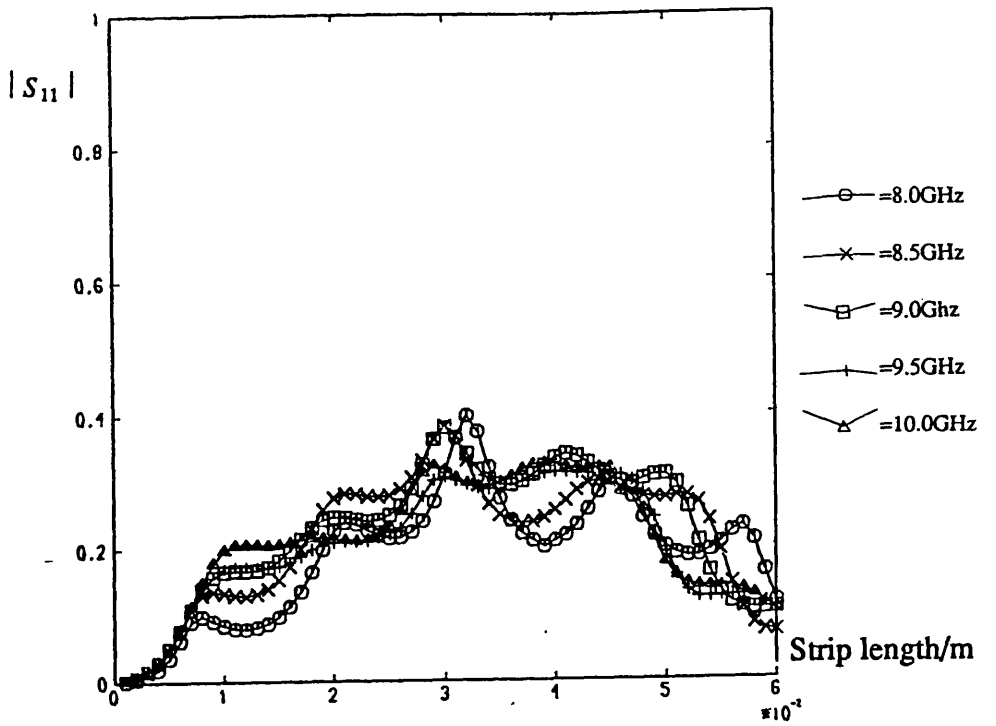

Figure 6.12f) Vector analysis : $|S_{11}|$ vrs strip length,width=5mm.

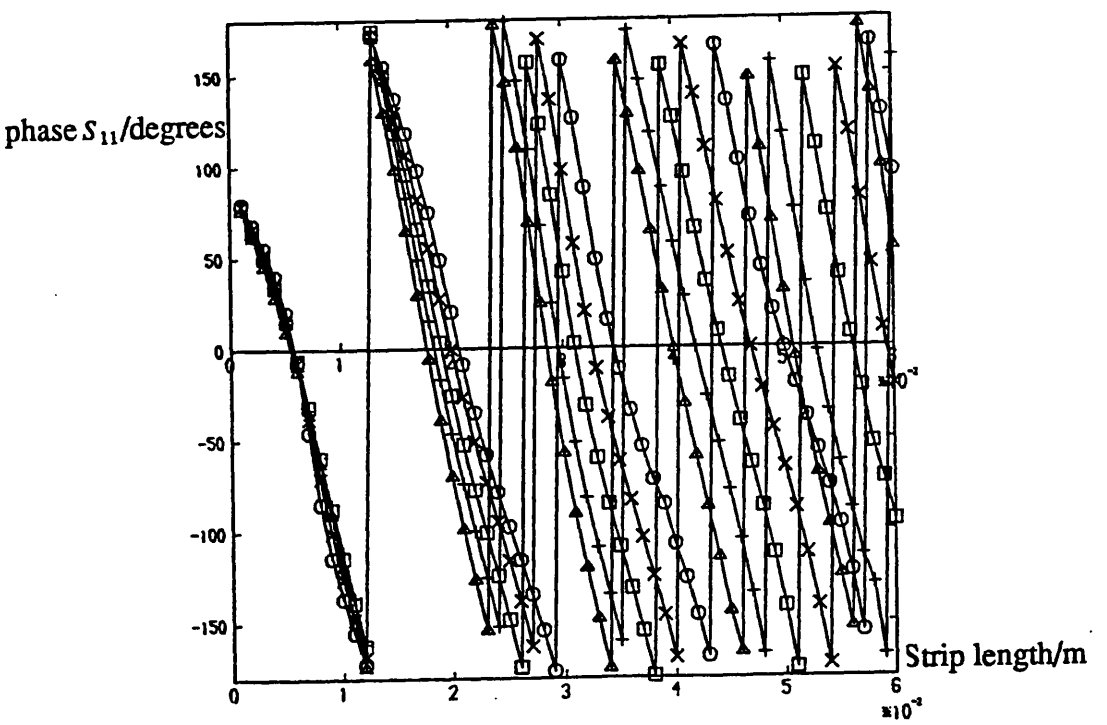

Figure 6.12g) Vector analysis : phase S_{11} vrs strip length,width=5mm.

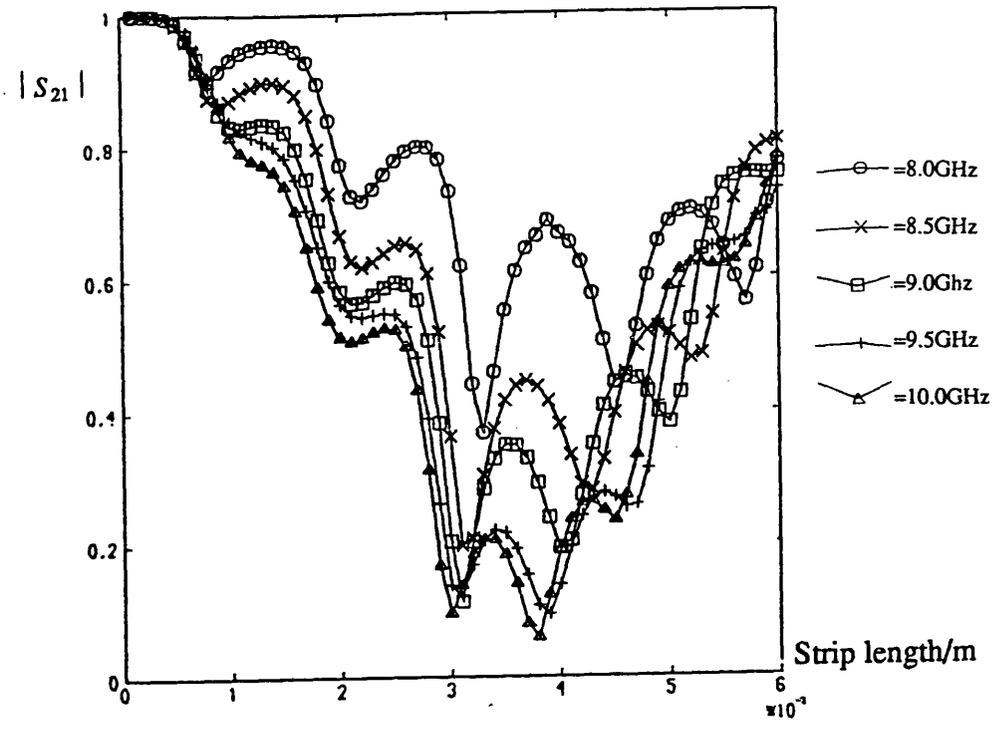

Figure 6.12h) Vector analysis : $|S_{21}|$ vrs strip length,width=5mm.

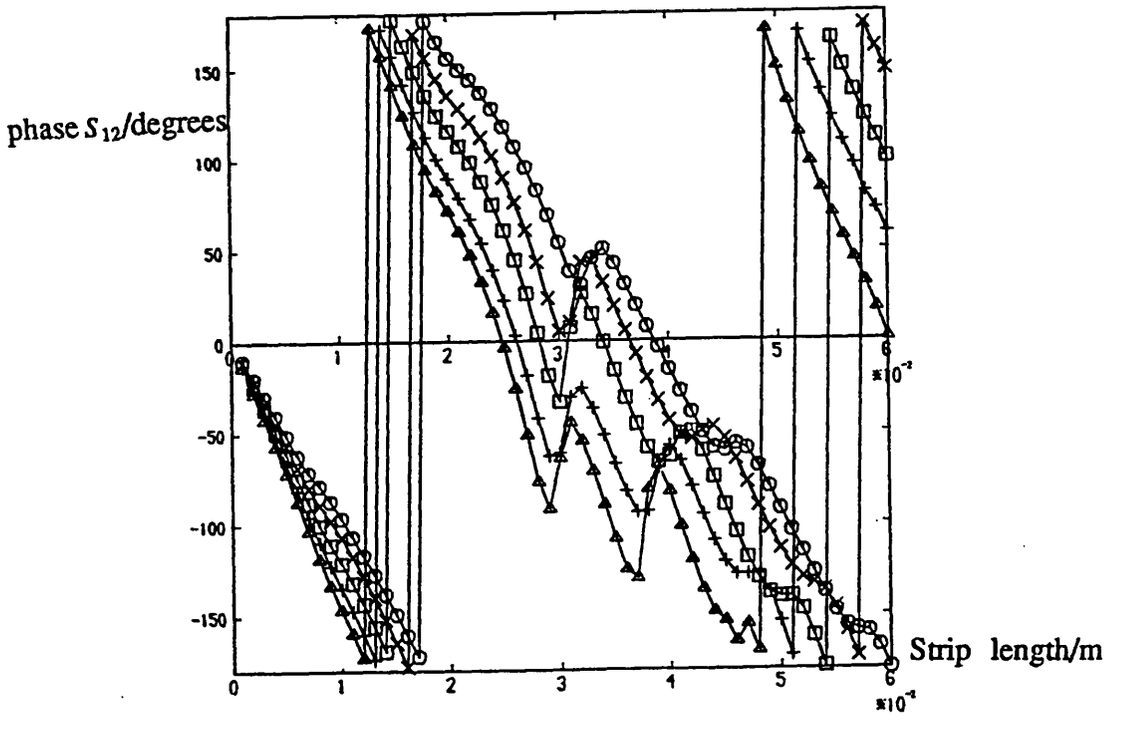

Figure 6.12i) Vector analysis : phase S_{21} vrs strip length,width=5mm.

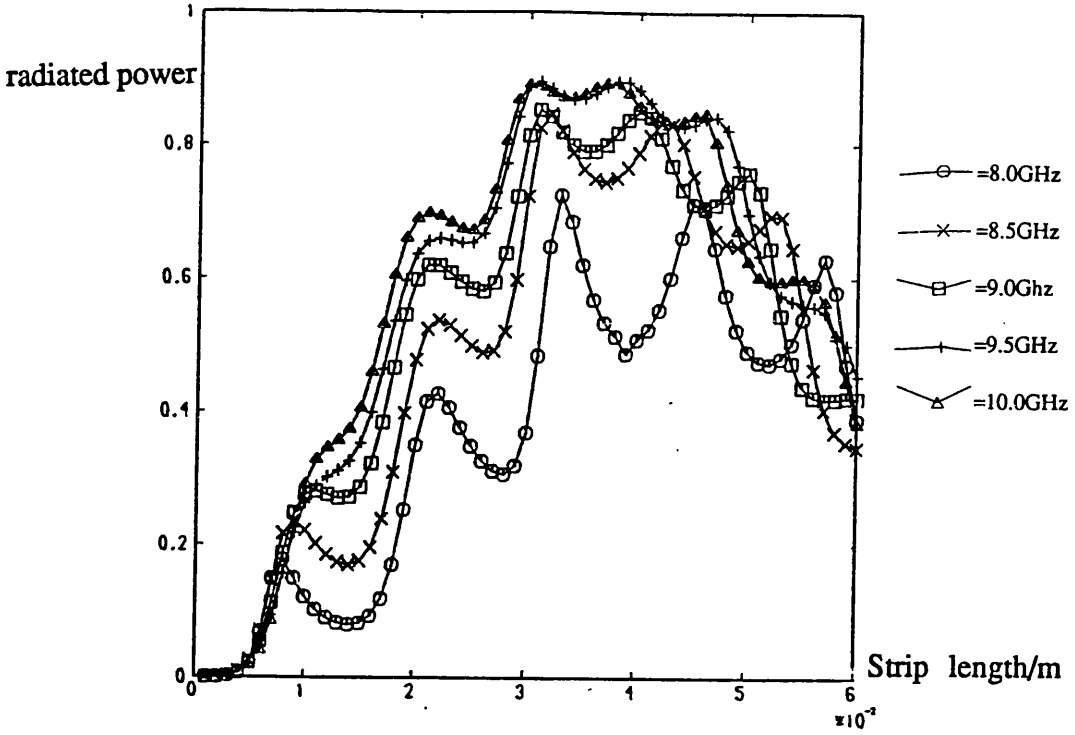

Figure 6.12j) Vector analysis : radiated power vrs strip length,width=5mm.

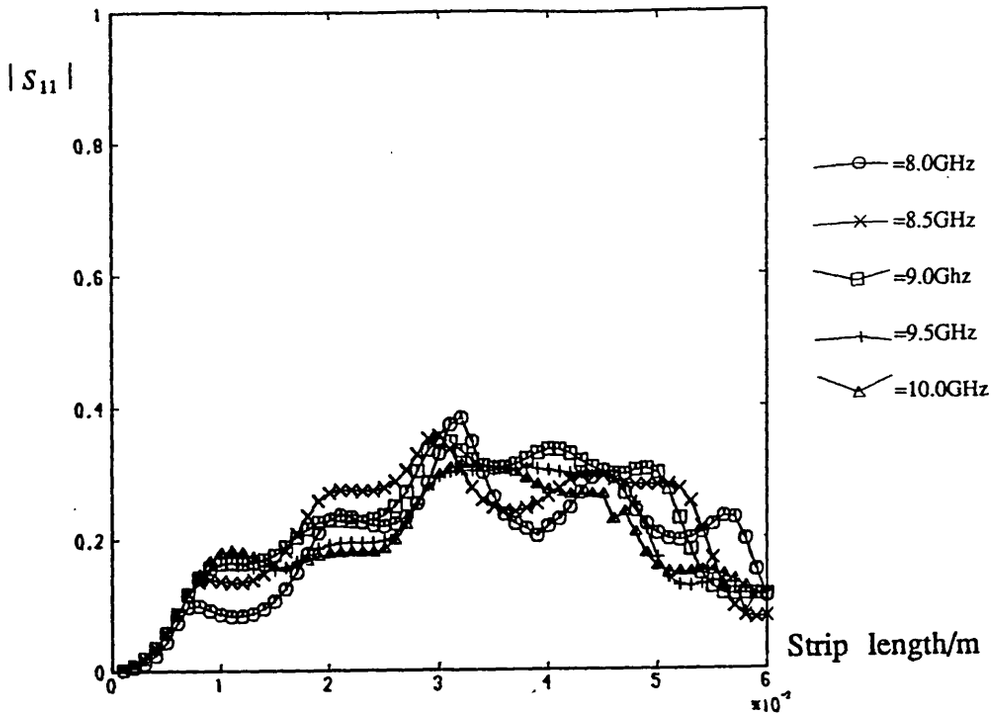

Figure 6.12k) Vector analysis : | S_{11} | vrs strip length,width=7mm.

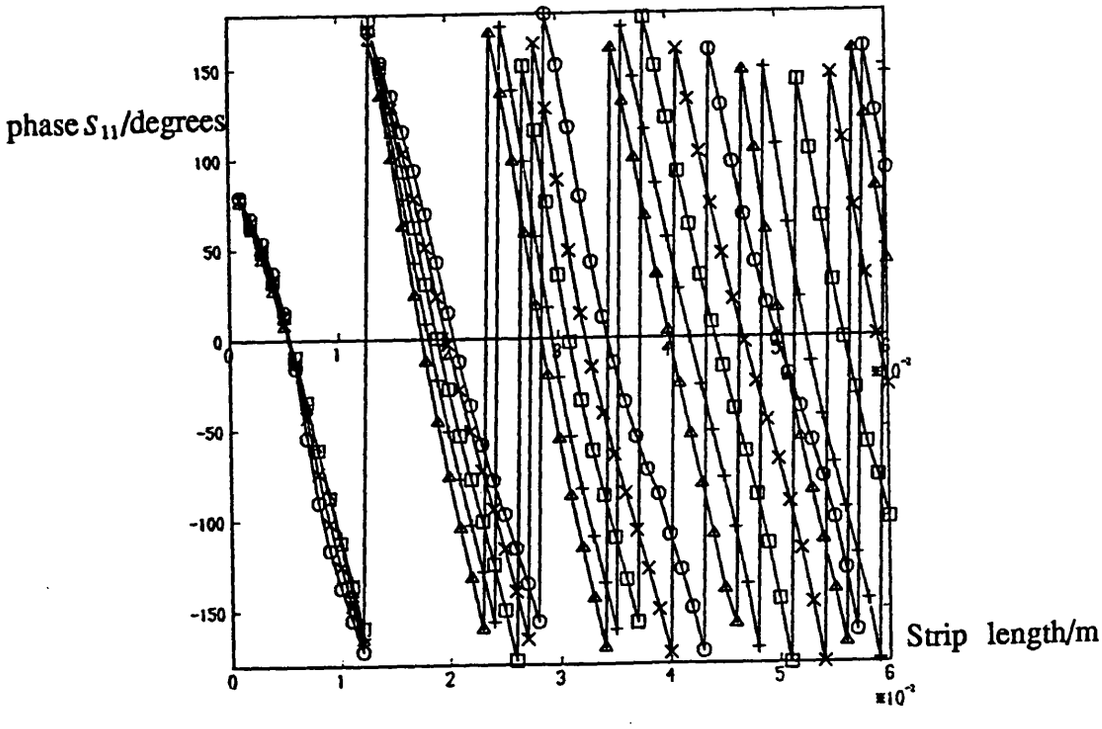

Figure 6.12l) Vector analysis : phase S_{11} vrs strip length,width=7mm.

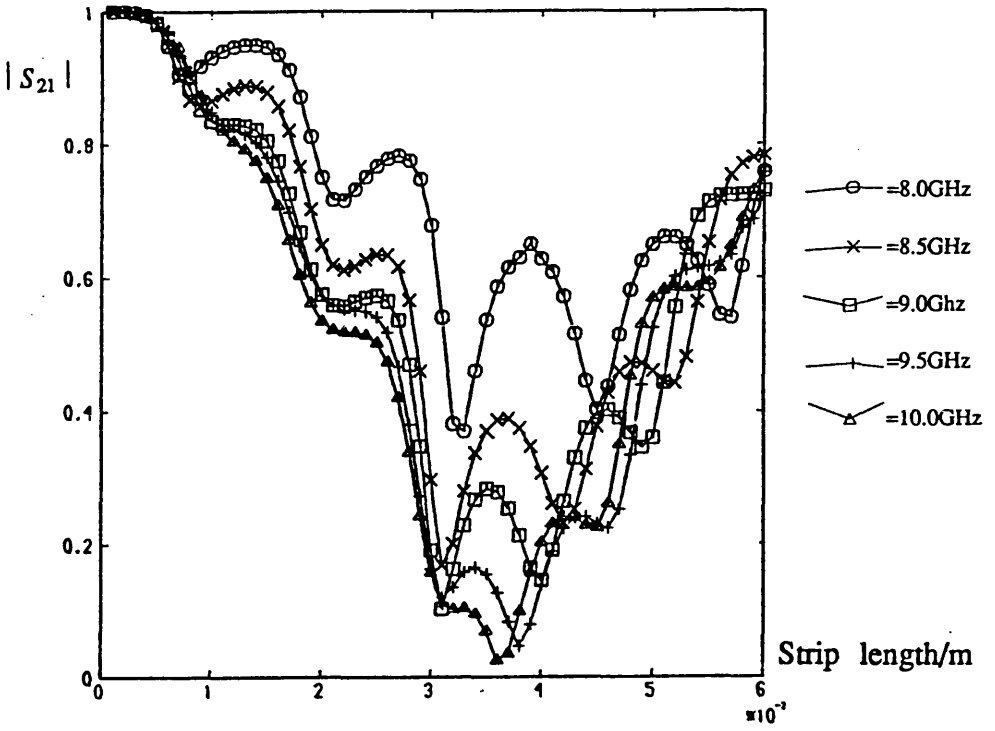

Figure 6.12m) Vector analysis : $|S_{21}|$ vrs strip length,width=7mm.

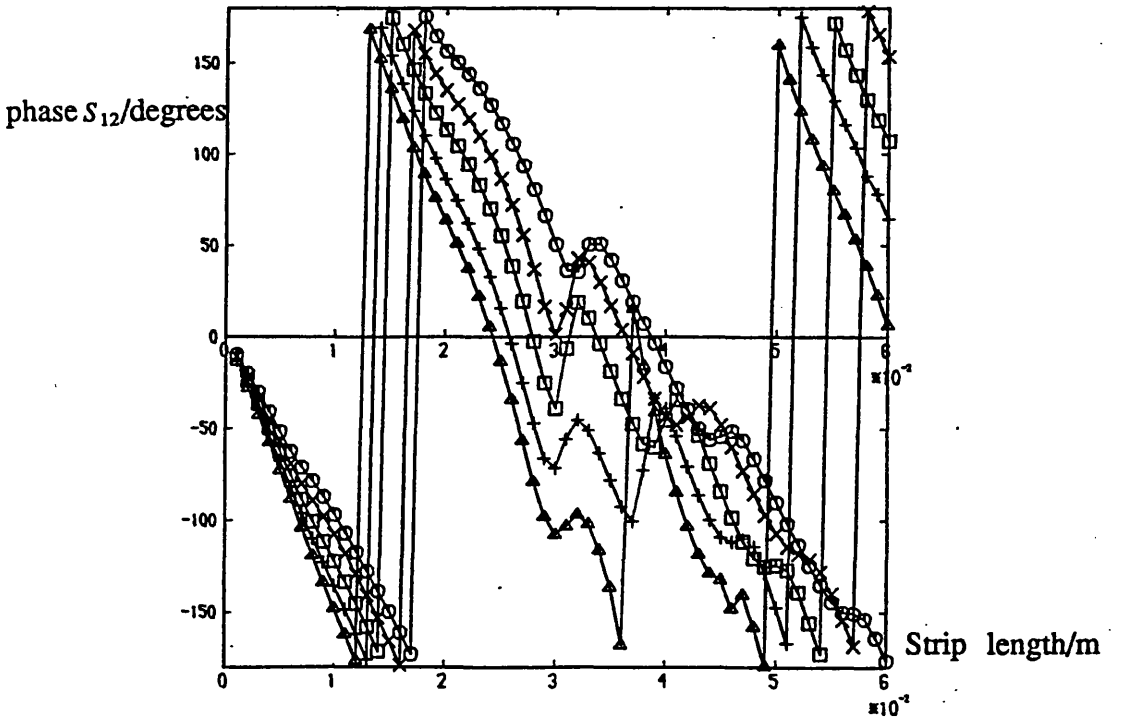

Figure 6.12n) Vector analysis : phase S_{21} vrs strip length,width=7mm.

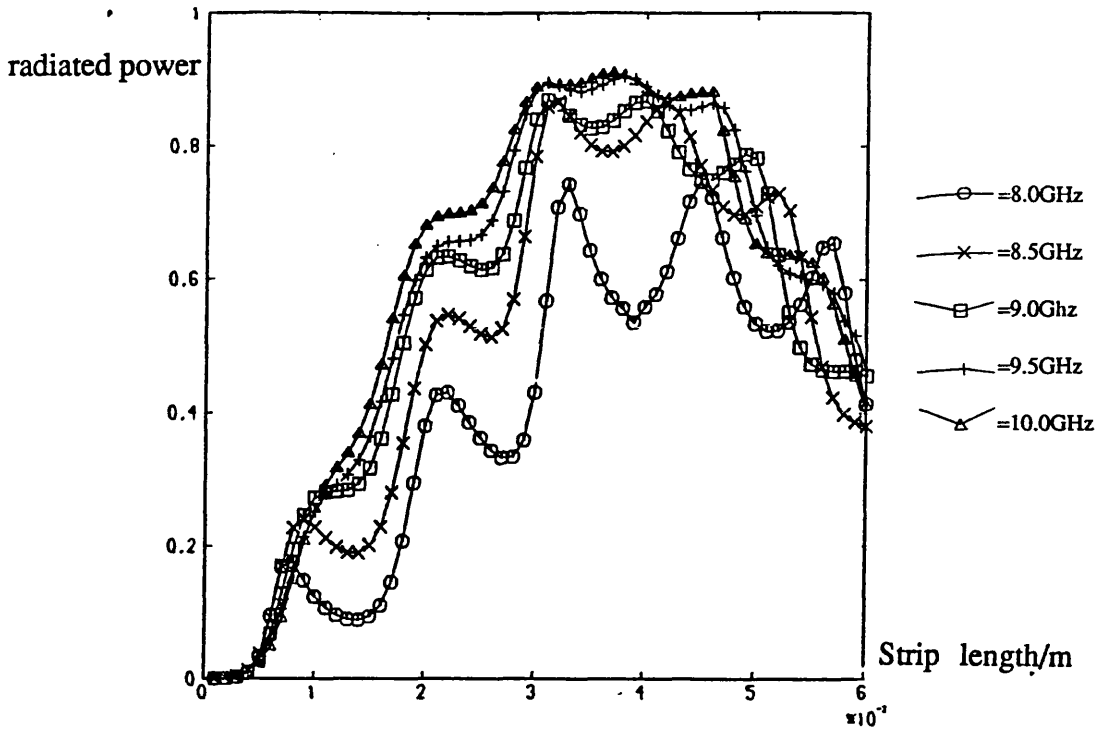

Figure 6.12o) Vector analysis : radiated power vrs strip length,width=7mm.

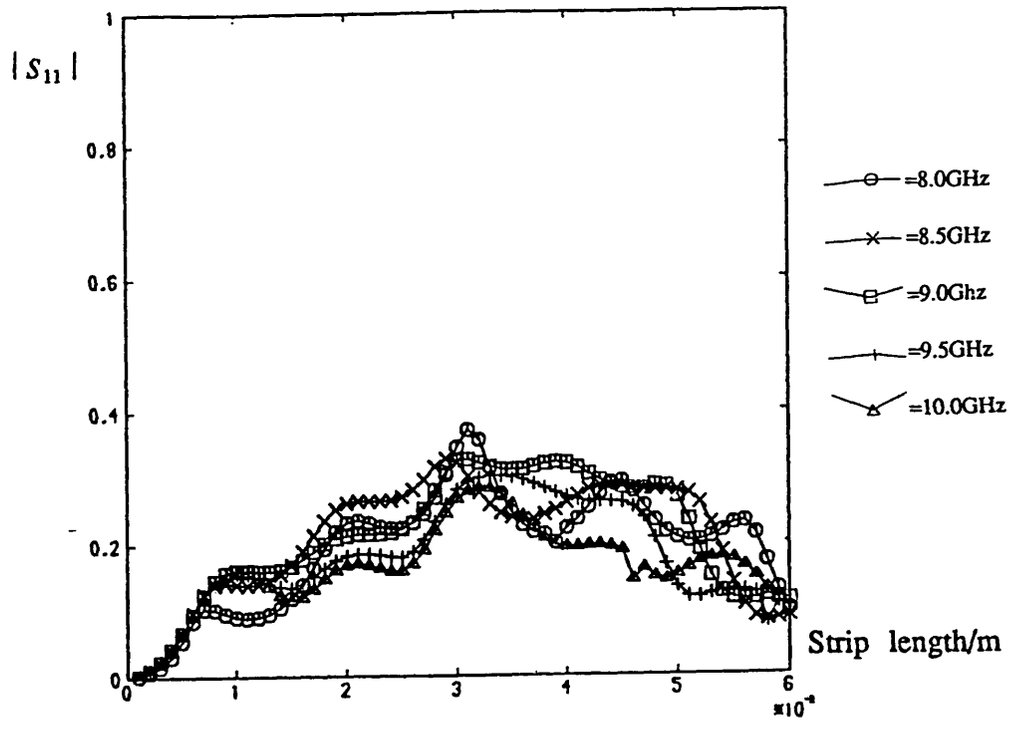

Figure 6.12p) Vector analysis : $|S_{11}|$ vrs strip length,width=10mm.

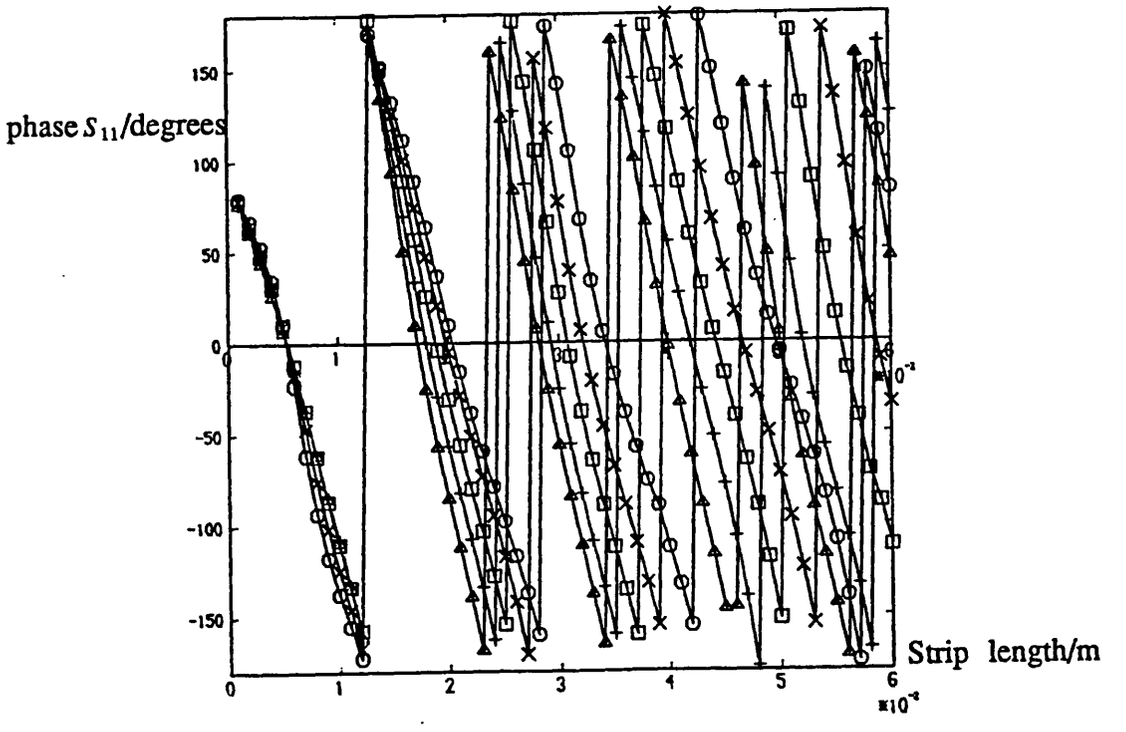

Figure 6.12q) Vector analysis : phase S_{11} vrs strip length,width=10mm.

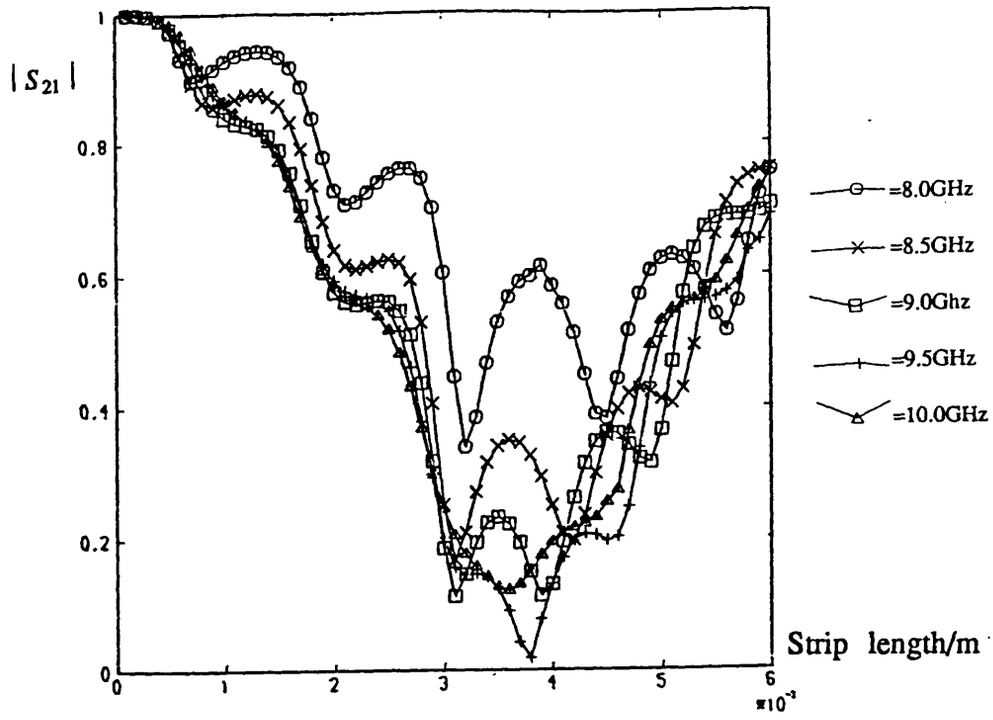

Figure 6.12r) Vector analysis : $|S_{21}|$ vrs strip length,width=10mm.

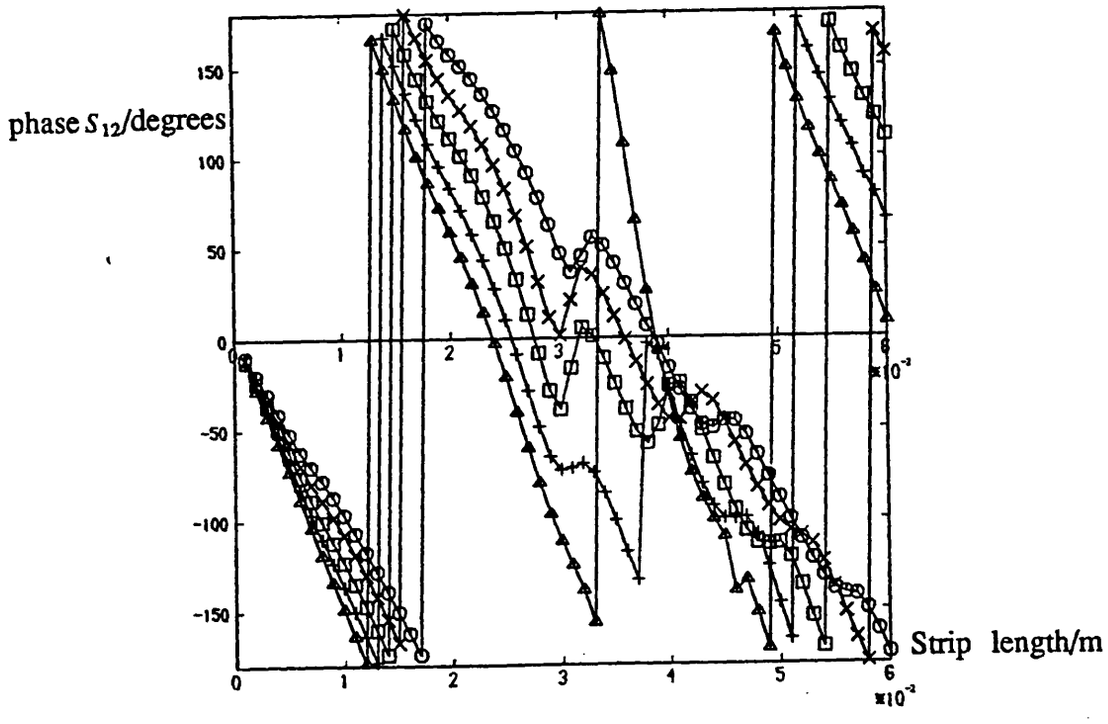

Figure 6.12s) Vector analysis : phase S_{21} vrs strip length,width=10mm.

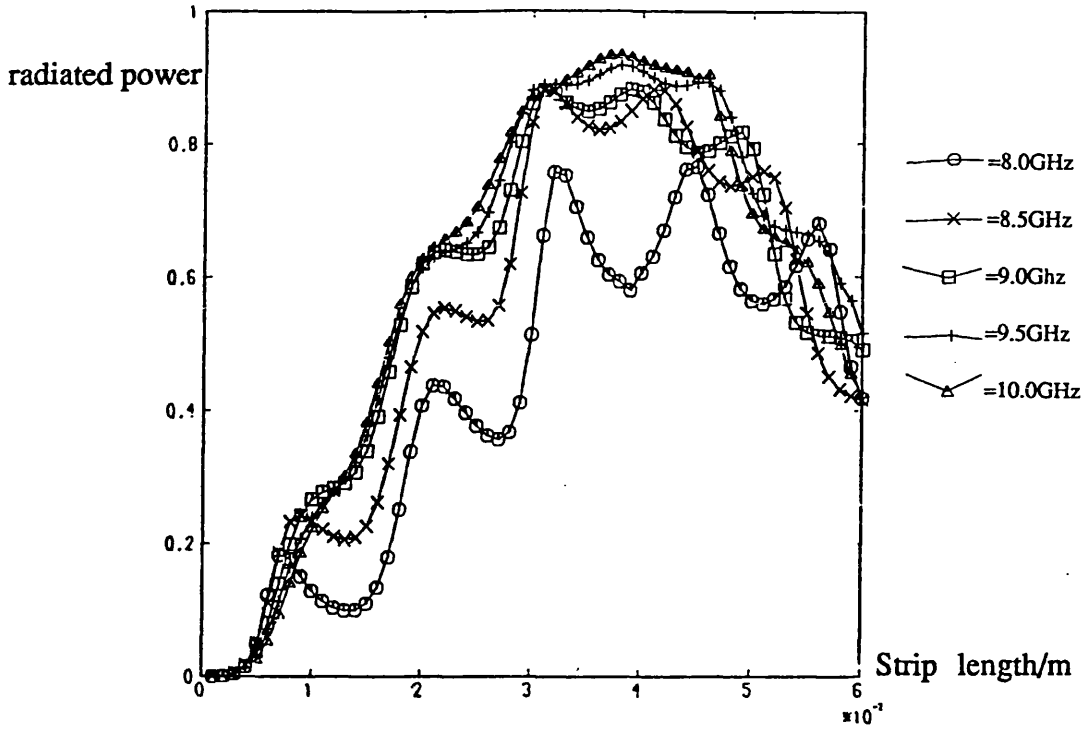

Figure 6.12t) Vector analysis : radiated power vrs strip length,width=10mm.

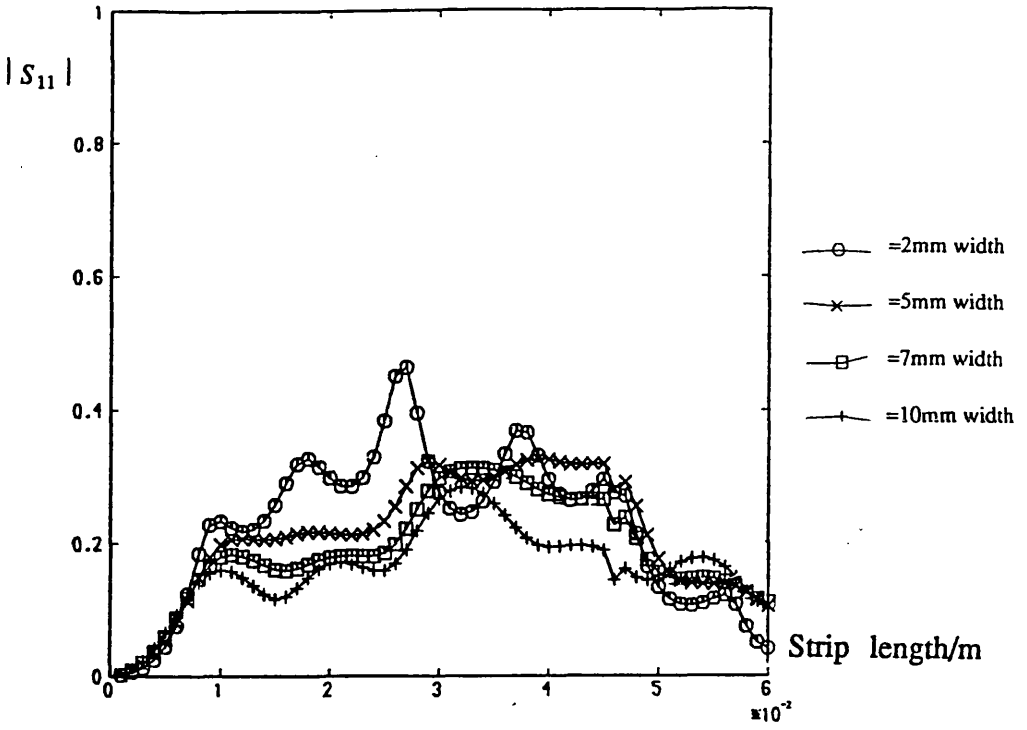

Figure 6.13a) Vector analysis : $|S_{11}|$ vrs strip length,at 8GHz.

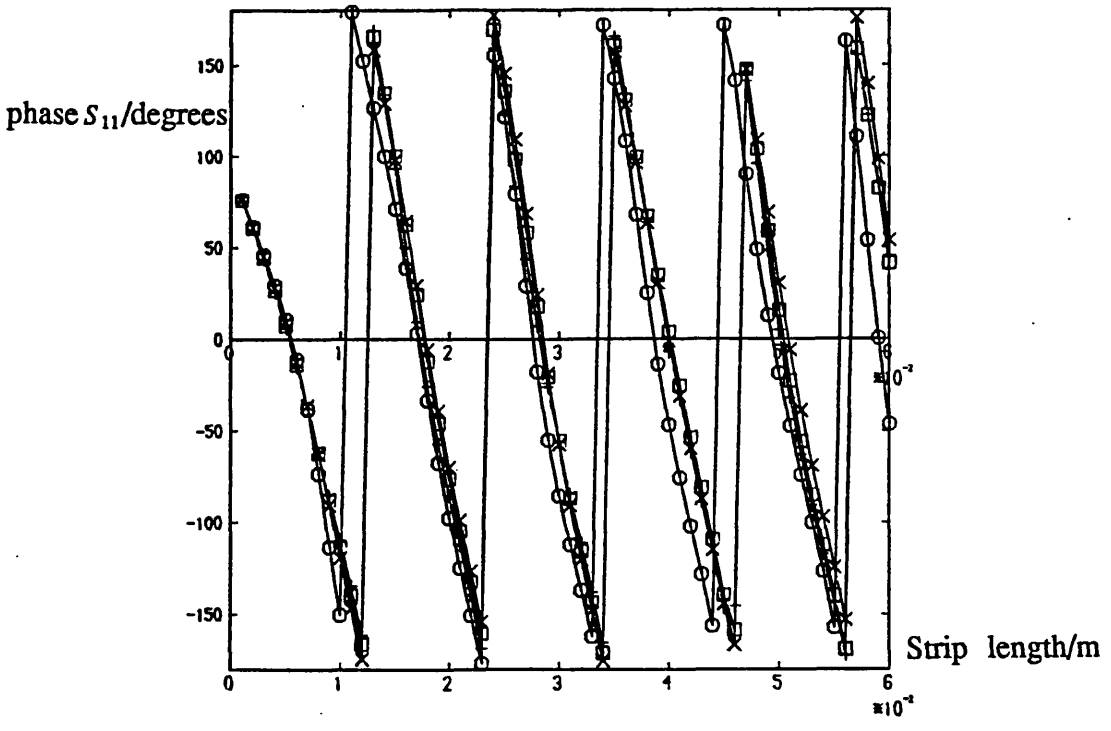

Figure 6.13b) Vector analysis : phase S_{11} vrs strip length,at 8GHz.

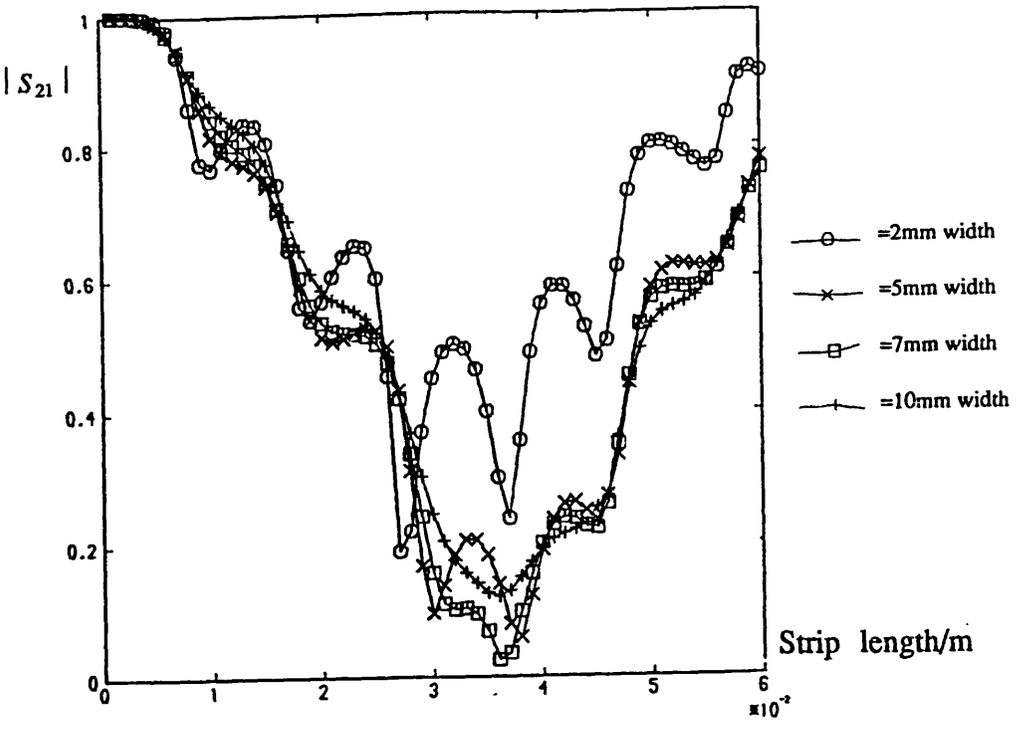

Figure 6.13c) Vector analysis : $|S_{21}|$ vrs strip length,at 8GHz.

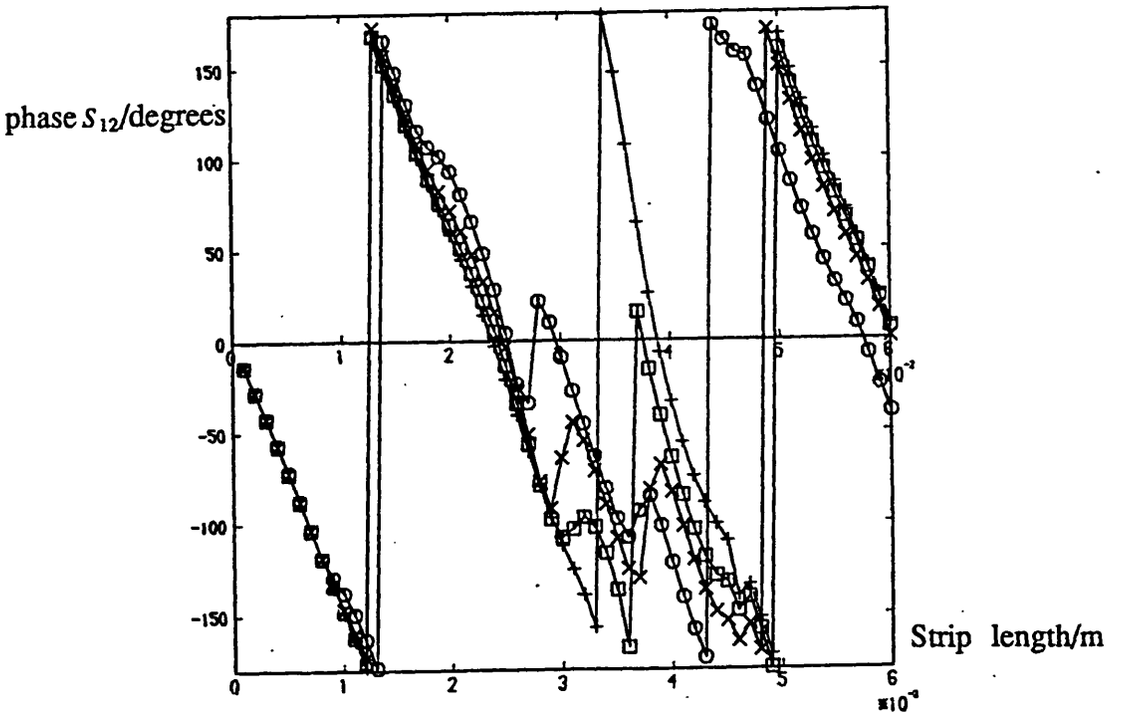

Figure 6.13d) Vector analysis : phase S_{21} vrs strip length,at 8GHz.

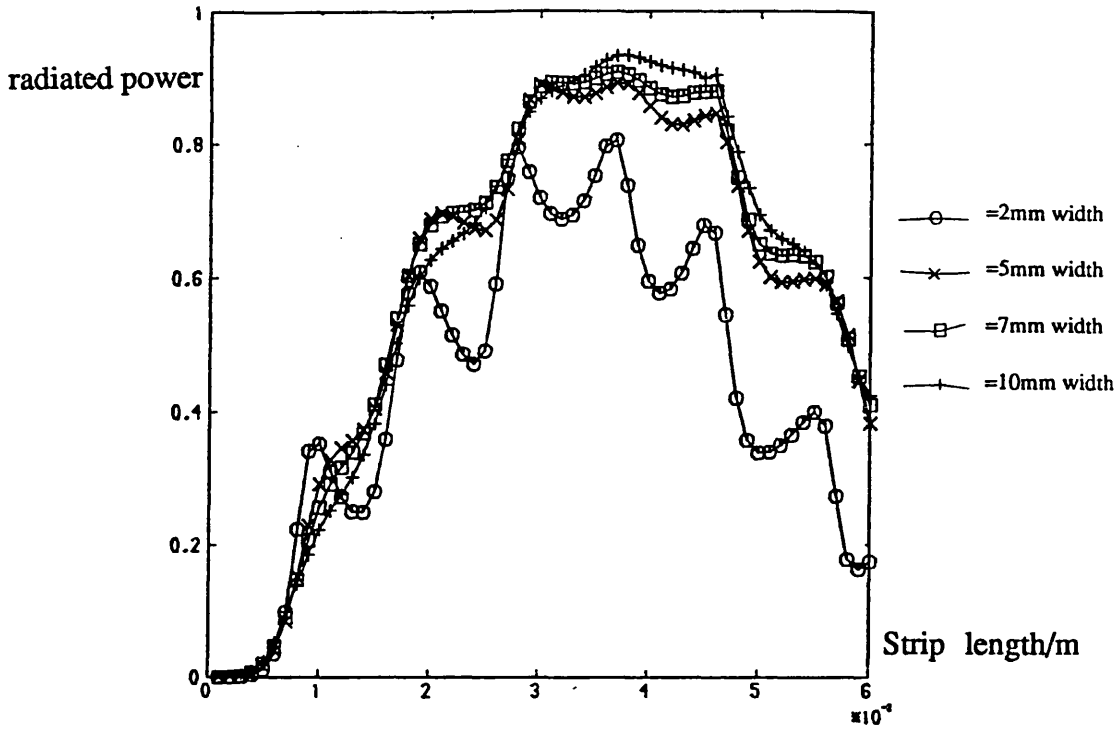

Figure 6.13e) Vector analysis : radiated power vrs strip length,at 8GHz.

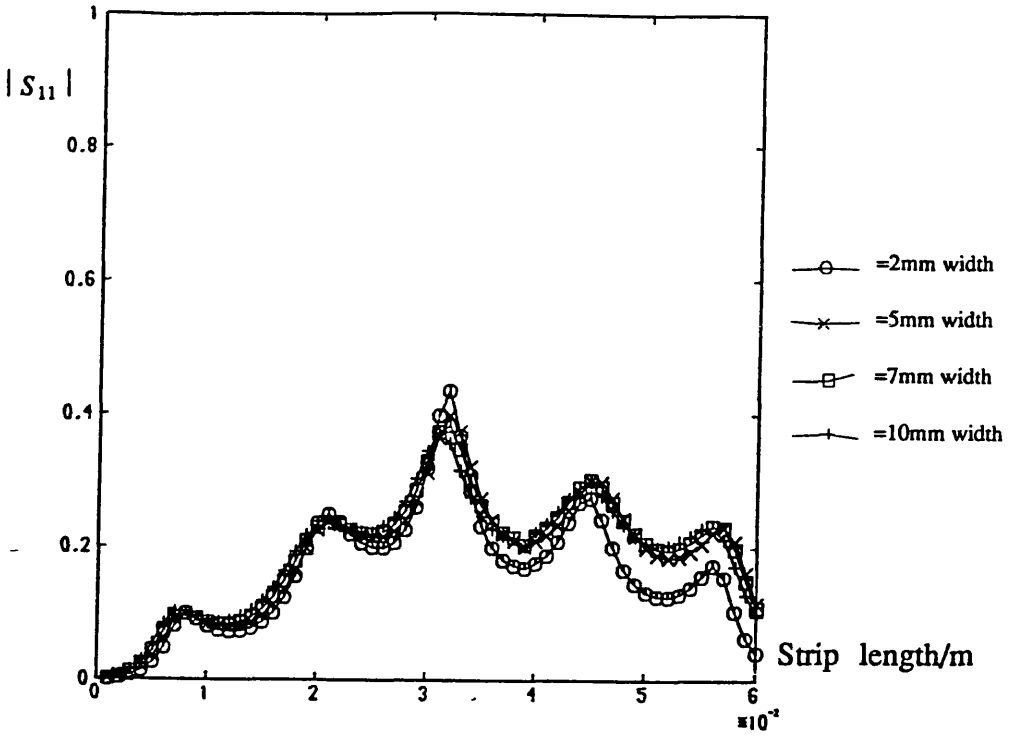

Figure 6.13f) Vector analysis : | S_{11} | vrs strip length,at 10GHz.

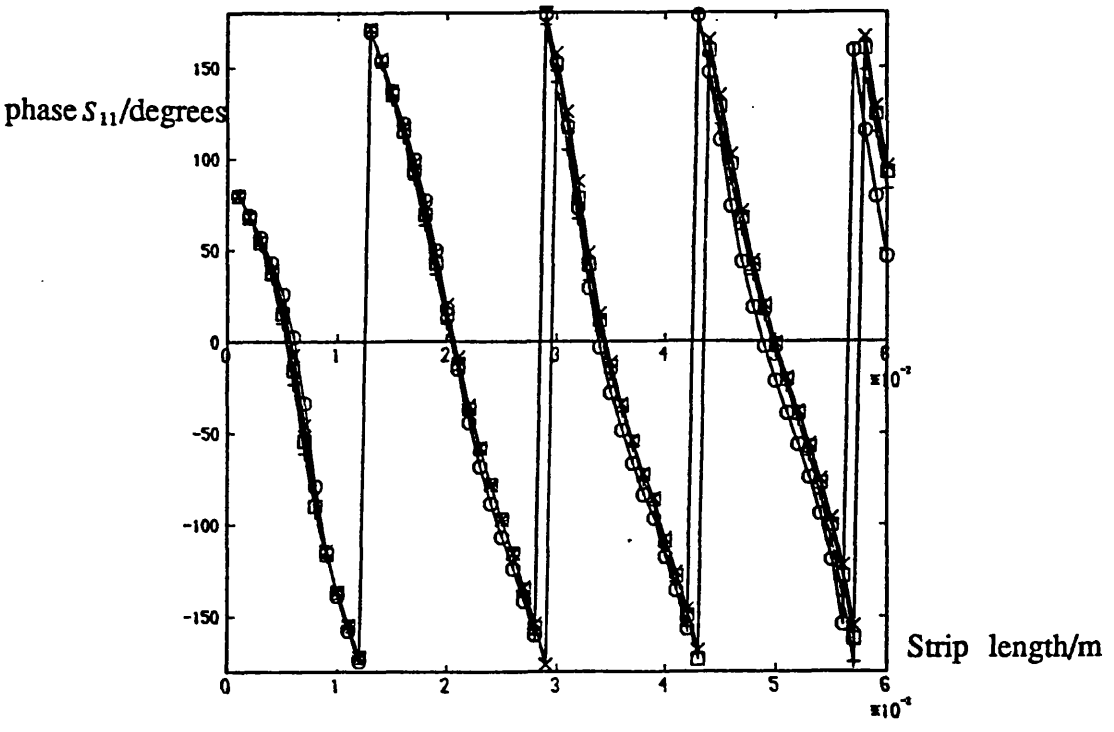

Figure 6.13g) Vector analysis : phase S_{11} vrs strip length,at 10GHz.

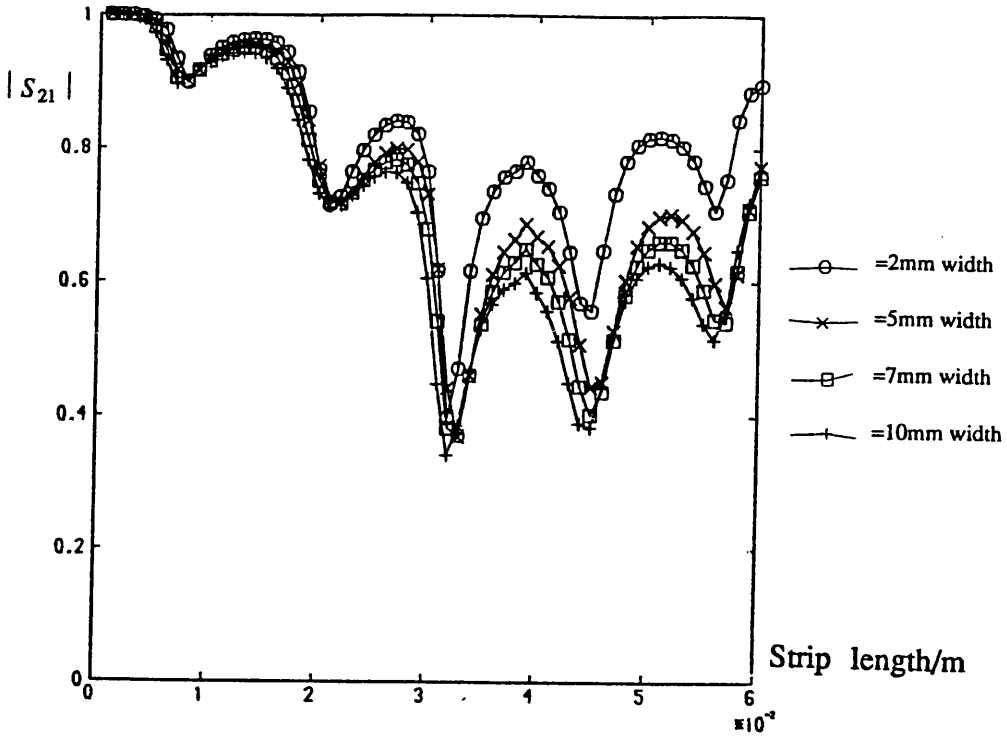

Figure 6.13h) Vector analysis : | S_{21} | vrs strip length,at 10GHz.

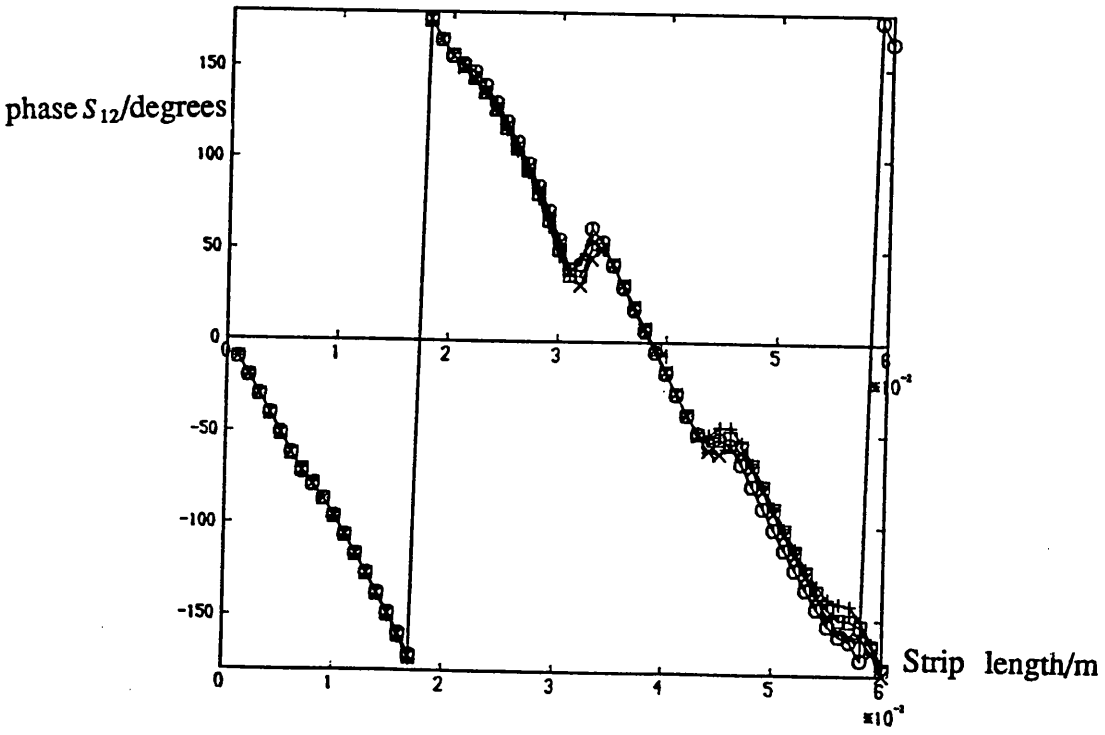

Figure 6.13i) Vector analysis : phase S_{21} vrs strip length,at 10GHz.

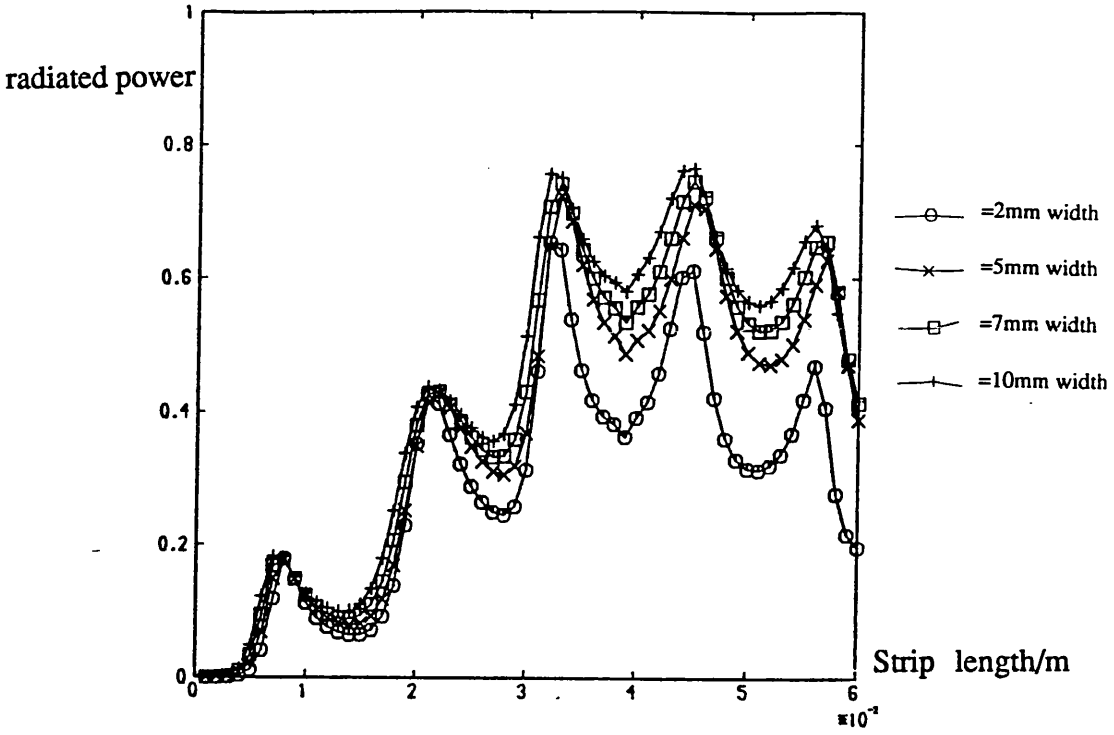

Figure 6.13j) Vector analysis : radiated power vrs strip length,at 10GHz.

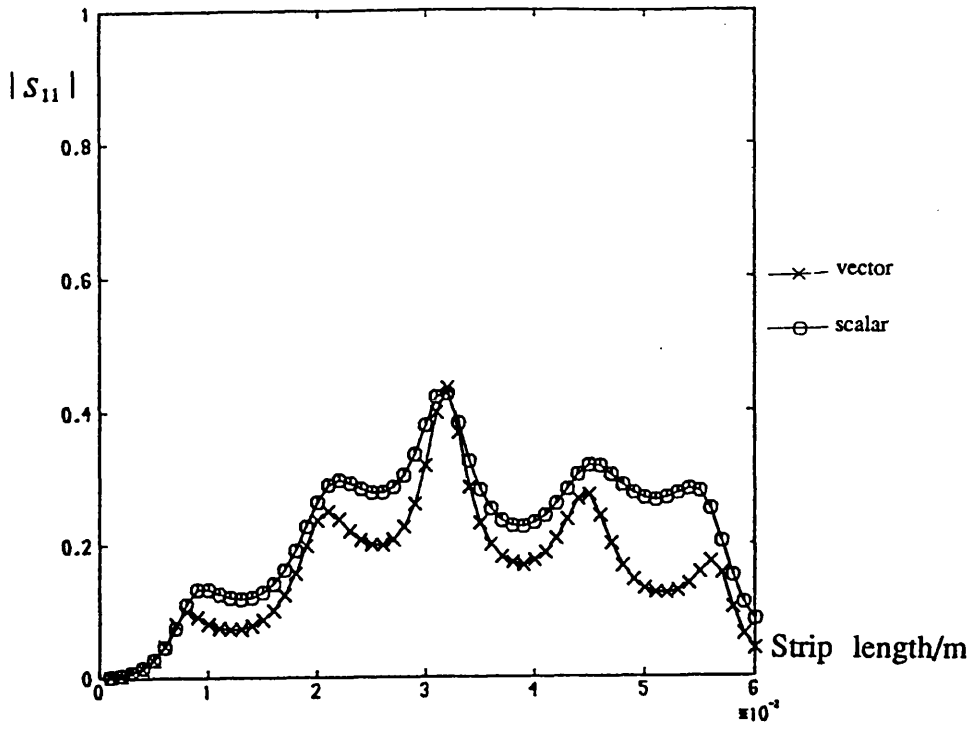

Figure 6.14a) Comparison of vector and scalar analyses : $|S_{11}|$ vrs strip length at 8GHz,width=2mm.

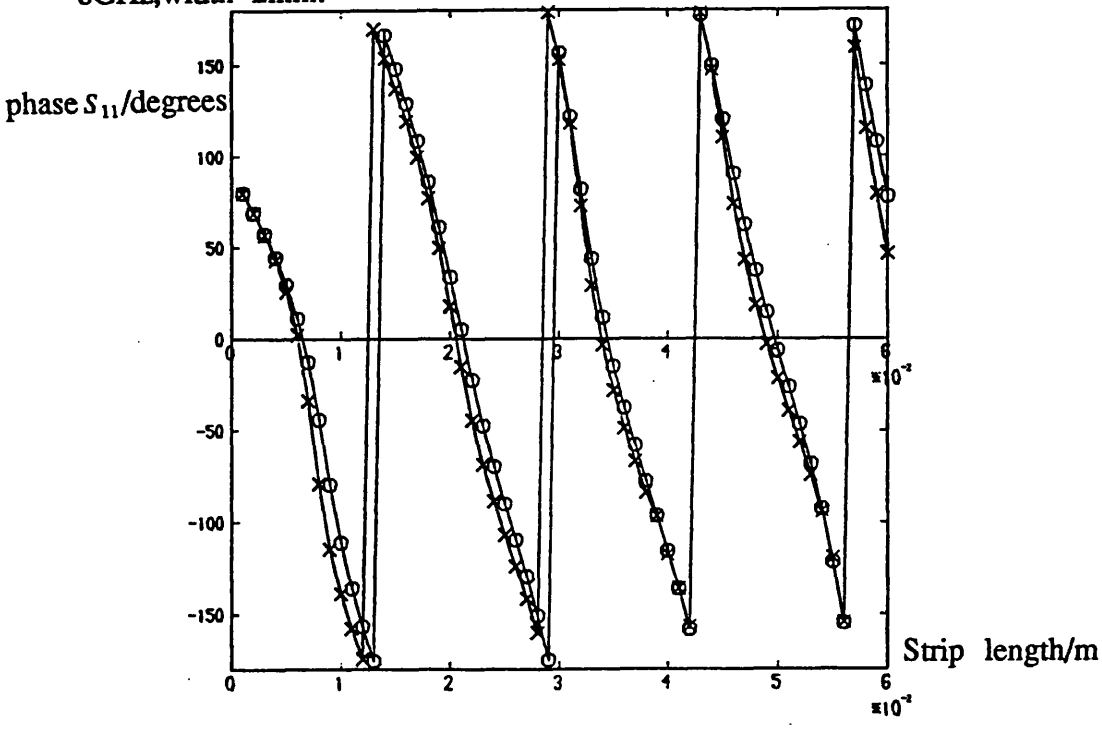

Figure 6.14b) Comparison of vector and scalar analyses :phase S_{11} vrs strip length at 8GHz,width=2mm.

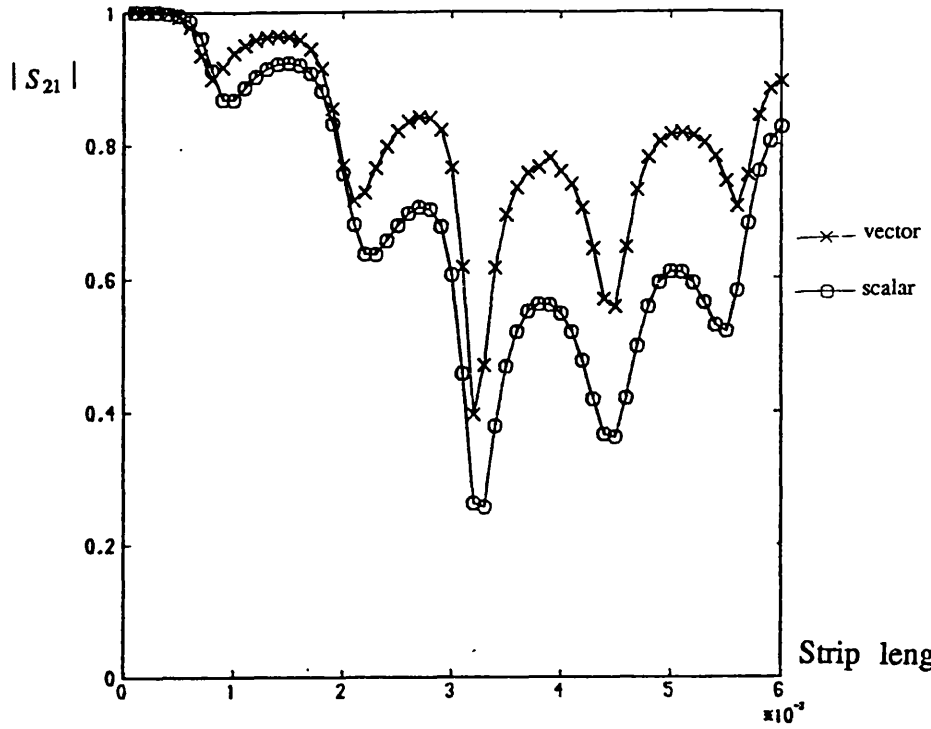

Figure 6.14c) Comparison of vector and scalar analyses : | S_{21} | vrs strip length at 8GHz,width=2mm.

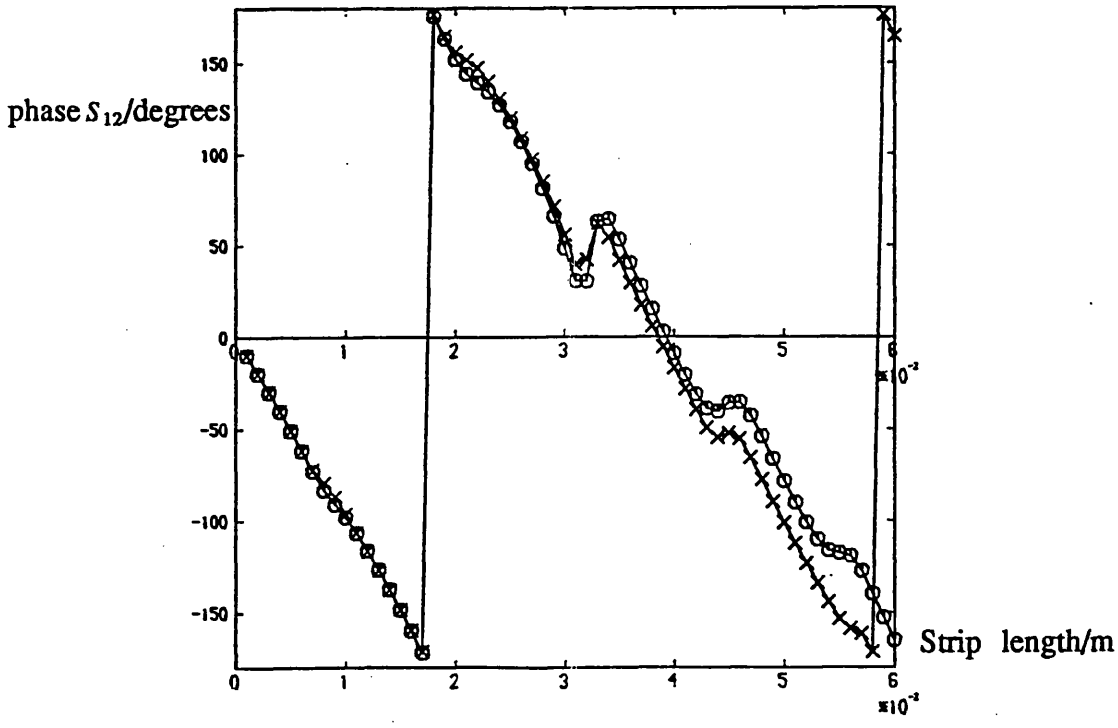

Figure 6.14d) Comparison of vector and scalar analyses :phase S_{21} vrs strip length at 8GHz,width=2mm.

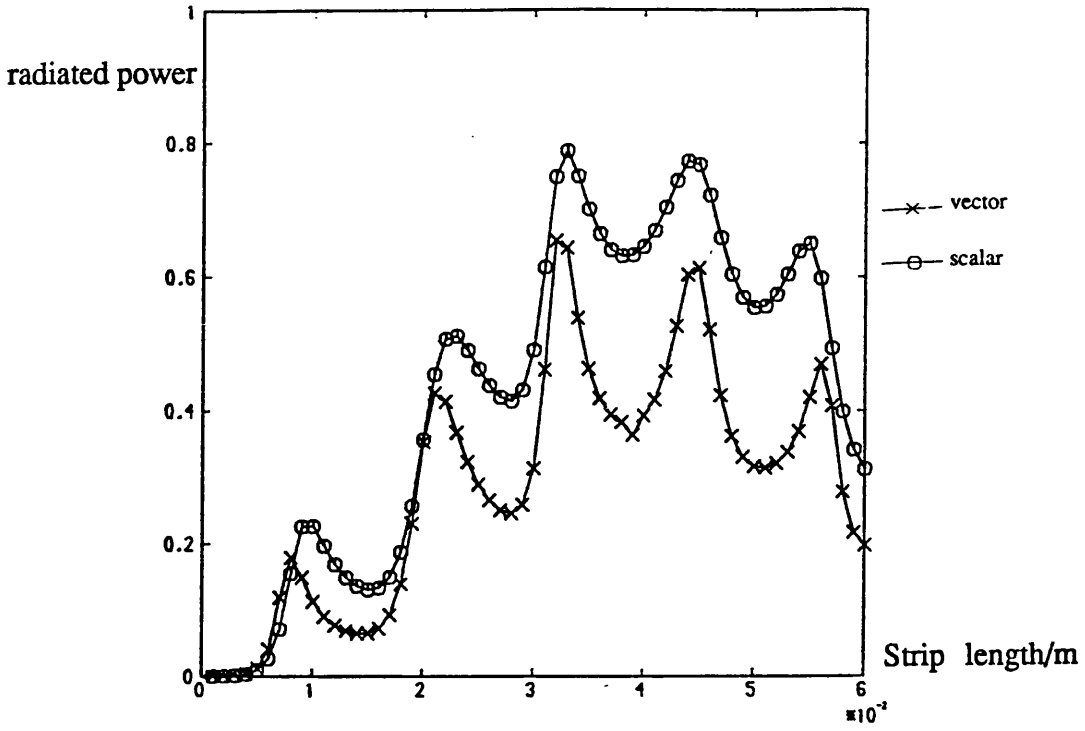

Figure 6.14e) Comparison of vector and scalar analyses :radiated power vrs strip length at 8GHz,width=2mm.

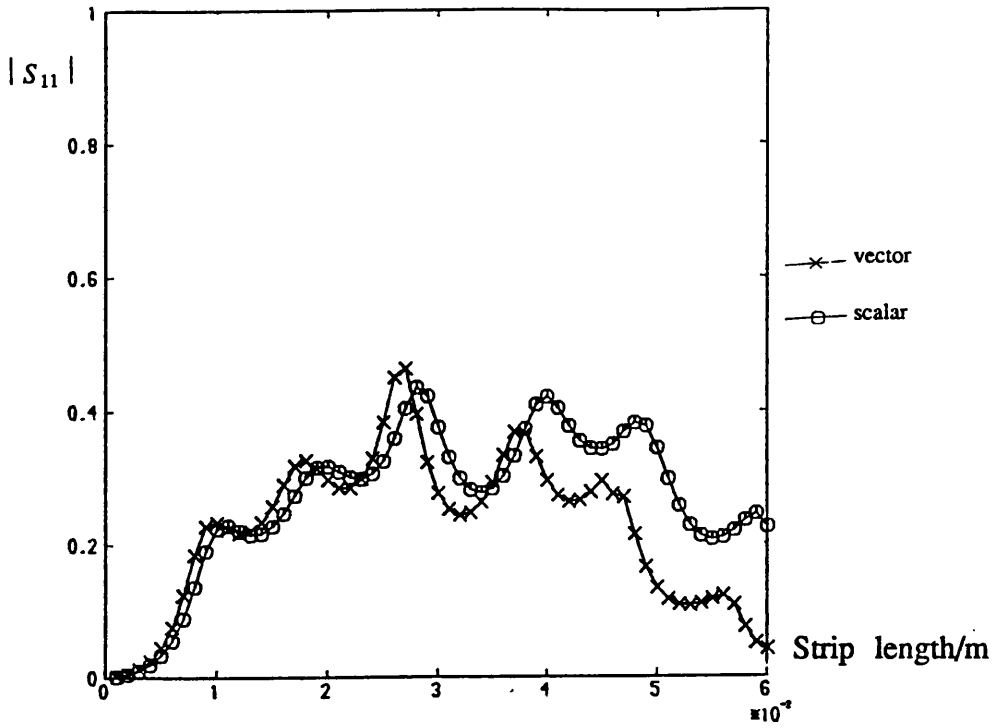

Figure 6.15a) Comparison of vector and scalar analyses : $|S_{11}|$ vrs strip length at 10GHz,width=2mm.

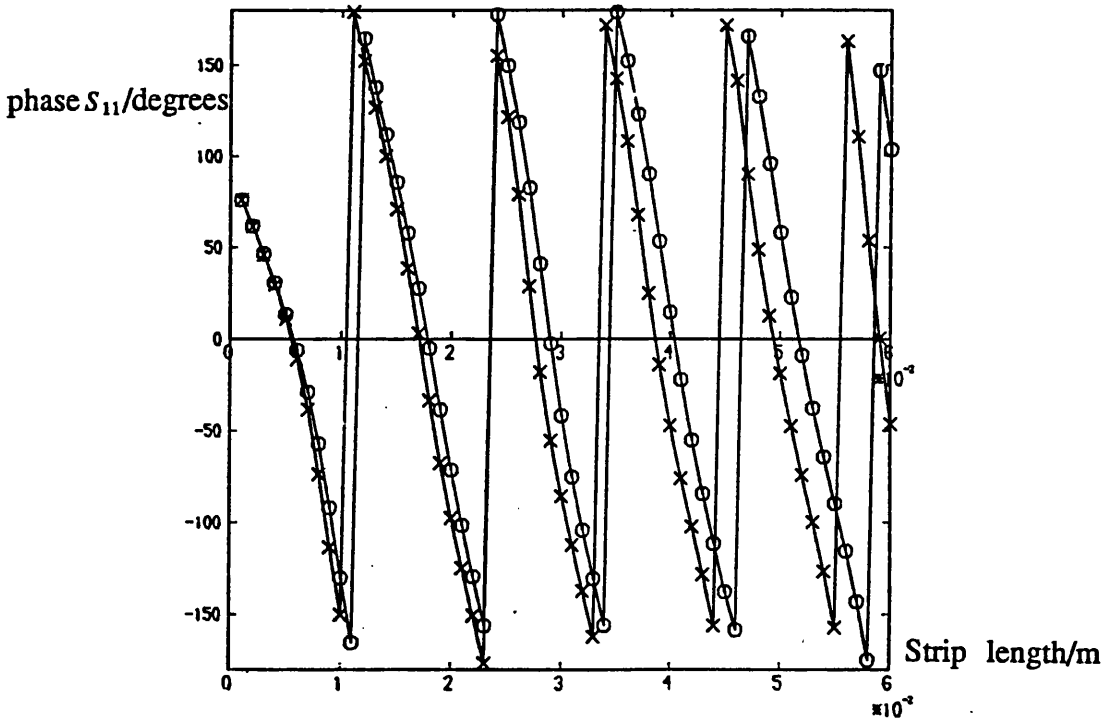

Figure 6.15b) Comparison of vector and scalar analyses :phase S_{11} vrs strip length at 10GHz,width=2mm.

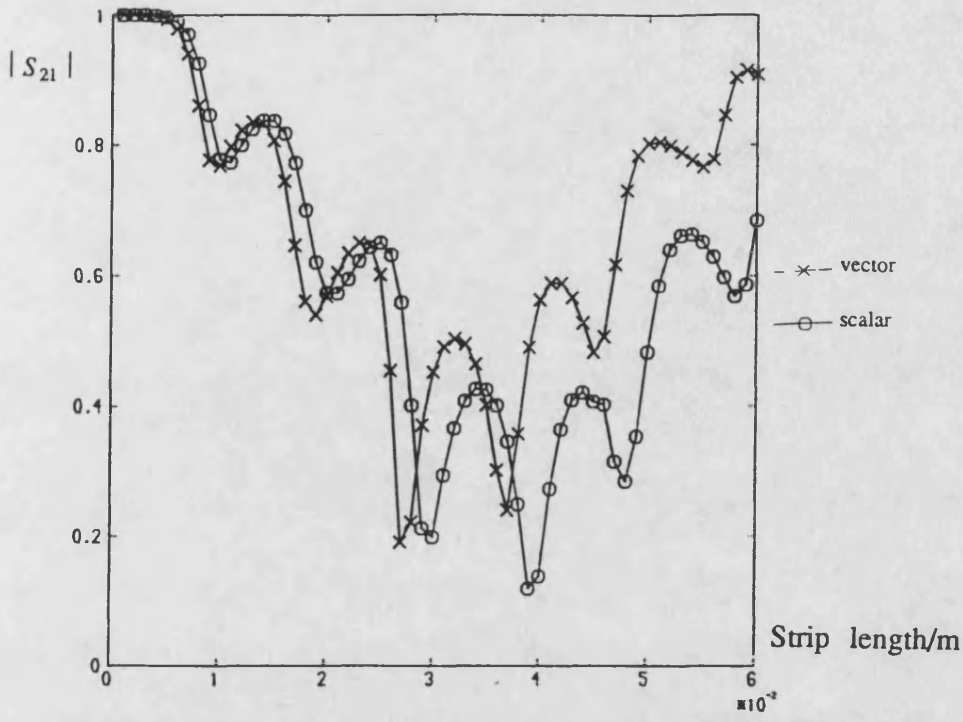

Figure 6.15c) Comparison of vector and scalar analyses : $|S_{21}|$ vrs strip length at 10GHz,width=2mm.

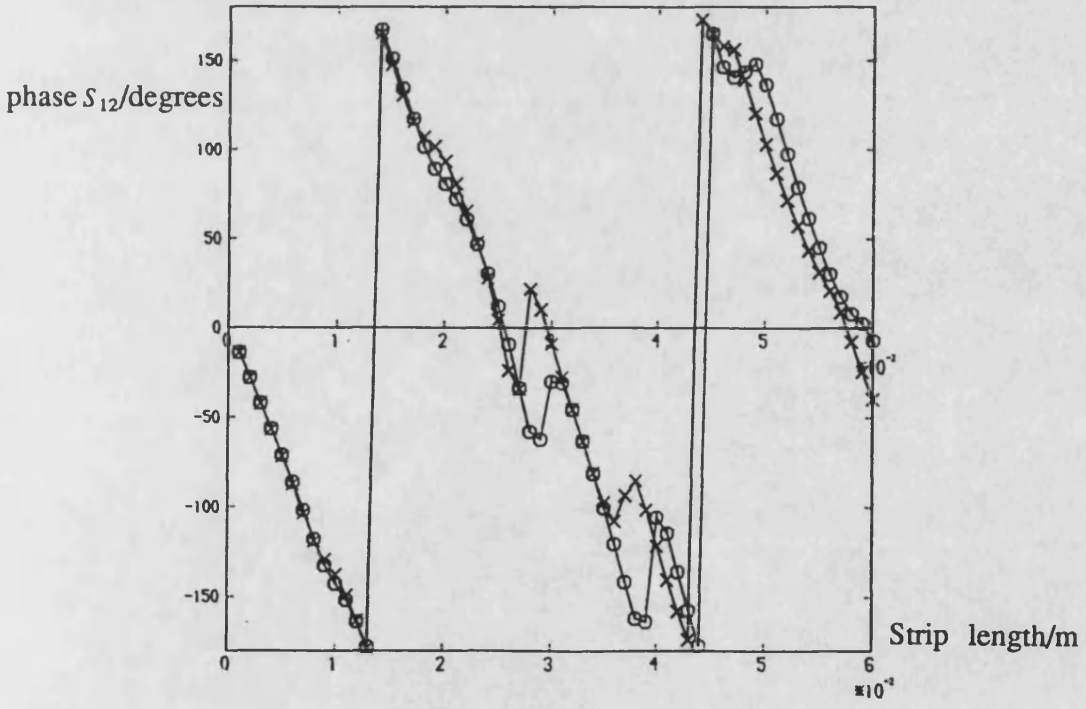

Figure 6.15d) Comparison of vector and scalar analyses :phase S_{21} vrs strip length at 10GHz,width=2mm.

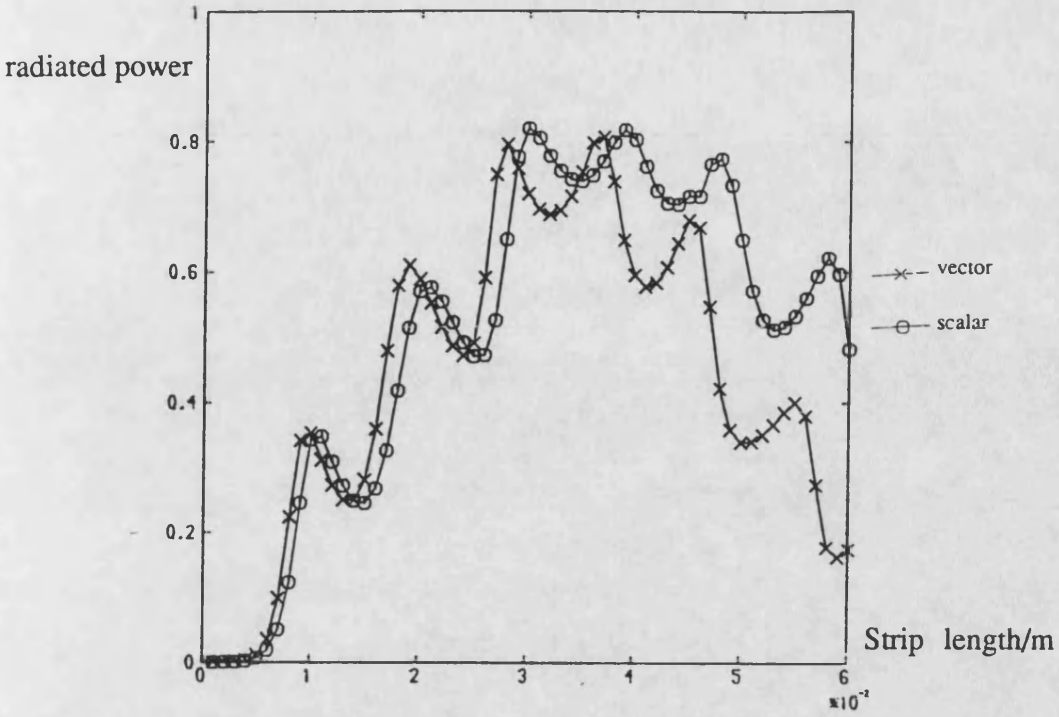

Figure 6.15e) Comparison of vector and scalar analyses :radiated power vrs strip length at 10GHz,width=2mm.

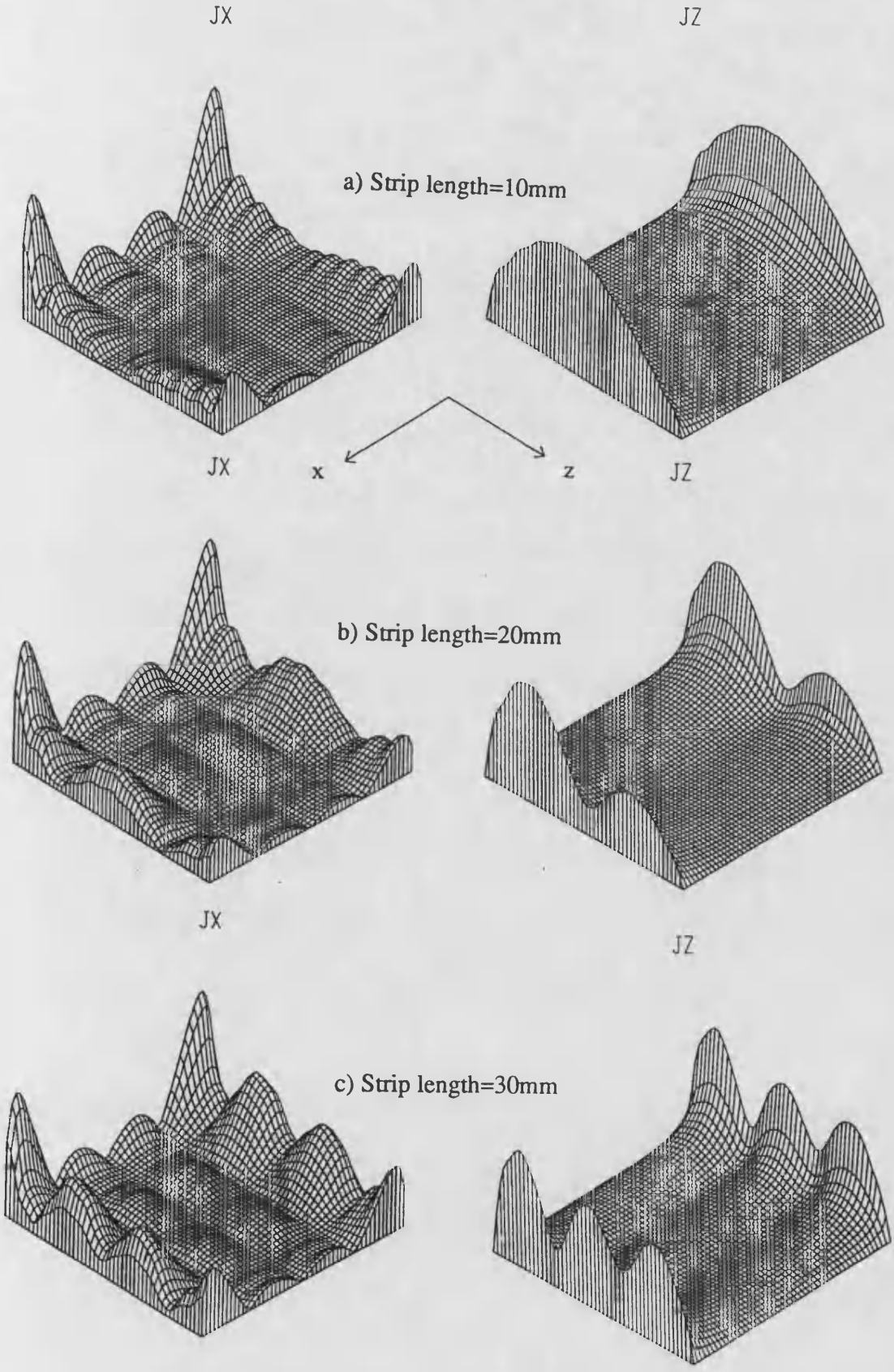

Figure 6.16) Patch currents on a 2mm wide strip at 10GHz.

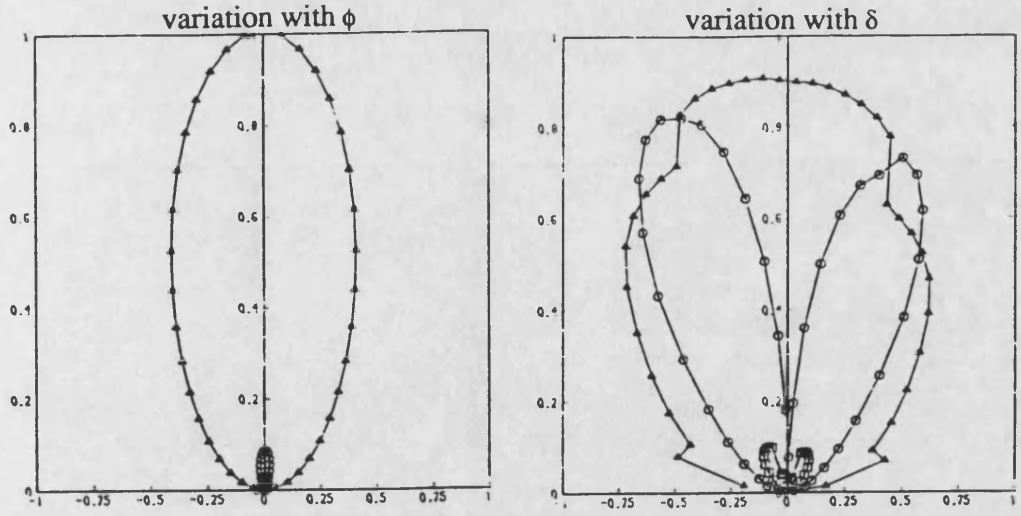

a) Strip length=10mm

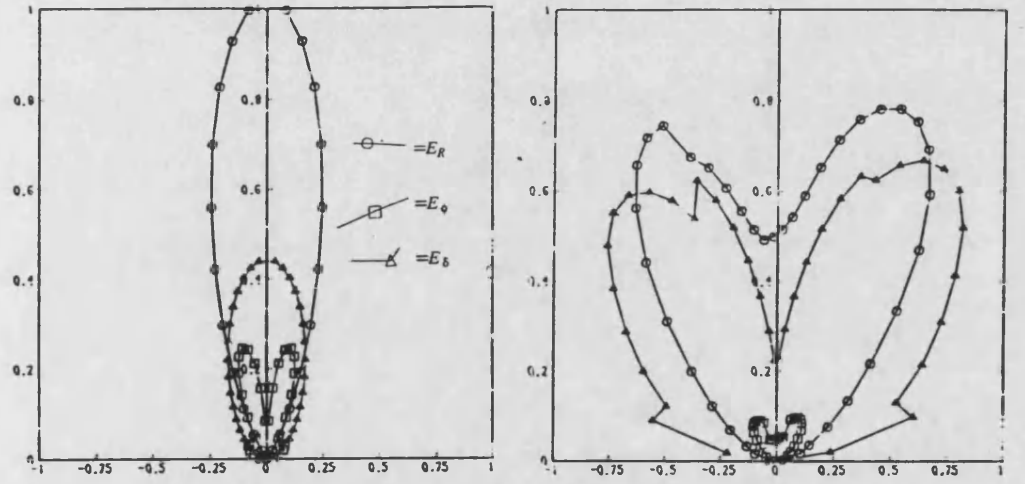

b) Strip length=20mm

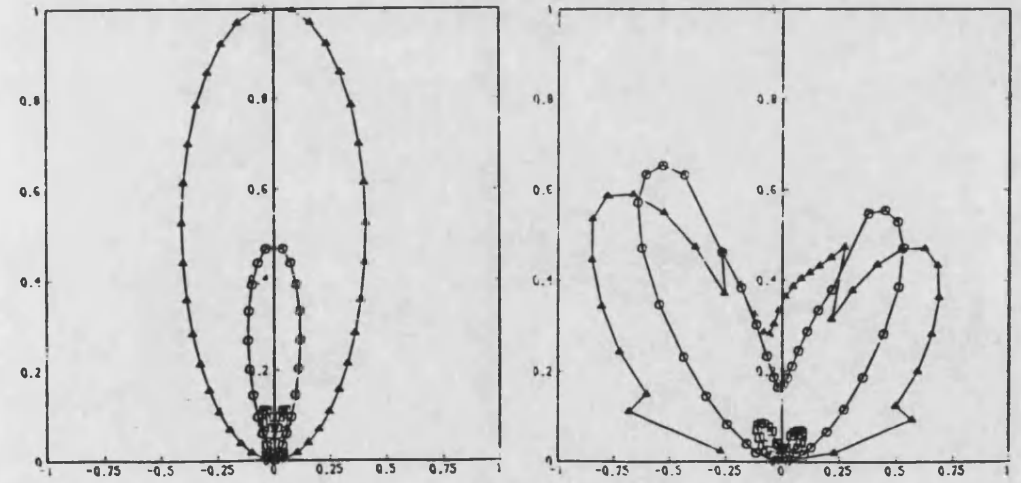

c) Strip length=30mm

Figure 6.17) Radiation Patterns for 2mm wide strip at 8GHz.

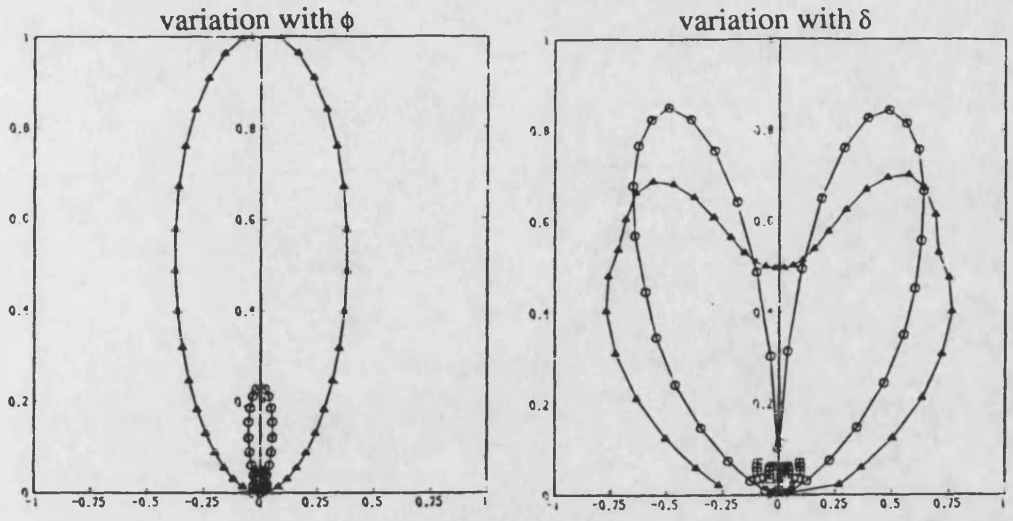

a) Strip length=10mm

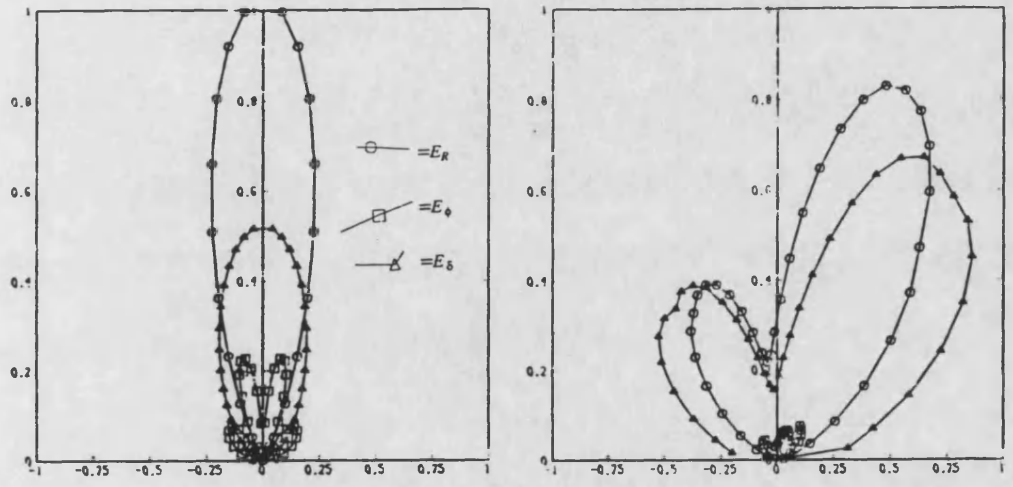

b) Strip length=20mm

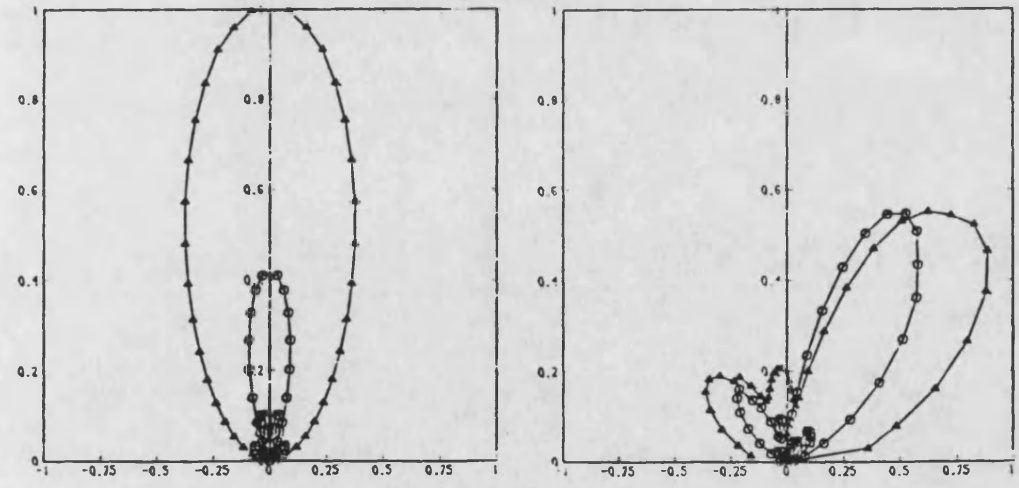

c) Strip length=30mm

Figure 6.18) Radiation Patterns for 2mm wide strip at 9GHz.

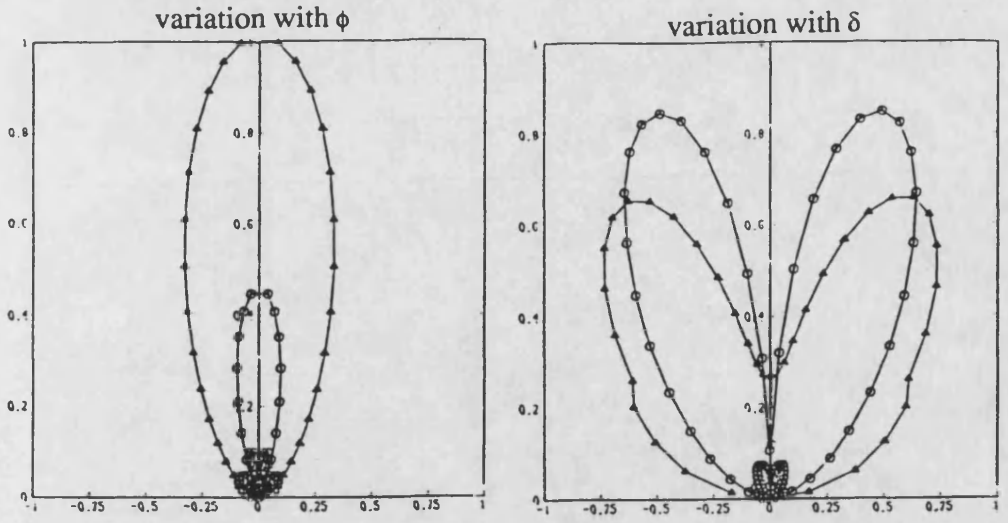

a) Strip length=10mm

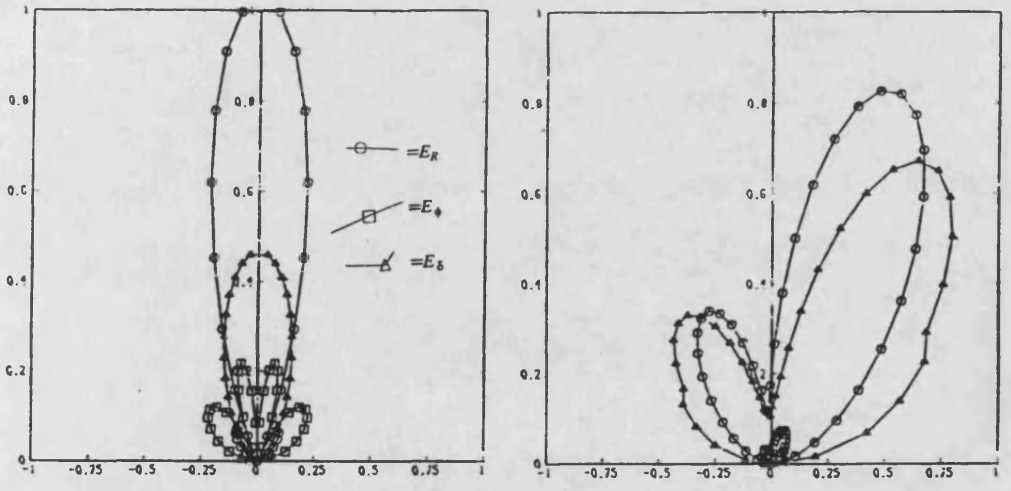

b) Strip length=20mm

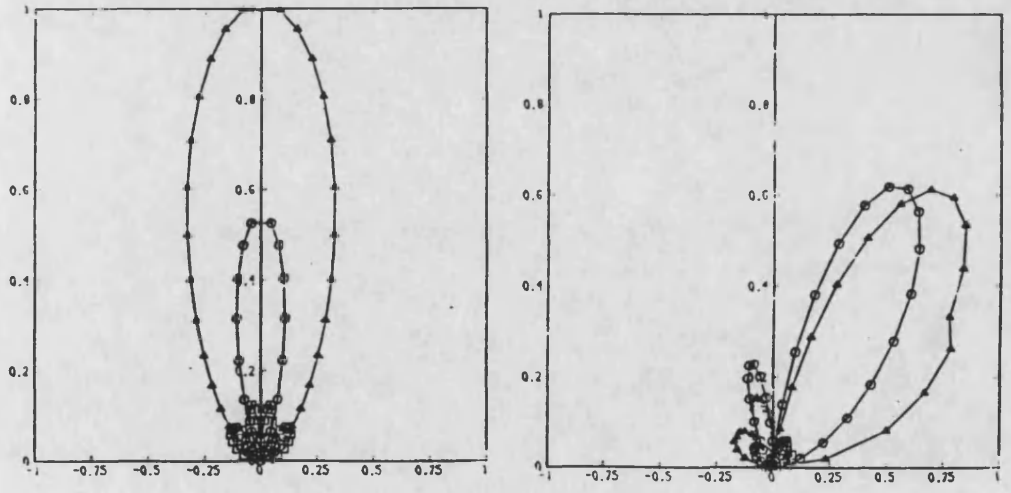

c) Strip length=30mm

Figure 6.19) Radiation Patterns for 2mm wide strip at 10GHz.

CHAPTER 7.

THE CONTINUOUS SPECTRUM OF THE MICROSTRIP LOADED I.D.G.

7.1) Introduction.

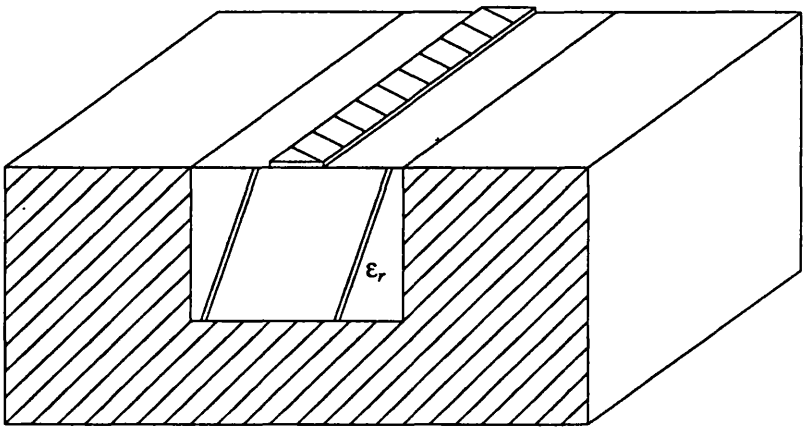

Figure 7.1) The Microstrip Loaded I.D.G.

The microstrip loaded I.D.G.,(M.I.G.),illustrated in figure 7.1,is of interest for two reasons.Firstly as a propagation medium in its own right,[1].The M.I.G. shares all the manufacturing advantages of the I.D.G. and,in addition,supports a quasi-T.E.M. mode resulting in a wide monomode bandwidth.It is possible that the M.I.G. may exhibit some of the disadvantages of microstrip at higher frequencies,such as unacceptable conduction loss,currently this aspect is under investigation.The similarity between M.I.G. and microstrip suggests that the integration of these two structures should be relatively straightforward.

The second,and probably more immediate reason for interest,is as a means of analysing leaky wave I.D.G. arrays formed from longitudinal metallic strips.These leaky wave antennas may be regarded as cascades of alternate sections of I.D.G. and M.I.G.,allowing them to be analysed using a mode matching approach.Associating transformer networks with each of the transitions from the I.D.G to M.I.G. and M.I.G. to I.D.G.,allows the array to be modelled as a sequence of multimodal transmission lines.This has already been undertaken,[1],although it was assumed that only the fundamental mode of each guide is significant in determining the the element length and the interelement spacing. As discussed in the previous chapter,this is not exactly the case,although in general the approach is promising and it is useful to have an independent means of corroborating the results of the previous chapter.

Finally,it also provides a further example of a nonseparable open structure whose spectrum cannot be fully characterised except by means of the method developed in chapter 2.

7.2) Formulation of the Transverse Characteristic Green's function for the Microstrip loaded I.D.G.

As the strip thickness has been assumed infinitesimal it is clear that the transverse characteristic Green's function and the eigenvalue equation characterising the modes of the M.I.G. will be identical those of the I.D.G.However the presence of the strip alters the domain of the basis functions used to expand the interface fields and,in contrast to the I.D.G.,it is not possible to use the functions $\phi_{hn}(x)$ as the basis.

It is known that the E_x field component will be singular at both the guide corners and the edges of the strip,the orders of singularity being $-\frac{1}{3}$ and $-\frac{1}{2}$

respectively.Intrinsic satisfaction of these edge conditions suggests the use of the weighted Jacobi polynomials as the basis and indeed,these these have successfully been used previously to recover the discrete modes of the M.I.G. [1].However the weighted Jacobi polynomials are even more numerically unwieldy than the weighted Gegenbauer polynomials proposed for the analysis of the I.D.G.,not even possessing an analytic Fourier transform.Again,at the expense of convergence,the use of a numerically expedient basis is attractive and this is the approach that has been adopted.

The basis that has been chosen are the functions;

$$f_p(x)=\frac{\delta_p}{\sqrt{a-w}}g(x)\sin\left(\frac{p\pi(|x|-\frac{w}{2})}{a-w}\right) \quad :\frac{w}{2}<|x|<\frac{a}{2} \quad :\delta_0=\frac{1}{\sqrt{2}} \quad :\delta_{p\neq 0}=2$$

$$=0 \quad :|x|>\frac{a}{2},\ |x|<\frac{w}{2} \tag{7.1}$$

where $g(x)$ is either 1 or $sgn(x)$ depending upon the polarity of the fields w.r.t. x. and m=0,2,4...

Again a significant saving in computational effort may be made by employing the following property of the continuous and discrete Fourier transforms of these functions,$Q_p(k_x)$ and Q_{pn}.

$$Q_p(k_x)=\frac{\delta_p}{\sqrt{a-w}}\left(\frac{2}{\pi}\right)^{\frac{1}{2}}\frac{k_x}{(\frac{m\pi}{a-w})^2-k_x^2}((-1)^{p/2}\cos(k_x\frac{a}{2})-\cos(k_x\frac{w}{2})) \tag{7.2}$$

$$Q_p(k_x)Q_q(k_x)=\frac{\delta_q}{\sqrt{a-w}}\left(\frac{2}{\pi}\right)^{\frac{1}{2}}\left[\frac{k_x}{(\frac{q\pi}{a-w})^2-(\frac{p\pi}{a-w})^2}((-1)^{q/2}\cos(k_x\frac{a}{2})-\cos(k_x\frac{w}{2}))Q_p(k_x)\right.$$

$$+\frac{k_x}{(\frac{p\pi}{a-w})^2-(\frac{q\pi}{a-w})^2}((-1)^{p/2}\cos(k_x\frac{a}{2})-\cos(k_x\frac{w}{2}))Q_q(k_x)\Bigg] \quad (7.3)$$

$$Q_{pn}=-\frac{\delta_p}{\sqrt{a-w}}\frac{2}{\sqrt{a}}\frac{\frac{n\pi}{a}\cos(\frac{n\pi w}{2a})}{(\frac{m\pi}{a-w})^2-(\frac{n\pi}{a})^2} \quad (7.4)$$

$$Q_{pn}Q_{q_n}=-\frac{1}{\sqrt{a-w}}\frac{2}{\sqrt{a}}\frac{n\pi}{a}\cos(\frac{n\pi w}{2a})\left[\frac{\delta_q Q_{pn}}{(\frac{q\pi}{a-w})^2-(\frac{p\pi}{a-w})^2}+\frac{\delta_p Q_{q_n}}{(\frac{p\pi}{a-w})^2-(\frac{q\pi}{a-w})^2}\right] \quad (7.5)$$

7.3) Discussion of the Modal Properties of the M.I.G. Continuum.

If the width of the strip is small compared to that of the guide,it is tempting to regard the microstrip loaded I.D.G. as a perturbed I.D.G.This argument suggests that the modes having an odd E_z component,which is therefore small at the center of the interface,differ only slightly from those of the I.D.G.Unfortunately,whilst the modes of the I.D.G. show some similar characteristics to those of the I.D.G.,they are in fact significantly different.These differences shall be discussed using the modes determined for a M.I.G. of width 22.86mm,depth 10.16mm and a strip width of 2mm operating at 10 GHz.The permittivity of the dielectric,P.T.F.E.,has been taken as 2.08.

In order to test the perturbation argument,modes of both odd and even polarity w.r.t. x shall be presented.All the results graphs are given in appendix A7 at the end of this chapter.

The main similarity between the M.I.G. and the I.D.G. modes is the existence of two classes of modes,characterised by finite and quasi-infinite eigenvalues respectively.In general the quasi-infinite eigenvalues of the M.I.G. tend to be much larger than those of the I.D.G.,which is unfortunate from a numerical point of view as it degrades the conditioning of the eigenvalue

problem.In fact it was not possible to determine the fields of many of the higher order modes due to numerical difficulties.The increase in the magnitude of the quasi-infinite eigenvalues is not surprising as they are related to the effective admittance presented by the interface to the mode,which is clearly increased by the presense of the strip.

Figure 7.2 shows the variation of the quasi-infinite eigenvalues against k_t for modes having an odd E_z component.It is again apparent,that a critical value of k_t exists above which the eigenvalue becomes finite.However it is also observed that,although a pair of modes still share a common critical value,they are no longer necessarily of opposite sign.Figure 7.3 illustrates that once finite the eigenvalues do not appear to follow any identifiable pattern and certainly do not resemble those of the I.D.G.

Figure 7.4 shows the interface fields for the first few modes.It is interesting to note that again,in many of the fields,there appears to be one dominant basis term combined with singularities at both the guide corners and the edge of the strip.It is not possible to discern any noticeable difference in the strengths of the two singularities which suggests that if,at a future date,intrinsic satisfaction of the edge conditions by the basis functions were contemplated,then distinguishing between these singularities does not justify the increased computational effort.

Figures 7.5 and 7.6 show respectively,the amplitudes of the basis terms and the Fourier transforms of the interface fields.It is difficult to identify any approximation to either set of spectra,although it is clear that the Fourier spectra are much wider than those of the I.D.G.

The eigenvalues of the modes having even E_z components,shown in figures 7.7 and 7.8,are even further from those of the I.D.G.Not only are the finite sized eigenvalues without any pattern,but also the existence of a critical value of k_t for

each is less apparent.The interface fields of these modes,given in figure 7.9,do not appear to differ in their general characteristics from those already discussed.For completeness the spectra of these modes are given in figures 7.10 and 7.11.

All the structures that have been analysed so far,both separable and nonseparable,have included only one interface.This does encompass a wide variety of practical waveguides,although it is clear that ideally it is desirable to extend the method to include structures containing an arbitrary number of interfaces.The next chapter shall undertake this extension and,in particular,derive the continuous spectrum of slotline with finite thickness metallisation.

7.4) References.

1) T.Rozzi,R de Leo and A.Morini,"Analysis of the 'Microstrip-Loaded Inset Dielectric Guide'",1989 MTT-S digest,pp923-926.

APPENDIX A7) GRAPHS OF THE M.I.G. MODES.

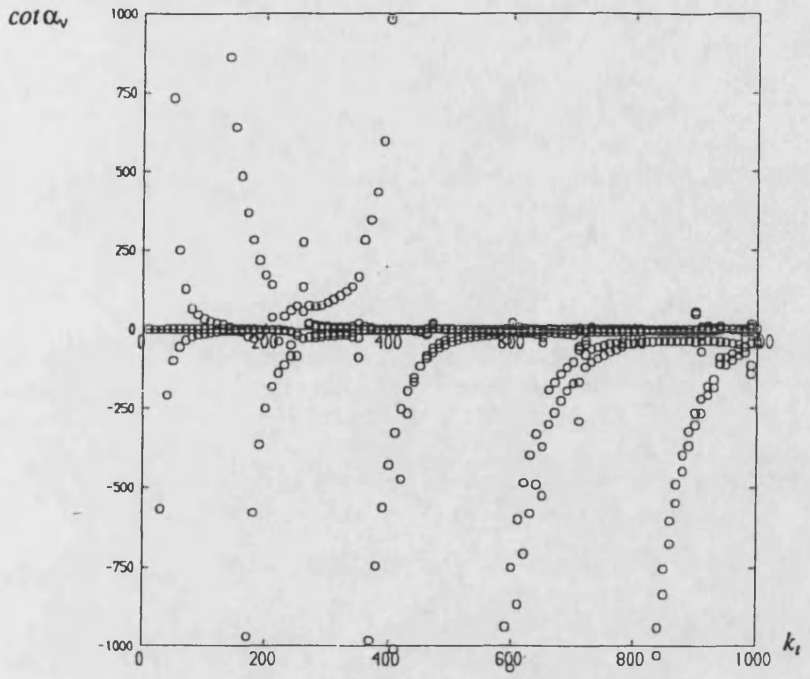

Figure 7.2) Variation of the quasi-infinite eigenvalues with k_t ;modes with odd E_z.

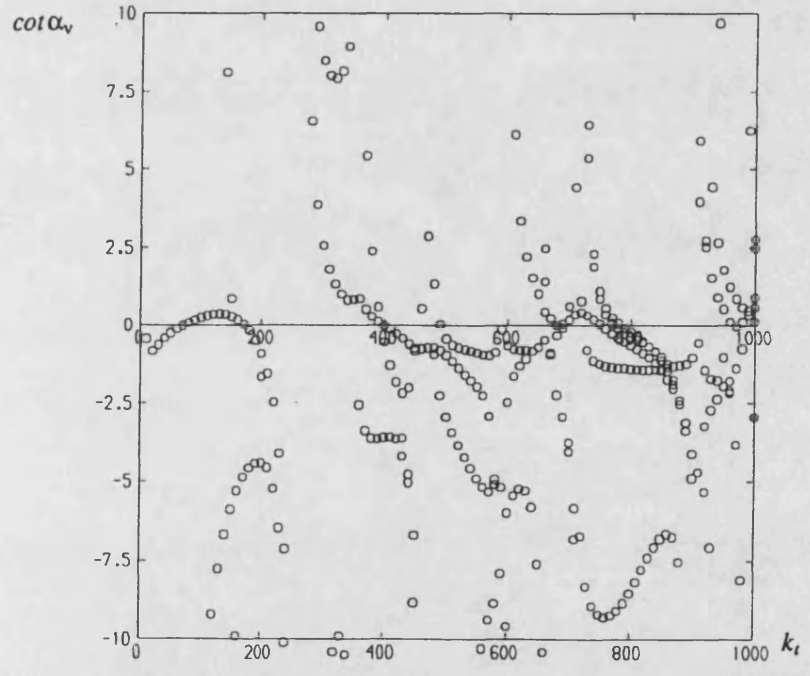

Figure 7.3) Variation of the finite eigenvalues with k_t;modes with odd E_z.

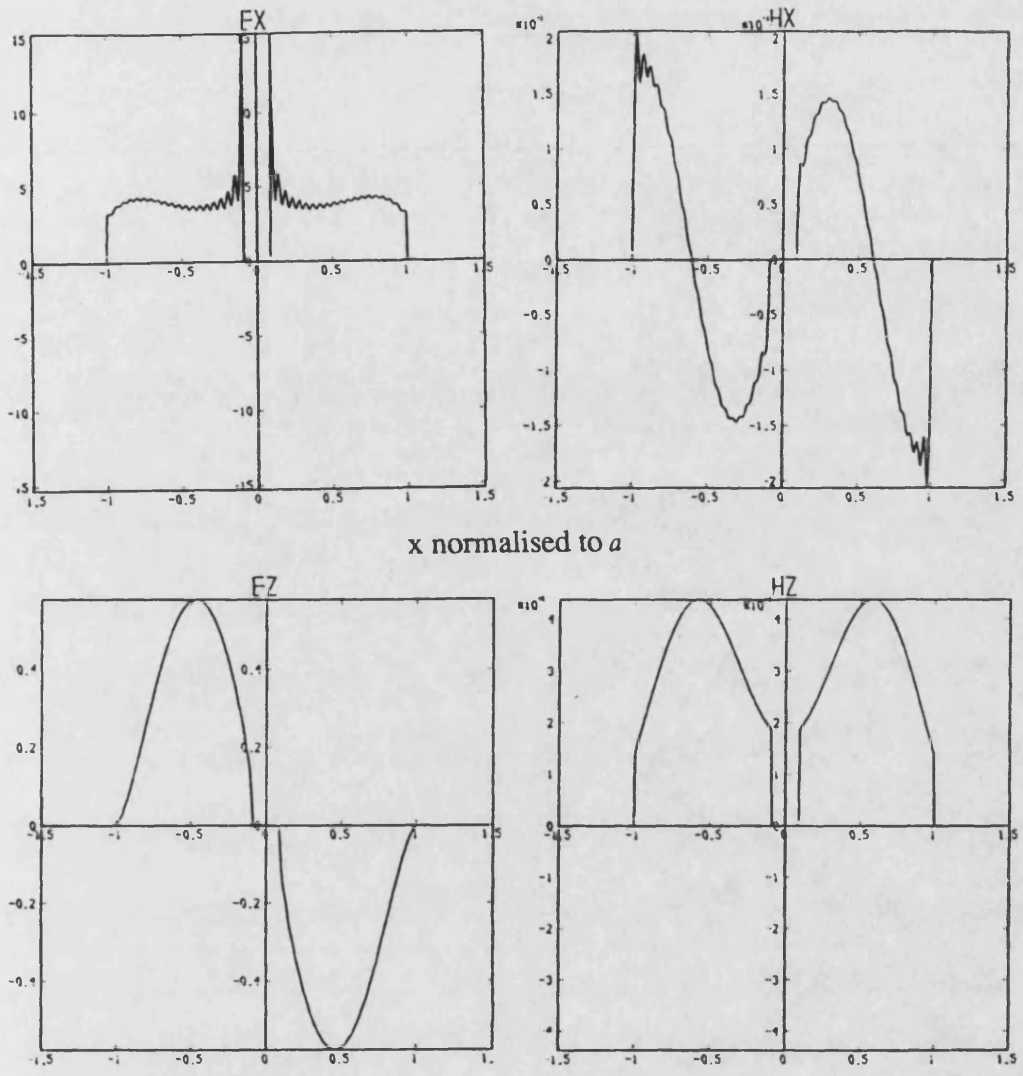

Figure 7.4a) Interface fields for the mode with $cot\alpha_v = -1.79$

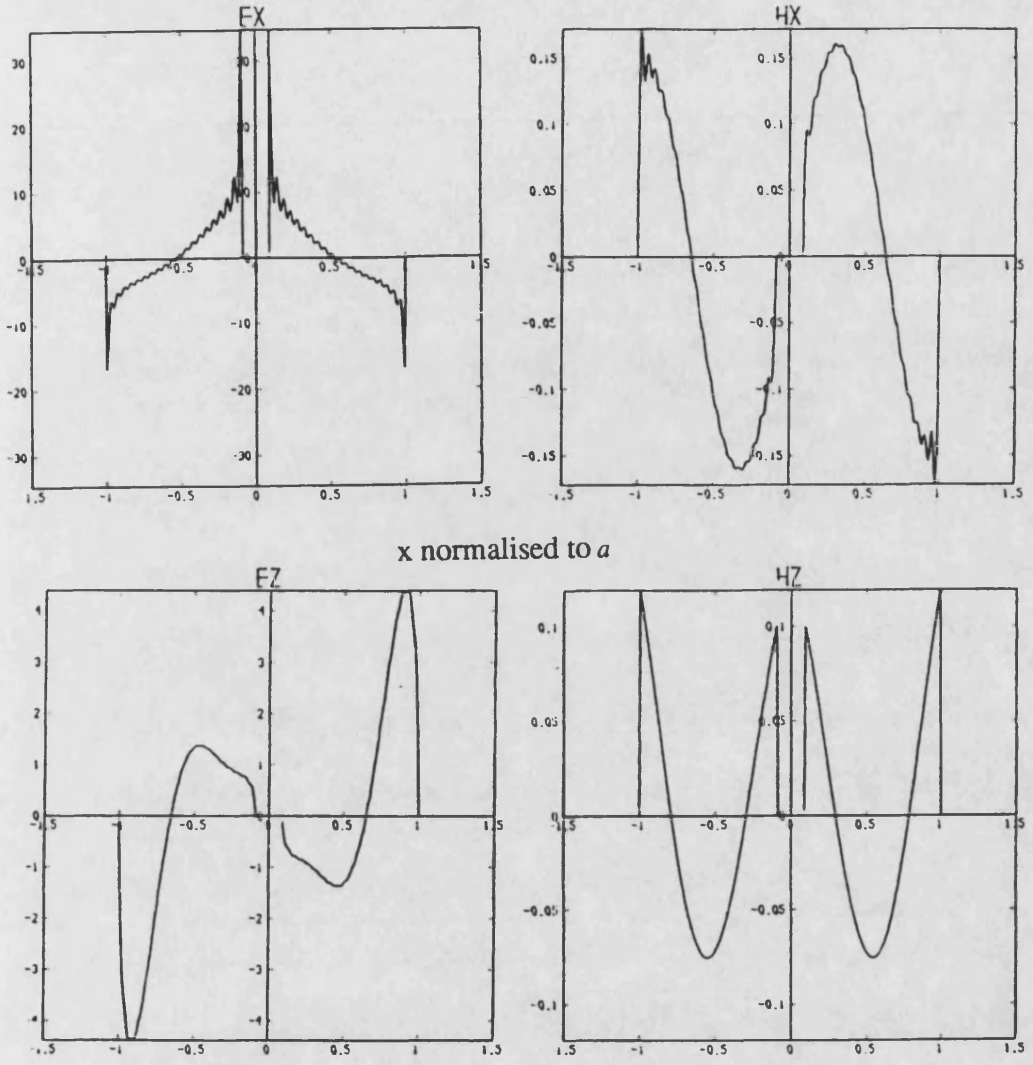

Figure 7.4b) Interface fields for the mode with $cot\alpha_v = -0.559$

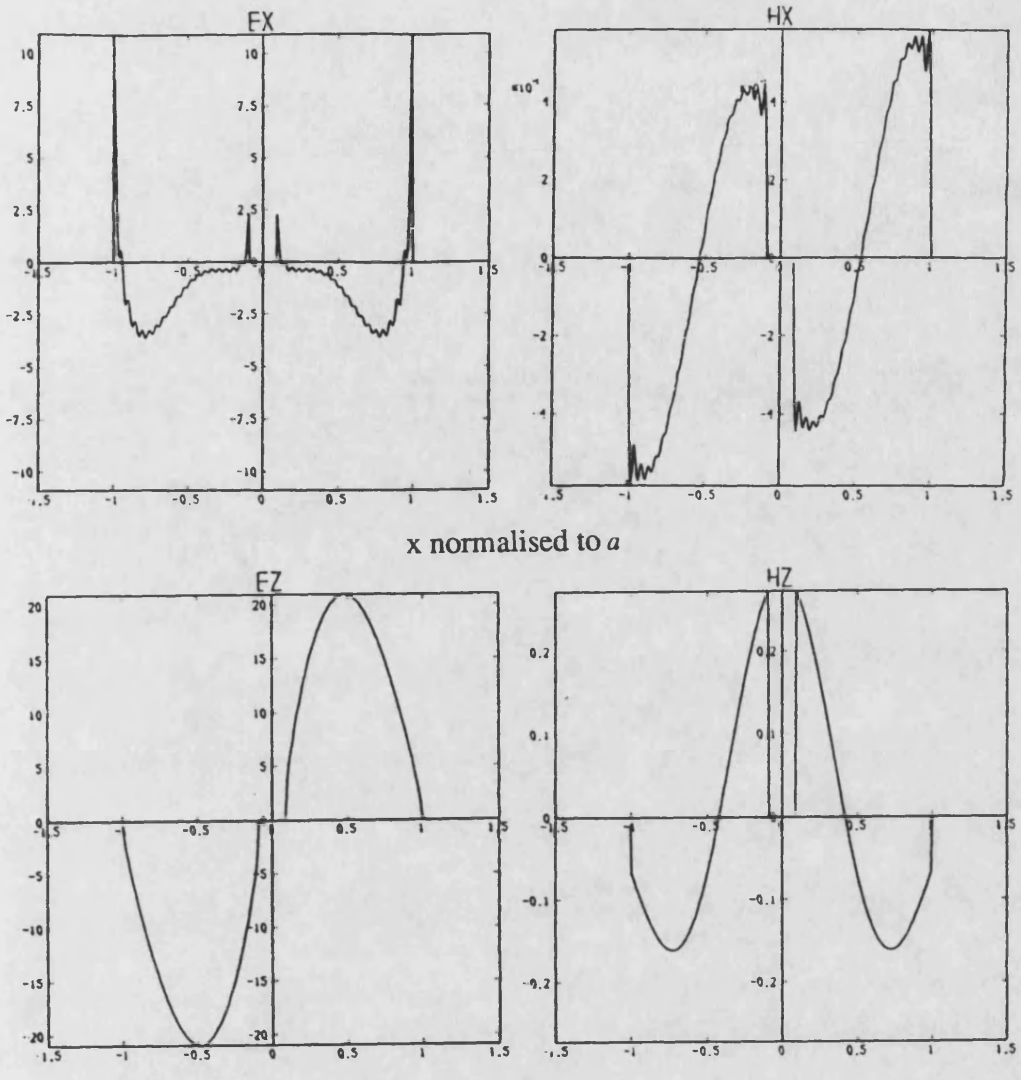

Figure 7.4c) Interface fields for the mode with $cot\alpha_v = -0.559$

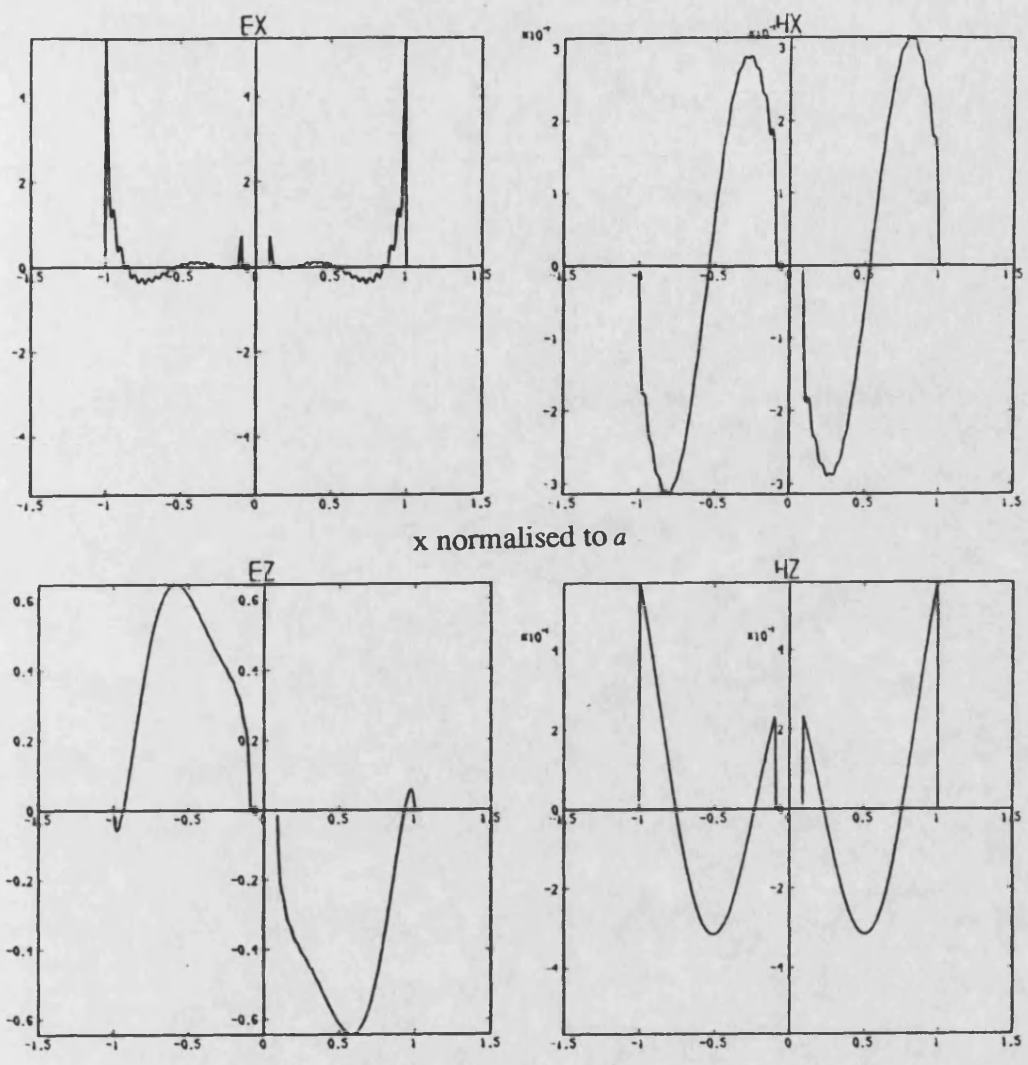

Figure 7.4d) Interface fields for the mode with $cot\alpha_v = -20.54$

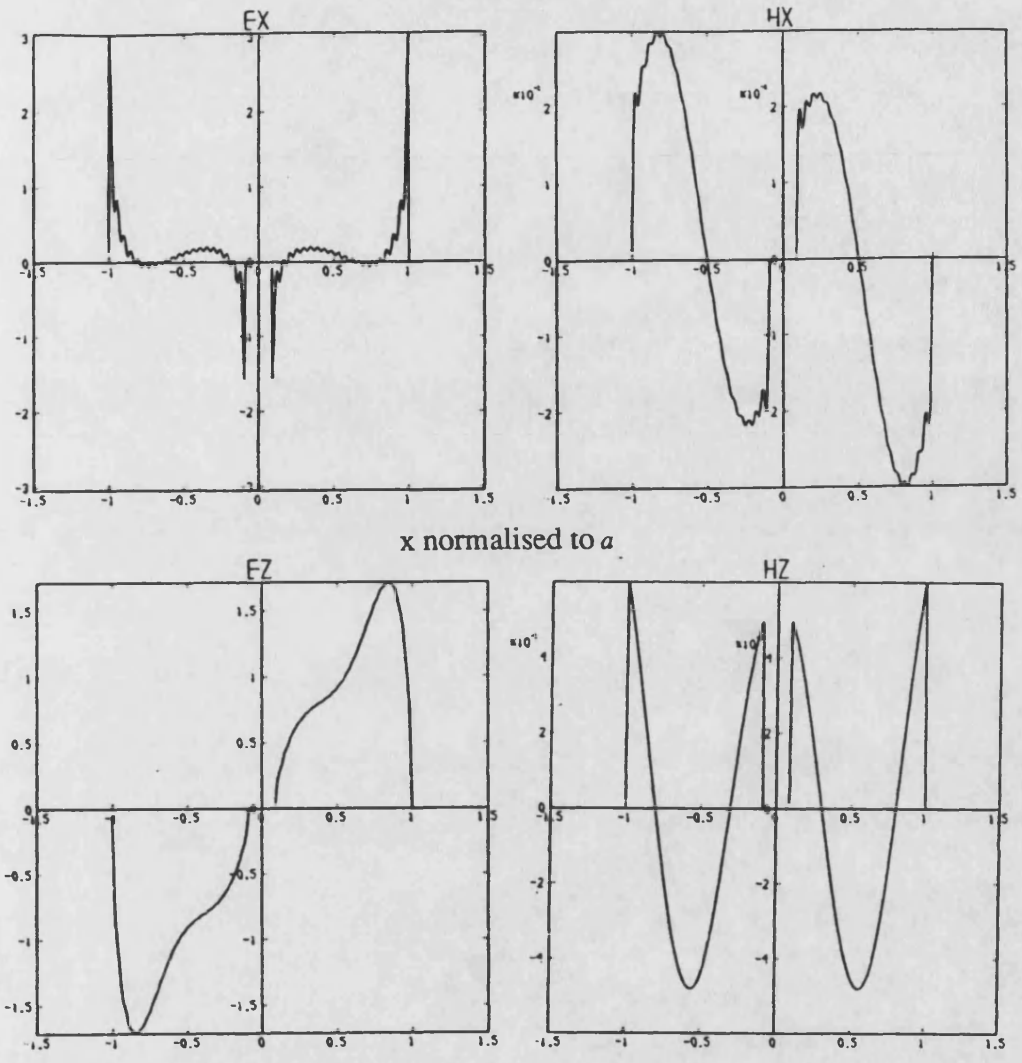

Figure 7.4e) Interface fields for the mode with $cot\alpha_v = -20.54$

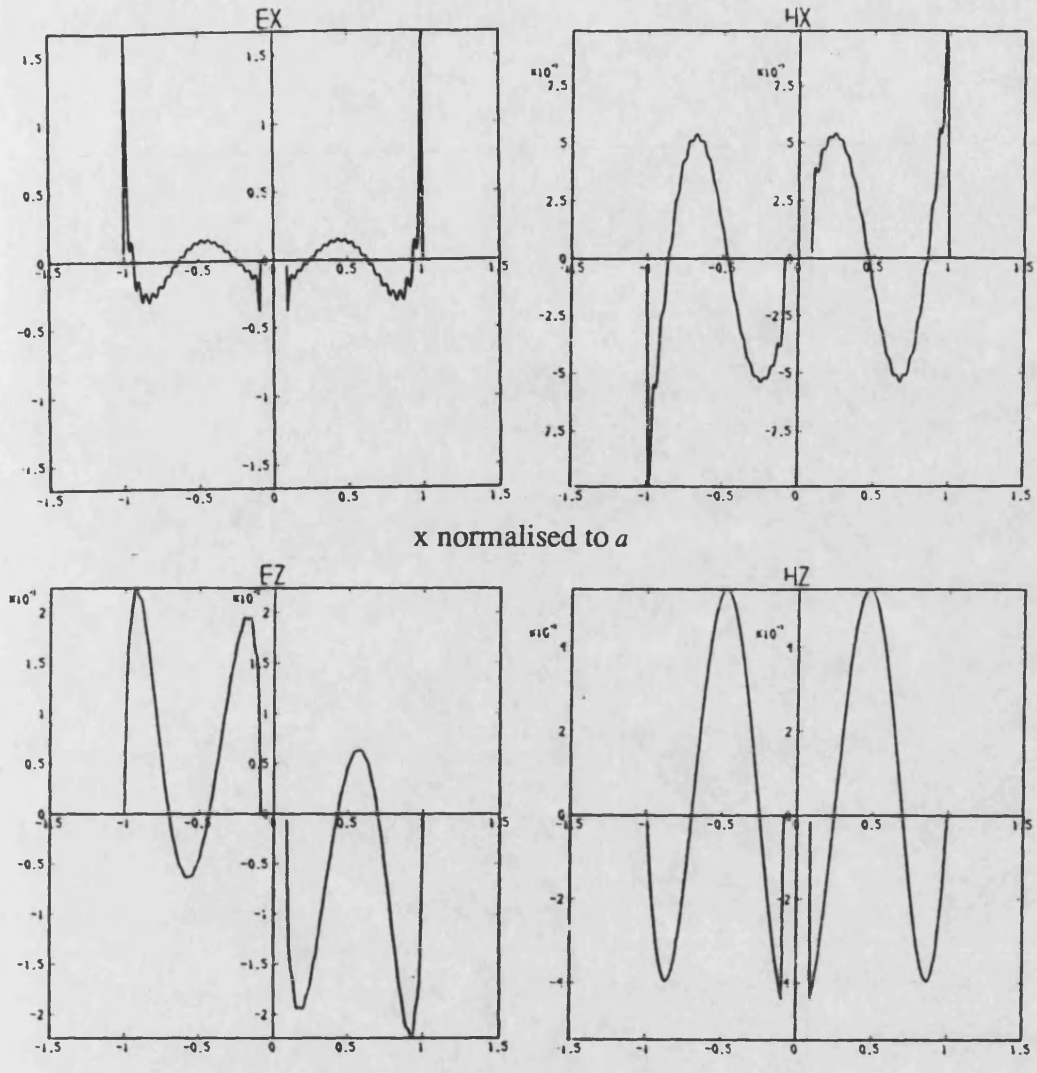

Figure 7.4f) Interface fields for the mode with $cot\alpha_v = -668$.

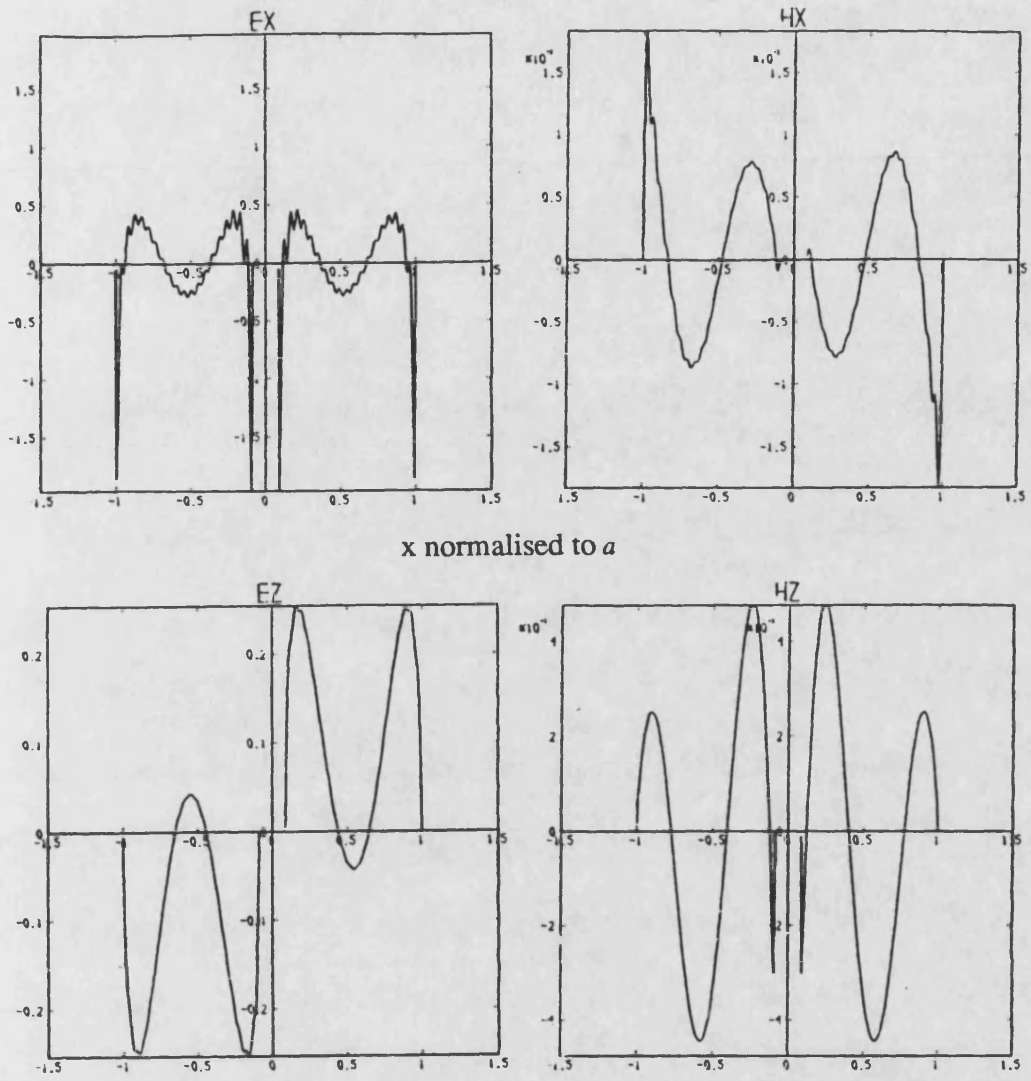

Figure 7.4g) Interface fields for the mode with $cot\alpha_v = -658$.

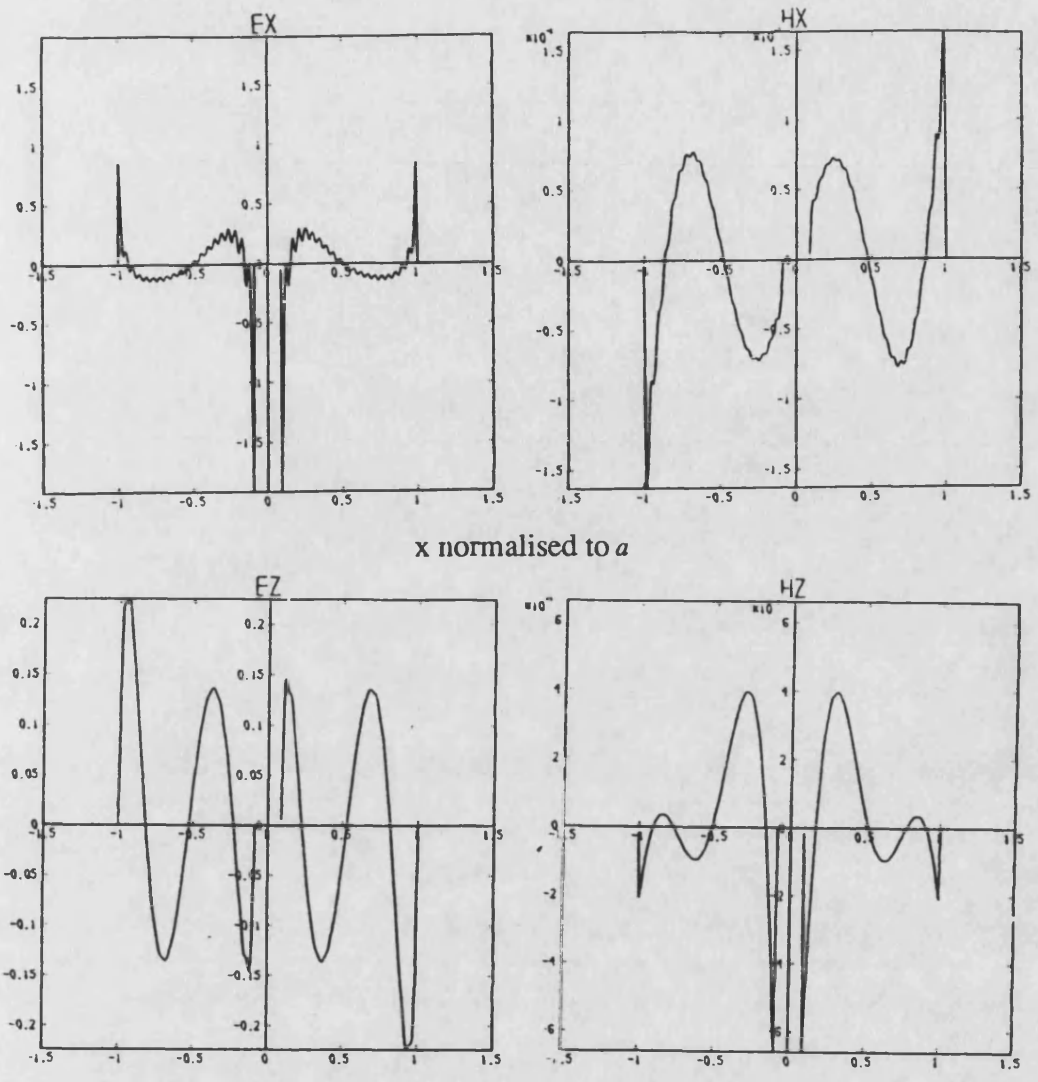

Figure 7.4h) Interface fields for the mode with $cot\alpha_v = -658$.

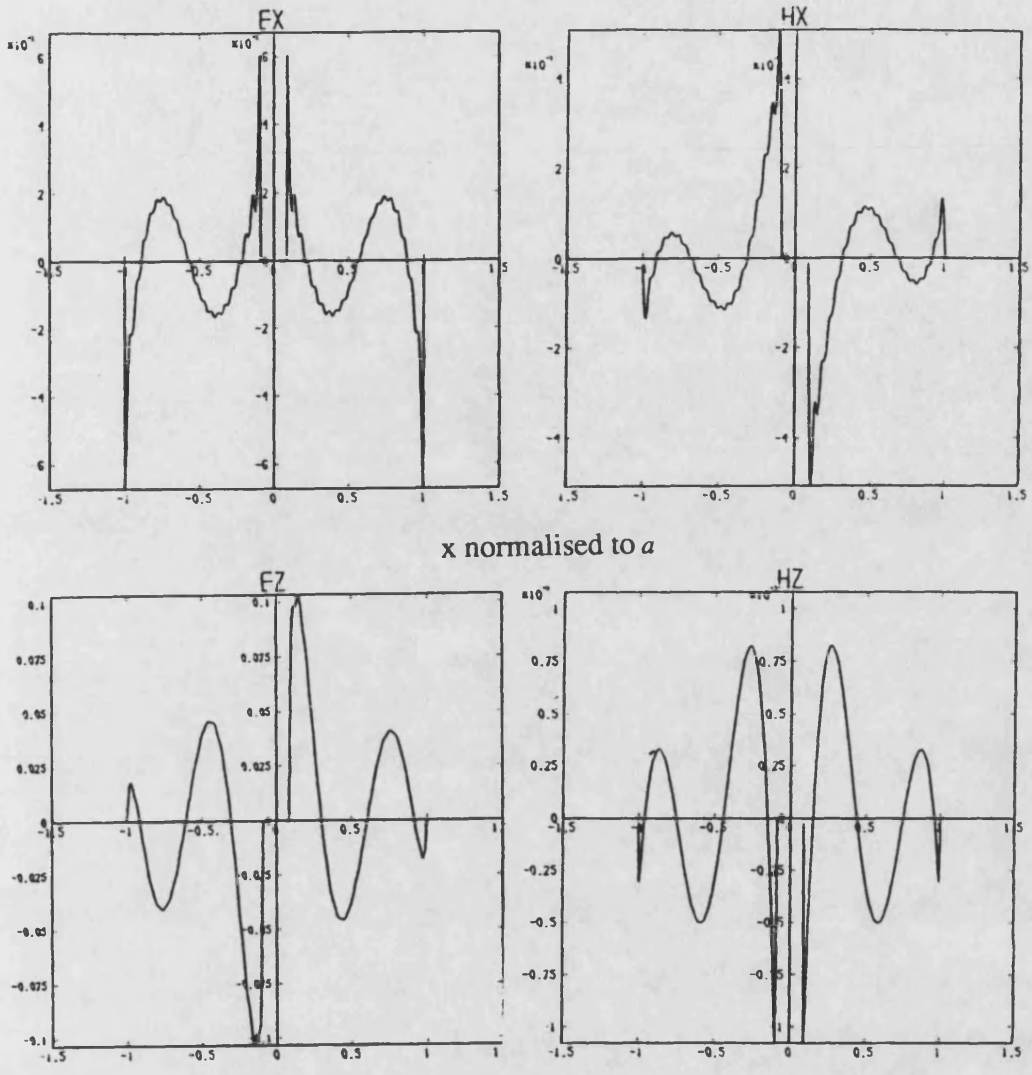

Figure 7.4i) Interface fields for the mode with $cot\alpha_v = -5255$.

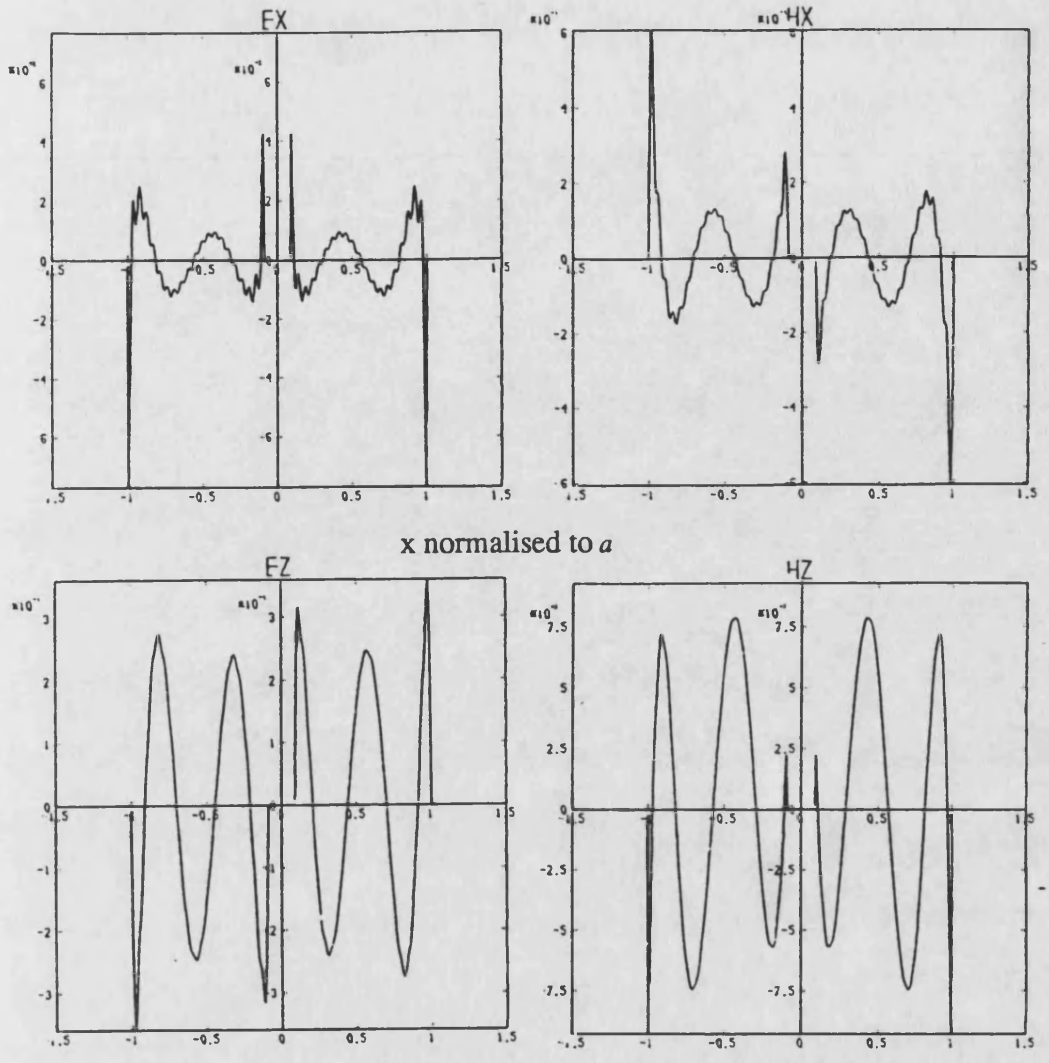

Figure 7.4j) Interface fields for the mode with $cot\alpha_v = -5.04 \times 10^5$

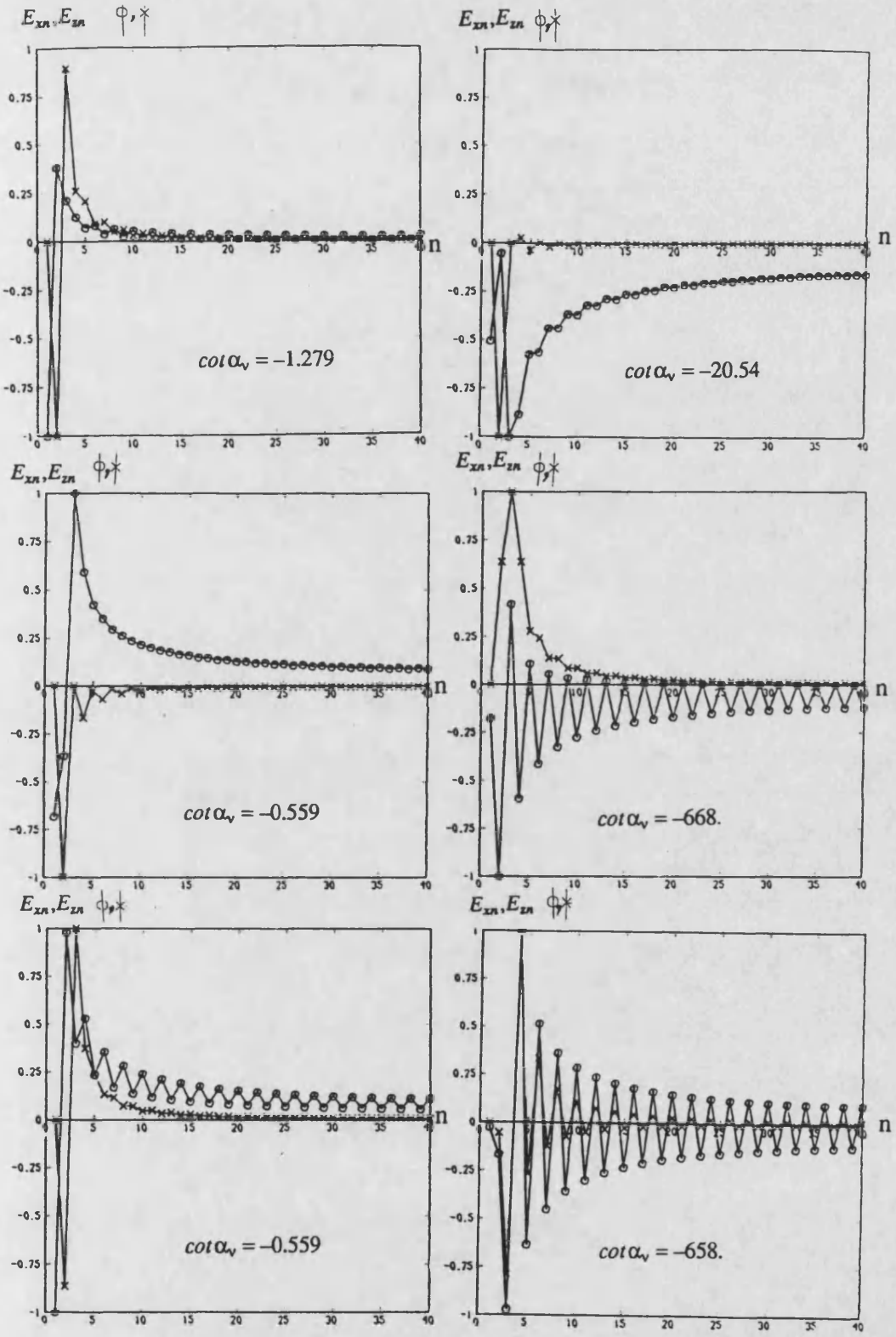

Figure 7.5) Basis amplitudes, E_{xn} and E_{zn}, of the odd E_z modes.

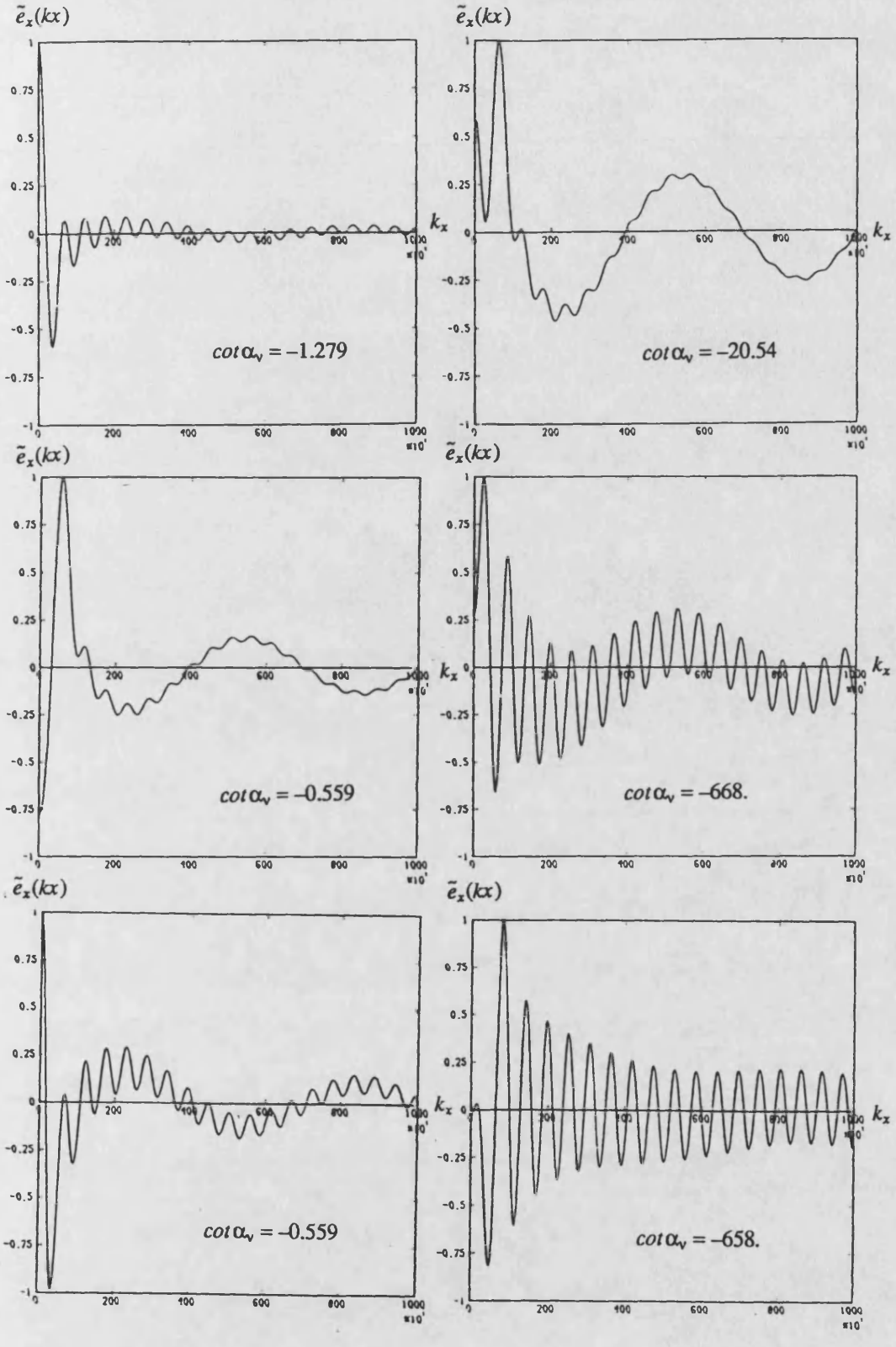

Figure 7.6) Fourier spectra of the odd E_z modes.

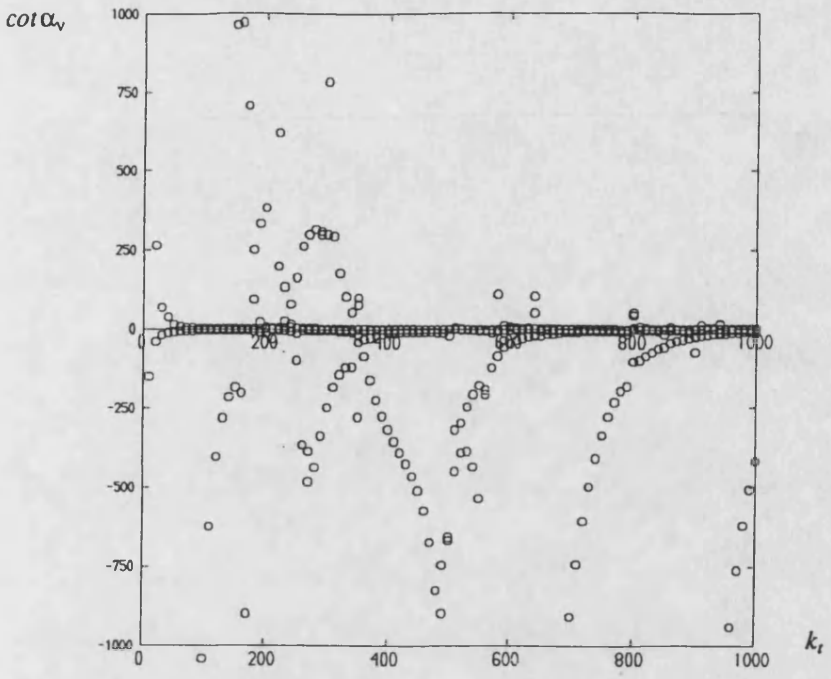

Figure 7.7) Variation of the quasi-infinite eigenvalues with k_t;modes with even E_z.

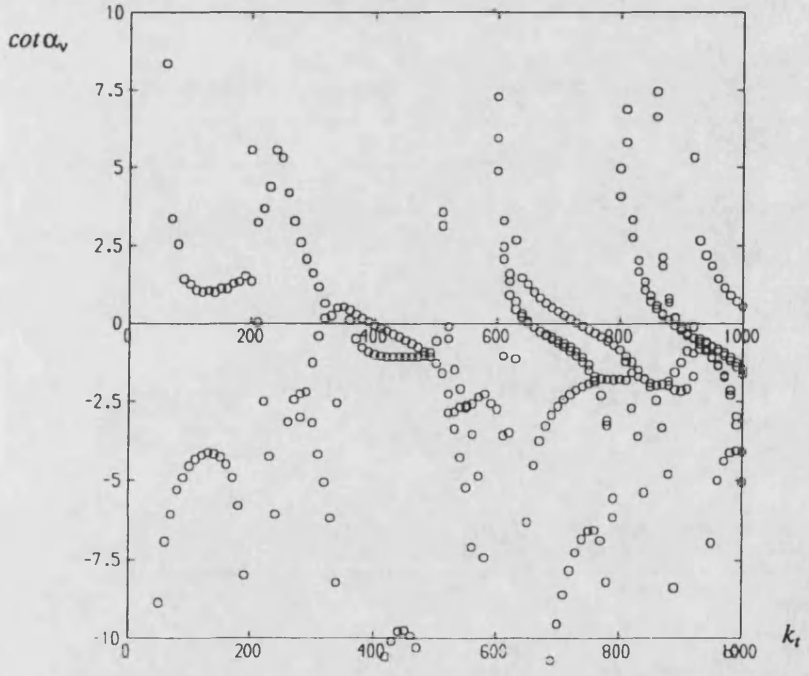

Figure 7.8) Variation of the finite eigenvalues with k_t;modes with even E_z.

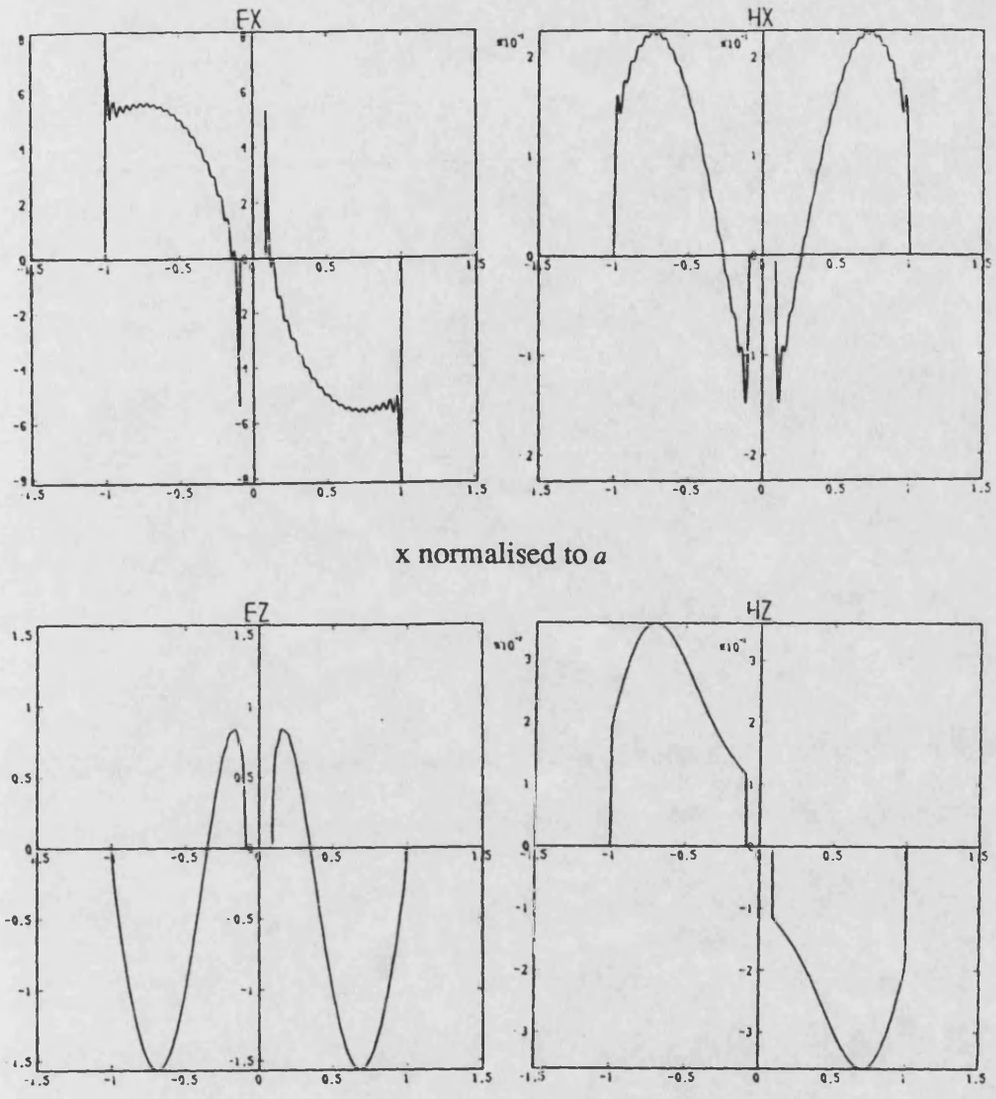

Figure 7.9a) Interface fields for the mode with $cot\alpha_v = -0.973$

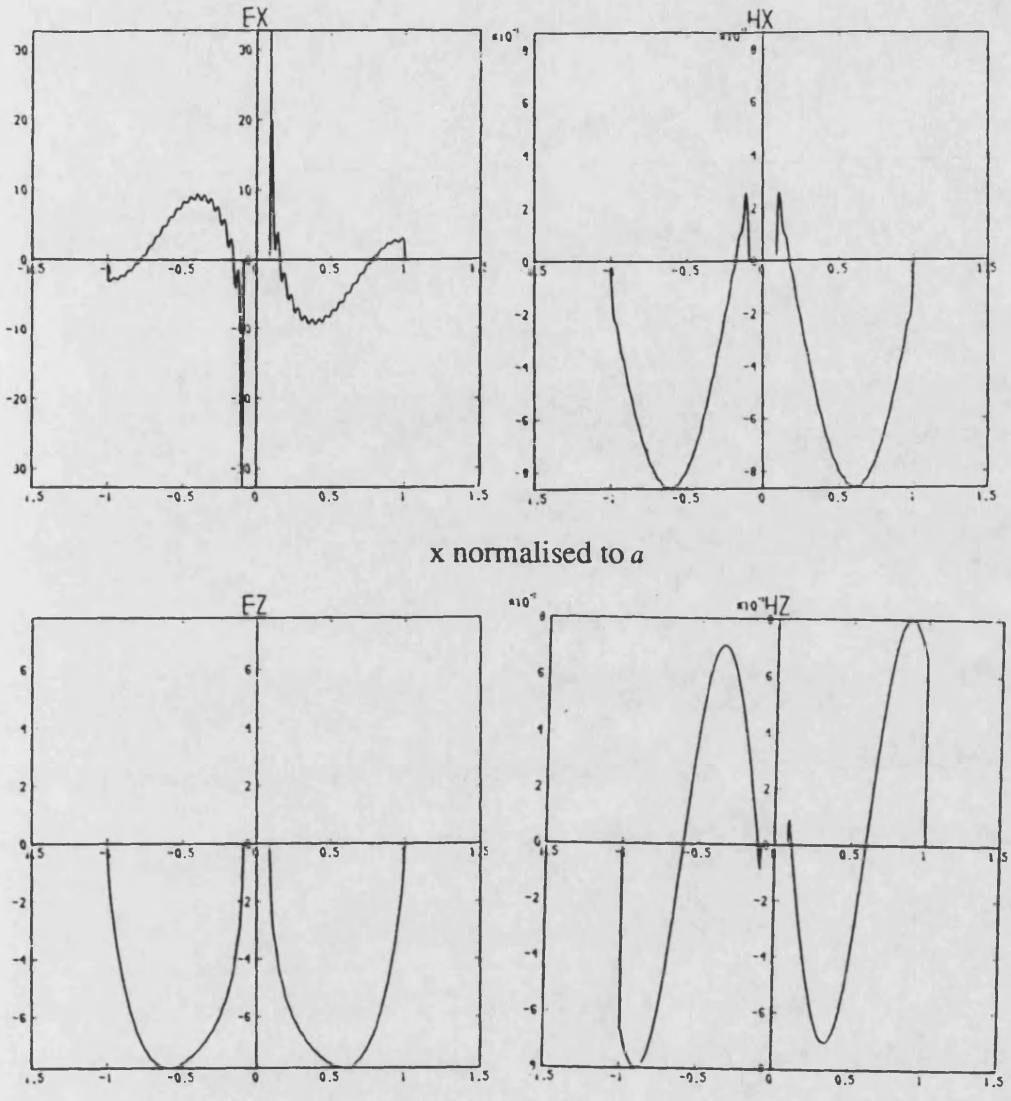

Figure 7.9b) Interface fields for the mode with $cot\alpha_v = -0.445$

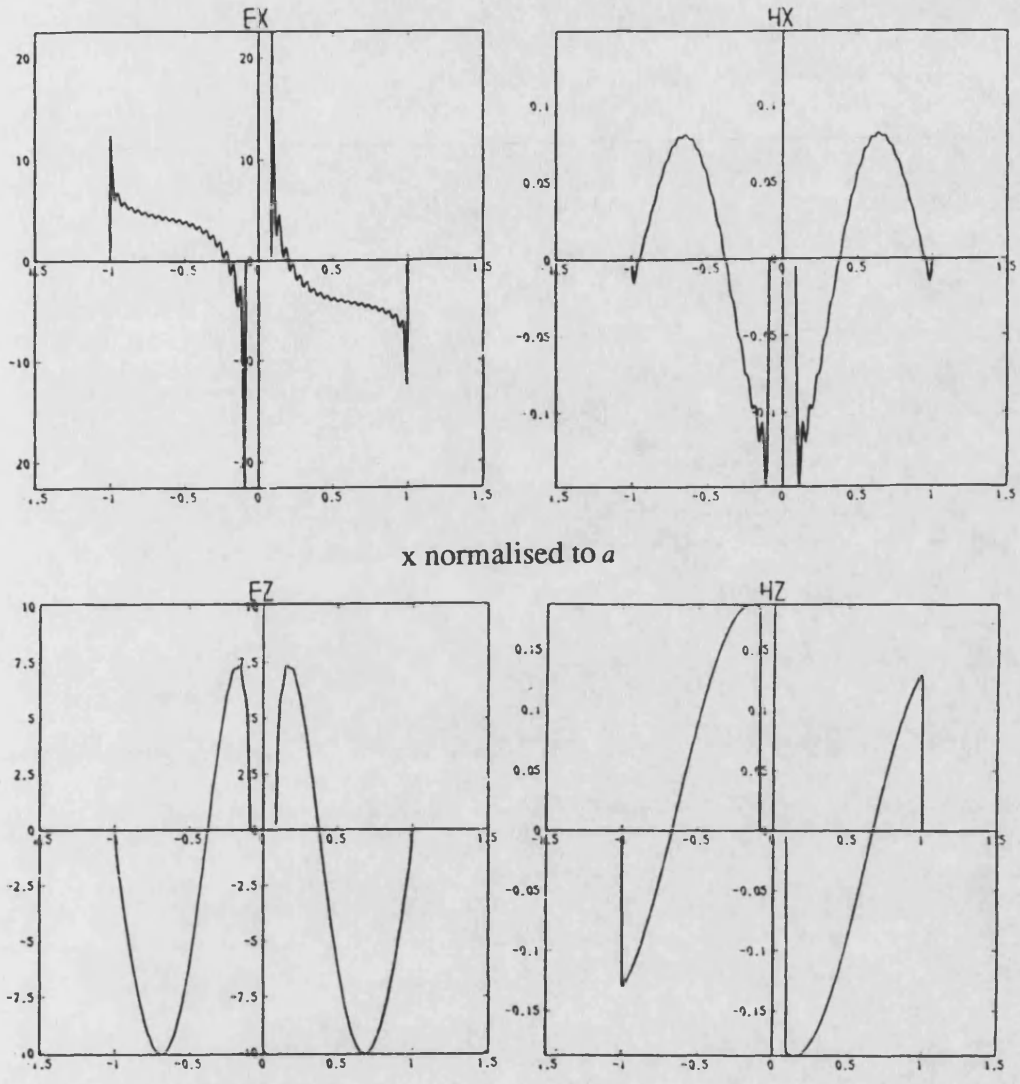

Figure 7.9c) Interface fields for the mode with $cot\alpha_v = -0.445$

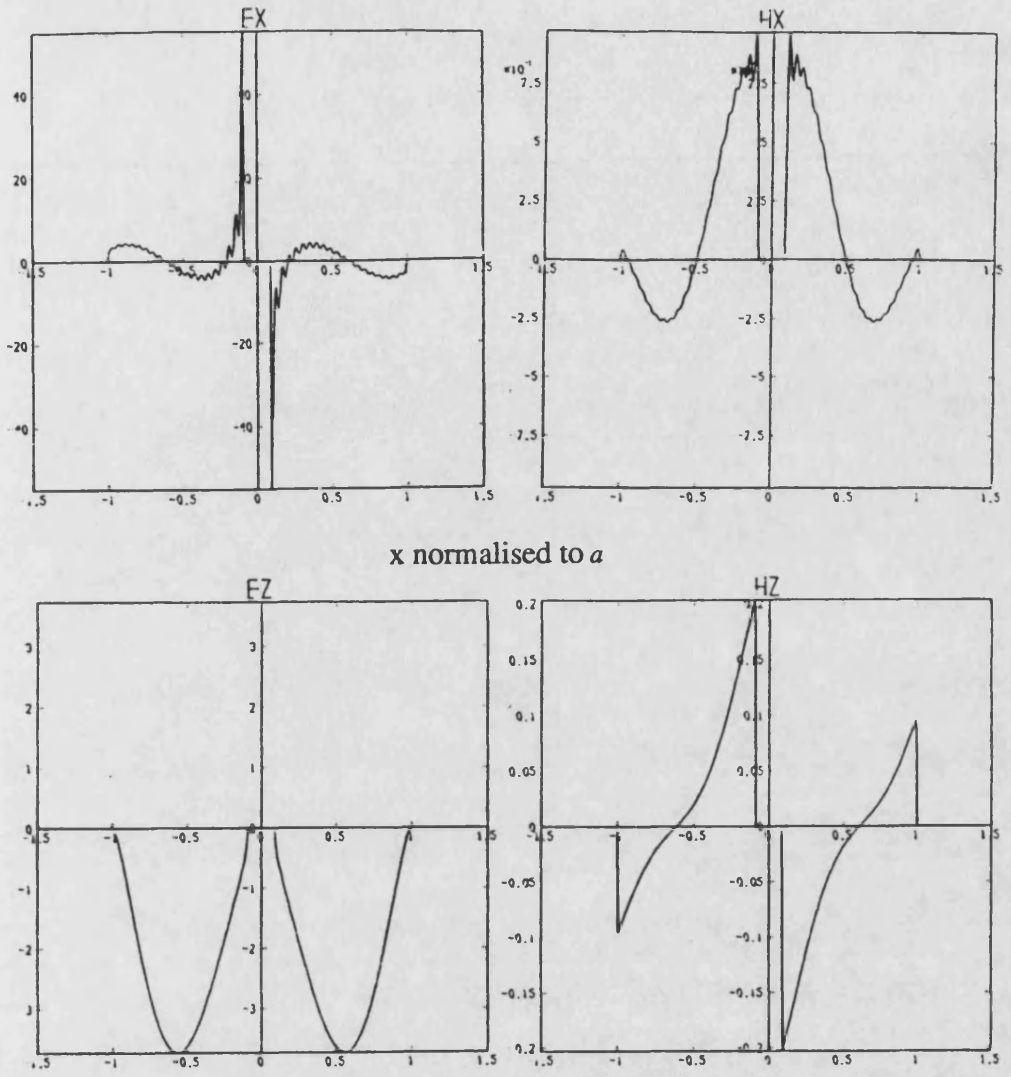

Figure 7.9d) Interface fields for the mode with $cot\alpha_v = -2.93$

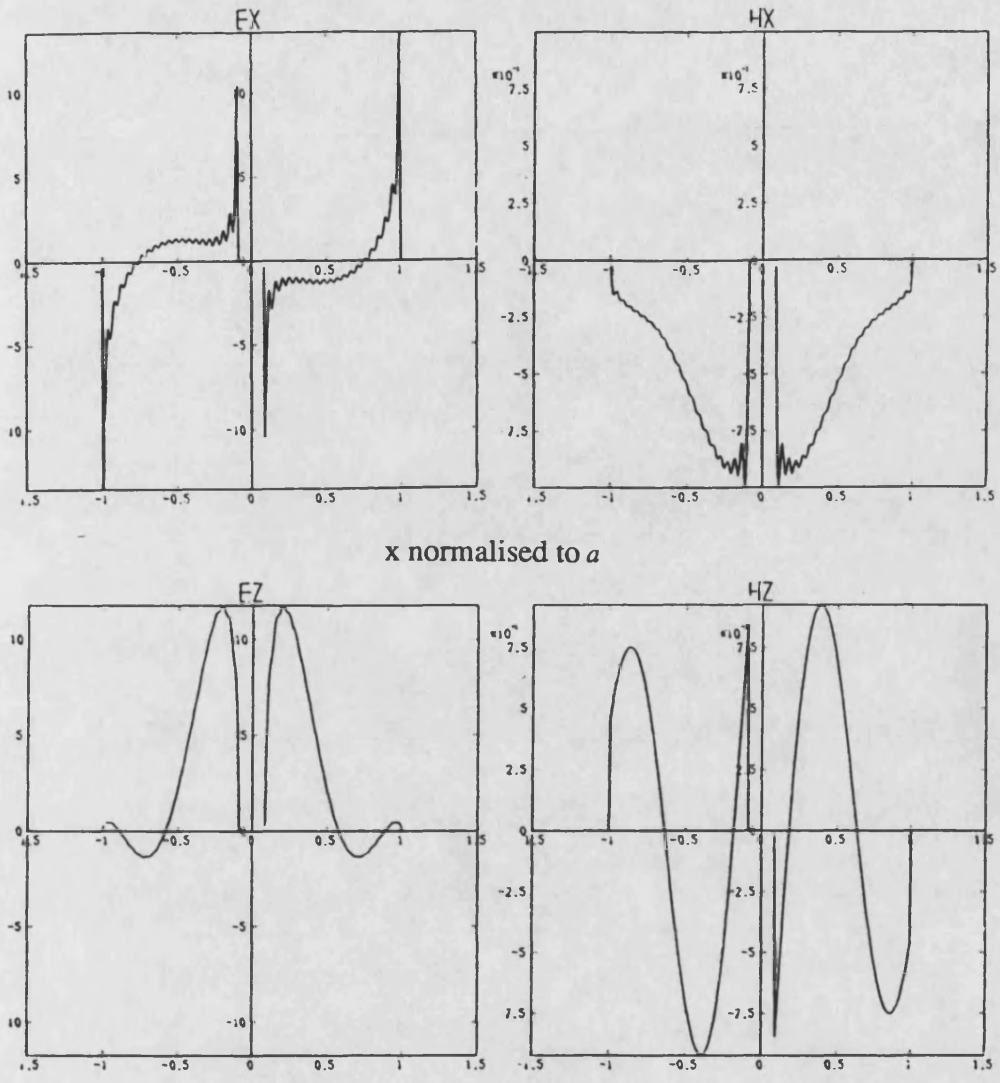

Figure 7.9e) Interface fields for the mode with $cot\alpha_v = -2.93$

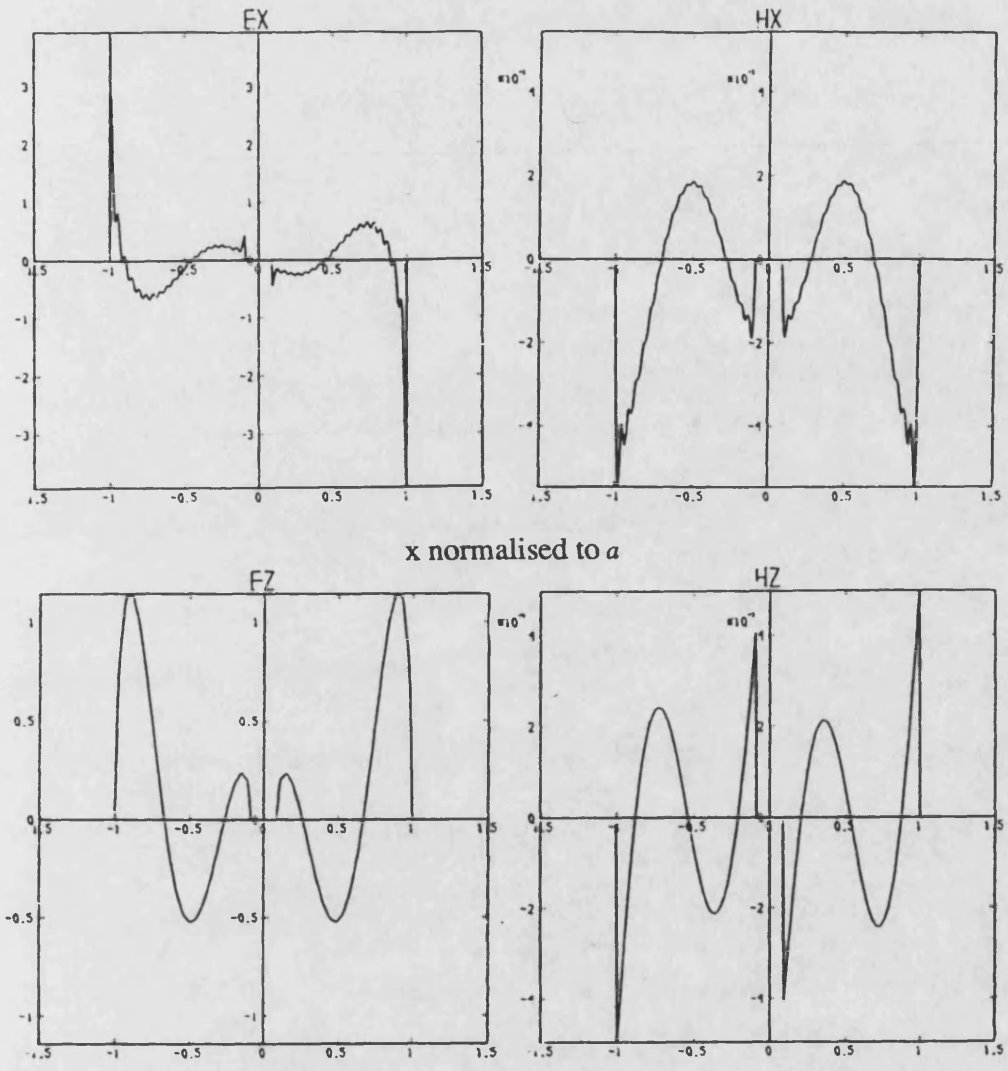

Figure 7.9f) Interface fields for the mode with $cot\alpha_v = -28.5$

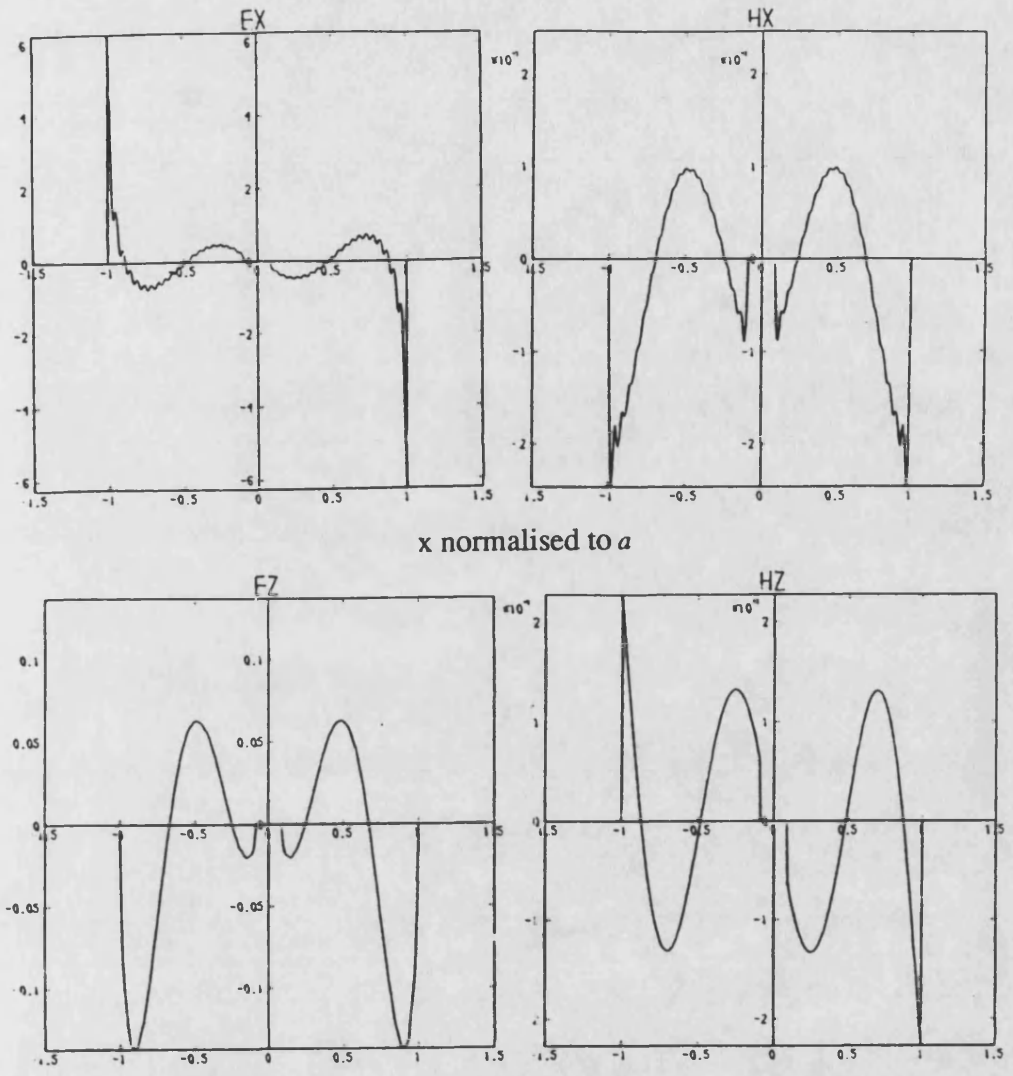

Figure 7.9g) Interface fields for the mode with $cot\alpha_v = -41.1$

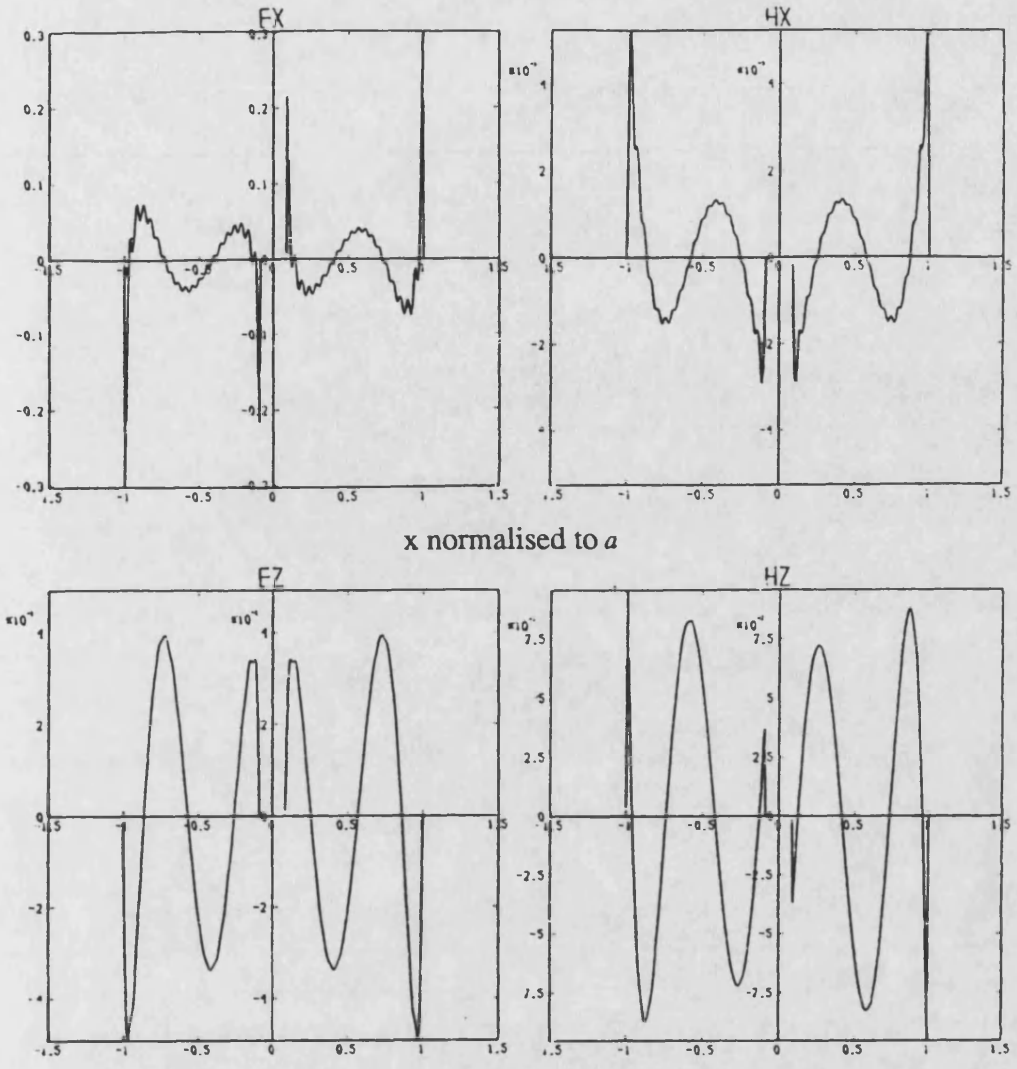

Figure 7.9h) Interface fields for the mode with $cot\alpha_v = -8101$.

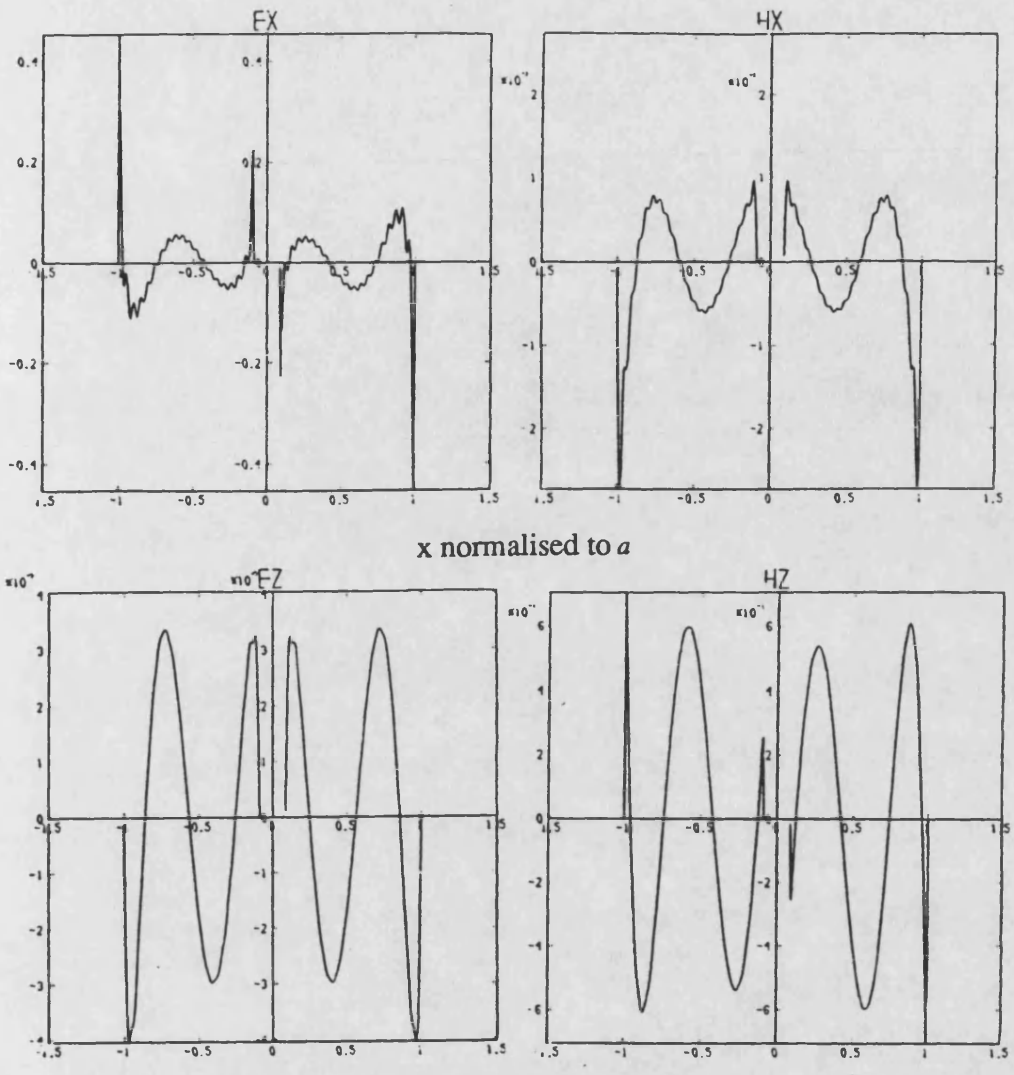

Figure 7.9i) Interface fields for the mode with $cot\alpha_v = -1.30 \times 10^4$

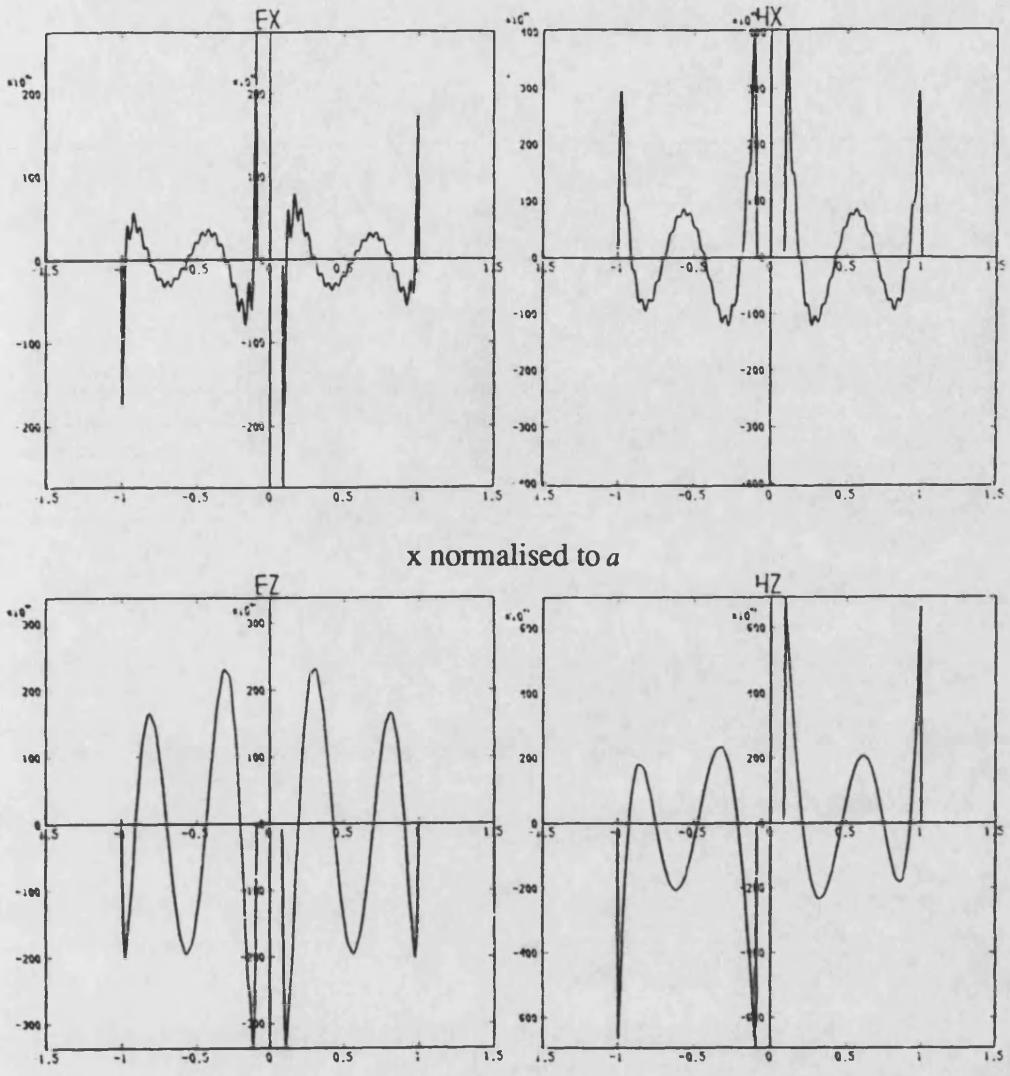

Figure 7.9j) Interface fields for the mode with $cot\alpha_v = 3.55 \times 10^4$

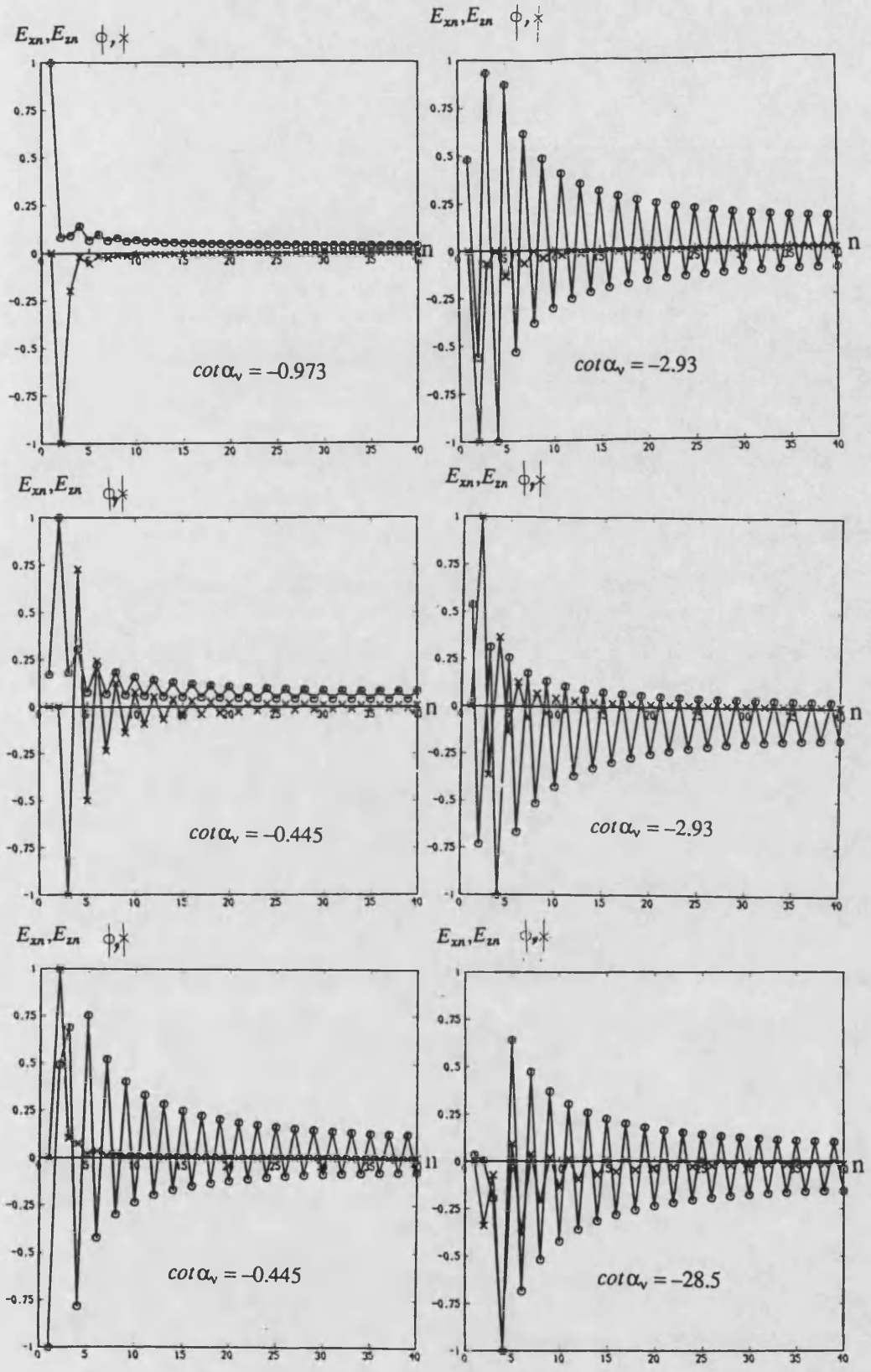

Figure 7.10) Basis amplitudes, E_{xn} and E_{zn}, of the even E_z modes.

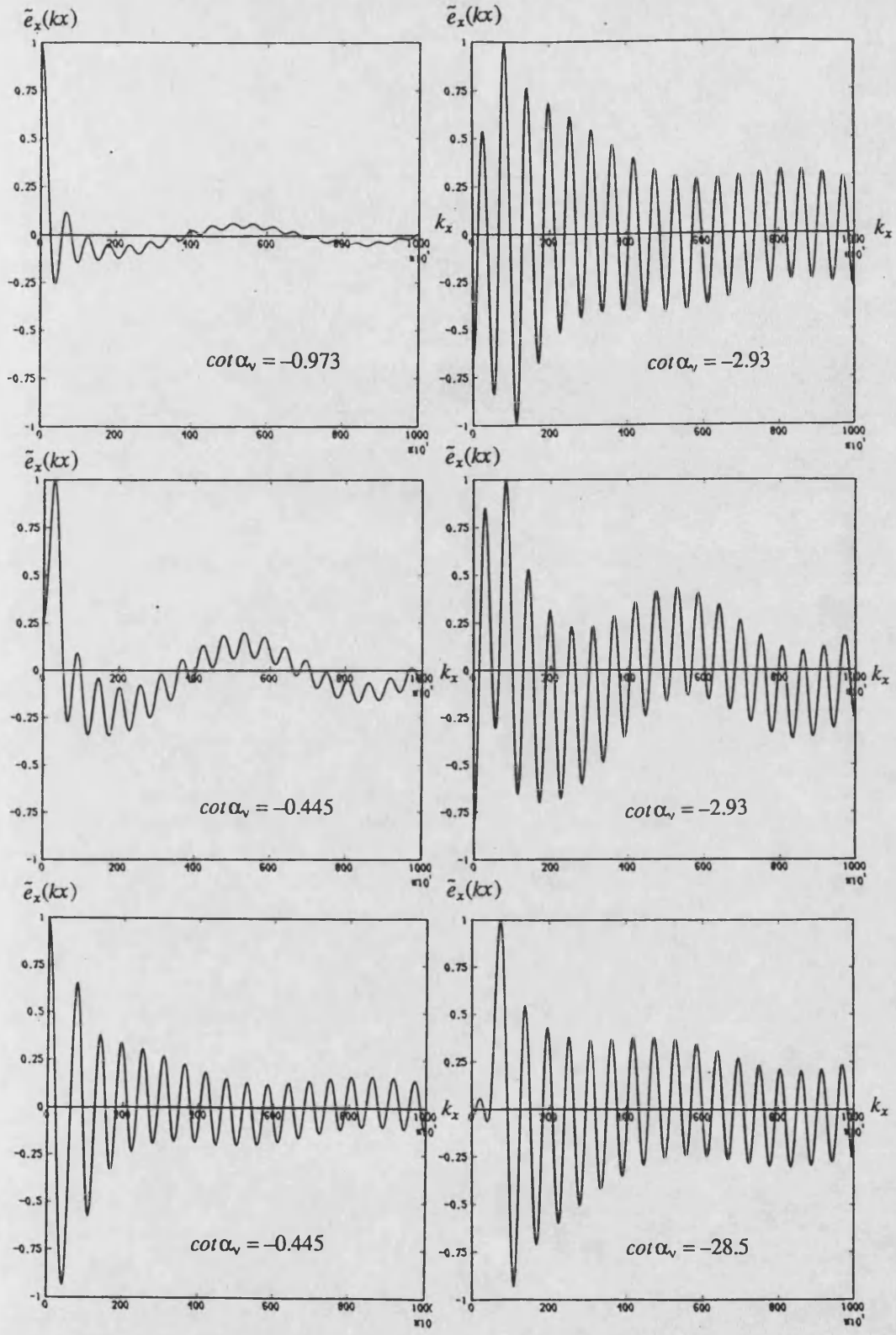

Figure 7.11) Fourier spectra of the even E_z modes.

CHAPTER 8.

THE CONTINUOUS SPECTRUM OF SLOTLINE WITH FINITE THICKNESS METALLISATION.

8.1) Introduction.

All the structures that have been considered so far,have been characterised by a single nonseparable interface.The objective of this chapter is to extend the transverse characteristic Green's function,presented in chapter 2,so that the complete mode spectra of structures containing multiple nonseparable interfaces may be recovered.

An example of such a structure is slotline with finite thickness metallisation.Slotline has proved popular due to its simple fabrication and the ease with which sources and active devices may be incorporated.However,in common with microstrip,the grounded dielectric slab of slotline can support surface modes which,when excited at discontinuities,give rise to losses and cross-talk.Accurately describing this effect and the modelling of circuit components requires the complete mode spectrum of slotline.

Previously,assuming infinitesimal metallisation thickness,transverse resonance has been used to recover the hybrid surface modes of slotline operating in the millimeter band,[1].As the frequency of operation is increased,not only do the continuous modes play a greater role,but also the assumption infinitesimal metallisation thickness becomes less appropriate.It is a simple matter to extend transverse resonance to the case of finite thickness metallisation and it shall now be shown how the continuous modes may also be found for this case.

8.2) The Transverse Characteristic Green's function for Structures with Multiple nonseparable interfaces.

This section shall demonstrate how the transverse characteristic Green's function may be formulated for structures with multiple nonseparable interfaces.Initially the theory shall be developed for a structure containing two nonseparable interfaces and then generalised to the case of N nonseparable interfaces.

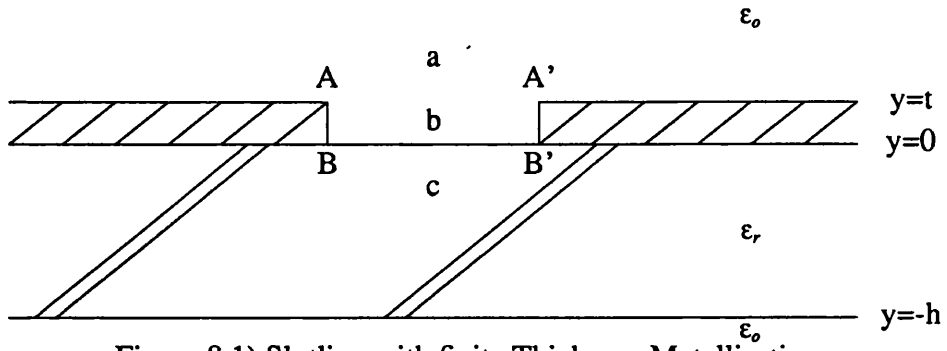

Figure 8.1) Slotline with finite Thickness Metallisation.

Consider as an example the finite thickness slotline illustrated in figure 8.1.The structure may be divided into three regions,a,b and c,separated by the two nonseparable interfaces AA' and BB'.It is immediately apparent,that the presence of the dielectric prevents the introduction of electric and magnetic walls midway between the two interfaces that would otherwise allow the problem to be tackled using symmetry.

One possible method to treat such structures is to consider each interface successively.For example the finite thickness slotline modes could be constructed from plane waves in the open region and those of the intermediate structure shown in figure 8.2,the latter having already been determined using the method given in

chapter 2.Although theoretically possible,such an approach is of negligible use as it would rapidly become computationally untenable.The alternative is to formulate the transverse characteristic Green's function in one fell swoop,using the method that shall now be presented.

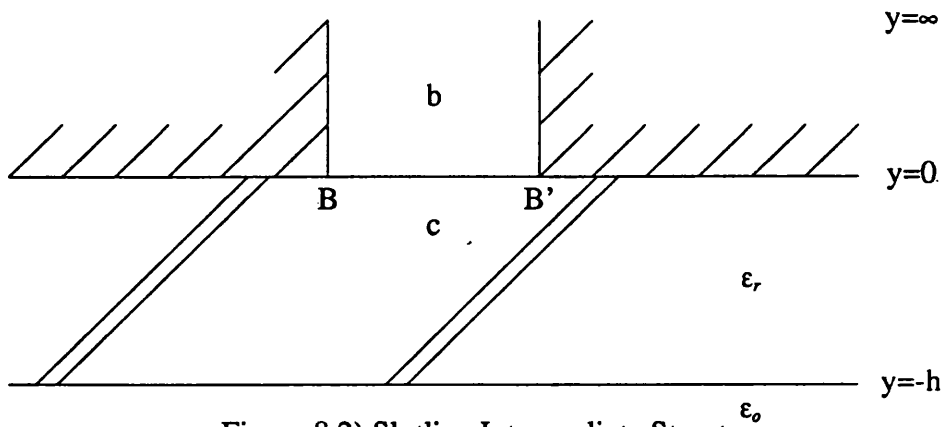

Figure 8.2) Slotline Intermediate Structure.

The formulation proceeds through the introduction of the two component magnetic vector potential and its associated transverse characteristic Green's function as discussed in chapter 2.The only difference in the method is the identification of the magnetic vector potential transverse characteristic Green's function,defined by;

$$(\nabla_t^2 + \lambda_{r_t})\underline{\underline{G}}_A(\underline{r}_t,\underline{r}_t';\lambda_{r_t}) = -(\hat{x}\hat{x} + \hat{z}\hat{z})\delta(\underline{r}_t-\underline{r}_t') \qquad (8.1)$$

where now $\underline{r}_t'$ may lie on either of the two interface planes AA' and BB'.

The solution to equation (8.1) is constructed from the solutions to the homogeneous Helmholtz equation in each of the three regions a,b and c in figure 8.1,which shall be identified as $\underline{A}_v^a(\underline{r}_t;\lambda_{r_t})$,$\underline{A}_v^b(\underline{r}_t;\lambda_{r_t})$ and $\underline{A}_v^c(\underline{r}_t;\lambda_{r_t})$.The function $\underline{A}_v(\underline{r}_t;\lambda_{r_t})$ and the adjoint function $\underline{E}_v^A(\underline{r}_t;\lambda_{r_t})$ shall be defined as;

$$\underline{A}_v(\underline{r}_t;\lambda_{r_t}) = \underline{A}_v^{a,b,c}(\underline{r}_t;\lambda_{r_t}) \qquad : \underline{r}_t \ in \ a,b,c$$

$$\underline{E}_v^A(\underline{r}_t;\lambda_{r_t}) = \left[\underline{E}_v^{a,b,c}(\underline{r}_t;\lambda_{r_t})\right]^A \qquad : \underline{r}_t \ in \ a,b,c \tag{8.2}$$

Continuity is ensured by requiring that;

$$\underline{A}_v^a(x,t;\lambda_{r_t}) = \underline{A}_v^b(x,t;\lambda_{r_t}) \ : \ \underline{A}_v^b(x,0;\lambda_{r_t}) = \underline{A}_v^c(x,0;\lambda_{r_t})$$

$$\underline{E}_v^a(x,t;\lambda_{r_t}) = \underline{E}_v^b(x,t;\lambda_{r_t}) \ : \ \underline{E}_v^b(x,0;\lambda_{r_t}) = \underline{E}_v^c(x,0;\lambda_{r_t}) \tag{8.3}$$

Consider expressing the magnetic vector potential transverse characteristic Green's function as;

$$\underline{\underline{G}}_A(\underline{r}_t,\underline{r}_t';\lambda_{r_t}) = \sum_v \frac{\underline{A}_v(\underline{r}_t;\lambda_{r_t})\underline{E}_v^A(\underline{r}_t';\lambda_{r_t})}{\gamma_v(\lambda_{r_t})} \tag{8.4}$$

If this expression is substituted into equation (8.1),then the discontinuity of its derivative w.r.t. y results in singularities of the form $f(x,x')\delta(y-0) + h(x,x')\delta(y-t)$.These may be found explicitly by integrating equation (8.1) w.r.t. y,ie;

$$\int_{-\infty}^{\infty} dy(\nabla_t^2 + \lambda_{r_t})\underline{\underline{G}}_A(\underline{r}_t,\underline{r}_t';\lambda_{r_t}) = -(\hat{x}\hat{x} + \hat{z}\hat{z})\delta(\rho - \rho')$$

$$= \mu\sum_v \frac{\underline{\underline{H}}_v^a(x,t;\lambda_{r_t})\times\hat{y}\ [\underline{E}_v^a(x',t;\lambda_{r_t})]^A - \underline{\underline{H}}_v^b(x,t;\lambda_{r_t})\times\hat{y}\ [\underline{E}_v^b(x',t;\lambda_{r_t})]^A}{\gamma_v(\lambda_{r_t})}$$

$$+ \frac{\underline{\underline{H}}_v^b(x,0;\lambda_{r_t})\times\hat{y}\ [\underline{E}_v^b(x',0;\lambda_{r_t})]^A - \underline{\underline{H}}_v^c(x,0;\lambda_{r_t})\times\hat{y}\ [\underline{E}_v^c(x',0;\lambda_{r_t})]^A}{\gamma_v(\lambda_{r_t})} \tag{8.5}$$

where ρ is a one dimensional parameter that lies on either of the nonseparable interfaces.This restriction on the field vectors may be expressed as the orthogonality condition;

$$\int_{-\infty}^{\infty} dx\, R\underline{E}_\mu(x,t;\lambda_{r_t}) \times \left[\underline{H}^a_\nu(x,t;\lambda_{r_t}) - \underline{H}^b_\nu(x,t;\lambda_{r_t})\right].\hat{y}$$

$$+ \int_{-\infty}^{\infty} dx\, R\underline{E}_\mu(x,0;\lambda_{r_t}) \times \left[\underline{H}^b_\nu(x,0;\lambda_{r_t}) - \underline{H}^c_\nu(x,0;\lambda_{r_t})\right].\hat{y} = \frac{\gamma_\nu(\lambda_{r_t})}{\mu}\delta_{\mu\nu} \tag{8.6}$$

where R is the reflection operator introduced in chapter 2.

As for the case of a single nonseparable interface,the solutions to this equation allow the electric field transverse characteristic Green's function to be written as;

$$\underline{\underline{G}}^s_E(\underline{r}_t,\underline{r}_t';\lambda_{r_t}) = \sum_\nu \frac{\underline{E}_\nu(\underline{r}_t;\lambda_{r_t})\underline{E}^A_\nu(\underline{r}_t';\lambda_{r_t})}{-j\omega\mu\gamma_\nu(\lambda_{r_t})} \tag{8.7}$$

The solution of equation (8.6) is facilitated by the introduction of the following admittance operators;

$$\underline{H}^a_\nu(x,t;\lambda_{r_t}) = \int_{-\infty}^{\infty} dx' \underline{\underline{Y}}^a(x,x')\underline{E}^a_\nu(x',t;\lambda_{r_t})$$

$$\underline{H}^c_\nu(x,t;\lambda_{r_t}) = \int_{-\infty}^{\infty} dx' \underline{\underline{Y}}^c(x,x')\underline{E}^c_\nu(x',0;\lambda_{r_t})$$

$$\begin{pmatrix} \underline{H}^b_\nu(x,t;\lambda_{r_t}) \\ -\underline{H}^b_\nu(x,0;\lambda_{r_t}) \end{pmatrix} = \int_{-\infty}^{\infty} dx' \begin{pmatrix} \underline{\underline{Y}}^b_{11}(x,x') & \underline{\underline{Y}}^b_{12}(x,x') \\ \underline{\underline{Y}}^b_{21}(x,x') & \underline{\underline{Y}}^b_{22}(x,x') \end{pmatrix} \begin{pmatrix} \underline{E}^b_\nu(x',t;\lambda_{r_t}) \\ \underline{E}^b_\nu(x',0;\lambda_{r_t}) \end{pmatrix} \tag{8.8}$$

allowing the denominator of $\underline{\underline{G}}^s_E(\underline{r}_t,\underline{r}_t';\lambda_{r_t})$ to be written as;

$$-j\omega\mu \int_{-\infty}^{\infty} dx \int_{-\infty}^{\infty} dx' (R\underline{E}_\mu(x,t;\lambda_{r_t})\ R\underline{E}_\mu(x,0;\lambda_{r_t})) \begin{pmatrix} \underline{\underline{Y}}^a(x,x') - \underline{\underline{Y}}^b_{11}(x,x') & -\underline{\underline{Y}}^b_{12}(x,x') \\ -\underline{\underline{Y}}^b_{21}(x,x') & -\underline{\underline{Y}}^c(x,x') - \underline{\underline{Y}}^b_{22}(x,x') \end{pmatrix} \begin{pmatrix} \underline{E}_\nu(x',t;\lambda_{r_t}) \\ \underline{E}_\nu(x',0;\lambda_{r_t}) \end{pmatrix}$$

$$= -jP_\nu(\lambda_{r_t})\delta_{\mu\nu}(1 - jcot\alpha_\nu(\lambda_{r_t})) \tag{8.9}$$

Not surprisingly,the problem is characterised by the transverse fields at both the interfaces,necessitating the use of two basis sets to discretise and hence solve equation (8.9).

The generalisation to structures divided by N-1 nonseparable interfaces into N regions,simply involves extending the definitions of $\underline{A}_v(\underline{r}_t;\lambda_{r_t})$ and $\underline{E}_v(\underline{r}_t;\lambda_{r_t})$ in equation (8.2) and the domain of the parameter ρ.The orthogonality condition may then be stated as;

$$-(\hat{x}\hat{x}+\hat{z}\hat{z})\delta(\rho-\rho') =$$

$$\mu\sum_v \frac{1}{\gamma_v(\lambda_{r_t})}\sum_n^N\left[\underline{H}_v^n(x,y_n;\lambda_{r_t})\times\hat{y}\,[\underline{E}_v^n(x',y'_n;\lambda_{r_t})]^A-\underline{H}_v^{n+1}(x,y_n;\lambda_{r_t})\times\hat{y}\,[\underline{E}_v^{n+1}(x',y'_n;\lambda_{r_t})]^A\right] \quad (8.10)$$

with $\underline{E}_v^n(x,y_n;\lambda_{r_t})=\underline{E}_v^{n+1}(x,y_n;\lambda_{r_t})$.

Defining admittance operators of the form;

$$\begin{pmatrix}\underline{H}_v^{n+1}(x,y_n;\lambda_{r_t})\\ -\underline{H}_v^{n+1}(x,y_{n+1};\lambda_{r_t})\end{pmatrix}=\int_{-\infty}^{\infty}dx'\begin{pmatrix}\underline{\underline{Y}}_{11}^{n+1}(x,x') & \underline{\underline{Y}}_{12}^{n+1}(x,x')\\ \underline{\underline{Y}}_{21}^{n+1}(x,x') & \underline{\underline{Y}}_{22}^{n+1}(x,x')\end{pmatrix}\begin{pmatrix}\underline{E}_v^{n+1}(x',y_n;\lambda_{r_t})\\ \underline{E}_v^{n+1}(x',y_{n+1};\lambda_{r_t})\end{pmatrix} \quad (8.11)$$

permits the denominator of $\underline{\underline{G}}_E^s(\underline{r}_t,\underline{r}_t';\lambda_{r_t})$ to be written as;

$$-jP_v(\lambda_{r_t})\delta_{\mu v}(1-jcot\alpha)=-j\omega\mu\int_{-\infty}^{\infty}dx\int_{-\infty}^{\infty}dx'(R\underline{E}_\mu(x,y_1;\lambda_{r_t})\;R\underline{E}_\mu(x,y_2;\lambda_{r_t})\ldots\ldots\ldots) \quad (8.12)$$

$$\begin{pmatrix}\underline{\underline{Y}}^1(x,x')-\underline{\underline{Y}}_{11}^2(x,x') & -\underline{\underline{Y}}_{12}^2(x,x') & 0 & 0\\ -\underline{\underline{Y}}_{21}^2(x,x') & -\underline{\underline{Y}}_{22}^2(x,x')-\underline{\underline{Y}}_{11}^3(x,x') & -\underline{\underline{Y}}_{12}^3(x,x') & 0\\ 0 & -\underline{\underline{Y}}_{21}^3(x,x') & -\underline{\underline{Y}}_{22}^3(x,x')-\underline{\underline{Y}}_{11}^4(x,x') & -\underline{\underline{Y}}_{12}^4(x,x')\\ 0 & 0 & -\underline{\underline{Y}}_{21}^4(x,x') & .\\ 0 & 0 & 0 & .\end{pmatrix}\begin{pmatrix}\underline{E}_v(x',y_1;\lambda_{r_t})\\ \underline{E}_v(x',y_2;\lambda_{r_t})\\ .\\ .\end{pmatrix}$$

8.3) Formulation for Slotline with finite thickness Metallisation.

In the previous section it has been demonstrated how the transverse characteristic Green's function of a structure containing multiple nonseparable

interfaces may be formulated.The detailed derivation of the continuum of slotline with finite thickness metallisation shall now be presented.Clearly many of the steps are identical to those undertaken for the I.D.G. and therefore shall not be repeated unnecessarily.

The fields in region (a) may be treated as for those of the I.D.G. yielding the admittance operator given in equation (4.2.15).

The transverse electric fields in region (b) may be represented by;

$$\begin{pmatrix} E_{vx}(\underline{r}_t;\lambda_{r_t}) \\ \partial x E_{vz}(\underline{r}_t;\lambda_{r_t}) \end{pmatrix} = \sum_{n=1,3..} \phi_{hn}(x)\frac{\sin(q_n y+\xi_n)}{\sin\xi_n}\underline{e}_{vn}(\lambda_{r_t}) \quad : \phi_{hn}(x) = \frac{2}{\sqrt{a}}\sin(\frac{n\pi}{a}x) \tag{8.13}$$

The amplitudes $\underline{e}_{vn}(\lambda_{r_t})$ and the phase shift ξ_n may be expressed in terms of the interface fields;

$$\underline{e}_{vn}(\lambda_{r_t}) = \int_{-\infty}^{\infty} dx\ \phi_{hn}(x)\underline{E}_v(x,0;\lambda_{r_t})$$

$$\underline{e}_{vn}(\lambda_{r_t})\frac{\sin(q_n t+\xi_n)}{\sin\xi_n} = \int_{-\infty}^{\infty} dx\ \phi_{hn}(x)\underline{E}_v(x,t;\lambda_{r_t}) \tag{8.14}$$

The transverse magnetic fields in region (b) are given by;

$$-\begin{pmatrix} H_{vz}(\underline{r}_t;\lambda_{r_t}) \\ \int dx H_{vx}(\underline{r}_t;\lambda_{r_t}) \end{pmatrix} = j\sum_n \phi_{hn}(x)\underline{\underline{Y}}_n\underline{e}_{vn}(\lambda_{r_t})\frac{\cos(q_n y+\xi_n)}{\sin\xi_n} \tag{8.15}$$

where;

$$\omega\mu_o q_n \underline{\underline{Y}}_n = \begin{pmatrix} k_t^2 & j\beta \\ -j\beta & \dfrac{k_o^2-(\frac{n\pi}{a})^2}{(\frac{n\pi}{a})^2} \end{pmatrix} \tag{8.16}$$

The admittance operator $\underline{\underline{Y}}^b(x,x')$ defined in equation (8.8) may now be identified

from equations (8.15) and (8.16) as;

$$\begin{pmatrix} \underline{H}_v(x,t;\lambda_{r_i}) \\ -\underline{H}_v(x,0;\lambda_{r_i}) \end{pmatrix} = j\sum_n \phi_{hn}(x,x') \begin{pmatrix} \overline{\overline{Y}}_n cotq_n t & -\overline{\overline{Y}}_n cosecq_n t \\ -\overline{\overline{Y}}_n cosecq_n t & \overline{\overline{Y}}_n cotq_n t \end{pmatrix} \int_{-\infty}^{\infty} dx' \phi_{hn}(x') \begin{pmatrix} \underline{E}_v(x',t;\lambda_{r_i}) \\ \underline{E}_v(x',0;\lambda_{r_i}) \end{pmatrix} \tag{8.17}$$

It is perfectly acceptable to treat the dielectric and open regions constituting region (c) separately.However,the drawback to this approach is that it introduces another set of interface fields that must be discretised by Galerkin's method.The alternative is to recognise that the separable nature of air-dielectric interface allows region (c) to be regarded as a set of uncoupled transmission lines terminated by known admittances.Recalling that the matrix $\overline{\overline{T}}^{-1}(k_x)$ introduced in chapter 3 decomposes the electric field into its L.S.E and L.S.M constituents,allows the transverse magnetic fields at $y=0^-$ to be written as;

$$\underline{H}_v(x,0;\lambda_{r_i}) = \int_0^{\infty} dk_x \phi_h(k_x,x) \overline{\overline{T}}(k_x) \begin{pmatrix} y_e' \dfrac{y_e + jy_e' \tan k_y' h}{y_e' + jy_e \tan k_y' h} & 0 \\ 0 & y_h' \dfrac{y_h + jy_h' \tan k_y' h}{y_h' + jy_h \tan k_y' h} \end{pmatrix}$$

$$\overline{\overline{T}}^{-1}(k_x) \int_{-\infty}^{\infty} dx' \phi_h(k_x,x') \underline{E}_v(x',0;\lambda_{r_i}) \tag{8.18}$$

where the primed quantities refer to the dielectric region and;

$$k_y^2 = k_i^2 - k_x^2 \quad : \quad k_y^{2\prime} = (\varepsilon_r - 1)k_o^2 + k_i^2 - k_x^2$$

$$y_h = \frac{k_y}{\omega\mu_o} \; ; \; y_h' = \frac{k_y'}{\omega\mu_o} \; ; \; y_e = \frac{\omega\varepsilon_o}{k_y} \; ; \; y_e' = \frac{\omega\varepsilon_r\varepsilon_o}{k_y'} \tag{8.19}$$

The admittance terms in equation (8.18) are complex quantities.It may be shown that a real term is present only if $k_x \le k_i$,which is not surprising as this corresponds to a propagating transmission line mode terminated by a real admittance.

If equations (8.17),(8.18) and (4.2.15) are substituted into equation (8.9) then the denominator of the transverse characteristic Green's function may be identified as;

$$P_v(\lambda_{r_l})\delta_{\mu v}(1-jcot\alpha_v(\lambda_{r_l}))=\int_{-\infty}^{\infty}dx\int_{-\infty}^{\infty}dx'(\underline{RE}_\mu(x,t;\lambda_{r_l})\ \underline{RE}_\mu(x,0;\lambda_{r_l}))\int_0^{\infty}dk_x\phi_h(k_x,x)$$

$$\left[\begin{pmatrix}\underline{\underline{Y}}^a(k_x) & 0\\ 0 & \underline{\underline{Y}}^c(k_x)\end{pmatrix}\phi_h(k_x,x')-j\sum_n\phi_{hn}(x)\begin{pmatrix}\underline{\underline{Y}}_n cotq_n t & -\underline{\underline{Y}}_n cosecq_n t\\ -\underline{\underline{Y}}_n cosecq_n t & \underline{\underline{Y}}_n cotq_n t\end{pmatrix}\right]\phi_{hn}(x')\begin{pmatrix}\underline{E}_v(x',t;\lambda_{r_l})\\ \underline{E}_v(x',0;\lambda_{r_l})\end{pmatrix} \quad (8.20)$$

which leads to the eigenvalue equation;

$$cot\alpha_v(\lambda_{r_l})\int_{-\infty}^{\infty}dx\int_{-\infty}^{\infty}dx'(\underline{RE}_\mu(x,t;\lambda_{r_l})\ \underline{RE}_\mu(x,0;\lambda_{r_l}))\int_0^{\infty}dk_x\phi_h(k_x,x)\begin{pmatrix}\underline{\underline{Y}}^a(k_x) & 0\\ 0 & -\mathrm{Re}\left[\underline{\underline{Y}}^c(k_x)\right]\end{pmatrix}\phi_h(k_x,x')$$

$$\begin{pmatrix}\underline{E}_v(x',t;\lambda_{r_l})\\ \underline{E}_v(x',0;\lambda_{r_l})\end{pmatrix}=\int_{-\infty}^{\infty}dx\int_{-\infty}^{\infty}dx'(\underline{RE}_\mu(x,t;\lambda_{r_l})\ \underline{RE}_\mu(x,0;\lambda_{r_l}))\left[\sum_n\phi_{hn}(x)\begin{pmatrix}\underline{\underline{Y}}_n cotq_n t & -\underline{\underline{Y}}_n cosecq_n t\\ -\underline{\underline{Y}}_n cosecq_n t & \underline{\underline{Y}}_n cotq_n t\end{pmatrix}\phi_{hn}(x')\right.$$

$$\left.+\begin{pmatrix}-\int_{k_l}^{\infty}dk_x\phi_h(k_x,x)\underline{\underline{Y}}^a(k_x)\phi_h(k_x,x') & 0\\ 0 & \int_0^{\infty}dk_x\phi_h(k_x,x)\mathrm{Im}\left[\underline{\underline{Y}}^c(k_x)\right]\phi_h(k_x,x')\end{pmatrix}\right]\begin{pmatrix}\underline{E}_v(x',t;\lambda_{r_l})\\ \underline{E}_v(x',0;\lambda_{r_l})\end{pmatrix} \quad (8.21)$$

Before solving equation (8.21),there are two aspects that need to be considered.Firstly,the existence of singularities in the matrix $\underline{\underline{Y}}^c(k_x)$.These occur at those values of k_x corresponding to the surface modes of a grounded dielectric slab and raise the question as to whether the integral over k_x should include a residue from these poles.The analysis presented in [1],included a residue,interpreted as a substrate leakage term.However,as pointed out by the same author in [2],the amplitude of $\underline{\tilde{e}}(k_x)$ at the poles is,in fact,identically zero and thus removes the residue from the calculation.Therefore,the integral over k_x is a principal value integral.

The second aspect that must be considered is a numerical one.If the metallisation thickness,t,tends to 0,then the elements of the matrix $\begin{pmatrix} \underline{\underline{Y}}_n cotq_n t & -\underline{\underline{Y}}_n cosecq_n t \\ -\underline{\underline{Y}}_n cosecq_n t & \underline{\underline{Y}}_n cotq_n t) \end{pmatrix}$ become infinite.In fact,if this matrix is written as $\begin{pmatrix} \underline{\underline{Y}}_n & -\underline{\underline{Y}}_n \\ -\underline{\underline{Y}}_n & \underline{\underline{Y}}_n \end{pmatrix} cosecq_n t$ as $t \to 0$,then it can be seen that this is the mechanism that forces $\underline{E}(x,0) \to \underline{E}(x,t)$,although numerically this causes problems.To overcome this difficulty,it is appropriate to redefine the unknowns as $\underline{E}(x,0)$ and $\delta\underline{E}(x)$,where $\underline{E}(x,t) = \underline{E}(x,0) + \delta\underline{E}(x)$.This redefines the problematic matrix as $\begin{pmatrix} \underline{\underline{Y}}_n(cotq_n t - cosecq_n t) & \underline{\underline{Y}}_n cotq_n t \\ \underline{\underline{Y}}_n(cotq_n t - cosecq_n t & -\underline{\underline{Y}}_n cosecq_n t) \end{pmatrix}$ which is numerically well behaved as $t \to 0$.

Equation (8.21) may be solved using Galerkin's method.As in the case of the I.D.G.,the functions $\phi_{hn}(x)$ have been used as the expansion basis for both interfaces.

8.4) Discussion of the continuous modes of slotline with finite thickness metallisation.

As the objective of this chapter is to demonstrate an extension to the transverse characteristic Green's function,rather than an exhaustive study of slotline,the properties of the modes shall only be briefly discussed.

The examples given are for a slotline with a slot of width 2mm,a dielectric of height 0.635mm and permittivity 9.8 and operating at 10GHz.Three metallisation thicknesses,10μm,20μm and 50μm have been considered.

Figure 8.3 shows the variation of the eigenvalues with k_t for a metallisation of thickness 10μm.Clearly,as observed for the I.D.G.,the existence of two classes of modes,characterised by finite and quasi-infinite eigenvalues,is apparent.This is not surprising as this effect is caused by the presence of a slotted groundplane,a feature common to both guides.

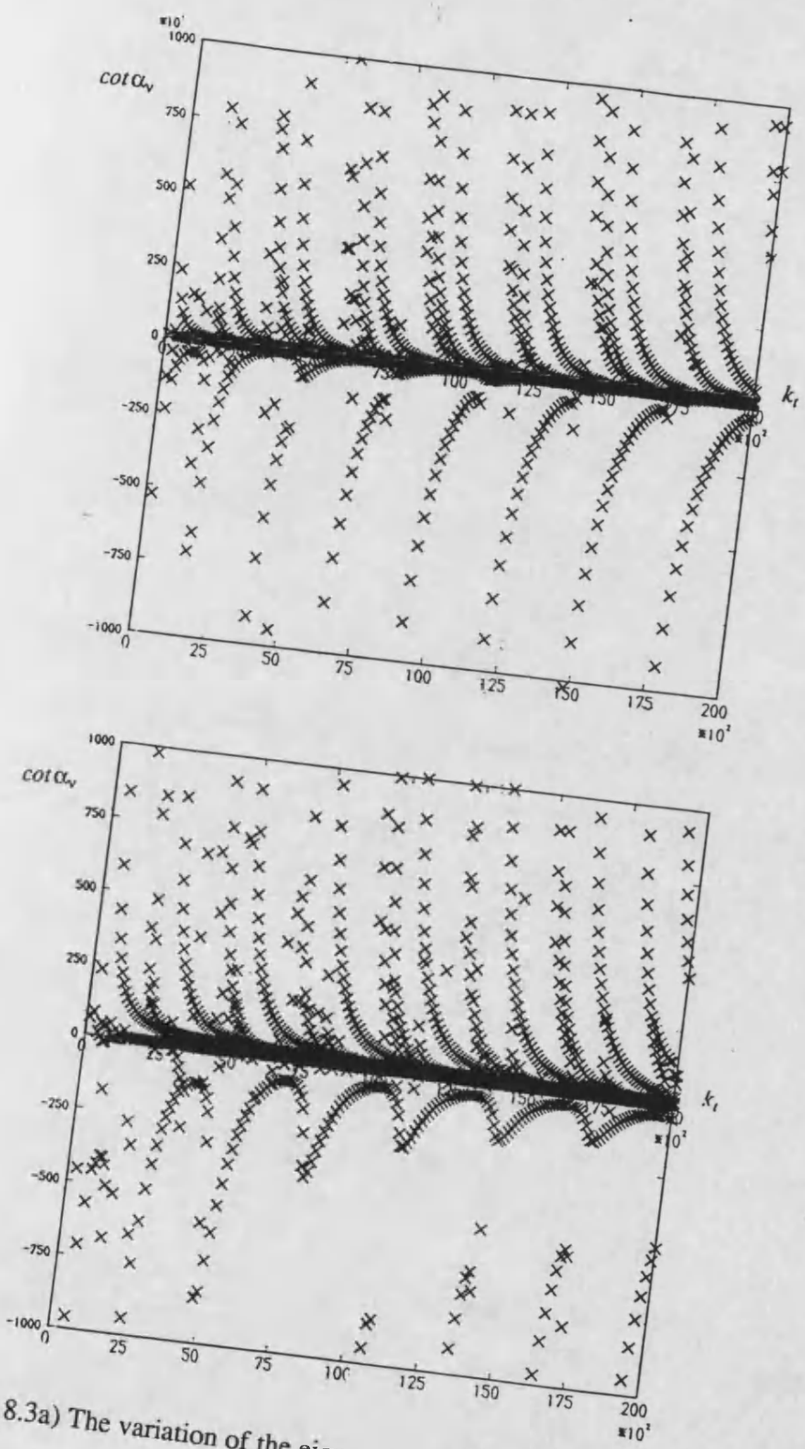

Figure 8.3a) The variation of the eigenvalues with k_t with a metallisation thickness of 10μm.

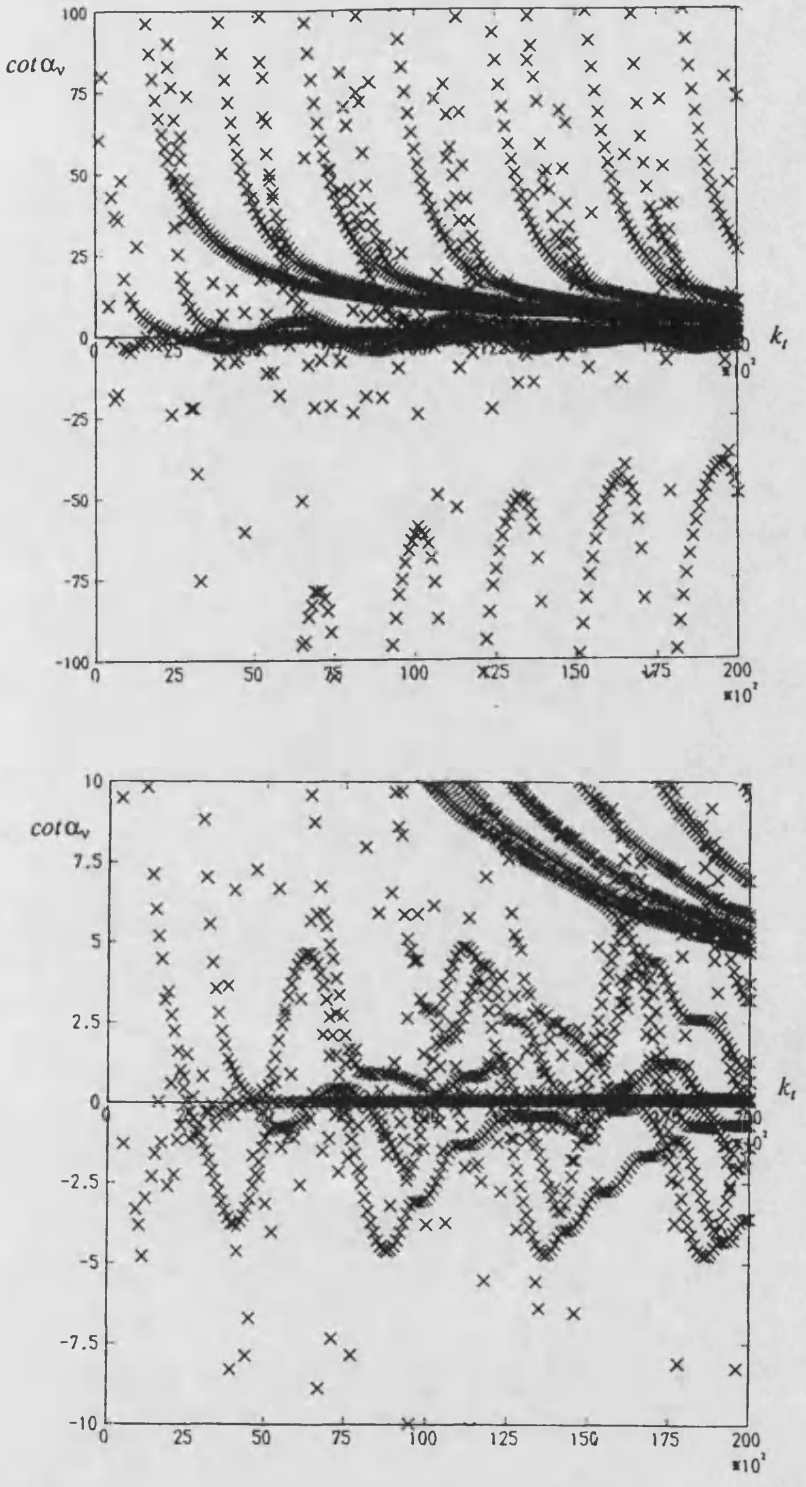

Figure 8.3b) The variation of the eigenvalues with k_t with a metallisation thickness of 10μm.

Obviously slotline has two open regions and this is manifested by the division of the open region modes into two types.It can be seen in figure 8.3a,that there is one type which has a pair of modes with eigenvalues of opposite sign sharing the same critical value of k_t and another type which has a pair of modes with eigenvalues of the same sign,sharing a different critical value of k_t.(Recalling that the critical value is the value of k_t above which a mode is a slot mode and below an open region mode.)

Once finite,the eigenvalues do not appear follow any clear pattern,although a sinusoidal behaviour is suggested.

Figures 8.4,8.5 and 8.6 given in appendix A8 at the end of this chapter,shown the interface fields for the first few modes with metallisation thicknesses of $10\mu m$,$20\mu m$ and $50\mu m$ and k_t=10000.Figure 8.4 demonstrates that,if the metallisation is thin,then for some of the modes,as expected,there is a negligible difference between the fields at the top and bottom of the slot.These are modes which could probably be accurately recovered by assuming infinitesimal metallisation thickness.However it can also be seen that there are modes whose fields differ significantly at the two interfaces,highlighting the need for a two interface analysis if they are to be accurately identified.Not surprisingly,as the metallisation thickness increases most of the modes fall into the latter catagory.

Finally,it is noted that although slotline,under certain circumstances,may be analysed by assuming infinitesimal thickness metallisation,many of the structures proposed for use in the millimeter band such as trapped image line and inverted strip dielectric waveguide,will always require the use of a multiple interface analysis to accurately recover their complete mode spectra.

8.5) References.

1) T.Rozzi,F.Moglie,A.Morini,E.Marchionna and M.Politi,"Hybrid Modes,Substrate leakage,and losses of Slotline at Millimeter-Wave Frequencies",IEEE trans. microwave theory and techniques,vol MTT-38,no 8,Aug 1990,pp1069-1078.

2) T.Rozzi and J.Kot,"The complete Spectrum of Image Line",IEEE trans. microwave theory and techniques,vol MTT-37,no 5,May 1989,pp868-874.

APPENDIX A8) THE INTERFACE FIELDS.

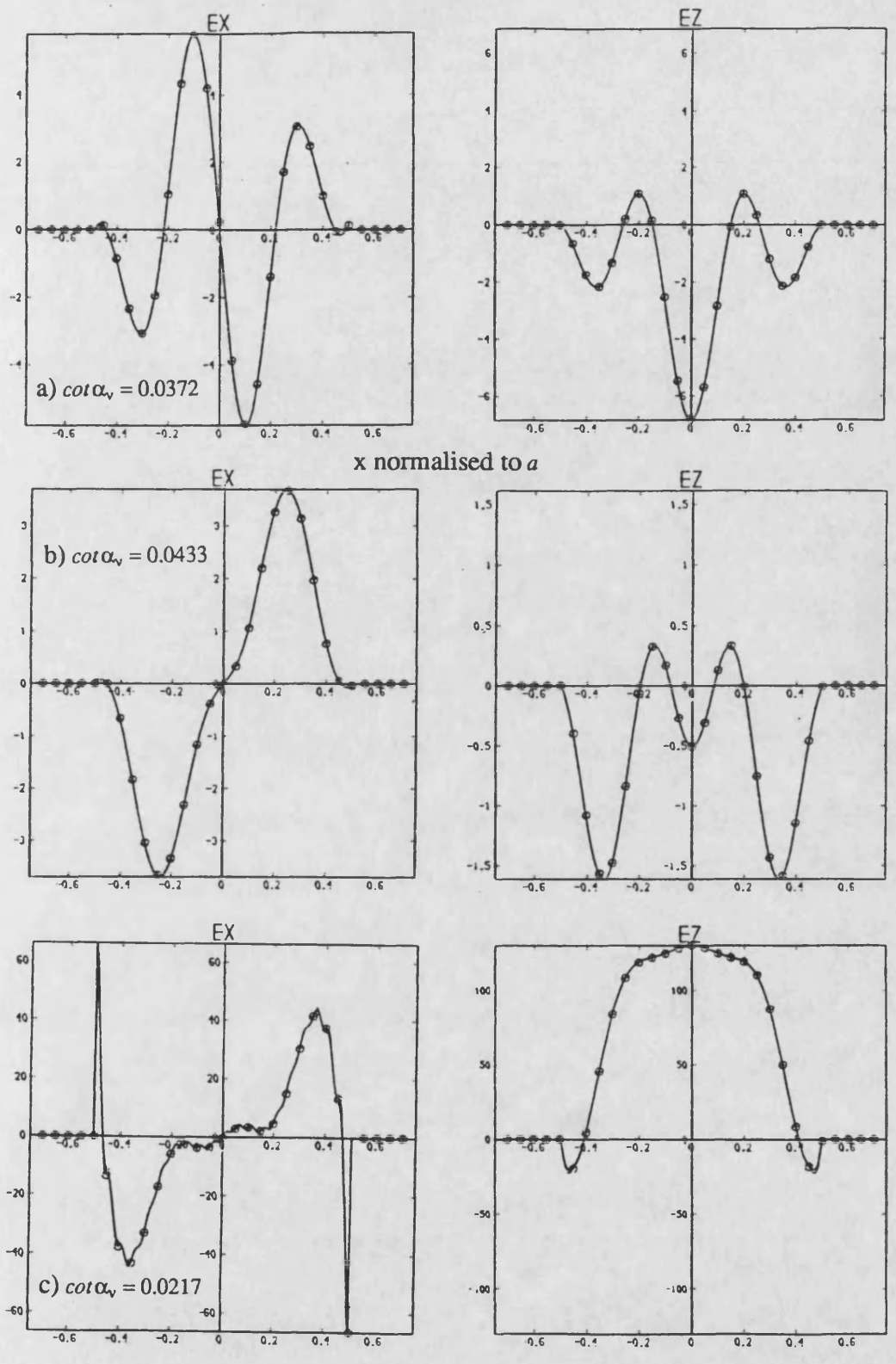

Figure 8.4) Interface fields with 10μm metallisation thickness.

y=t,0

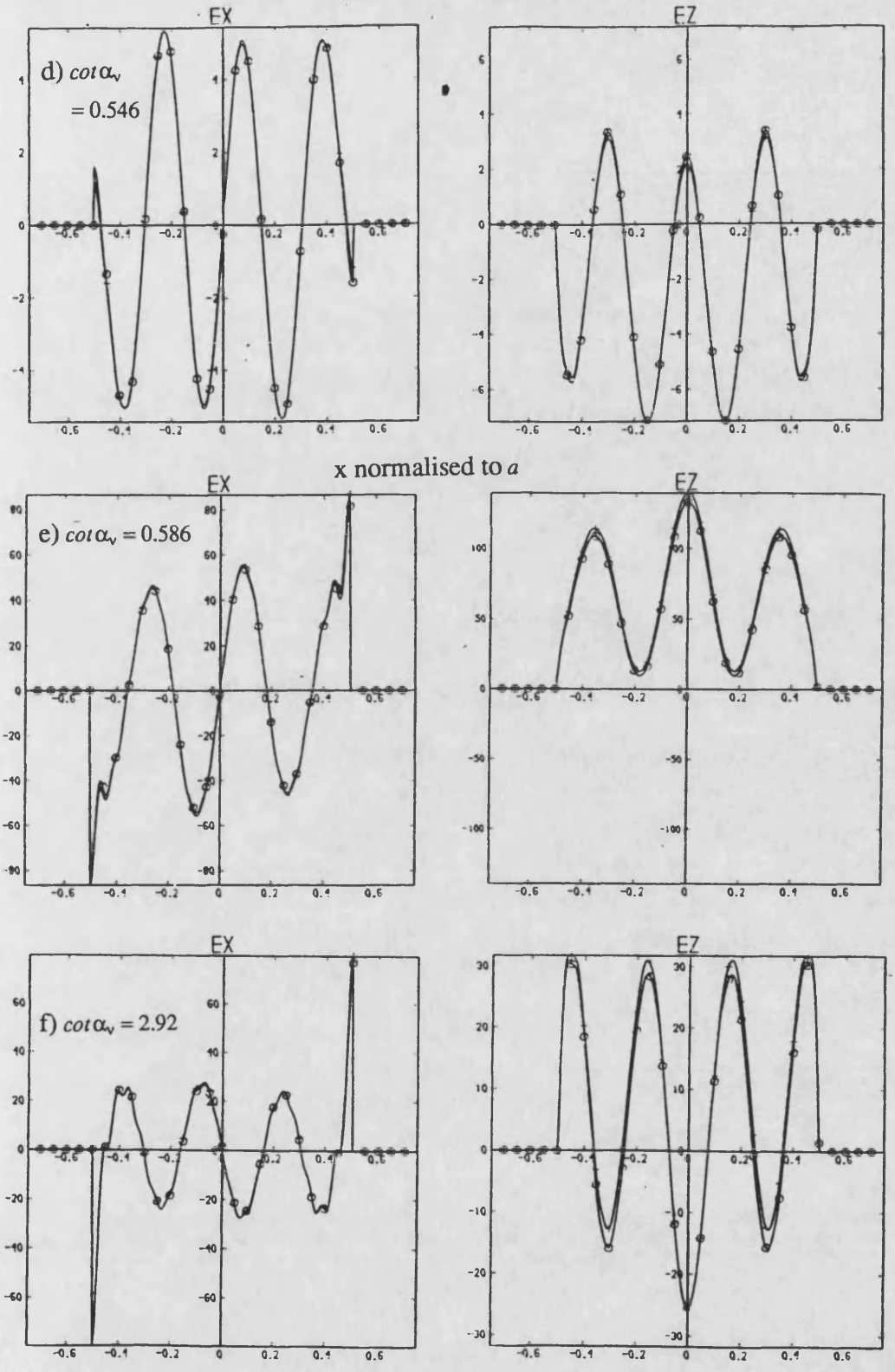

Figure 8.4) Interface fields with 10μm metallisation thickness.

y=t,0

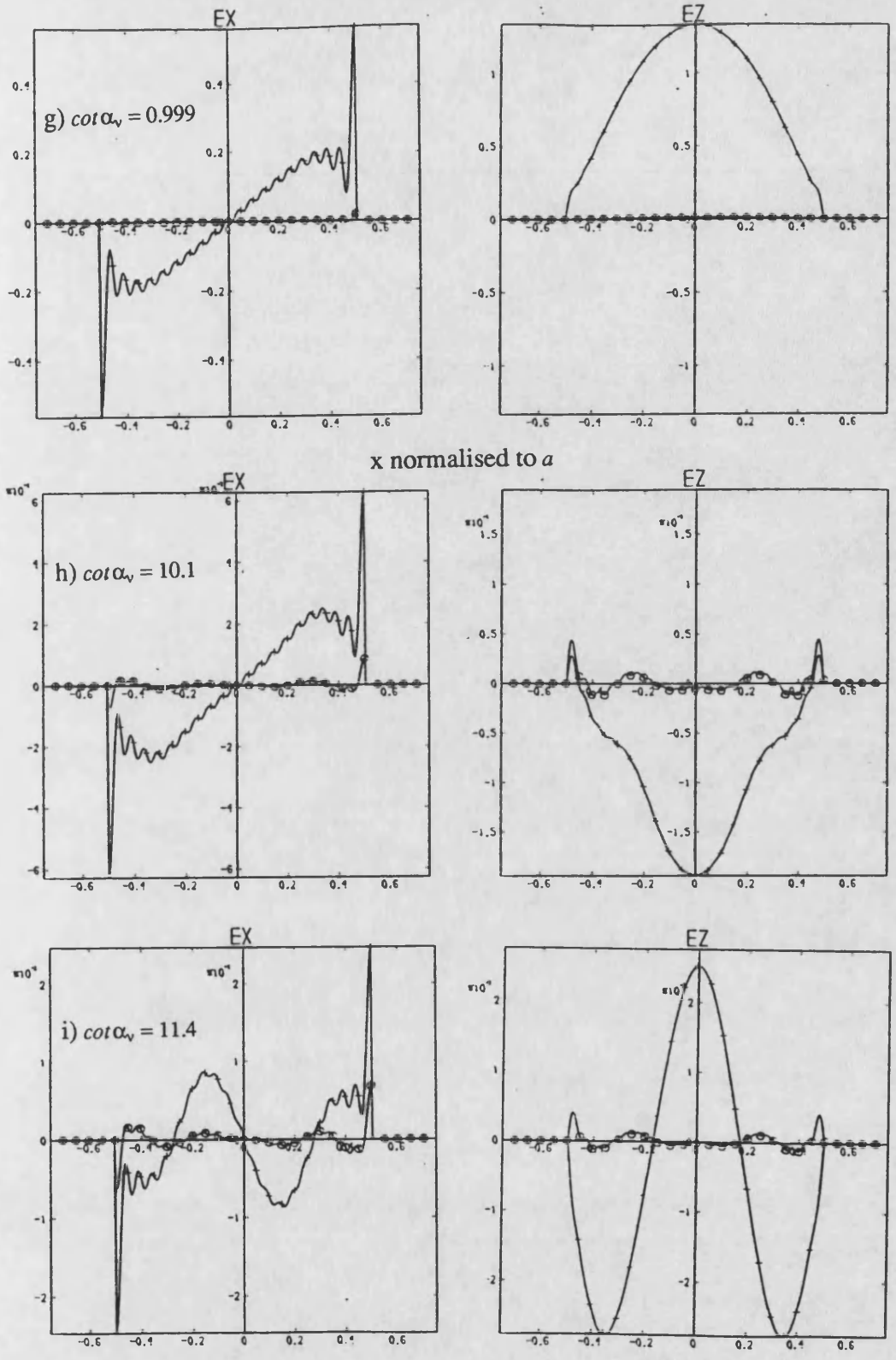

Figure 8.4) Interface fields with 10μm metallisation thickness.

y=t,0

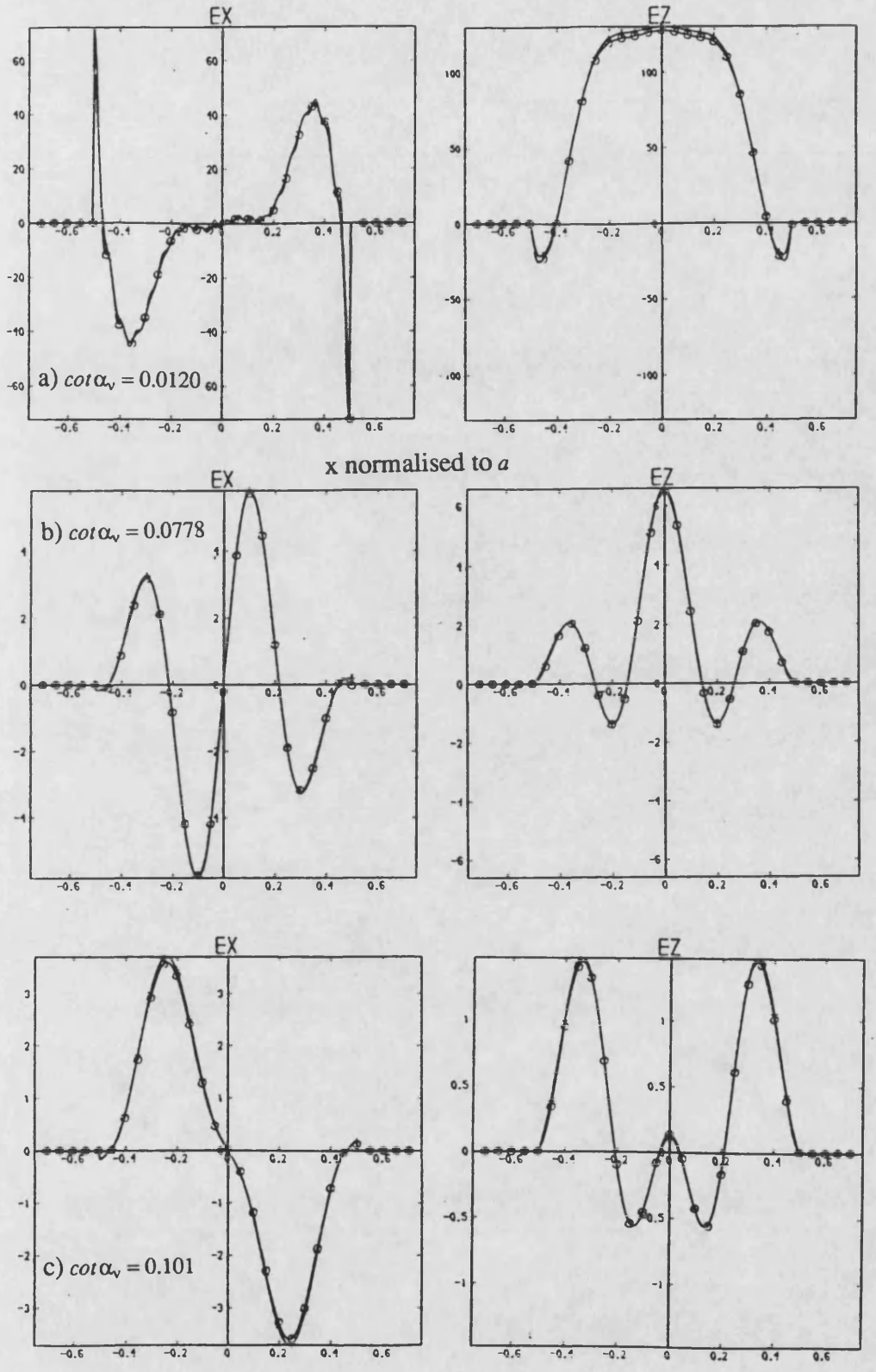

Figure 8.5) Interface fields with 20μm metallisation thickness.

y=t,0

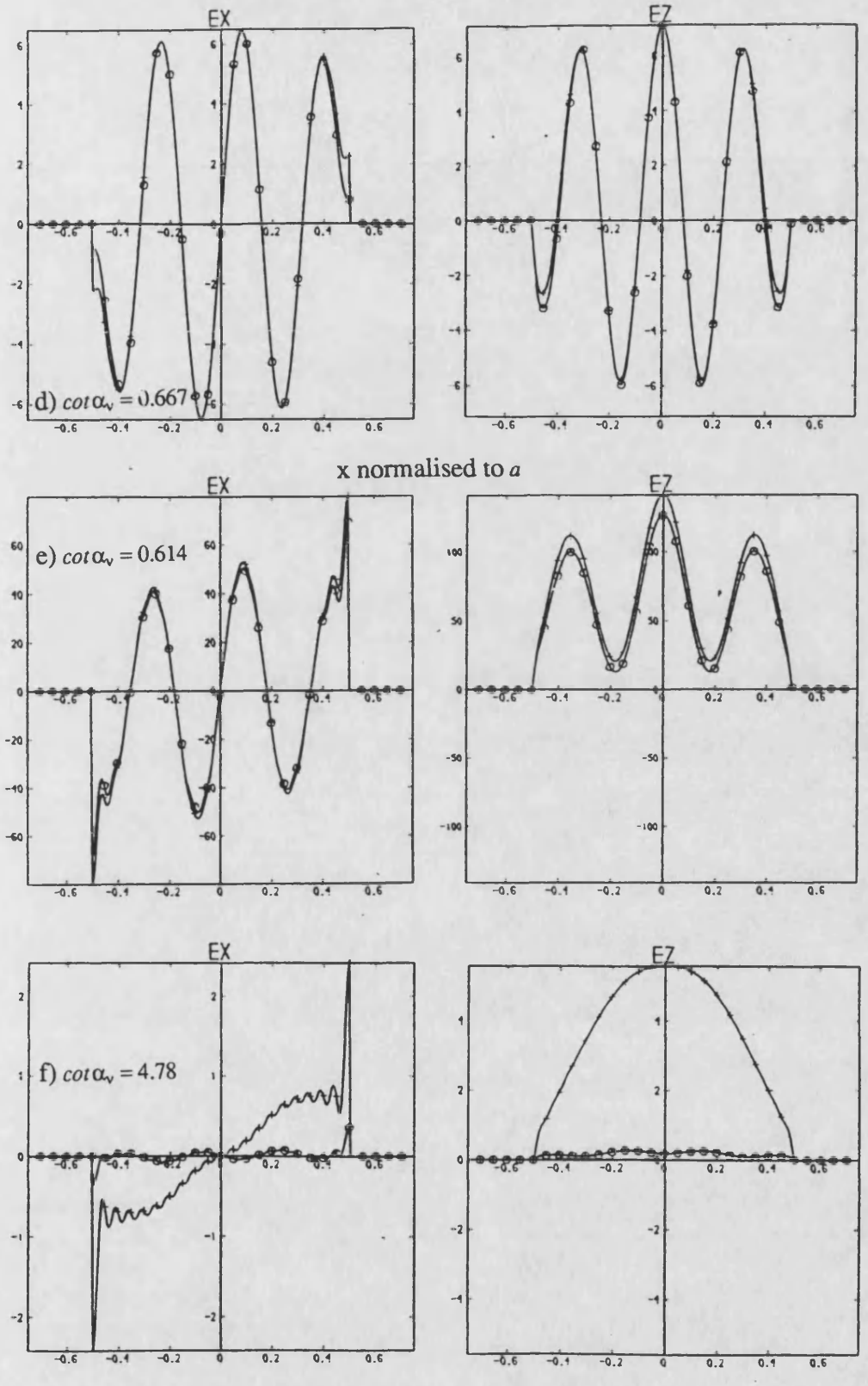

Figure 8.5) Interface fields with 20μm metallisation thickness.

y=t,0

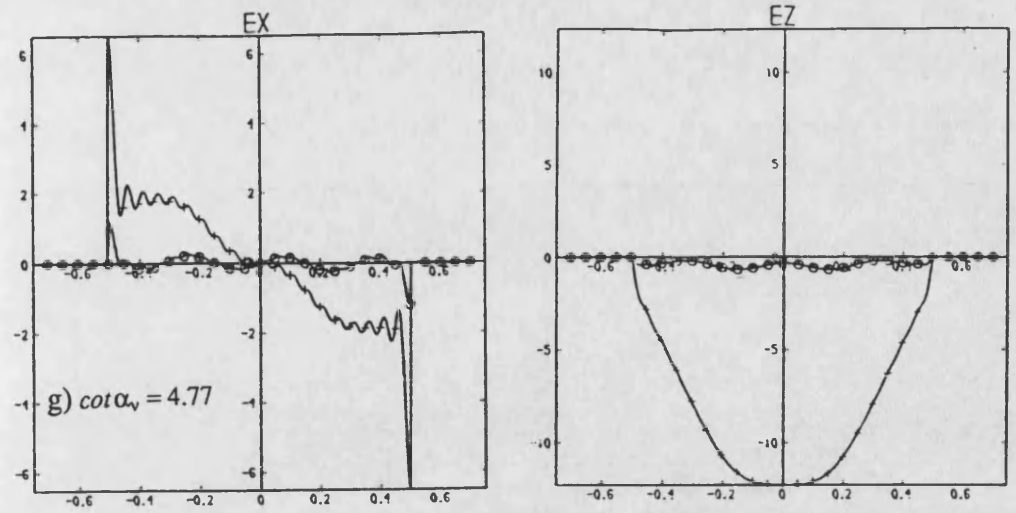

x normalised to *a*

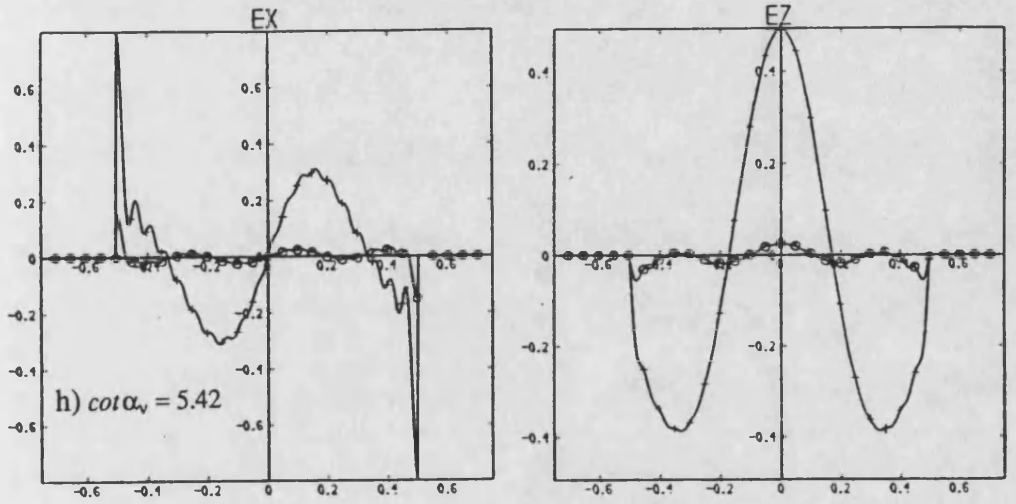

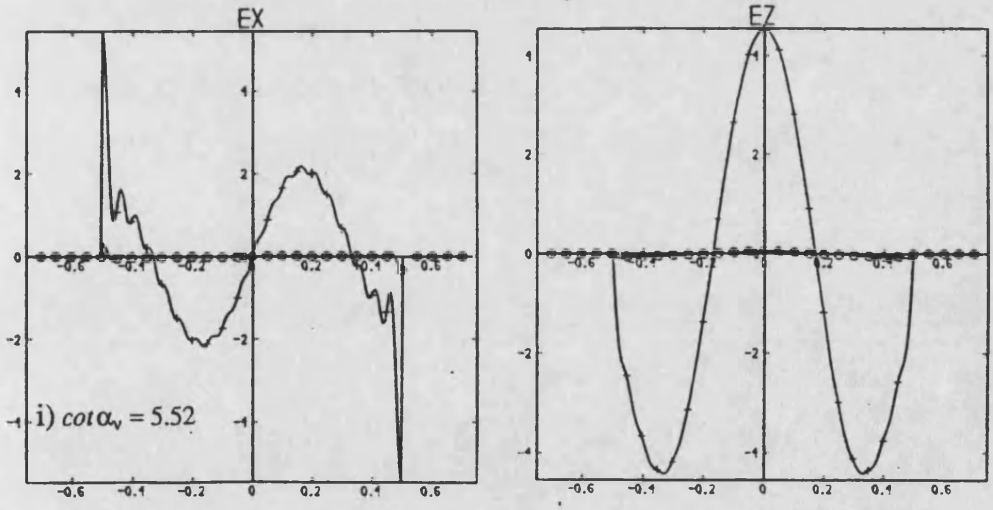

Figure 8.5) Interface fields with 20μm metallisation thickness.

y=t,0

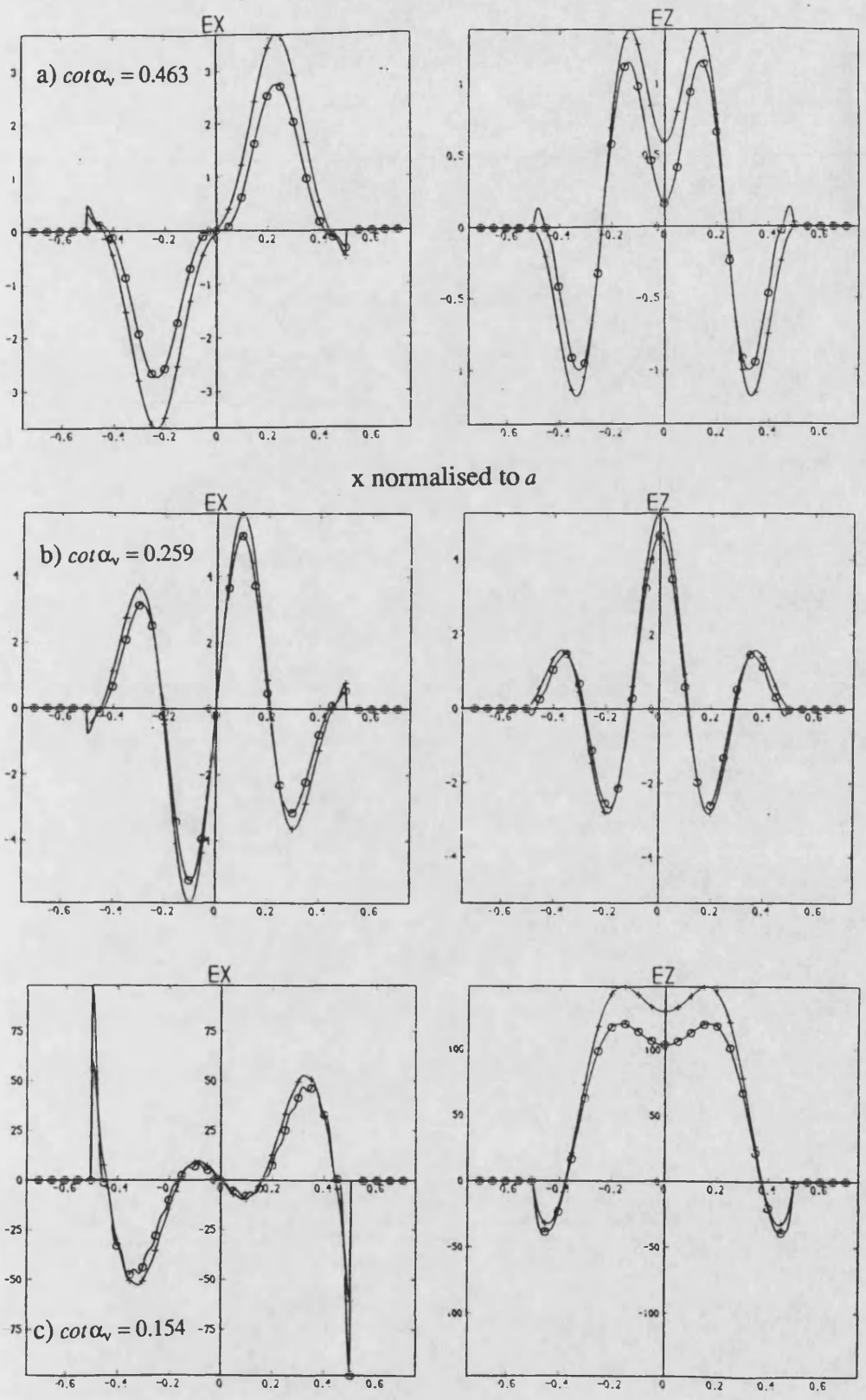

Figure 8.6) Interface fields with 50μm metallisation thickness.

ϕy=t,0

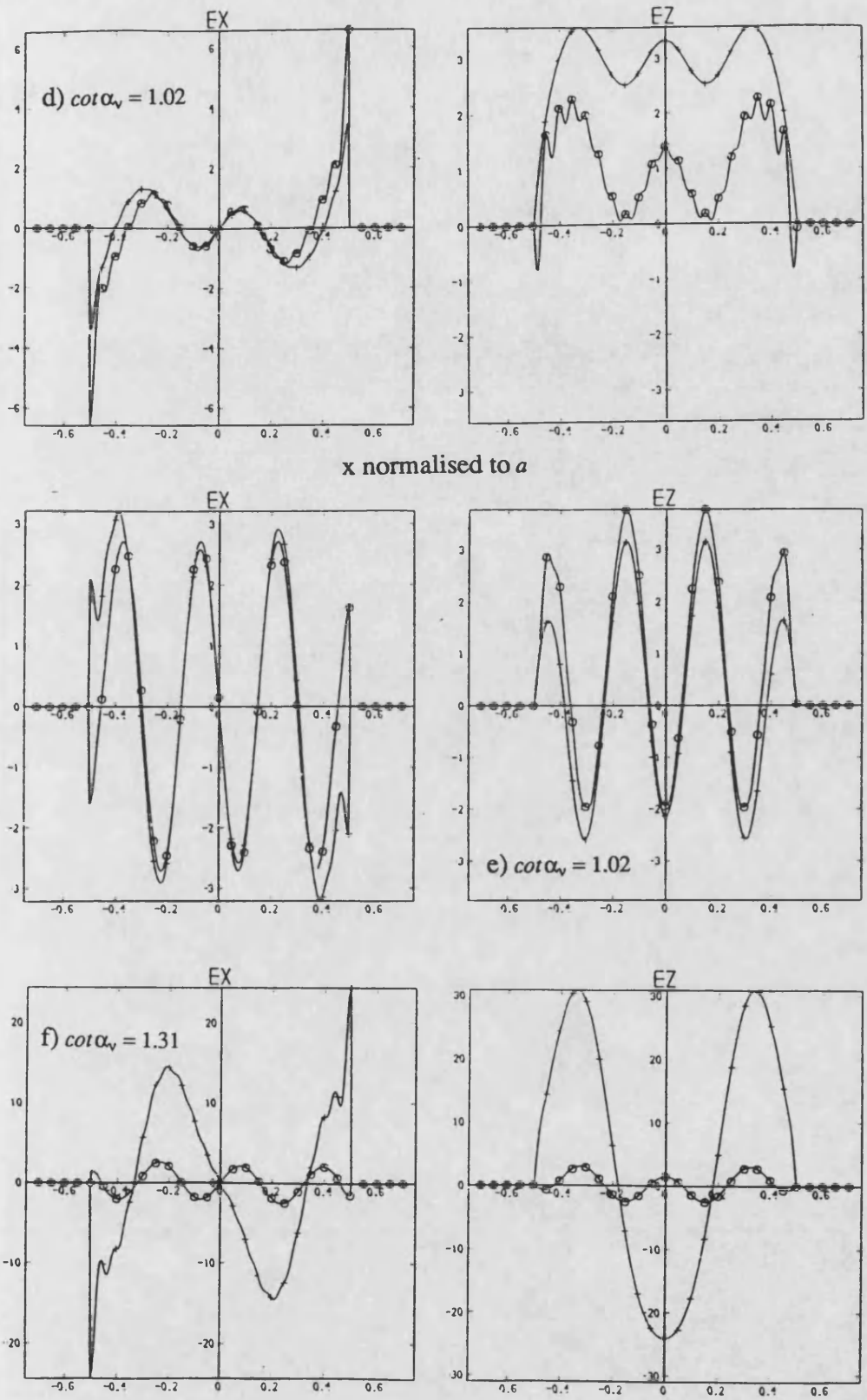

Figure 8.6) Interface fields with 50μm metallisation thickness.

y=t,0

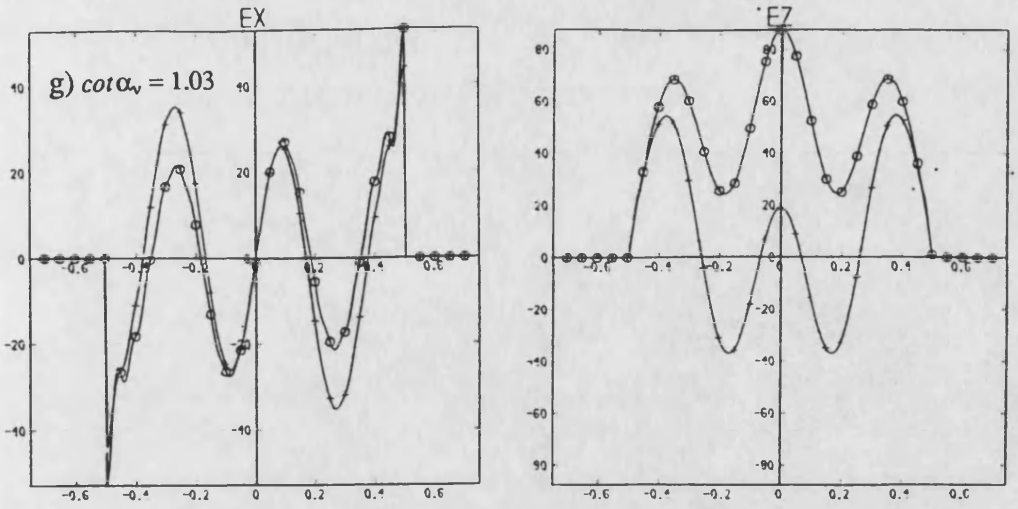

x normalised to *a*

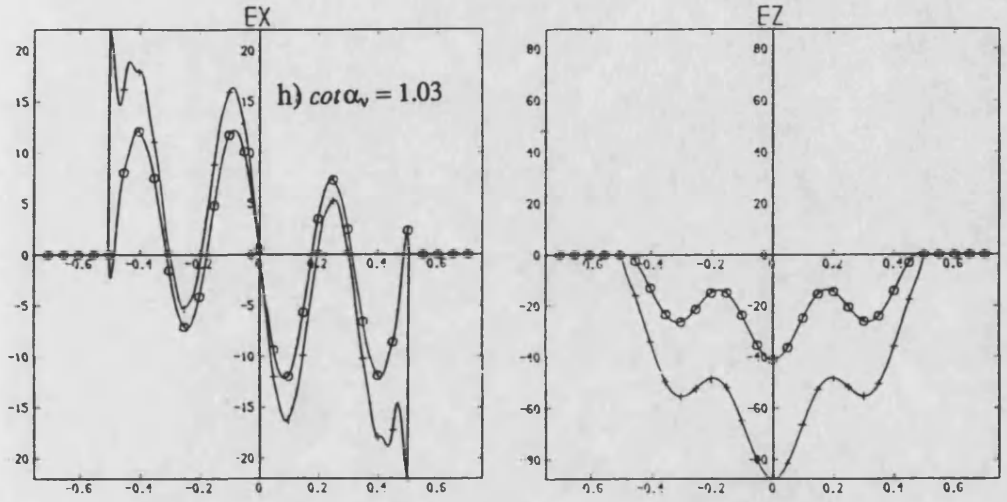

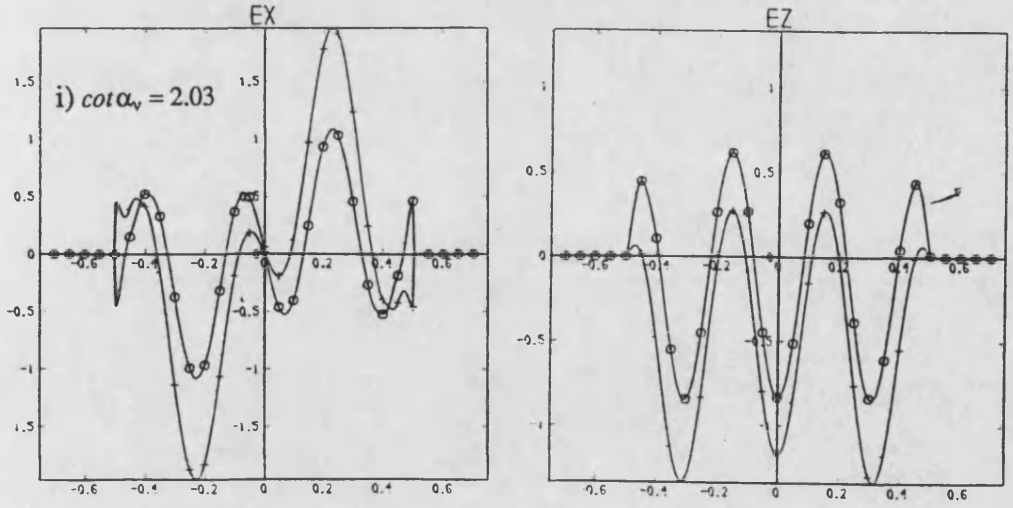

Figure 8.6) Interface fields with 50μm metallisation thickness.

y=t,0

CHAPTER 9.

CONCLUSION.

The purpose of this chapter is to review and draw conclusions from the work presented in this thesis and to suggest areas for future work.

9.1) Review of the work presented in this thesis.

The original objective of this work was to develop a method to permit leaky-wave antennas formed in I.D.G. to be analysed and accurately synthesised.The analytical approach adopted requires the rigorous hybrid spectrum of the I.D.G.The open nonseparable nature of the I.D.G. necessitated the development of a novel hybrid transverse characteristic Green's function method to recover this spectrum,the derivation of which,presented in chapter 2,has a rigorous basis in functional analysis and includes as a particular case,the familiar transverse resonance method.

This Green's function is constructed from solutions of the homogeneous wave equation in each region of the guide,the amplitudes of which are defined by continuity and an eigenvalue equation.The eigenvalue equation may be solved in the space domain using Galerkin's method.

The hybrid transverse characteristic Green's function is important as it allows the complete mode spectra of many of the guides proposed for use in the millimeter band to be recovered.Without these spectra,the accurate design of circuit elements based upon these guides would have to be undertaken using purely numerical methods such as the finite element method.As discussed in chapter 1,whilst finite elements has a role to play,it is neither the most efficient nor

enlightening method to apply in many circumstances.

To illustrate the use of the hybrid transverse characteristic Green's function,open separable structures whose modes may also be identified by the separation of variables,were analysed in chapter 3.

Chapter 4 refocused attention upon the I.D.G.,demonstrating how its complete mode spectrum,and in particular its continuous spectrum,could be recovered.Careful consideration was given to the numerical aspects,illustrating,for example,that the choice of basis functions used to expand the modal fields must be a comprimise between numerical expediency and the rate of convergence.

The continuous modes of the I.D.G. were found to divide into two classes,slot region modes and open region modes,each class further dividing into L.S.E.- and L.S.M.-dominated variants.The slot region modes,characterised by finite eigenvalues,may be recovered from a matrix equation of moderate order and the near fields of the open region modes,characterised by quasi-infinite eigenvalues,were found to be very amenable to an analytic approximation.

To validate this spectrum,chapter 5 presented an analysis of transitions from closed rectangular waveguide to the I.D.G.Excellent agreement was obtained between theoretical and experimental values,not only confirming the validity of the mode spectrum but also its practical utility.

Chapter 6 presented an analysis of radiating strips and patches placed upon the I.D.G.Elements producing both vertically and horizontally polarised radiation were considered and several interesting phenomena were observed.For example,single transverse strips give rise to a beam that is offset from broadside,a phenomenon that may be explained by considering the strength of coupling between the strip and each continuous mode.Also,the network parameters of longitudinal strips suggest that the ends of the strip are strongly coupled by both

the fundamental mode and the continuous modes,a phenomenon previously observed for interacting steps in planar dielectric guide.Finally,a network model of linear arrays that accounts for mutual coupling was discussed which permits linear arrays to be synthesised from standard building blocks.

Chapter 7 derived the continuous spectrum of the microstrip loaded I.D.G.,a structure that is not only of interest as a transmission medium,but also as one of the building blocks discussed in chapter 6.Again the continuous modes split into slot region and open region modes,although as yet,approximations to neither have not been found.

Finally,as many of the guides proposed for use in the millimeter band possess multiple nonseparable interfaces,chapter 8 presented an extension of the transverse characteristic Green's function developed in chapter 2,to allow the spectra of this class of structures to be recovered.In particular,the continuous spectrum of slotline with finite thickness metallisation was identified.

9.2) Areas for future Work.

The work presented in this thesis has encompassed a reasonably wide variety of subjects,each of which has suggested areas for future work.In particular;

i) Theoretical formulations.

The hybrid transverse characteristic Green's function has been developed for structures that consist of isotropic,piecewise inhomogeneous materials.Whilst this includes many practical structures,it is conceivable,that in the future the use of anisotropic,chiral or non-linear materials in either waveguides or particular circuit elements,will motivate a generalisation of the transverse characteristic Green's function to include these effects.

Secondly,as discussed in section 2.4.5.,it could prove useful to seek an

alternative derivation of the transverse characteristic Green's function based upon the scattering of a packet of plane waves by the nonseparable interface.Although leading to the same result,it is probable that the conceptual insight gained will provide more efficient methods of deriving the complete mode spectra of certain structures.

ii) Numerical Evaluation.

The efficient and accurate numerical evaluation of the equations resulting from the theoretical process is an important aspect of any analysis.The work presented in this thesis has identified two specific areas that require careful consideration.Firstly,the choice of basis functions used to expand the modal fields and secondly the solution of ill-conditioned matrix eigenvalue problems.Both these aspects have been examined within the context of this work,although there is certainly scope for improvement.

iii) Rectangular waveguide to I.D.G. transitions.

The rectangular waveguide to I.D.G. transitions analysed in chapter 5 are an important method of feeding the I.D.G.Having demonstrated that these transitions may be theoretically analysed,it is now possible to optimise their performance.Obviously this is an important topic and requires further investigation.

iv) I.D.G. leaky-wave array design.

The analysis of single radiating elements on the I.D.G. is only one step toward the goal of providing a C.A.D. system for the design and synthesis of I.D.G. leaky-wave antennas.It has been indicated that the next step is to produce a library of basic building blocks from which linear arrays may be constructed.There is certainly scope for future investigation of many aspects of

I.D.G. based antennas which,to date,have demonstrated excellent potential.

v) The development of I.D.G. circuit components.

Now that the complete mode spectrum of the I.D.G. is available,it is possible to theoretically investigate the design of a wide variety of I.D.G. circuit components such as filters,couplers,transitions to other guides and the integration of sources and active devices.

vi) Application of the transverse characteristic Green's function to other structures.

The transverse characteristic Green's function method and its extension given in chapter 8 permits the complete mode spectra of many important structures to be developed for the first time.

9.3) Concluding remarks.

The development of dielectric waveguides for use in the millimeter band has been hampered by their open nonseparable nature.Without their continuous radiation modes it has been difficult to theoretically minimise radiation losses from circuit components.Similarly,the promise of compact,lightweight,electrically scannable leaky-wave arrays has been,to some degree,offset by difficulties in their theoretical synthesis.

A method of deriving the complete mode spectra of this class of waveguides has been presented in this thesis and has been shown to be useful in overcoming these difficulties.

With the ever increasing demands being placed upon electromagnetic systems,it is inevitable that the commercial exploitation of the millimeter band will motivate continued research in this field.

SYMBOLS.

SUPERSCRIPTS.

A	Adjoint quantity.
T	Transpose.
*	Conjugate.
$\pm$	For $y \gtrless y'$
a,b,c	In region a,b,c.
$\rho,\kappa=e,h$	T.M. or T.E. polarisation.
s	Solenoidal.
l	Lamellar.
$\sim$	Fourier transform variable.

CAPITAL LETTERS.

$\underline{\tilde{A}}_v(k_x,k_t)$	Far field amplitude vector.
$\underline{A}(\underline{r},t)$	Magnetic vector potential.
$\underline{E}(\underline{r},t)$	Electric field vector.
$E.H._{11}$	I.D.G. surface mode vector:quasi-L.S.M. polarised.
$E.H._n(k_t)$	I.D.G. continuum mode vector:quasi-L.S.M. polarised slot mode.
$F(x)$ $\tilde{F}(k_x)$	Near field approximation to the open modes of the I.D.G. continuum.
$\underline{E}^{\rho}_{mn}(r_t)$	Electric field vector of a rectangular waveguide mode.
$\underline{E}_i(r_t)$	Incident electric field.
$\underline{E}_s(r_t)$	Scattered electric field.
$\underline{\underline{G}}(\underline{r},\underline{r}')$	Modal Green's function.
$\underline{\underline{G}}_E(\underline{r},\underline{r}')$	Electric field modal Green's function.

$\underline{\underline{T}}(k_x)$ Continuous coordinate rotation matrix.

$\underline{\underline{T}}_n$ Discrete coordinate rotation matrix.

$W(x)$ Weight function.

$\tilde{V}(k_x)$ The continuous amplitude of the magnetic type Hertzian potential.

V_n The discrete amplitude of the magnetic type Hertzian potential.

$Z(z;\lambda_z)$ The eigenfunctions in z.

SMALL LETTERS.

a I.D.G. slot width.

$\underline{\tilde{e}}_v(k_x)$ Fourier transform of the transverse electric fields at the air-dielectric interface of the I.D.G.

$\underline{e}_{vn}$ Discrete Fourier transform of the transverse electric fields at the air-dielectric interface of the I.D.G.

$f(\underline{r})$ Source function.

$f_A(\underline{r})$ Magnetic vector potential source.

$f_E(\underline{r})$ Electric field source.

$f_p(x)$ Basis functions used to discretise the transverse electric fields.

h I.D.G. slot depth.

k_o Free space wavenumber.

k_x x-directed wavenumber in the open region.

k_y y-directed wavenumber in the open region.

k_t Transverse wavenumber in the open region.

q_n y-directed wavenumber in the bound region.

$\underline{r}$ Spatial coordinate vector.

$\underline{\underline{G}}_M(\underline{r},\underline{r}')$ Magnetic field modal Green's function.

$\underline{\underline{G}}_E(\underline{r},\underline{r}';\lambda_\tau)$ Electric field characteristic Green's function.

$\underline{\underline{G}}_A(\underline{r},\underline{r}';\lambda_\tau)$ Magnetic vector potential characteristic Green's function;

$\underline{H}(\underline{r},t)$ Magnetic field.

$H.E._{10}$ I.D.G. surface mode vector:quasi-L.S.E. polarised.

$H.E._n(k_t)$ I.D.G. continuum mode vector:quasi-L.S.E. polarised slot mode.

$\underline{H}^p_{mn}(r_t')$ Magnetic field vector of a rectangular waveguide mode.

$\underline{\underline{I}}$ Dyadic identity operator.

$\tilde{I}(k_x)$ The continuous amplitude of the electric type Hertzian potential.

I_n The discrete amplitude of the electric type Hertzian potential.

$\underline{J}(\underline{r},t)$ Surface current density.

L An operator.

L^{-1} The inverse operator to L.

N_p Normalisation coefficient.

$P_v(\lambda_{\tau_t})$ Defined on p2-29

$Q_v(\lambda_{\tau_t})$ Defined on p.2-29

$Q_p(k_x)$ Inner product = $\int_{-\infty}^{\infty} dx \phi_h(k_x,x) f_p(x) W(x)$

Q_{pn} Inner product = $\int_{-\infty}^{\infty} dx \phi_{hn}(x) f_p(x) W(x)$

$R = (\underline{\underline{I}}_t - \hat{z}\hat{z})$ The reflection operator,

R_e The reflection coefficient under even excitation.

R_o The reflection coefficient under odd excitation.

$T(t;\lambda_t)$ The eigenfuntions in time.

r_t Spatial coordinate vector in the transverse plane.

t Time.

y_{on} $y_o(\rho')$ Characteristic admittances.

$y_e(k_z)$ $y_h(k_z)$ T.M. and T.E. characteristic admittances.

$z_e(k_z)$ $z_h(k_z)$ T.M. and T.E. characteristic impedances.

GREEK LETTERS.

$\alpha_\nu(\lambda_{\tau_t})$ Phase shift in the standing waves,w.r.t. y, of a continuous mode.

β z-directed propagation constant.

$\gamma_\nu(\lambda_{\tau_t})$ Denominator of the characteristic Green's function.

δ_{mn} Kronecker delta function.

$\delta(\lambda-\lambda')$ Dirac delta function.

$\underline{\underline{\varepsilon}}$ Permittivity dyadic.

ε Scalar permittivity.

ε_r Relative permittivity.

$\underline{e}(r_t)$ Electric field vector at the waveguide transition.

λ Complex arguments of the characteristic Green's function.

$\underline{\phi}_n(\underline{r})$ Eigenfunction.

$\underline{\phi}_\lambda(\underline{r})$ Improper eigenfunction.

$\underline{\phi}(r_t;\lambda_{\tau_t})$ Transverse eigenfunction.

δ ϕ Observation angles in cylindrical coordinates.

ω Angular frequency.

$\underline{\underline{\mu}}$ Permeability dyadic.

μ Scalar permeability.

ν Variable characterising the continuous modes for a given value of k_t

$\underline{\Pi}_e^{\pm}(\underline{r}_t;k_t)$ $\underline{\Pi}_h^{\pm}(\underline{r}_t;k_t)$ Electric and magnetic type Hertzian potentials.

$<\underline{a}(r_t),\underline{b}(r_t)>$ Inner product notation.

$|\ |$ Modulus.

arg argument.

res residue from a pole.